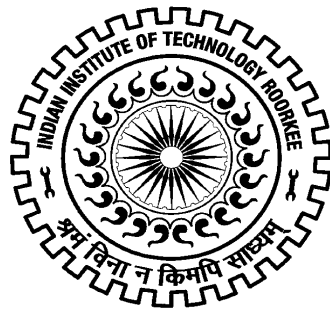


TREATMENT OF PETROLEUM REFINERY WASTEWATER

Ph.D THESIS

by

CHANDRAKANT THAKUR



**DEPARTMENT OF CHEMICAL ENGINEERING
INDIAN INSTITUTE OF TECHNOLOGY ROORKEE
ROORKEE - 247 667 (INDIA)**

DECEMBER, 2013

TREATMENT OF PETROLEUM REFINERY WASTEWATER

A THESIS

*Submitted in partial fulfilment of the
requirements for the award of the degree*

of

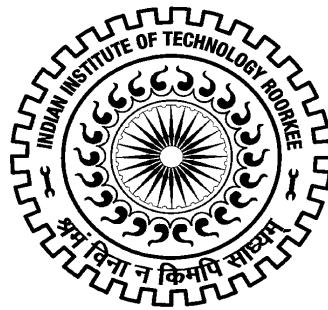
DOCTOR OF PHILOSOPHY

in

CHEMICAL ENGINEERING

by

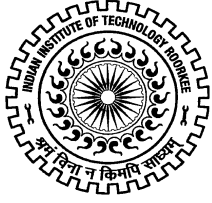
CHANDRAKANT THAKUR



**DEPARTMENT OF CHEMICAL ENGINEERING
INDIAN INSTITUTE OF TECHNOLOGY ROORKEE
ROORKEE - 247 667 (INDIA)**

DECEMBER, 2013

**©INDIAN INSTITUTE OF TECHNOLOGY ROORKEE, ROORKEE-2013
ALL RIGHTS RESERVED**



INDIAN INSTITUTE OF TECHNOLOGY ROORKEE ROORKEE

CANDIDATE'S DECLARATION

I do hereby certify that the work which is being presented in this thesis entitled “**TREATMENT OF PETROLEUM REFINERY WASTEWATER**” in partial fulfilment of the requirement for the award of the Degree of Doctor of Philosophy and submitted in the **Department of Chemical Engineering of the Indian Institute of Technology Roorkee** is an authentic record of my own work carried out during a period from December, 2009 to December, 2013 under the supervision of Dr. I.D. Mall, Professor, Department of Chemical Engineering, Indian Institute of Technology Roorkee, Roorkee.

The matter presented in the thesis has not been submitted by me for the award of any other degree of this or any other Institute.

(CHANDRAKANT THAKUR)

This is to certify that the above statement made by the candidate is correct to the best of my knowledge.

Date: December , 2013

(I.D. MALL)
Supervisor

The Ph.D. Viva-Voice Examination of **Mr. CHANDRAKANT THAKUR**, Research Scholar, has been held on.....

Signature of Supervisor

Chairman, SRC

External Examiner

Head of the Department/Chairman, ODC

ABSTRACT

Petroleum industries transform crude oil into useful products such as kerosene, gasoline, and other petrochemical feedstocks. This process consumes large amount of water, consequently significant amount of wastewater gets generated during processing of crude oil in refineries. Wastewater generated in refinery process is about 0.4-1.6 times the crude oil processed [Coelho et al., 2006]. Petroleum refinery wastewater (PRW) contains phenolic compounds (such as phenol, resorcinol, catechol, etc.), oil and grease, and other toxic compounds which can cause serious environmental problem if discharged to various aquatic bodies. Refineries follow traditional treatment technologies that consist of different mechanical, physico-chemical and biological treatment methods. Refractory toxic compounds present in PRW reduce the efficiency of biological treatment processes.

Among physico-chemical methods, adsorption as a wastewater treatment process has aroused considerable interest during recent years. Granulated activated carbon is generally used as a commercial adsorbent. However, because of its high cost, industrial and agricultural wastes such as rice husk ash (RHA), bagasse fly ash, etc. have gained a lot of attention as potential low-cost adsorbents [Kumar et al., 1987; Sharma et al., 2010; Alam et al., 2007]. However, only few studies [McKay and Al-Duri, 1991; Allen et al., 2004; Suresh et al., 2012a,b] have been reported in the open literature for the multi-component adsorption of phenolic compounds on various types of adsorbents. Since, actual effluents generated in industries such as petroleum refineries contain several phenolic compounds; therefore, equilibrium adsorption data

for closely related binary and ternary compounds is of utmost importance for the design of adsorption systems.

Sequential batch reactor (SBR) is a biological treatment method which has gained more importance as compared to other biological treatment methods because of its inherent flexibility in treatment time. SBR treatment system consists of five operations in sequence: fill phase in which reactor is fed with wastewater; react phase in which the organic matter degradation occurs; settle phase in which biomass is allowed to settle; draw phase in which wastewater is withdrawn from reactor to retain the biomass and idle phase [Chan and Lim, 2007; Thakur et al., 2013a]. Survey of the open literature for treatment of petroleum wastewater by SBR [Viero et al., 2008; Shariati et al., 2011; Kutty et al., 2011] shows that previous researchers did not use fill time as an operating parameter, and kinetic study was not performed in any of the previous studies for the treatment of PRW in SBR.

Recently electrochemical treatment using various types of electrodes has been used for the treatment of various type of industrial wastewaters [Sengil et al., 2009; Verma et al., 2013]. Only a few studies are available in open literature for the electrochemical treatment of PRW. Yavuz et al. [2010] performed electrochemical oxidation of PRW using boron doped diamond anode, ruthenium mixed metal oxide electrode, and electrofenton and electrocoagulation using iron electrode. Yan et al. [2011] treated PRW using electrochemical process with three dimensional multi-phase porous graphite plate electrodes. Thus, the most common iron/stainless steel (SS) electrodes have not been used earlier for the electrocoagulation (EC) treatment of PRW. More over in previous studies, the sludge was not characterized from disposal point of view.

The present study has been undertaken with endeavor to study treatment of wastewater containing phenolic compounds and actual PRW by following methods:

1. Individual and simultaneous adsorptive removal of phenol, catechol and resorcinol from aqueous solution by RHA.
2. Treatment of synthetic phenolic wastewater containing phenol, catechol and resorcinol by SBR.
3. Treatment of actual PRW by SBR.
4. Treatment of actual PRW by EC method using SS as an electrode.

Adsorptive removal of phenolic compounds like phenol, catechol and resorcinol was studied by means of adsorption onto low-cost RHA [Thakur et al., 2013b,c]. Physico-chemical characterization including surface area, X-ray diffraction analysis, scanning electron microscopy (SEM), and Fourier transform infrared spectroscopy (FTIR) of the RHA before and after adsorption have been done to understand the adsorption mechanism. Effect of adsorbent dose and contact time was studied out by varying the dosages in the range of 2-20 g/L at natural pH. All the batch experiments were carried out at $30\pm 1^\circ\text{C}$. Optimum adsorbent dose for all the compounds was found to be 20 g/L. Contact time for adsorption equilibrium was found to be 16 h. The pseudo-second-order kinetics represented the adsorption process well for all the adsorbates. Redlich–Peterson isotherm model was found to best-represent the individual equilibrium data for all the three compounds by RHA. The adsorption of phenol, catechol and resorcinol from the binary and ternary solutions onto RHA has been generally found to be antagonistic in nature. Equilibrium isotherms for the binary and ternary adsorption have been analyzed by using non-modified Langmuir, modified Langmuir, extended-Langmuir, extended-Freundlich and Sheindorf–Rebuhn–Sheintuch models. Extended

Langmuir model which assumes overlapping of sites for different adsorbate better represented the binary isotherm data for all three phenol-catechol, catechol-resorcinol and phenol-resorcinol systems and the ternary system data.

Treatment of synthetic wastewater containing phenol, resorcinol and catechol was studied in a SBR [Thakur et al., 2013a]. Activated sludge was collected from sewage treatment plant located in Rishikesh, Uttarakhand, India. The sludge was first screened for the removal of coarse and bigger particles and then it was aerated for 1-2 d and acclimatized for treatment of phenol containing wastewater. The reactor was composed of Plexi glass, with the dimension of 7.37 cm×40.64 cm (radius × height) and having 5 litre working volume. Aeration in the SBR was achieved by an aquarium-type air pump with sintered-sand diffusers at the bottom of the reactor. Mixed liquor suspended solid (MLSS) concentration was controlled between 1200 and 2200 mg/L with a sludge age of ≈20 d. Excess sludge, which grew during the aeration stage, was drawn out at the end of every operating cycle, in order to maintain proper MLSS concentration. The reactors were operated in an isothermal chamber with temperature at 30±1°C. Parameters such as hydraulic retention time (HRT) and filling time have been optimized to increase the phenol, resorcinol, catechol and chemical oxygen demand (COD) removal efficiencies. The optimum HRT value was found to be 1.25 d whereas optimum fill time was found to be 1.5 h. More than 99% phenol, 95% resorcinol and 96% catechol and 89% COD removal efficiencies have been obtained at optimum conditions. EDAX analysis shows the increased carbon content and utilization of nutrients in the sludge after the treatment of wastewater in the SBR. The heating value of the activated sludge was found to be 12.09 MJ/kg. The filtered sludge can be dried and fired as fuel in the furnaces/incinerators for its heat recovery. The bottom ash can

be used for blending with organic manure for its use in agriculture/horticulture or can be blended with clay/coal fly ash for use in making bricks/ceramic tiles for the building industry [[Thakur et al., 2013a](#)].

SBR was also used for the treatment of actual PRW in terms of COD and total organic carbon (TOC) removal. Actual PRW was collected from a nearby petroleum refinery and was characterized for its various physico-chemical characteristics. In this study, reactor was operated on a fill-and-draw basis, with a cycle time of 8 h, while, settle time, decant time and idle time were 1, 0.5 and 0.5 h, respectively. React time was varied according to the fill phases strategies to degrade the carbonaceous materials and nitrogen present in PRW. For this, two phases study was carried out. In the phase-I of SBR operation, instantaneous filling strategy was implemented by varying the volume exchange ratio (VER) and HRT in the range of 0.10-0.60 d and 0.56-3.33 d, respectively. Aeration was given during the react phase only. Maximum COD and TOC removal of 77% and 79% was observed at HRT=0.83 d. Further experiments were performed by varying the fill time from 0.5-2 h at HRT=0.83 d. Maximum COD and TOC removal of 79.7% and 83.5%, respectively, was achieved when the fill time was 2 h. FTIR and UV-visible analysis were done so as to understand the degradation mechanism [[Thakur et al., 2013e](#)].

Performance of a batch EC treatment of actual PRW was studied using SS electrode [[Thakur et al., 2013d](#)]. A rectangular perspex glass lab-scale batch reactor having a working volume of 1.5 l (110 mm×110 mm×125 mm) was used for the EC experiments. Four SS electrodes of 3 mm thickness and 80 mm×80 mm dimension were used in the present study. The inter-electrode gap was varied in the range of 0.5-2.5 cm. A digital direct current power supply (0–20 V, 0–5 A) was used to maintain

constant current in the range of 1-5 A during the run. Solution was agitated with magnetic stirrer during the experimental run so as to achieve proper mixing. Full factorial central composite (CCD) design was used to study the effect of four key process parameters on the reduction of COD and TOC. The parameters used in this study are initial pH (pH_0): 2–10; current density (j): 39.06–195.31 A/m^2 ; inter-electrode distance (g): 1–2.5 cm and electrolysis time (t): 30–150 min. Quadratic models were developed in terms of input parameters such as pH_0 , j , g and t by carrying out experiments as per the CCD design. These quadratic models were further used for determining parametric condition for maximum COD and TOC removal. COD and TOC removal efficiencies of 61% and 51.6%, respectively, were obtained at optimized operating condition of $\text{pH}_0=6.0$, $j=182 \text{ A}/\text{m}^2$, $g=1.5 \text{ cm}$ and $t=145 \text{ min}$. Mechanism of EC treatment was studied by carrying out zeta potential measurement, UV-visible and FTIR analysis of PRW before and after treatment. Overall treatment of PRW was because of the charge neutralization of colloids, adsorption onto generated iron hydroxides and by degradation of the organic pollutants by oxidizing agents generated in situ during EC treatment. Sludge generated has also been characterized by FTIR, SEM, energy dispersive X-ray analysis and thermo-gravimetric analysis so as to evaluate its disposal aspect [Thakur et al., 2013d].

For treatment of synthetic wastewater containing phenolic compounds like phenol, catechol and resorcinol, SBR was found to show better treatment efficiency as compared to adsorption with RHA. Comparison of various treatment methods for actual PRW shows that treatment in SBR removes highest amount of COD, however, it requires higher treatment time as compared to EC treatment.

ACKNOWLEDGEMENT

“COMMIT YOURSELF TO CONSTANT IMPROVEMENT AND QUALITY”

to what I have tried to do so in this thesis. To do the present work and write this thesis, I was lucky to be supported by professors, seniors, friends, family members, and many more. It is really very difficult to express my thanks to all of them in these few words.

I express my deep sense of gratitude to my guide Dr. I. D. Mall, Professor, Department of Chemical Engineering, Indian Institute of Technology Roorkee, Roorkee, for his keen interest, constant guidance and encouragement throughout the course of this work. His experience, assiduity and deep insight of the subject held this work always on a smooth and steady course.

I am also extremely thankful to Dr. Vimal Chandra Srivastava, Assistant Professor, Department of Chemical Engineering, Indian Institute of Technology Roorkee, Roorkee for his constant motivation, guidance and support.

My sincere and grateful thanks are also due to Dr. Indra Mani Mishra and Dr. B. Prasad, Professors, Department of Chemical Engineering and Dr. Pradeep Kumar, Professor, Department of Civil Engineering, IIT Roorkee for their kind assistance and encouragement. I would like to take this opportunity to put on record my respects to Dr. V. K. Agarwal, Prof. and Head of the Department, for providing me various facilities during the course of the present investigation and Dr. B. Mohanty, Prof. and Chairman DRC, Department of Chemical Engineering; and all faculty members for their help, motivation and moral support during my research.

I owe grateful thanks to my friends and seniors, especially, Dr. J.P. Kushwaha, Dr. S. Suresh, Dr. V. Subbaramaiah, Seema Singh, Ajay Hiwarkar, Nilambar Bariha, Ramkishore, Praveen Toni, Prateek, Mohd. Nasir, Raj Kumar, Rajesh Bilotia, Ankit

Ranjan, Abhishek Singh Tomar, Gagan Mandal and many others who generously helped me during my research work.

Special thanks are due to technical staff of the Department: Shri Rajendra Bhatnagar, Shri S.K. Sisodia, Shri Tara Chand, Shri Satpal Singh, Shri Vipin Ekka, Shri Arvind Kumar, etc. who helped me during the course of my experimental work. Thanks are also due to Shri Shadab Ali, Shri Arun Sharma, Shri Ram Avatar, Shri Sudesh and other ministerial staff of the Department of Chemical Engineering for their assistance.

I sincerely thank Indian Institute of Technology Roorkee and Ministry of Human Resource and Development, Government of India, for providing financial support to undertake the work.

I felt highly privileged to be associated as a research scholar with Prof. I.D. Mall, honest teacher, good researcher and dynamic person. I am also thankful to Mrs. Indira Mall who has been so kind to me, whenever I went to her residence.

Above all, I want to express my heartiest gratitude to all my family members for their love, faith and support for me, which has always been a constant source of inspiration and encouragement.

I fully understand that the research experience and knowledge that I have gathered during Ph.D. would be highly useful in my career. This work was possible due to contributions of many. I am thankful to all of them and extremely sorry if anyone is left out in the acknowledgement. I thank God for encouraging me in every possible way and providing me strength to withstand the adversities during my past years.

CHANDRAKANT THAKUR

CONTENTS

Candidate's Declaration	i
Abstract	ii
Acknowledgement	viii
List of Figures	xiv
List of Tables	xviii
Abbreviations and Notations	xxi
Chapter I INTRODUCTION	
1.1 General	1
1.2 Petroleum Refinery Process	2
1.3 Wastewater Characteristics and Discharge Standard For Petroleum Refinery	5
1.4 Wastewater Treatment in Petroleum Refinery	10
1.5 Objectives	13
Chapter II PETROLEUM REFINEING & WASTEWATER MANAGEMENT	
2.1 General	15
2.2 Petroleum Refining Process	15
2.3 Generation of Wastewater in Petroleum Refineries	21
2.4 Management of Wastewater and Treatment Strategies	26
Chapter III LITERATURE REVIEW	
3.1 General	31
3.2 Adsorption	32
3.3 Sequential Batch Reactor	40
3.4 Electrocoagulation Treatment	51
3.5 Research Gap	60

Chapter IV ADSORPTION

4.1	General	62
4.2	Adsorption Theory	62
4.3	Materials and Methods	64
4.3.1	Adsorbent Characterization	64
4.3.2	Adsorbates	65
4.3.3	Batch Experimental Programme	67
4.3.4	Adsorption Kinetic Study	68
4.3.5	Adsorption Isotherm Study	69
4.3.5.1	Single Component Isotherm Modeling	69
4.3.5.2	Multi Component Isotherm Modeling	71
4.4	Results and Discussion	73
4.4.1	Characterization of Adsorbent	73
4.4.2	Effect of Initial pH	75
4.4.3	Effect of Adsorbent Dose and Contact Time	77
4.4.4	Adsorption Kinetic Study	80
4.4.5	Adsorption Isotherm Modeling	83
4.4.5.1	Individual adsorption of Phenol, Catechol and Resorcinol	83
4.4.5.2	Binary adsorption of Phenol-Catechol, Catechol-Resorcinol and Phenol-Resorcinol	89
4.4.5.3	Ternary adsorption of Phenol, Catechol and Resorcinol	108

Chapter V SEQUENTIAL BATCH REACTOR TECHNOLOGY

5.1	General	117
5.2	Sequential Batch Reactor	117
5.2.1	Operation of Sequential Batch Reactor	118
5.2.2	Operating Parameter in SBR Process	121
5.3	Materials and Methods	122
5.3.1	Experimental Setup	122
5.3.2	Experimental Procedure	123
5.3.3	Analytical Measurements	125

5.4	Treatment of Synthetic Wastewater containing Phenolic Compounds (Phenol, Catechol and Resorcinol)	127
5.4.1	Characteristics of Wastewater and Acclimatization of Sludge	127
5.4.2	Effect of HRT	128
5.4.3	Effect of Fill Time	131
5.4.4	Characterization of Sludge	131
5.5	Treatment of Actual Petroleum Refinery Wastewater	138
5.5.1	Characteristics of Wastewater and Acclimatization of Sludge	138
5.5.2	Effect of HRT on COD and TOC removal	139
5.5.3	Effect of Fill Time on COD and TOC removal	145
5.5.4	Determination of Kinetic Parameters	150
5.5.5	Characterization of Wastewater and Activated Sludge	151

Chapter VI ELECTROCOAGULATION TREATMENT

6.1	General	154
6.2	Electrocoagulation Theory	154
6.3	Materials and Methods	156
6.3.1	Wastewater	156
6.3.2	Experimental Setup	156
6.3.3	Experimental Design and Procedure	159
6.4	Results and Discussion	162
6.4.1	Statistical Analysis and Fitting of Second-Order Polynomial Equation	162
6.4.2	Effects of Parameters	167
6.4.3	Optimization Analysis	168
6.4.4	Mechanism Study	171
6.4.5	Physico-chemical Analysis of Electrodes and Residues	176

Chapter VII CONCLUSIONS AND RECOMMENDATIONS

7.1	Conclusions	179
7.1.1	Treatment of Synthetic Wastewater containing Phenol, Catechol and Resorcinol	179

7.1.2	Treatment of Actual PRW	180
7.2	Recommendations	182
REFERENCES		183
PUBLICATIONS FROM THESIS		211
BIO-DATA		212

LIST OF FIGURES

Figure No.	Title	Page No.
Figure 1.2.1	Typical flow diagram of petroleum refinery process	3
Figure 2.2.1	Overview of petroleum refinery	17
Figure 2.3.1	Sources of pollutants from petroleum refinery process	25
Figure 2.4.1	Management of wastewater generated in petroleum industry	29
Figure 2.4.2	Typical petroleum refinery wastewater treatment plant	30
Figure 4.4.1	Point of zero charge of rha	78
Figure 4.4.2	Effect of pH_0 on the adsorption of phenol, catechol and resorcinol by RHA, $C_0 = 250$ mg/L, $m = 20$ g/L, $t = 24$ h, $T = 30$ °C	79
Figure 4.4.3	Effect of adsorbent dose and contact time on the adsorption of phenol, catechol and resorcinol by RHA, $C_0 = 250$ mg/L, $pH_0 = 6$, $T = 30$ °C	79
Figure 4.4.4	Pseudo-second-order kinetic plot for the removal of phenol, catechol and resorcinol by RHA, $pH_0=6.0$, $C_0=250$ mg/L, $m=20$ g/L, $T=30$ °C	82
Figure 4.4.5	Equilibrium adsorption isotherms for the individual adsorption of phenol, catechol and resorcinol onto rice husk ash. experimental data represented by points and r-p isotherm fitting represented by lines	88
Figure 4.4.6	FTIR analysis of raw rha, phenol, catechol and resorcinol loaded rha	88
Figure 4.4.7	Comparison of the experimental and calculated q_e values for phenol and catechol adsorption from a binary mixture of phenol and catechol	102
Figure 4.4.8	Comparison of the experimental and calculated q_e values for catechol and resorcinol adsorption from a binary mixture of catechol and resorcinol	103
Figure 4.4.9	Comparison of the experimental and calculated q_e values for phenol and resorcinol adsorption from a binary mixture of phenol	104

	and resorcinol	
Figure 4.4.10	Binary adsorption isotherms of simultaneous phenol and catechol adsorption onto RHA. The surfaces are predicted by the extended Langmuir model and the symbols are experimental data (a) Phenol uptake and (b) Catechol uptake	105
Figure 4.4.11	Binary adsorption isotherms of simultaneous catechol and resorcinol adsorption onto RHA. The surfaces are predicted by the extended Langmuir model and the symbols are experimental data (a) Catechol uptake and (b) Resorcinol uptake	106
Figure 4.4.12	Binary adsorption isotherms of simultaneous phenol and resorcinol adsorption onto RHA. the surfaces are predicted by the extended Langmuir model and the symbols are experimental data (a) Phenol uptake and (b) Resorcinol uptake	107
Figure 4.4.13	Three-dimensional adsorption isotherm surfaces created by using a multicomponent extended Langmuir model for the phenol + catechol + resorcinol systems with $C_{e,R}$ as a parameter. (a) The effect of catechol concentration on the equilibrium uptake of phenol; (b) The effect of phenol concentration on the equilibrium uptake of catechol; (c) The effect of phenol and catechol concentration on the equilibrium total uptake of phenol + catechol by RHA.	115
Figure 4.4.14	Three-dimensional adsorption isotherm surfaces created by using a multicomponent extended langmuir model for the phenol + catechol + resorcinol systems with $C_{e,p}$ as a parameter. (a) The effect of resorcinol concentration on the equilibrium uptake of catechol; (b) The effect of catechol concentration on the equilibrium uptake of resorcinol; (c) The effect of catechol and resorcinol concentration on the equilibrium total uptake of catechol + resorcinol by RHA.	116
Figure 5.2.1	Sequencing batch reactor (SBR) operation principle	119
Figure 5.3.1	Schematic diagram of experiment setup	124

Figure 5.3.2	Actual photograph of experimental setup	124
Figure 5.4.1	Peaks corresponding to phenol, catechol and resorcinol present in wastewater before and after treatment in sbr	129
Figure 5.4.2	Effect of hydraulic retention time (HRT) on the removal of resorcinol, catechol, phenol and COD at SRT=20 d, instantaneous filling	130
Figure 5.4.3	Effect of hydraulic retention time (HRT) on the final MLSS and MLVSS concentration at SRT=20 d, instantaneous filling	130
Figure 5.4.4	Effect of fill time on the removal of resorcinol, catechol, phenol and COD at SRT=20 d and HRT=1.25 d	133
Figure 5.4.5	Effect of fill time on the final MLSS and MLVSS concentration at SRT=20 d and HRT=1.25 d	133
Figure 5.4.6	EDX of activated sludge before and after treatment	135
Figure 5.4.7	DTA-DTA-TG plot of activated sludge in various conditions in air atmosphere (a) before and (b) after growth	136
Figure 5.5.1	Effect of HRT on (a) COD removal, and (b) TOC removal	142
Figure 5.5.2	Effect of HRT on (a) pH, and (b) Dissolved oxygen	143
Figure 5.5.3	Effect of HRT on MLSS and SVI	144
Figure 5.5.4	Effect of fill time on (a) COD removal, and (b) TOC removal	147
Figure 5.5.5	Effect of fill time on (a) pH, and (b) Dissolved oxygen	148
Figure 5.5.6	Effect of fill time on MLSS and SVI	149
Figure 5.5.7	FTIR of treated and raw refinery wastewater by SBR	152
Figure 5.5.8	UV–Visible spectrum analysis of treated and raw refinery wastewater by SBR	152
Figure 6.3.1	Schematic diagram of experimental setup	158
Figure 6.3.2	Actual photograph of experimental setup	158
Figure 6.4.1	Effect of current density (A/m^2) and pH on (a) COD removal, (b) TOC removal, and (c) Desirability factor	169
Figure 6.4.2	Effect of time (min) and electrode gap (cm) on (a) COD removal, (b) TOC removal, and (c) Desirability factor	170
Figure 6.4.3	UV–Visible spectra of PRW at different time intervals during the	173

	EC treatment at $\text{pH}_0=6.0$, $j=182 \text{ A/m}^2$, $g=1.5 \text{ cm}$	
Figure 6.4.4	Variation of zeta potential with time in the EC reactor at optimum condition of treatment, $\text{pH}_0=6.0$, $j=182 \text{ A/m}^2$, $g=1.5 \text{ cm}$	173
Figure 6.4.5	FTIR of sludge generated, treated and raw refinery wastewater by EC	174
Figure 6.4.6	SEM images of fresh and used stainless steel electrode and sludge generated during experiment	177
Figure 6.4.7	Thermogravimetric analysis of sludge under air atmosphere	178

LIST OF TABLES

Table No.	Title	Page No.
Table 1.3.1	Generation of wastewater during refining process of crude oil	7
Table 1.3.2	Typical characteristics of different petroleum refinery wastewater	8
Table 1.3.3	Minimal national standards [MINAS] for discharge of effluents from petroleum refineries	9
Table 2.2.1	Major unit operations typically involved in petroleum refinery	18
Table 2.3.1	Typical material outputs from selected refining processes	23
Table 2.4.1	Characteristics of wastewater and pollution/toxicants discharged from petroleum refineries in India	28
Table 3.2.1	Studies on the treatment of wastewater containing metals, dyes and other compounds by adsorption	37
Table 3.2.2	Studies on the treatment of phenolic by adsorption	39
Table 3.3.1	Brief review on industrial application of SBR	43
Table 3.3.2.	Comparison of studies on treatment of various wastewater by SBR	48
Table 3.3.3	Studies on the Treatment of Phenolic Compounds using Sequential Batch Reactor Process	49
Table 3.4.1	Studies on treatment of various industry wastewater by electrocoagulation	53
Table 3.4.2	Studies on treatment of PRW by electrocoagulation	57
Table 4.3.1	Physico-chemical properties and solvatochromic parameter of phenol, catechol and resorcinol	66
Table 4.3.2	Multi-component isotherm models	72
Table 4.4.1	Characterization of rice husk ash (RHA)	74
Table 4.4.2	Kinetic parameter for the removal of phenol, catechol and resorcinol by RHA, $pH_0=6.0$, $C_0=250$ mg/L, $m=20$ g/L, $T=30$ °C	81
Table 4.4.3	Individual adsorption equilibrium uptakes and yields of phenol, catechol and resorcinol adsorption at different initial concentrations onto RHA	86
Table 4.4.4	Isotherm parameter fitted on isotherm model for the removal of	87

	phenol, catechol and resorcinol by RHA	
Table 4.4.5	Comparison of individual and total adsorption equilibrium uptakes and yields found at different catechol concentrations in the absence and presence of increasing concentrations of phenol onto RHA	96
Table 4.4.6	Comparison of individual and total adsorption equilibrium uptakes and yields found at different catechol concentrations in the absence and presence of increasing concentrations of resorcinol onto RHA	97
Table 4.4.7	Comparison of individual and total adsorption equilibrium uptakes and yields found at different resorcinol concentrations in the absence and presence of increasing concentrations of phenol onto RHA	98
Table 4.4.8	Multi-Component isotherm parameter values for the simultaneous removal of phenol and catechol by RHA	99
Table 4.4.9	Multi-Component isotherm parameter values for the simultaneous removal of catechol and resorcinol by RHA	100
Table 4.4.10	Multi-Component isotherm parameter values for the simultaneous removal of phenol and resorcinol by RHA	101
Table 4.4.11	Comparison of Individual and total adsorption equilibrium uptakes and yields found at different resorcinol concentrations in the absence and presence of increasing concentrations of phenol ions onto RHA	112
Table 4.4.12	Multi-component isotherm parameter values for the simultaneous removal of phenol and catechol by RHA	114
Table 5.3.1	Analytical techniques/instruments/equipment used in the determination of various parameters	127
Table 5.5.1	Details of acclimatization procedure for SBR	138
Table 5.5.2	Characterization of PRW before and after treatment by SBR	139
Table 5.5.3	Effect of HRT with instantaneous fill on COD and TOC removal efficiency	141
Table 5.5.4	Variation in fill time with HRT 0.83 d on COD and TOC removal Efficiency	146
Table 5.5.5	Kinetic constant for COD degradation of PRW in SBR at various HRT	151

Table 6.3.1	Dimensional characteristics of EC-Cell	157
Table 6.3.2	Parameters and their level used to design the experiment runs	160
Table 6.3.3	Full factorial design with actual and predicted values of percentage COD and TOC removal	161
Table 6.4.1	Adequacy of the models tested for Y_1 and Y_2	164
Table 6.4.2	ANOVA for response surface quadratic model for Y_1	165
Table 6.4.3	ANOVA for response surface quadratic model for Y_2	166
Table 6.4.4	FTIR Band assignment for untreated and treated PRW and sludge generated during EC experiment	175

ABBREVIATIONS AND NOTATIONS

ABBREVIATIONS

AC	: Activated charcoal
ACC	: Activated carbon commercial
ACL	: Activated carbon laboratory
ANOVA	: Analysis of variance
APHA	: American public health association
API	: American petroleum institute
AS	: Activated sludge
BET	: Brunaur-Emmett-Teller
BFA	: Bagasse fly ash
BJH	: Barret-Joyner-Halenda
BOD	: Biological oxygen demand, mg/L
C/N	: Carbon nitrogen ratio
CC	: Central composite
CDU	: Crude distillation unit
CHNS	: Carbon hydrogen nitrogen sulphur
CN	: Cyanide
COD	: Chemical oxygen demand, mg/L
CSTR	: Continuous stirred tank reactor
D	: Overall desirability
DAF	: Dissolved air flotation
DDW	: Double distilled water
DF	: Degree of freedom
DO	: Dissolved oxygen
DTG	: Differential thermal analysis
DTA	: Differential thermal analysis
EC	: Electrocoagulation

EF	: Electro-flotation
FCC	: Fluid catalytic cracker
2FI	: Two factor interaction
FTIR	: Fourier transform infrared
GAC	: Granular activated carbon
GSBR	: Granular sequential batch reactor
HPLC	: High performance liquid chromatography
HRT	: Hydraulic retention time
IAF	: Induced air flotation
MLSS	: Mixed liquor suspended solids, mg/L
MLVSS	: Mixed liquor volatile suspended solids, mg/L
MPSD	: Marquardt's percent standard deviation
MSBR	: Membrane-couple sequential batch reactor
N	: Nitrogen
O & G	: Oil and Grease
ORW	: Oil refinery wastewater
OWS	: Oily water sewer
PAC	: Poly aluminum chloride
PRESS	: Predicted residual sum of square
PRW	: Petroleum refinery wastewater
PUF	: Polyurethane foam
PW	: Petrochemical wastewater
R-P	: Redlich-Peterson isotherm
RBC	: Rotating biological contactor
RH	: Rice husk
RHA	: Rice husk ash
RSM	: Response surface methodology
SBAR	: Sequencing batch airlift reactor
SBR	: Sequencing batch reactor
SEM	: Scanning electron microscope
SMBR	: Submerged membrane bioreactor

SRS	: Sheindorf-Rebhum-Sheintuch
SRT	: Sludge retention time
SS	: Suspended solid
SSE	: Sum of square error
SVI	: Sludge volume index
TA	: Thermo analysis
TDS	: Total dissolved solids
TGA	: Thermo-gravimetric analysis
TN	: Total nitrogen
TOC	: Total organic carbon
TS	: Total solid
TSS	: Total suspended solid
UASB	: Up flow anaerobic sludge blanket
VER	: Volume exchange ratio
XRD	: X-ray diffraction
WC	: Wood charcoal

NOTATION

l/n	: Heterogeneity factor
a_{ij}	: Competition coefficients of component i by component j , dimensionless
a_R	: R-P isotherm constant, L/mg
a_R	: Constant of Redlich-Peterson isotherm, L/mmol
Ad_{Tot}	: Total adsorption yield
Ad_i	: Individual adsorption yield
b_i	: Model coefficient
C_o	: Initial concentration of adsorbate in solution, mmol/L
$C_{o,i}$: Initial concentration of each component in solution, mmol/L
C_e	: Unadsorbed concentration of the single-component at equilibrium, mmol/L

- $C_{e,i}$: Unadsorbed concentration of each component in the binary mixture at equilibrium, mmol/L
 C_f : Final concentration of adsorbate in solution, mmol/L
 d_i : Desirability of response i
 g : Inter-electrode gap, cm
 h : Initial sorption rate, mg/g min
 HRT_{opt} : Optimum hydraulic retention time, d
 J : Current density, A/m²
 k : Number of responses
 k_A : Adsorption rate constant for the adsorption equilibrium
 k_d : Endogenous coefficient, h⁻¹
 k_f : Pseudo-first order rate constant
 k_o : Frequency factor (same unit as that k)
 k_s : Pseudo-second order rate constant
 $K_{EL,i}$: Extended Langmuir constant, L/mg
 K_F : Mono-component (non-competitive) constant of Freundlich isotherm of the single component, (mmol/g)/(L/mmol)^{1/n}
 $K_{F,i}$: Individual Freundlich isotherm constant of each component, (mmol/g)/(L/mmol)^{1/n}
 K_i : Individual extended Langmuir isotherm constant of each component, L/mmol
 K_L : Constant of Langmuir isotherm, L/mmol
 $K_{L,i}$: Individual Langmuir isotherm constant of each component, L/mmol
 K_R : Constant of Redlich-Peterson isotherm, L/g
 K_T : Equilibrium binding constant (l/mol)
 m : Mass of adsorbent per liter of solution, g/L
 n : Mono-component (non-competitive) Freundlich heterogeneity factor of the single component, dimensionless
 n_i : Individual Freundlich heterogeneity factor of each component, dimensionless

n_m	: Number of measurements
n_p	: Number of parameters
N	: Number of data points
N_C	: Number of cycles per day
pH_o	: Initial pH of the solution
pH_{pzc}	: Point of zero charge
q_e	: Equilibrium single-component solid phase concentration, mmol/g
$q_{e,calc}$: Calculated value of solid phase concentration of adsorbate at equilibrium, mmol/g
$q_{e,exp}$: Experimental value of solid phase concentration of adsorbate at equilibrium, mmol/g
$q_{e,i}$: Equilibrium solid phase concentration of each component in binary mixture, mmol/g
q_m	: Adsorption capacity of adsorbent, mmol/g
q_{max}	: Constant in extended Langmuir isotherm, mmol/g
q_t	: Adsorbate adsorbed, mg/g at any time t
Q	: Daily waste water flow rate, L/d
R	: Universal gas constant, 8.314 J/K mol
R^2	: Coefficient of determination
t	: Time, min
t_{AE}	: Aerobic react time, h
t_{AN}	: Anaerobic react time, h
t_{AX}	: Anoxic react time, h
t_D	: Decant time, h
t_F	: Fill time, h
t_I	: Idle time, h
t_R	: React time, h
t_S	: Settle time, h
t_C	: Total cycle time, h
T	: Absolute temperature, °C

V	: Volume of adsorbate containing solution, L
V_F	: Filled volume, L
V_T	: Total volume, L
V_W	: Waste sludge volume, L
V_{SI}	: Sludge volume, L
w	: Mass of adsorbent, g
X	: MLSS in the reactor with full filled, mg/L
X_{Ae}	: Fraction of the adsorbate adsorbed on the adsorbent under equilibrium
X_W	: MLSS in waste stream, mg/L
Y	: Yield coefficient
Y_1	: Percentage COD removal
Y_2	: Specific energy consumed (KWh per kg of COD removed)
Y_i	: Response values of i
Y_{i-max}	: Maximum acceptable value of response i
Y_{i-min}	: Minimum acceptable value of response i ,

GREEK SYMBOLS

α_i	: Constant in SRS model for each component, dimensionless
β	: Constant of Redlich-Peterson isotherm ($0 < \beta < 1$)
β_i	: Constant in SRS model for each component, dimensionless
$\eta_{L,i}$: Multi-component (competitive) Langmuir adsorption constant of each component, dimensionless
$\eta_{R,i}$: Multi-component (competitive) R-P adsorption constant of each component, dimensionless
μ	: Specific growth rate

SUBSCRIPTS AND SUPERSSCRIPTS

0	: Initial concentration of a substance
e	: Equilibrium concentration of a substance

INTRODUCTION

1.1 GENERAL

Petroleum refining industries play a vital role in the economic growth of any country. The economic development of many countries gets hindered due to “energy poverty”. Crude oil fulfills almost 35.1% of the global energy demand [[World Petroleum Scenario, 2011](#)]. Petroleum refineries have revolutionized human life and are providing major basic needs of energy in domestic, industrial and transportation sectors. They also provide feed stocks for fertilizers, synthetic fibers, synthetic rubbers, polymers, intermediates, explosives, dyes, paints, etc.

Global and Indian oil reserves were 235.8 and 0.8 thousand million ton per annum respectively by the end of year 2012 [[BP statistics report, 2013](#)]. In the year 2011-12, crude oil production in India was about 42 million metric tonne (MMT), with share of national oil companies at 72.4%. Indian refineries have the capacity of 215.07 MMT with refinery production (crude throughput) of 211.42 MMT as on 1.8.2012. The indigenous production of petroleum products during 2011-12 was 198.9 MMT, while consumption was 148 MMT [[MoPNG, 2011-2012](#)]. According to Ministry of Petroleum and Natural Gas, India has just 0.3% oil and gas resources of the world, but has 18% of the world’s population. India’s crude oil consumption has grown at a rate of 4.3% for the last 10 years, driven primarily by the crude oil consumption in transportation sector [[Care Rating, 2013](#)].

Petroleum refining industry uses various conversion processes to convert crude oil into valuable products and by-products like liquefied petroleum gas (LPG), fuel, naphtha, petrochemical feed stocks, etc. However, industry also generates huge amount of waste containing high chemical oxygen demand (COD), biological oxygen demand (BOD), oil and grease, suspended solids and toxic compounds like phenolic compounds that are not easily biodegradable. Industries use various treatment options consisting of primary, secondary and tertiary treatment methods depending upon the concentration of its contaminant so that the contaminant level in the treated effluent is below the discharge limits of wastewater set by various environmental protection agencies.

1.2 PETROLEUM REFINERY PROCESS

Petroleum refining processes consist of chemical, physical, and thermal separation of crude oil into its major distillate fractions which are further processed through a series of separation and conversion steps to produce finished petroleum products. Typical petroleum refinery processes are shown in [Figure 1.2.1](#). Major categories of refinery processes/units are:

Physical separation processes: Atmospheric distillation, vacuum distillation, aromatics extraction, de-waxing/de-asphalting, gas separation plant, etc.

Chemical conversion process: Alkylation, catalytic cracking, isomerisation, reforming, Hydrocracking, asphalt blowing, thermal cracking/visbreaking, etc.

Purification or treating processes: Desalting, hydrotreating/hydrodesulphurization (HDS)/hydrofinishing, sulphur recovery from hydrogen sulphide, sour gas concentration (acid gas removal), sour water treatment, lubricating oil refining, etc.

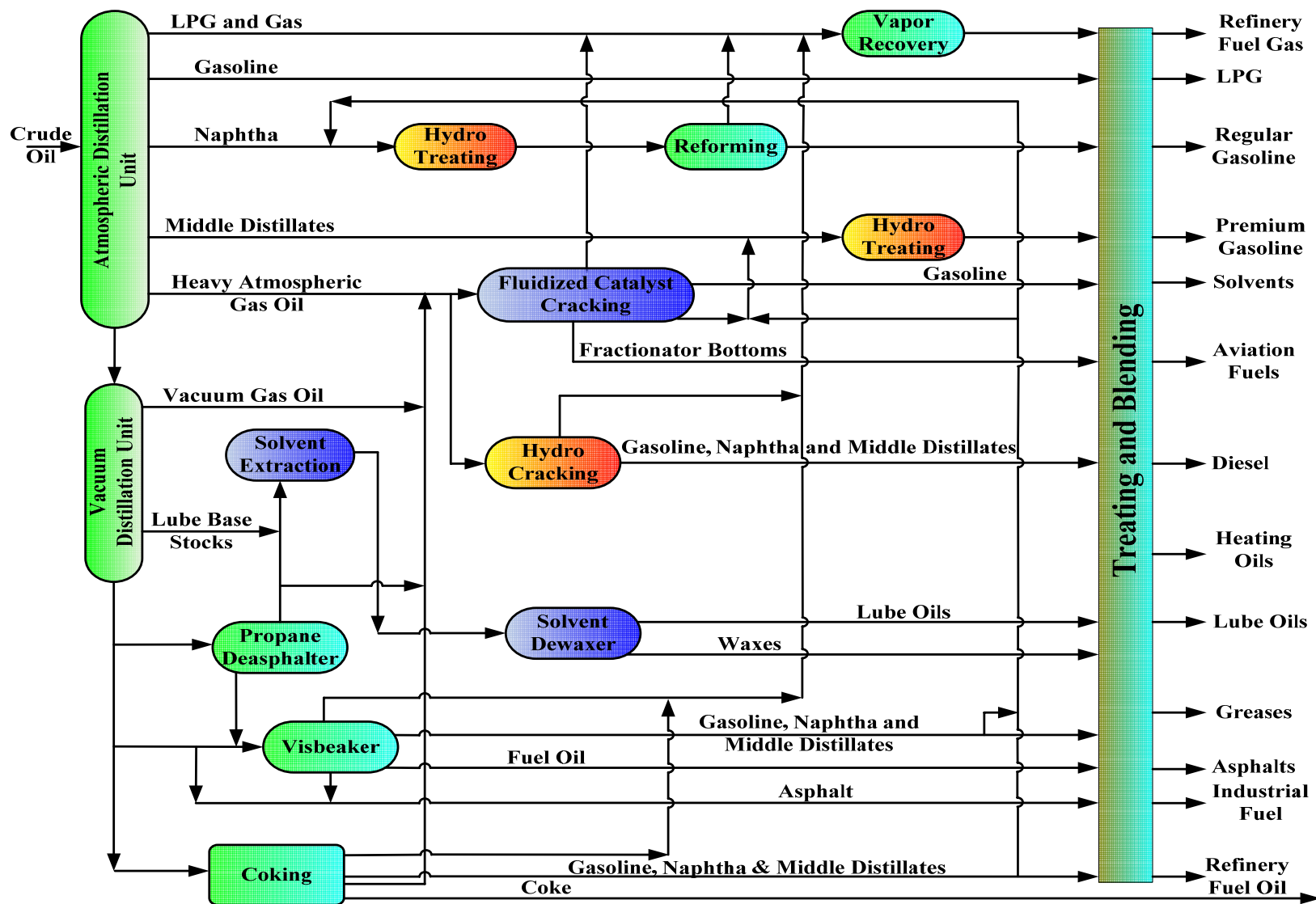


Figure 1.2.1. Typical flow diagram of petroleum refinery process.

Utilities and general facilities: Refinery liquid/gas fuel system, steam and/or power supply, flare system for disposal of vapor releases, water, air, hydrogen, and nitrogen supply, cooling water system, wastewater and hydrocarbon slops treatment, blending, storage and loading facilities, etc.

Environmental Controls: Aqueous effluent treatment, combustion and other air emission control, waste disposal, odor and noise control, etc.

Crude oil is processed through desalting process followed by distillation units where crude oil is fractionated into various intermediate products. Final petroleum products are formed by combining, reshaping and breaking of various distillate fraction (or intermediate product) in various combinations of alkylation, coking, cracking, and reforming processes.

Petroleum refineries use large amount of water to transform crude oil into valuable refined products. During processing of the crude oil, 80% of used water goes as waste stream since water does not go into the final petroleum product. Wastewater generated during the refining process is 0.4-1.6 times the amount of the crude oil processed [Coelho et al., 2006]. These waste streams are sent to common wastewater treatment unit of the refinery [Dorn, 1998; IPEICA, 2010]. Thus, based on the current yield of 84 million barrels per day (mbpd) of crude oil, a total of 33.6 mbpd of effluent is generated globally [Doggett and Rascoe, 2009; Diyaudddeen et al., 2011]. Wastewater contains oil and grease along with various toxic compounds (such as heavy metals, non-volatile and volatile aromatic compounds, phenol, etc.) which can cause serious problems to treatment, if the treatment processes are ineffective [Beg et al., 2003; Gasim et al., 2010]. Amount of pollutants present in petroleum refinery wastewater (PRW) depends upon the type of water processing being done throughout various

processes and operations of the plant. Toxic pollutants generated must be treated on-site or sent to common treatment unit depending upon its toxicity.

1.3 WASTEWATER CHARACTERISTICS AND DISCHARGE STANDARDS FOR PETROLEUM REFINERY

[Table 1.3.1](#) gives the details of various types of waste generated during the refining process of crude oil. Wastewater generated in petroleum refinery depends upon the complexity of refining process, presence of free and emulsified oil, COD and other hazardous chemicals such as hydrocarbons, phenols, sulphides, cyanide, ammonia as nitrogen, etc. [[Zarooni and Elshorbagy, 2006](#)].

The effluents contain high amount of oily and viscous residues, which are formed during production, transportation and refining process. Such residues, called oily sludge are basically composed of oil, water, solids, and their varied composition make their reutilization very difficult and confer on them high recalcitrance. Due to their chemical composition and concentration, their effects on the environment are not desirable (e.g. eutrophication) as well as dangerous to human health. Typical characteristics of PRW as reported by various investigators are given in [Table 1.3.2](#).

PRW contains phenol and associated compounds like catechol and resorcinol along with other pollutants. Majority of these phenolic compounds originate from the catalytic cracking process. The reaction products from the catalytic cracker contain steam which is subsequently used by the main fractionator. Thus, the main fractionator overhead reflux drum produces sour and foul condensate containing phenolic compounds along with ammonia, light hydrocarbons, hydrogen sulfide, cyanide, etc. Caustic treatment of cracked gasoline removes aliphatic sulfur compounds like

mercaptans, thiophenols, etc. and some amount of other phenolic compounds. Hence, spent caustics also contain phenolic compounds.

Phenol and associated compounds like catechol and resorcinol which are generated in petroleum refineries have been listed as priority pollutants by environmental protection agencies. These compounds are considered as toxic to aquatic organisms at 5–25 mg/L and impart taste and odor above 2 mg/L concentration [Kumar et al., 2003]. United States environmental protection agency (USEPA) has put phenol in priority pollutants list and has proposed stringent limits on the discharge of phenol [Beszedits and Silbert, 1990]. According to usage of water, some of the agencies have recommended phenol concentration limit in various types of water. It is mandatory for the industries to meet the discharge standards of the effluents. The Ministry of Environment and Forests (MOEF), Govt. of India, and the Central Pollution Control Board (CPCB) are authorized under the law to impose the standards and to monitor and regulate the effluent being discharged. Typical discharge limits of wastewater from petroleum refinery, as suggested by CPCB, are given in Table 1.3.3. For drinking water, Bureau of Indian Standards (BIS) recommends phenol limit of 0.001 mg/L. For potable water, World Health Organization (WHO) recommends maximum phenol concentration of 0.001 mg/L, whereas for discharge in surface waters phenol should not exceed 1.0 mg/L. For discharge of phenol containing water into the public sewers, on land for irrigation, and marine coastal areas; the BIS limit is 5 mg/L [Suresh et al., 2011b; Kamble et al., 2008]. The threshold value of phenols in water is 4000 µg/L [Knop et al., 1985; Qadeer, 2002].

Table 1.3.1. Generation of wastewater during refining process of crude oil.

Process	Process wastewater
Crude oil desalting	Oil, H ₂ S, NH ₃ , phenol, high levels of suspended solids, dissolved solids, high BOD, high temperature
Atmospheric distillation	Oil, H ₂ S, NH ₃ , suspended solids, chlorides, mercaptans, phenol, elevated pH
Thermal cracking/ Visbreaking	Oil, H ₂ S, NH ₃ , phenol, suspended solids, high pH, BOD, COD
Coking	High pH H ₂ S, NH ₃ , suspended solids, COD
Catalytic cracking	High levels of oil, suspended solids, phenols, cyanides, H ₂ S, NH ₃ , high pH, BOD, COD
Catalytic hydrocracking	High COD, suspended solids, H ₂ S, relatively low levels of BOD
Hydrotreating/ Hydroprocessing	H ₂ S, NH ₃ , high pH, phenols suspended solids, BOD, COD
Alkylation	Low pH, suspended solids, dissolved solids, COD, H ₂ S, spent sulfuric acid
Isomerisation	Low pH, chloride salts, caustic wash, relatively low H ₂ S and NH ₃
Polymerization	H ₂ S, NH ₃ , caustic wash, mercaptans and ammonia, high pH
Catalytic Reforming	High levels oil, suspended solids, COD, relatively low H ₂ S
Solvent Extraction	Oil and solvents
Dewaxing	Oil and solvents
Propane Deasphalting	Oil and propane
Gas treatment and sulfur recovery	H ₂ S, NH ₃ , amines, Stretford solution
Heat exchanger cleaning	Oily wastewater generated
Storage tanks	Water drained from tanks contaminated with tank product

Sources: Assessment of Atmospheric Emissions from Petroleum Refining, Radian Corp., 1980; Petroleum Refining Hazardous Waste Generation, U.S. EPA, Office of Solid Waste, 1994.

Table 1.3.2. Typical characteristics of different petroleum refinery wastewater (composition in mg/L, except for pH).

Waste Type	pH	COD	BOD ₅	O&G	TOC	Phenols	TSS	Sulfate	Reference
PRW	NR	658-710.5	NR	NR	NR	30	NR	NR	Serafim, 1979
PRW	NR	300-800	150-350	NR	NR	20-200	100	NR	Dold, 1989
PRW	6.5-8.5	800	350	3000	NR	8	NR	17	Demirci et al., 1997
OW	6-10	1722-7826	953-4106	NR	NR	NR	1805-7758	NR	Lee et al., 2004
PRW	NR	68-220	0.2-1.2	1.1-3.5	NR	0.85-3.75	NR	NR	Rahman and Al-Malack, 2006
PRW	8.0-8.2	850-1020	570	12.7	NR	98-128	NR	15-23	Coelho et al., 2006
PRW	NR	300-800	150-350	3000	NR	20-200	NR	NR	Al Zarooni and Elshorbagy, 2006
PRW	6.7	200	NR	NR	NR	3.7	NR	NR	Santos et al., 2006
PRW	NR	5500	220	NR	NR	NR	NR	NR	Sun et al., 2008
PW	7-9	300-600	150-360	≤50	NR	NR	150	NR	Ma et al., 2009
PRW	NR	590	NR		NR	192.9	NR	NR	Yavuz et al., 2010
ORW	7.6	3150	323	NR	1550	NR	NR	NR	Wei et al., 2010
PRW	8.2	3504	NR	NR	NR	88	0.08	NR	El-Naas et al., 2010
PW	7.5-10.3	330-556	NR	NR	NR	NR	130-250	NR	Khaing et al., 2010
PRW	6.5	1021	NR	NR	NR	95	NR	450	Yan et al., 2011
PRW	7.0	1343	849	NR	398	NR	74	NR	Hasan et al., 2012

PRW-Petroleum Refinery Wastewater; PW-Petrochemical Wastewater; ORW-Oil Refinery Wastewater; OW-Oil Refinery Wastewater; COD-Chemical Oxygen Demand; TOC-Total Organic Carbon; TSS-Total Suspended Solids; BOD₅-5 day Biological Oxygen Demand; O&G-Oil and grease; NR-Not reported.

Table 1.3.3 Minimal national standards [MINAS] for discharge of effluents from petroleum refineries.

S No.	Parameter	Limiting value for concentration [mg/L, except for pH]	Limiting value for quantum [kg/1000 tonnes of crude processed, except for pH]	Averaging period
1	pH	6.0-8.5	-	Grab
2	Oil & grease	5	2	-do-
Parameters to be monitored daily: composite sample [with 8 h interval]				
3	BOD _{3 days, 27° C}	15	6	24 hours
4	COD	125	50	-do-
5	Suspended solids	20	8	-do-
6	Phenols	0.35	0.14	-do-
7	Sulphides	0.5	0.2	-do-
8	Cyanide	0.2	0.08	-do-
Parameters to monitored once in a month: composite sample [with 8 h interval]				
9	Ammonia as N	15	6	-do-
10	Total Kjeldahl nitrogen	40	16	-do-
11	Phosphorous	3	1.2	-do-
12	Chromium (VI)	0.1	0.04	-do-
13	Total Chromium	2.0	0.8	-do-
14	Lead	0.1	0.04	-do-
15	Mercury	0.01	0.004	-do-
16	Zinc	5.0	2	-do-
17	Nickel	1.0	0.4	-do-
Parameters to monitored once in a month: grab samples for each shift with 8 h interval				
19	Benzene	0.1	0.04	Grab
20	Benzol Pyrene	0.2	0.08	-do-

Sources: Industries Effluent Standard CPCB, 2012.

Drinking of water containing phenol above threshold value can cause protein degeneration, paralysis, and tissue erosion of the central nervous system and also damages the kidney of the human body. Wastewater containing oil products and chemicals like phenol, catechol, resorcinol, etc. is not easily degradable and requires special attention for treatment. Several in-plant and end-of-process technologies have been developed which are capable of handling petroleum refining industry wastewater.

1.4 WASTEWATER TREATMENT IN PETROLEUM REFINERY

Due to the ineffectiveness of purification systems, wastewater may become dangerous, leading to the accumulation of toxic products in the receiving water bodies with potentially serious consequences on the ecosystem [Bay et al., 2003]. Typical PRW treatment plant carries out treatment in three steps:

- Pretreatment : Removal of oil and suspended solids, pH control and primary sedimentation
- Intermediate treatment : Neutralization, coagulation and sedimentation, dissolved air floatation, precipitation and detoxification
- Secondary/Tertiary treatment : Biological/chemical oxidation, filtration and adsorption

To reduce toxicity load on wastewater treatment plants, aqueous streams generated from various units are segregated and pre-treated before sending to the effluent treatment plant [Gomkale et al., 1996]. Refineries follow traditional treatment technologies that consist of different mechanical, physico-chemical and biological treatment methods. Biological treatment is the back bone of the overall treatment. However, refractory toxic compounds present in PRW reduce the efficiency of biological treatment processes. Therefore, these compounds need to be removed before

wastewater reaches biological treatment processes. Tertiary treatment methods may also be used by the industries for polishing the effluent to the final discharge limits.

Various researchers have made effort to modify the secondary treatment methods or have implemented tertiary treatment methods to reach the standard discharge limit of the wastewater. Various treatment methods like coagulation [Demirci et al., 1997; El-Naas et al., 2009b], adsorption [El-Naas et al., 2009a; Serafim, 1979], chemical oxidation [Abdelwahab et al., 2009], electrochemical oxidation [Yavuz et al., 2010], biological techniques [Jou and Huang, 2003; Ma et al., 2009], membranes [Li et al., 2006; Rahman and Al-Malack, 2006], membrane filtration [Tansel et al., 2001], membrane bioreactors [Viero et al., 2008] and microwave-assisted catalytic wet air oxidation [Sun et al., 2008] have been reported. Although biological treatment is simple, cheap, and cost-effective; however, traditional biological treatment by activated sludge method is not fully capable of treating recalcitrant compounds [Mizzouri and Shaaban, 2010; Thakur et al., 2013a].

There are number of new biological techniques which are being researched for biological treatment. Sequential batch reactor (SBR) has gained more importance as compared to other biological treatment methods because of its inherent flexibility in cycle time. It can be applied to treat wastewater having high concentration of COD, BOD, phenolic compounds and other hazardous pollutants [Barrios-Martinez et al., 2006; Tsang et al., 2007]. SBR can handle shock loads and is easy to operate and requires less area for operation. SBR has been used for treatment of various types of wastewaters [Danesh and Oleszkiewicz, 1997; Colmenarejo et al., 1998]. SBR process is a sequential suspended growth (activated sludge (AS)) process in which all major steps of conventional ASP occur in the same tank in sequential order. SBR treatment system consists of five sequencing operations: fill phase, in which reactor is fed with wastewater; react phase, in which the organic matter degradation occurs; settle phase,

in which biomass is allowed to settle; draw phase, in which wastewater is withdrawn from reactor to retain the biomass; and the idle phase [Dague et al., 1992]. Some refineries also perform tertiary treatment of wastewater using activated carbon, anthracite coal, sand, etc., to filter out remaining impurities like biomass, trace materials etc.

Electrocoagulation (EC) has been used for the treatment of numerous types of wastewaters generated in various industries such as textile, distillery, tannery, pulp and paper, etc. It has been used for the removal of various types of pollutants such as dyes, arsenic, phenolic compounds, polyaromatic organic, spent caustic, etc. from aqueous solutions [Panizza et al., 2000; Can et al., 2003; Mahesh et al., 2006; Thakur et al., 2009; Cotillas et al., 2013; Hariz et al., 2013; Bhatnagar et al., 2013]. Chen [2004] reviewed in detail fundamentals and application of EC methods for the treatment of wastewater containing suspended solids, oil and grease, and even organic or inorganic pollutants. Efficiency of EC treatment depends on various process parameters like conductivity, pH, type of electrode used, current density (j), type of pollutant, etc. Due to this multiple ingredient, the process is complex and requires some statistically experimental design that reduces the number of experimental runs with a better combination of input parameters. The application of this statistical design is to reduce the process variability, time of trial and error in experiments results [Chen et al., 2012; Prasad et al., 2008; Moreno et al., 2009]. Previous studies carried out in our laboratory show that among stainless steel (SS), iron and aluminum electrodes for treatment of textile, distillery and dairy wastewaters, amount of sludge generated with SS electrode is least and that the SS electrode has wide working pH range. SS electrode showed performance comparable with those iron and better than aluminum in term of removal efficiencies [Thakur et al., 2009; Kumar et al., 2009; Kushwaha et al., 2010,2011; Mondal et al., 2012,2013].

Refinery organics like phenolic substrates are sometimes difficult to remove by conventional biological treatment method and may require tertiary treatment. Adsorption treatment process is one of the efficient methods for removal of various types of contaminants from effluent, especially for the moderate and low concentration effluents [Nigam et al., 1996; Imagawa et al., 2000; Malik, 2003]. In most of the industries, commercial activated carbon is used as an adsorbent because of its extended surface area, microporous structure, high adsorption capacity and high degree of surface reactivity. However, it is expensive and has led to the search for low cost adsorbents [Abdelwahab et al., 2005].

Rice husk ash (RHA) has good porosity, high amount of silica and a number of functional groups on its surface which make it good adsorbent. Besides, its availability in abundance makes it highly economical as the only cost involved is the transportation cost from the place of generation to its place of use as an adsorbent [Aksu and Yener, 2001]. RHA can be used as an adsorbent because of its low cost and availability in abundance [Mall et al., 1996; Srivastava et al., 2006a].

1.5 OBJECTIVES

In view of the literature survey presented in Chapter 3, research gaps identified in section 3.5 and considering the fact that PRW contains a number of toxic phenolic compounds such as phenol, catechol, resorcinol, etc., it was decided to first study the treatment of synthetic wastewater containing phenolic compounds by adsorption onto RHA and by SBR. Also, it was decided to study treatment of actual PRW by SBR and EC method with SS electrode. Specific aims and objectives are as follows:

1. Adsorptive removal of phenolic compounds from aqueous solution by RHA.

- To characterize RHA using various characterization techniques and use it in batch process for adsorptive removal of phenol, catechol and resorcinol from aqueous solution.
 - To study the effects of adsorbent dosage, pH and time on removal efficiency.
 - To study multicomponent adsorption isotherm behavior of the competitive adsorption of phenol, catechol and resorcinol in individual, binary and ternary systems.
 - To model the binary and ternary adsorption data by various multi-component isotherm models.
2. Treatment of synthetic phenolic wastewater containing phenol, catechol and resorcinol by SBR.
- To study the effects of HRT and filling time on simultaneous removal of phenol, catechol and resorcinol.
 - To perform the sludge disposal study.
3. Treatment of actual PRW by SBR.
- To characterize actual PRW before and after treatment.
 - To study the effects of HRT, filling time on COD and TOC removal from actual PRW.
 - To determine the kinetic parameters for COD removal process in SBR.
4. Treatment of refinery wastewater by EC method using stainless steel as an electrode.
- To study the effects of current density, electrolysis time, initial pH and electrode gap on COD and TOC removal of actual PRW and maximize the removal efficiencies using desirability approach.
 - To understand the treatment process by characterizing the PRW, sludge and electrode before and after treatment; and performing sludge disposal study.

PETROLEUM REFINING AND WASTEWATER MANAGEMENT

2.1 GENERAL

This chapter describes the different sections of petroleum refining process, wastewater generation and its management. In the refinery, crude oil is processed through a number of unit operations at various temperatures to breakdown the carbon chain and make various valuable products. During the refining process, various effluents containing various toxic compounds are generated. Proper management of wastewater can reduce its quantity and contaminant load that may further reduce the operating and maintenance costs of wastewater treatment plant. Furthermore, reuse of treated wastewater could also potentially reduce the consumption of fresh water used during different operations.

2.2 PETROLEUM REFINING PROCESS

Crude oil is a liquid mixture of hydrocarbons. It mainly consists of straight-chain alkanes, some amounts of cycloalkanes and aromatic hydrocarbons, which can be separated based on their boiling points. Refining technology has evolved considerably over the last century; largely in response to changing product requirements: gasoline for automobile, petrochemicals as building block for clothing and consumer goods, and more environmental friendly processes and products [Katzner et al., 2000]. Petroleum refineries consist of a complex system with multiple operations depending upon the

properties of crude oil to be refined and the desired products. For these reasons, no two refineries are alike.

Crude oil is first distilled, and then it goes through more complex refining processes for further conversion into valuable products. The most important distillation processes are atmospheric distillation and vacuum distillation. Crude oil processed in the petroleum refinery is transformed into more than 2500 refined products including liquefied petroleum gas, gasoline, kerosene, aviation fuel, diesel fuel, fuel oils, lubricating oils and petrochemical feedstock [Benyahia et al., 2006].

Petroleum refining processes and operations can be classified into the following basic areas: physical separation process, chemical conversion process, purification or treating, environmental control, utilities and general facilities which are shown in [Figure 2.2.1](#). Supporting operations may include wastewater treatment, sulphur recovery, additive production, blow down system, heat exchanger cleaning, blending of products and storage of products.

Some of the major crude oil refining processes are mentioned below:

Fractional distillation: In this process, heavier and lighter distillates are separated from which gasoline, fuel oil, wax and lubricants are produced.

Cracking: In this process, decomposition of crude petroleum and their fractions take place because of heating.

Treating: In this process, the quality of product is improved and undesired components are removed.

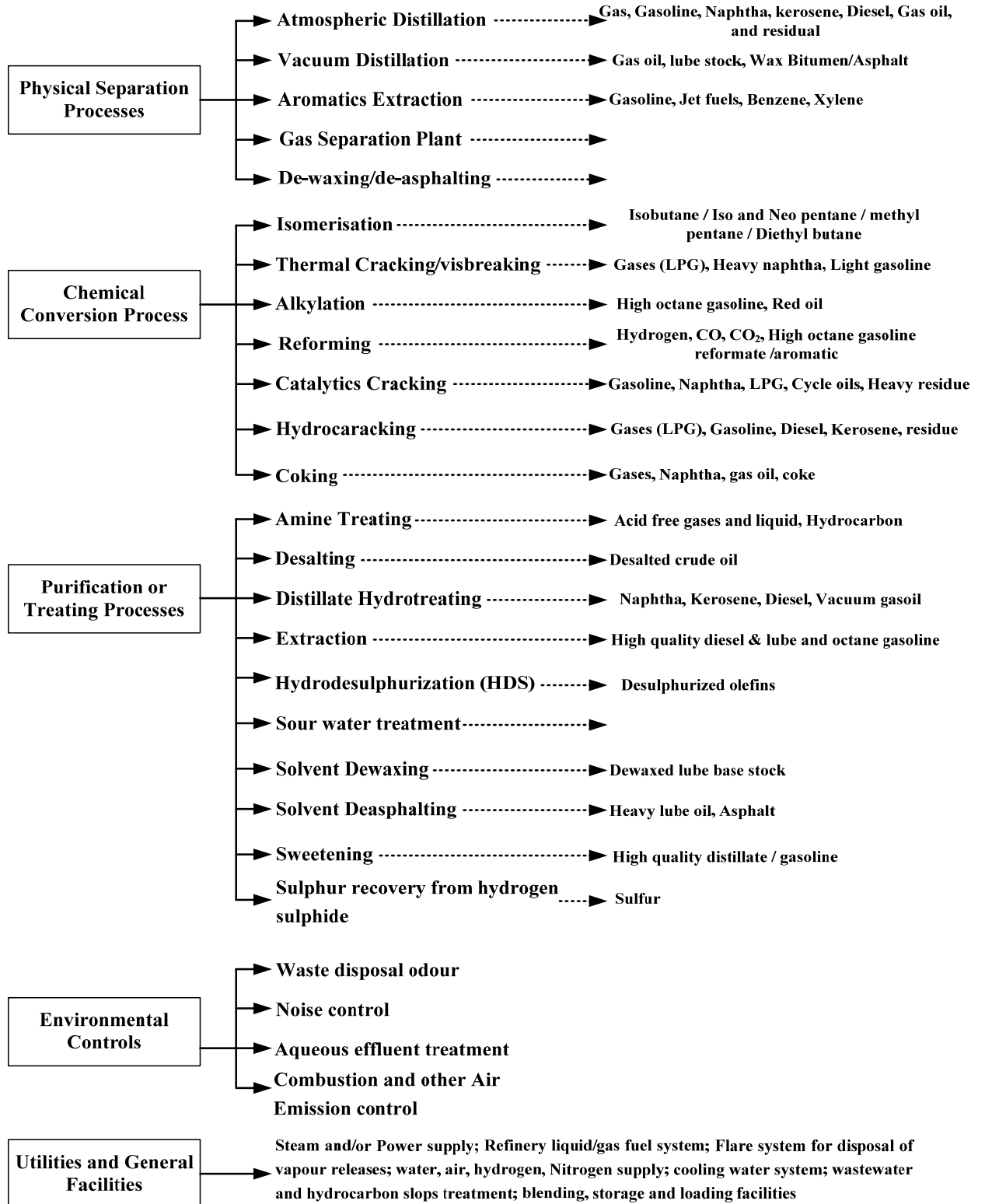


Figure 2.2.1. Overview of petroleum refinery.

Table 2.2.1. Major unit operations typically involved in petroleum refinery.

Process	Description
Desalting	In this process, salts like chlorides of Ca, Mg, Na, and impurities in crude oil are separated to avoid corrosion, plugging, and fouling of process equipment used in refining process and also to prevent poisoning of catalysts in processing units.
Atmospheric distillation	Desalted crude oil is fed into distillation column for the first thermal conversion process. Pressure of the feed is kept slightly above atmospheric. At successively higher points on the tower, various major products including heating oil, lubricating oil, gasoline, kerosene, and uncondensed gases (which condense at lower temperatures) are drawn off from different height of distillation and heavy fuel oil or asphalt residue is taken out from the bottom.
Vacuum distillation	Distillation of the residue (which cannot be distilled) from atmospheric distillation column to make it suitable for catalytic cracking or hydrocracking for manufacturing of lubricating oils, and a residue (which is blown further to form bitumen).
Thermal cracking/ visbreaking	Cracking of heavy residue products from atmospheric and vacuum distillation column under high temperature without use of any catalyst. Thermal cracking or visbreaking, uses heat and pressure to break large hydrocarbon molecules into smaller and lighter molecules. In thermal cracking, heavy gas oils and residue from the vacuum distillation process are typically the feedstocks. The feedstock is heated in a furnace or other thermal unit up to 400°C and then fed to a reaction chamber that is kept at a pressure of 140 psi (gauge). Visbreaking is used to reduce the pour point of waxy residues and to reduce the viscosity of residues used for blending with lighter fuel oils.
Coking	Coking is a cracking process used primarily to reduce refinery production of low-value residual fuel oils to transportation oils, such as gasoline and diesel.

Catalytic cracking	Catalytic cracking uses heat, pressure, and a catalyst to break complex hydrocarbons into simpler molecules in order to increase the quality and quantity of lighter, more desirable products and decrease the amount of residuals. The catalysts used in refinery cracking units are typically solid materials like (zeolite, aluminum hydrosilicate, treated bentonite clay, fuller's earth, bauxite and silica-alumina) that come in the form of powders, beads, pellets or shaped materials.
Catalytic hydrocracking	Catalytic hydrocracking converts the feedstocks (fractions that are more difficult to crack and cannot be cracked effectively in catalytic cracking units) into gasoline, high octane isoparaffins, jet fuels, diesel fuels, low-pressure gas, and low-sulphur fuel oil. In hydrocracking temperature ranges from 205 to 428°C, which is still lower than the temperature required for catalytic cracking; whereas the pressure is much higher, ranging from 100 to 2,000 psi.
Hydrotreating/ hydroprocessing	Hydrotreating/hydroprocessing are similar processes used to remove impurities such as sulphur, nitrogen, oxygen, and trace metal impurities that may deactivate process catalyst.
Alkylation	Alkylation is used to produce a high octane gasoline blending stock from isobutane formed primarily during catalytic cracking and coking operations but also from catalytic reforming, crude distillation, and natural gas processing. Alkylation reactions occur in presence of a catalyst at controlled temperatures and pressures. The different catalysts used in this process are AlCl ₃ , H ₂ SO ₄ and HF.
Isomerization	Isomerization is used to alter the arrangement of molecule without adding or removing anything from original molecule. Typically, paraffins (C ₄ H ₁₀ and C ₅ H ₁₂) are converted to isoparaffins having a much higher octane number.
Polymerization	Polymerization in the petroleum industry is the process of converting light olefin gases including ethylene, propylene and butylene into hydrocarbons of higher molecular weights and higher octane numbers that can be used

	as gasoline blending stocks. Polymerization combines two or more identical olefin molecules to form a single molecule with the same elements in the same proportions as the original molecules. The reaction occurs at a temperature of 149-232°C and at a pressure of 150-1200 psi.
Catalytic reforming	Catalytic reforming uses catalytic reactions to process primarily low octane heavy straight run (from CDU) gasoline and naphtha into high octane aromatics. Feedstocks to the catalytic reforming processes are usually hydrotreated first to remove sulphur, nitrogen, and metallic contaminants.
Solvent extraction	Solvent extraction uses solvents to dissolve and remove aromatics from lube oil feedstocks, improving viscosity, oxidation resistance, color, and gum formation. This process also helps to prevent corrosion, protect catalyst in subsequent processes, and improve finished products by removing unsaturated, aromatic hydrocarbons from lubricant and grease stocks. The solvent extraction process separates aromatics, naphthenes, and impurities from the product stream by dissolution or precipitation.
Dewaxing	Dewaxing is a process of removing wax from lube oil, generally after deasphalting and solvent extraction so as to produce lubricants with low pour point and to recover wax for further processing. Usually two solvents toluene and methyl ethyl ketone are used in this process.
Propane deasphalting	Deasphalting is a solvent extraction process for removing asphalt or resins from viscous hydrocarbons to produce feedstocks for lube oil refining or catalytic cracking processes.
Merox extraction	This process is used for removal of mercaptans or for conversion of mercaptans into disulphide using a catalyst. The process is a combination of merox extraction and sweetening.
Hydro desulphurization	It is done to reduce the sulphur content of raw kerosene.

Sources: Mall, 2006; Prasad, 2000; Pachouri, 2008

Hydrocarbons are vaporized at different temperatures depending on their boiling points and further collected at various heights in the distillation column. The boiling points of some of the petroleum products obtained from atmospheric distillation column are petroleum gas (20°C), naphtha (40°C), petrol (70°C), kerosene, jet fuel (120°C), diesel (200°C), lubricant (300°C) and furnace oil (370°C). Solid petroleum coke collects at the bottom after the liquid fractions are removed. Various catalytic or thermal conversion processes are further used for converting the distilled fractions into valuable products. Catalytic reformer is an important conversion process where the heavy naphtha, produced in the crude distillation unit, is converted to gasoline. In the fluid catalytic cracker (FCC), the distillate of the vacuum distillation unit is cracked to form valuable products. Some conversion processes like hydrocracking is used to produce more lighter products from the heavy bottom products. Finally, all products may be treated to upgrade the product quality. Some of the unit operations typically involved in petroleum industries are briefly discussed in [Table 2.2.1](#).

2.3 GENERATION OF WASTEWATER IN PETROLEUM REFINERIES

The petroleum refining industry is a complex and an integrated industry that includes a large variety of processes and products. Petroleum refineries use tremendous amount of water and steam in a variety of processes ranging from crude oil desalting to atmospheric and vacuum distillation units, visbreaking, FCC units, cokers, hydroprocessing units, and cooling towers. These units are responsible for the

generation of wastewater containing high amount of oily sludge, variety of toxic organic and inorganic substances and viscous residues [Coelho et al., 2006].

In the petroleum industries, water is also used in hydrometallurgy where many suspended solids as well as large varieties of metals get added up in the wastewater [Bagajewicz, 2000]. Petroleum refineries use relatively large volumes of water for cooling systems. Cooling system generate around 3.5-5 m³ of wastewater generated per ton of crude processed [<http://www.lenntech.com/petrochemical.htm#ixzz2LocyhxhN> (accessed 23.02.13)]. Cooling water typically does not come into direct contact with process oil streams, and therefore, contains less contaminant than process wastewater.

Table 2.3.1 gives the details of amount of wastewater generated during refining process. Figure 2.3.1 shows the details of wastewater generated during refinery process.

Refineries generate polluted wastewaters containing high biochemical oxygen demand (BOD) and chemical oxygen demand (COD), oil, benzene, benzo-pyrene, heavy metals like chromium, lead, etc. [Chen et al., 2003; Zhao et al., 2006].

Refineries also generate solid wastes and sludge (ranging from 3 to 5 kg per ton of crude processed), 80% of which may be considered hazardous because of the presence of toxic organics and heavy metals. If these wastes are not treated to the desired degree, the pollutants reach the water course and bring out a number of changes in the water quality of the receiving water, which ultimately renders the water unsafe for aquatic life, domestic and industrial use.

Table 2.3.1. Typical material outputs from selected refining processes.

Process	Process wastewater	Residual wastes generated
Crude oil desalting	Flow = 2.1 Gal/Bbl. Oil, H ₂ S, NH ₃ , phenol, high level of suspended solids, dissolved solids, high BOD, high temperature	Crude oil/desalter sludge (iron rust, clay, sand, water, emulsified oil, wax, and metals)
Atmospheric distillation	Flow = 26.0 Gal/Bbl. Oil, H ₂ S, NH ₃ , suspended solids, chlorides, mercaptans, phenol, elevated pH	Typically, little or residual waste generated
Vacuum distillation	Flow = 26.0 Gal/Bbl. Oil, H ₂ S, NH ₃ , suspended solids, chlorides, mercaptans, phenol, elevated pH	Typically, little or residual waste generated
Thermal cracking/ visbreaking	Flow = 2.0 Gal/Bbl. Oil, H ₂ S, NH ₃ , suspended solids, phenol, high pH, BOD, COD	Typically, little or residual waste generated
Coking	Flow = 1.0 Gal/Bbl. High pH, H ₂ S, NH ₃ , suspended solids, COD	Coke dust (carbon particles and hydrocarbons)
Catalytic cracking	Flow = 15.0 Gal/Bbl. High levels of oil, suspended solids, phenol, cyanides, H ₂ S, NH ₃ , high pH, BOD, COD	Spent catalyst (metals from crude oil and hydrocarbons), spent catalyst from electrostatic precipitators (aluminium silicate and metals)
Catalytic hydrocracking	Flow = 2.0 Gal/Bbl. High COD, suspended solids, H ₂ S, relatively low levels of BOD	Spent catalyst fines (metals from crude oil and hydrocarbons)
Hydrotreating/	Flow = 1.0 Gal/Bbl.	Spent catalyst fines (aluminium

Hydroprocessing	H ₂ S, NH ₃ , high pH, phenols, suspended solids, BOD, COD	silicate and metals)
Alkylation	Low pH, suspended solids, dissolved solids, COD, H ₂ S, spent sulphuric acid.	Neutralized alkylation sludge (sulphuric acid or calcium chloride hydrocarbons)
Isomerization	Low pH, chloride salts, caustic wash, relatively low H ₂ S and NH ₃	Calcium chloride sludge from neutralized HCl gas
Polymerization	H ₂ S, NH ₃ , caustic wash, mercaptans and NH ₃ , high pH	Spent catalyst containing H ₃ PO ₄
Catalytic reforming	Flow = 6.0 Gal/Bbl. High level oil, suspended solids, COD, relatively low H ₂ S	Spent catalyst fines from electrostatic precipitators (alumina silicate and metals)
Solvent extraction	Oil and solvents	Little or no residue wastes generated
Dewaxing	Oil and solvents	Little or no residue wastes generated
Propane deasphalting	Oil and propane	Little or no residue wastes generated
Merox treating	Little or no wastewater generated	Spent merox caustic solution, waste oil-disulphide mixture
Wastewater treatment	Not applicable	API separator sludge (phenols, metals, and oil), chemical precipitation sludge (chemical coagulants, oil), DAF floats, biological sludges (metals, oils, and suspended solids), spent lime

Source: Assessment of Atmospheric Emissions from Petroleum Refining, Radian Corp., 1980; Petroleum Refining Hazardous Waste Generation, U.S. EPA, Office of Solid Waste, 1994.

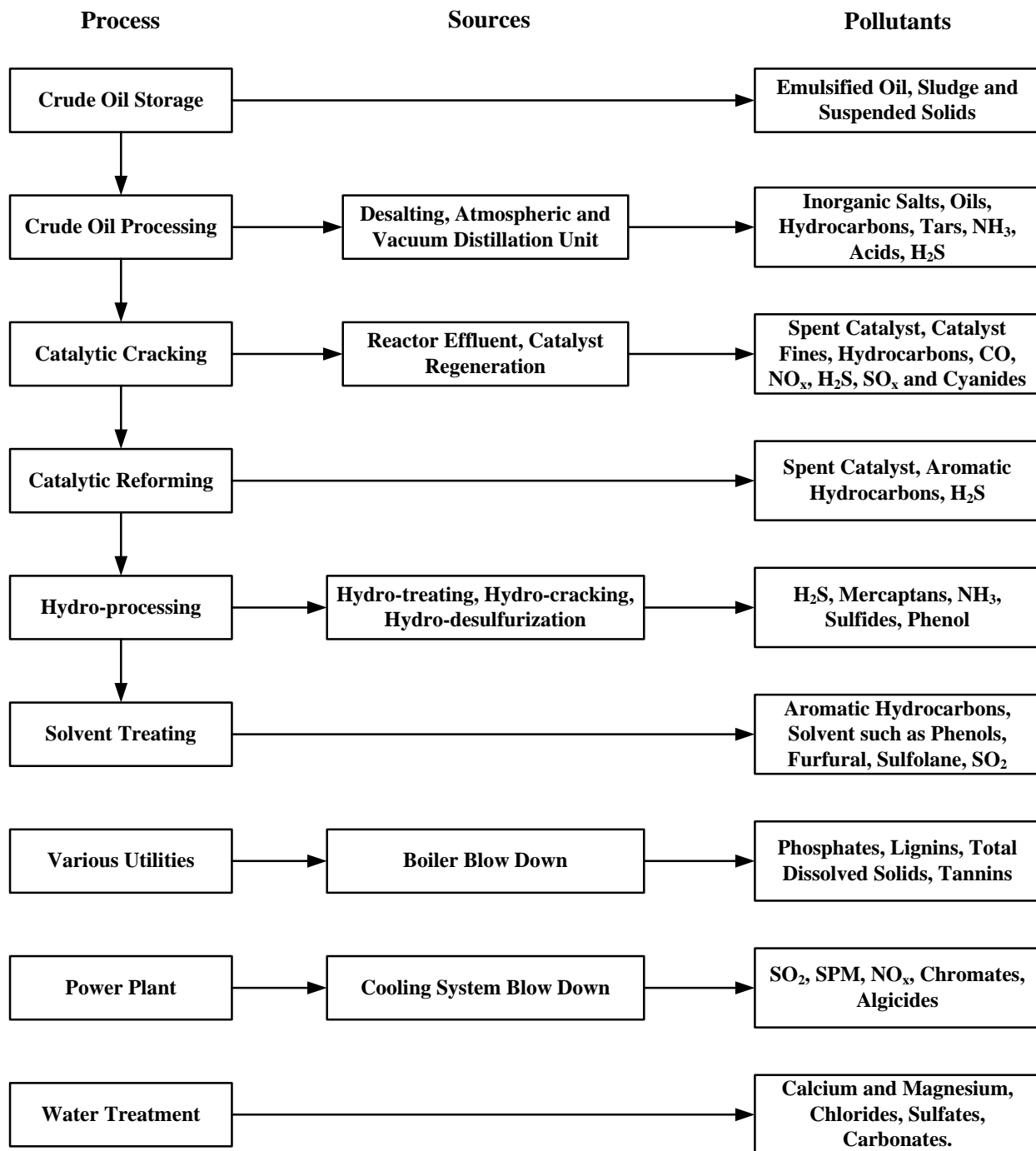


Figure 2.3.1. Sources of pollutants from petroleum refinery process.

Sources: Gomkale et al., 1996.

2.4 MANAGEMENT OF WASTEWATER AND TREATMENT STRATEGIES

Waste management comprises of quick identification of the waste generated, efficient collection and handling, optimal reuse and recycling, effective disposal leaving no environmental problems.

Petroleum refineries consist of multiple unit operation with complex systems which depend on the type of crude oil refined and the desired products. Depending on the size, crude, products and complexity of operations, a petroleum refinery can be a large consumer of water. A large portion of the water used in a petroleum refinery can be continuously recycled with in a refinery. To reuse, recycle and discharge the water from the refinery, wastewater should be treated to its discharge limit set by pollution control agency.

Refinery wastewaters often require a combination of treatment methods to remove oil and contaminants before discharge. Separation of different streams, such as storm water, cooling water, process water, sanitary, sewage, etc., is essential for minimizing treatment requirements. A typical system may include sour water stripper, gravity separation of oil and water, American petroleum institute (API) separator, dissolved air flotation (DAF), biological treatment and clarification. A final polishing step using filtration, activated carbon, or chemical treatment may also be required. Sludge treatment is usually performed using land application (bioremediation) or solvent extraction followed by combustion of the residue or by use for asphalt, where ever feasible. In some cases, the residue may require stabilization prior to disposal to reduce the leachability of toxic metals. Oil is recovered from slops using separation

techniques such as gravity separators and centrifuges. [Figure 2.4.1](#) shows the management of wastewater generated in the petroleum refinery

The unit operation used in wastewater treatment plant are classified as physical (air flotation, oil coalescing, evaporation, filtration, etc.), biological, thermal and chemical (precipitation, coagulation, ion exchange, etc.) treatment methods.

Primary wastewater treatment consists of separation of oil, water, and solids in two stages. During the first stage, an API separator, a corrugated plate interceptor, or other separator design is used. Wastewater moves very slowly through the separator allowing free oil to float to the surface and be skimmed off and solids to settle to the bottom and be scraped off to a sludge collecting hopper. The second stage utilizes physical or chemical methods to separate emulsified oils from the wastewater. Physical methods may include the use of a series of settling ponds with a long retention time, or the use of DAF. In DAF, air is bubbled through the wastewater, and both oil and suspended solids are skimmed off from the top. Chemicals, such as ferric hydroxide or aluminum hydroxide, can be used to coagulate impurities into a froth or sludge which can be more easily skimmed off from the top. As removal of oil is achieved wastewater is fed to biological treatment system.

Secondary treatment is the heart of the treatment plant which is helpful in removing COD, suspended solids, organic matter and nutrients (nitrogen, phosphorus or both) from the wastewater which make the effluent quality within the standard limit. Biological treatment is the backbone of the overall treatment. Biological treatment processes can be considered as clean technology for treating wastewater from oil industry as it generates no secondary pollutants [[Jou et al., 2003](#); [Bertin et al., 2007](#); [Gasim et al., 2010](#); [Bhattacharya et al., 2005](#)]. At present, most of the industries have

biological processes (activated sludge units, trickling filters, and rotating biological contactors) as the secondary treatment process which requires huge installation cost, large installation area and high maintenance, thus requiring some modification in the process so that all these deficiencies can be eliminated. Combination of biological process and electrocoagulation, adsorption, etc. are useful to reduce the cost of treatment and increase the efficiency of wastewater treatment plant.

Some refineries employ an additional stage of wastewater treatment called tertiary treatment process for polishing to meet discharge limits. The polishing step can involve the use of activated carbon, anthracite coal, or sand to filter out any remaining impurities such as biomass, silt, trace metals and other inorganic chemicals, as well as any remaining organic chemicals. [Figure 2.4.2](#) describes the typical wastewater treatment of petroleum refinery.

Characterization of the wastewater discharged from a typical petroleum refinery in India containing a variety of objectionable and toxic organic and inorganic substances is shown in [Table 2.4.1](#).

Table 2.4.1. Characteristics of wastewater and pollution/toxicants discharged from petroleum refineries in India.

Effluent characteristics	Value	Pollution/toxic constituents
Flow, L/kg oil	1.5	Free oil (2,000-3,000 mg/L)
pH	6.8-7.2	Emulsified oil (80-120 mg/L)
Suspended solids, mg/L	200-400	H ₂ S and RSH (10-220)
BOD, mg/L	100-300	Phenols (10-100 mg/L)
COD, mg/L	400-600	Ammonium and chromium if cooling water is also mixed with process water.
BOD load, g/unit product	0.3	

Sources: Pauchouri, 2008

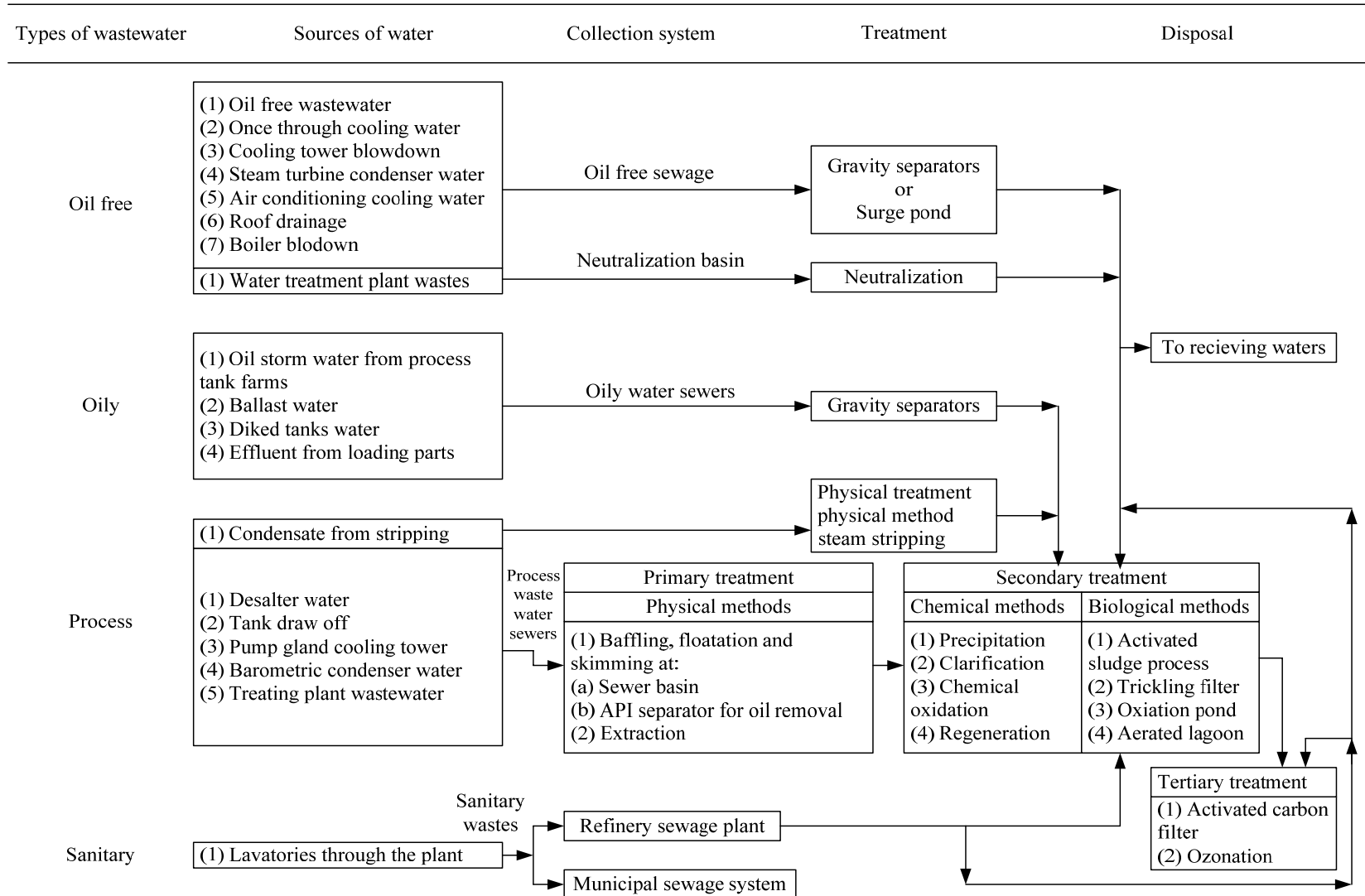


Figure 2.4.1. Management of wastewater generated in petroleum industry.

Sources: Mall, 2006; Pachouri, 2008

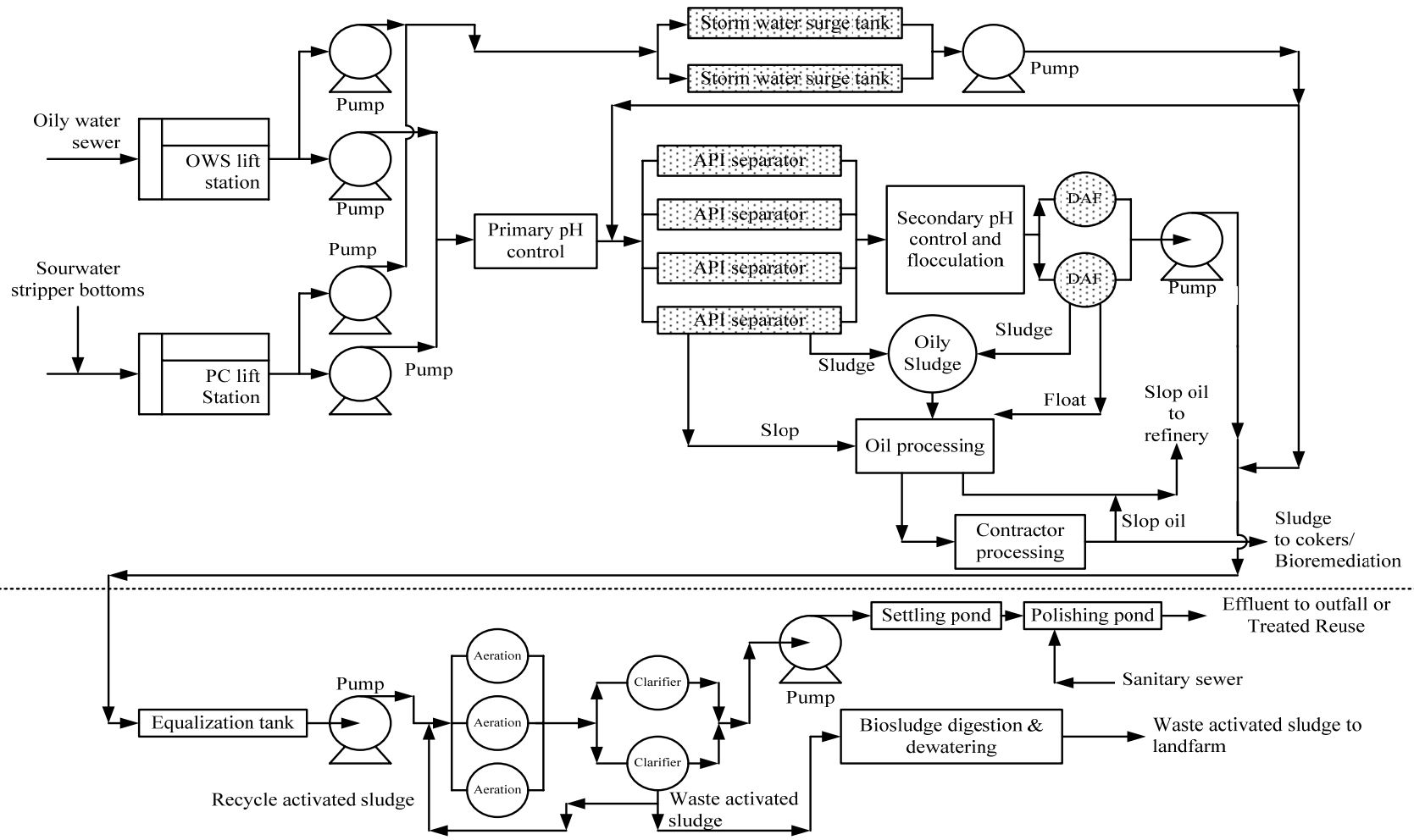


Figure 2.4.2. Typical petroleum refinery wastewater treatment plant
 Sources: Mall, 2006; Pachouri, 2008

LITERATURE REVIEW

3.1 GENERAL

Petroleum refineries use large amount of water to transform crude oil into valuable refined products such as LPG, gasoline, kerosene, etc. However, while processing the crude oil, 80% of used water goes as waste stream since water does not go into the final product. These waste streams are sent to common wastewater treatment unit of the refinery [Dorn, 1998; IPEICA, 2010]. This petroleum refinery wastewater (PRW) contains oil and grease along with various toxic compounds (such as heavy metals, phenol and other associated compounds such as catechol, resorcinol, etc.) which can cause serious problems to ecosystem, if the treatment processes is ineffective [Beg et al., 2001]. Typical PRW treatment is done in three steps. During primary treatment, physicochemical separation is done in which free oil, suspended solids and colloidal materials are removed. However, emulsified or dissolved oil still remains in the PRW and is removed during the secondary treatment [Shariati et al., 2011; Hasan et al., 2011]. Primary, mechanical and physicochemical treatment (flotation and coagulation) remove around 10% of the suspended matter and 20–30% of oil and grease from PRW [Stepnowski et al., 2002]. Most of the treatment of PRW takes place during secondary treatment. Secondary treatment methods consist of aerobic and/or anaerobic biological oxidation, settling, etc. After that, tertiary treatment is done so as to remove remaining recalcitrant pollutants. Various researchers have used

various treatment methods for the treatment of various types of petroleum or petrochemical industry wastewaters.

Industrial units such as petrochemical, petroleum refinery, etc. discharge phenol and its derivatives such as catechol and resorcinol in their effluents. Various research efforts have been made to abate phenolic wastewater using various treatment methods like adsorption, ultrafiltration, catalytic wet oxidation, etc. [Khieu et al., 2009; Cordero et al., 2008; Rengaraj et al., 2002; Cam et al., 2011; Purkait et al., 2005; Alam et al., 2007; Sharma et al., 2010c]. Biological degradation of these substrates is little rigid since it is highly toxic to the environment.

Present work focuses on treatment of PRW and phenolic compounds by adsorption, sequential batch reactor (SBR) and electrocoagulation (EC) methods. This chapter presents an overview of the research work available in the open literature for the treatment of wastewater by adsorption, SBR and EC method. Various sections in this chapter focus on the treatment of PRW, phenol and associated compounds such as catechol and resorcinol which are commonly found in PRW. Areas where further research and attention are required have been identified in the last section of this chapter.

3.2 ADSORPTION

Adsorption process is considered an attractive process that is used as a tertiary treatment method. Adsorption process is one of the efficient methods for removal of various types of contaminants from effluent, especially for moderate and low concentrations effluents and has attracted considerable interest recently.

In most of the industries, commercial granular activated carbon (GAC) is used as an adsorbent because of its extended surface area, microporous structure, high adsorption capacity and high degree of surface reactivity. However, its high initial cost and the need for a costly regeneration system makes it economically less viable as an adsorbent [Abdelwahab et al., 2005; Suresh et al., 2011a]. Because of the expensive nature of commercial adsorbents like activated carbon, many investigators have done research on more economic and efficient adsorbent such as those which can be obtained as an agricultural or industrial wastes/by-products like rice husk ash (RHA), bagasse fly ash (BFA), coconut shell carbon, peat, chitin and chitosan, etc. [Mall et al., 1996; Allen et al., 2004; Rengaraj et al., 2002; Armagan et al., 2003; Smith et al., 1993; Kim et al., 1997; Kumar et al., 2003; Wagner et al., 2001; Toth, 2002; Ahmaruzzaman, 2008; Soto et al., 2011]. Some of the studies on the treatment of wastewater containing metals, dyes and other compounds by adsorption are given in Table 3.2.1.

Mall et al. [1996] suggested RHA is an economical adsorbent for the treatment of wastewater and effluents. RHA can be used as an adsorbent because of its low cost and availability in abundance. Rice husk is a byproduct of the rice mill and is used as supplement fuel in rice husk-fired boilers. RHA has good porosity, high amount of silica and a number of functional groups on its surface which makes it good adsorbent. Besides its availability in abundance, it is highly economical as the only cost involved is transportation cost from the place of generation to its place of use as an adsorbent [Aksu and Yener, 2001]. Consequently, various researchers have used RHA for adsorptive removal of various types of adsorbates like metal ions, dyes and organics [El-Said et al., 2010; Lakshmi et al., 2009; Mane et al., 2007; Srivastava et al., 2006; Srivastava et al., 2009a].

Sharma et al. [2010a] had studied removal of methylene blue using pretreated rice husk (RH) and RHA. Adsorption treatment process was performed by adjusting the pH around 7, equilibration time of 30 min, and system temperature of 30°C. The thermodynamic study indicated that the adsorption of dyes was spontaneous and endothermic. Adsorption data were fitted to Langmuir and Freundlich isotherm models. The former model achieved best fit with the experimental data and its calculated maximum monolayer adsorption capacity have a value of 1347.7 mg/g for adsorption on RH and 1455.6 mg/g for adsorption on RHA at a temperature of 323°C. RHA is very effective than rice husk for phenol removal. RHA obtained from a rice mill in Kenya was used for removal of some phenolic compounds in water [Damaris et al., 2002]. Richard et al. [2009] studied the adsorption of complex phenolic compounds (phenols, chlorophenols and nitrophenols) on active charcoal and the adsorption capacity and isotherms study was done.

Various researchers have used various types of adsorbents for the removal of phenol and associated compounds like catechol and resorcinol. Table 3.2.2 summarizes adsorption studies on the removal of phenol, catechol and resorcinol from aqueous solution using various types of adsorbents. Khanna and Malhotra [1977] first examined the potential of fly ash for the removal of phenol. They reported kinetics and mechanism of phenol removal by fly ash and provided useful data in the design of phenol-fly ash adsorption systems. Adsorption of phenol, cresol, and their mixtures from aqueous solutions on activated carbon and fly ash were compared [Kumar et al., 1987]. The effects of contact time and initial solute concentration have been studied and isotherm parameters were evaluated. Freundlich isotherm was more suitable for all the systems investigated.

Sun et al. [2005] studied the adsorptive removal of resorcinol and catechol from aqueous solution by aminated hypercrosslinked polymers (AH-1, AH-2 and AH-3). Huang [2009] prepared a hypercrosslinked polymeric adsorbent HJ-1 from chloromethylated poly(styrene-co-divinylbenzene) (PS) and its several factors on adsorption, adsorption dynamics and adsorption equilibriums for phenol and p-cresol in aqueous solution were studied. Huang et al. [2009] developed an easily water-compatible hypercrosslinked resin HJ-1 for adsorption of catechol and resorcinol in aqueous solution. Kaleta [2006] used modified clarion clay and clinoptylolite as adsorbents for the removal of phenolic compounds from aqueous solution. Activated carbon showed an adsorptive capacity of 13.22 g/kg, modified Clarion clay 1.24 g/kg, and clinoptylolite 0.23 g/kg.

The removal of phenol and 4-nitrophenol using BFA was also reported by Gupta et al. [1998]. They concluded that the adsorption data followed both the Langmuir and Freundlich isotherms and adsorption process as exothermic in nature. Srivastava et al. [2006c] had reported adsorption behavior of phenol on carbon rich BFA and activated carbon-commercial grade (ACC) and laboratory grade (ACL). Optimum conditions for phenol removal were attained to be $pH_0 \approx 6.5$, adsorbent dose ≈ 10 g/L of solution, initial concentration of phenol ≈ 100 mg/L and equilibrium time ≈ 5 h. Adsorption of phenol followed pseudo-second order kinetics with the initial sorption rate for adsorption on ACL being the highest followed by those on BFA and ACC. Redlich–Peterson isotherm was found to best represent the data for phenol adsorption on all the adsorbents. Richard et al. [2009] studied the adsorption of

complex phenolic compounds (phenols, chlorophenols and nitrophenols) on active charcoal and the adsorption capacity and isotherms study were done.

Phenolic compounds are usually present in various forms, therefore, it is important to understand the competitive effects that can take place in such systems. Since, actual effluents generated in industries such as petroleum refineries contain several phenolic compounds; therefore, equilibrium adsorption data for closely related binary and ternary compounds is of utmost importance for the design of adsorption systems. Unfortunately, very few researcher have studied the competitive adsorption of phenol and its derivatives and its associated compounds in adsorption systems [Mondal and Balomajumder, 2007; Srivastava et al., 2008a,b; Kumar et al.,2011; Aghav et al., 2011].

Kumar et al. [2011] performed the modeling studies on simultaneous adsorption of phenol and resorcinol onto granular activated carbon from multi-component aqueous solution. Suresh et al. [2011b] studied the simultaneous adsorptive removal of phenol and aniline as well as phenol and nitro-phenol from aqueous solutions using GAC as an adsorbent. Suresh et al. [2011b] used Taguchi's method design to understand the simultaneous adsorptive removal of phenol with aniline and nitrophenol from aqueous solutions using GAC. They performed 27 set of experimental run by varying four process parameter. At the optimum condition $T = 45^{\circ}\text{C}$, $m = 10 \text{ g/L}$, $t = 660 \text{ min}$, 83.1% phenol and 76.2% aniline removals were observed for phenol–aniline system, whereas for phenol–aniline system, 99% phenol and 98% nitrophenol removals were observed.

Table 3.2.1. Studies on the treatment of wastewater containing metals, dyes and other compounds by adsorption.

Wastewater type	Adsorbent	Adsorbate	C ₀ (mg/L)	Optimized condition	Percentage reduction	Model fitted	Reference
Pulp and paper mill	PAC & BFA	-	COD =2380	PAC pH=3 Dose =3 g/L BFA pH =4 Dose= 2 g/L t = 120 min	PAC COD=80% Color=90% BFA COD=50% Color=55%	-	Srivastava et al., 2005
Synthetic wastewater	RHA	Mercury (II)	100	pH=6.0 Dose=20 g/L t =3h	98%	Langmuir	Tiwari et al., 1995
Synthetic wastewater	RHA	Cd(II), Ni(II), Zn(II)	100	pH=6.0 Dose=10 g/L t =60 min	>98%	Taguchi's method	Srivastava et al., 2008b
Synthetic wastewater	RH	Chromium (VI)	10-70	pH =2.0 Dose=20 g/L t =180 min	71.0%	Freundlich and D-R models	Bansal et al., 2009
Synthetic wastewater	RHA & MRHA	Chromium (VI)	10	pH =2.0 Dose=40 g/L Contact time=3 h	RHA = 59.12% MRHA = 81.39%	Freundlich	Wongjunda and Saueprasearsit, 2010

Wastewater type	Adsorbent	Adsorbate	C ₀ (mg/L)	Optimized condition	Percentage reduction	Model fitted	Reference
Synthetic wastewater	BFA	Orange-G (OG) and Methyl Violet (MV) dyes	-	Time=4 h OG pH=4; Dose=2 g/L MV pH =9; Dose=4 g/L	> 90 %	OG - Freundlich isotherm MV- R-P isotherm	Mall et al., 2006
Synthetic wastewater	RHA	Indigo Carmine dye	20-1000	pH=5.4 Time=8 h Dose=10 g/L	>90%	R-P and Freundlich isotherm	Lakshmi et al., 2009
Synthetic wastewater	RHA & GAC	Pyridine	600	pH=6.2 Dose : GAC=30 g/L BFA=50 g/L t =5h	RHA 79% GAC 85%	Redlich and Peterson (R-P) isotherm	Lataye et al., 2008
Synthetic wastewater	BFA & GAC	Quinoline	100	pH=5.5 Dose: GAC=5 g/L BFA=10 g/L t =8h	BFA 84% GAC 96%	Redlich and Peterson (R-P) isotherm	Rameshraj et al., 2012
Synthetic wastewater	BA, AC & WC	Phenol	30-50	-	BA=90% AC=98% WC=90%	Freundlich	Mukherjee et al., 2007

AC-activated charcoal; RHA-rice husk ash; MRHA-modified rice husk ash; RH-rice husk; GAC-granular activated carbon;

WC-wood charcoal; BFA-bagasses fly ash; PAC-poly aluminum chloride; *t*-contact time

Table 3.2.2. Studies on the treatment of phenolic by adsorption.

Adsorbent	Adsorbate	t (h)	K_F (mg/g)/(mg/L) ^{1/n}	1/n	q_m (mg/g)	K_L (L/mg)	Reference
PAC	P	10	0.60	0.43	64	0.24	Tancredi et al., 2004
GAC	P	48	0.17	0.56	46	0.06	Tancredi et al., 2004
BFA	P	24	4.5782	0.3678	23.832	0.0885	Srivastava et al., 2006c
ACC	P	24	2.4143	0.5031	30.2187	0.0291	Srivastava et al., 2006c
ACL	P	24	7.3771	0.3146	24.6458	0.2391	Srivastava et al., 2006c
GAC	C	48	42.40	0.205	143.47	0.08	Kumar et al., 2003
ACC	C	24	0.015	0.23	0.0013	0.000007	Bayram et al., 2009
GAC	C	48	1.49	0.81	238.1	0.004	Blanco-Martinez et al., 2009
CTAB-B	C	4.16	33.02	-	53.41	0.003	Shakir et al., 2008
TiO2	C	2	-	0.337	11.172	0.0589	Arana et al., 2007
GAC-SAB	R	10	23.43	0.877	49.75	0.074	Mondal and Balomajunder, 2007
GAC	R	48	34.83	0.226	142.8	0.047	Kumar et al., 2003
CZ	R	48	-	-	0.880	-	Mohamed et al., 2006
GAC	R	10	34.52	0.236	140.72	0.046	Mondal and Balomajunder, 2007
TiO2	R	2	-	0.703	7.870	0.0089	Arana et al., 2007

GAC-granular activated carbon; BFA-Bagasses fly ash; PAC-poly aluminum chloride; ACC-activated carbon cloth; CTAB-B-cetyltrimethylammonium bromidemodified bentonite; HJ-1-hypercrosslinked resin; SAB-simultaneous adsorption biodegradation; P-phenol; C-catechol; R-resorcinol.

3.3 SEQUENTIAL BATCH REACTOR

Biological treatment is one of the most widely used method for wastewater treatment because of the fact that it mineralizes the pollutants and generates no secondary pollutants [Bertin et al., 2007; Bhattacharya et al., 2005]. Stringfellow and Alvarez-Cohen [1999] reported biological wastewater treatment for the removal of dissolved oil in petroleum refining effluent. Puyol et al. [2009] studied wide range of HRT for UASB treatment method which was found to be highly effective for the treatment of medium and high-strength wastewaters. Various researchers have also reported use of biological treatment technology for PRW [Viero et al., 2008; Shariati et al., 2011; Rastegara et al., 2011; Kutty et al., 2011; Mizzouria and Shaabana, 2013]. However, the efficiency of biological treatment processes reduces with an increase in concentration of toxic compounds in wastewater. Therefore, these compounds need to be removed before wastewater reaches biological treatment process.

Sequential batch reactor (SBR) is a biological treatment method which has gained more importance as compared to other biological treatment methods because of its inherent flexibility in cycle time which can handle shock load of influent characteristics, easy to operate and requires less area for operation. SBR treatment system consists of five sequencing operation: fill phase in which reactor is fed with wastewater; react phase in which the organic matter degradation occurs; settle phase in which biomass is allowed to settle; draw phase in which wastewater is withdrawn from reactor to retain the biomass and idle phase [Dague et al., 1992]. SBR has been originally used for reduction of COD from various types of wastewaters [Danesh and

Oleszkiewicz, 1997; Carucci et al., 1997; Colunga and Martinez, 1996; Colmenarejo et al., 1998]. Table 3.3.1 gives an overview of application of SBR for the treatment of industrial wastewaters whereas Table 3.3.2 compares operational details of the SBR operation and its efficiency for treatment of various wastewaters.

Various studies have been reported for treatment of phenolic wastewater in SBR. Table 3.3.3 compares SBR studies for removal of phenolic compounds from aqueous solutions. Yu and Gu [1996] evaluated the performance of the two SBRs with aerated fill and unaerated fill treating synthetic phenolic wastewater. At low influent phenol concentrations (e.g. 400 mg/L), SBR with unaerated fill performed better than SBR with aerated fill. However, when the influent phenol concentration was high (e.g. >800 mg/L), phenol accumulated during the fill period in the SBR with unaerated fill became inhibitory to micro-organisms. This led to a reduction in substrate removal efficiency and the growth of dispersed biomass. The selection of fill strategies for the SBR was dependent not only on the wastewater composition and biodegradability, but also on the concentration of toxic organic matters in wastewater. Sarfaraz et al. [2004] conducted studies on the anoxic phenol removal using granular denitrifying sludge in SBR at different cycle lengths and influent phenol concentrations. Results showed that removal exceeded 80% up to an influent phenol concentration of 1050 mg/L at 6 h cycle length, which corresponded to 6.4 kg COD/m³d. Beyond this, there was a steep decrease in phenol and COD removal efficiencies. Tomei et al. [2003] studied the biodegradation kinetics of 4-nitrophenol (4NP) in a lab-scale sequencing batch reactor fed with the compound as the sole carbon source. The experimental results showed that

both long feed phase and high biomass concentration are effective in reducing the substrate concentration peak and then improving the process efficiency. [Sahinkaya and Dilek \[2007\]](#) investigated the biodegradation kinetics of 4-chlorophenol (4-CP) and 2,4-dichlorophenol (2,4-DCP) separately in batch reactors and mixed in SBRs. [Fang et al. \[2006\]](#) investigated removal efficiency of phenol from synthetic wastewater using anaerobic thermophilic condition (55°C). Maximum phenol removal 99% was achieved at HRT 40 h.

[Shariati et al. \[2011\]](#) had used membrane SBR for the treatment of synthetic petroleum wastewater operated at different HRT. [Kutty et al. \[2011\]](#) employed six different SBR for the treatment PRW having COD concentration of approximately 500-750 mg/L. Experiments were performed at various anaerobically stirred and aerobic modes with a 24 h cycle in 2 L reactor. Removal efficiency of COD was 91%, 91%, and 88% for aerobic reactor, combined anaerobic-aerobic reactors and aerobic mixed, respectively.

Table 3.3.1. Brief review on industrial application of SBR.

Industry/ Application	Experimental Setup/ Waste properties	Parameters observed	Result/ Conclusion/ Recommendations	Reference
Wastewater from pulp and paper mill.	The Laboratory scale reactor consists of four 4 L reactors of acrylic boards with the use of aquarium type air pump for aeration. Minimum of 2 mg/L of DO level were maintained throughout the experiment. The experiment was performed in a air-conditioned laboratory with temperature of 25 ± 1°C. Wastewater characterized as COD of 1200-1400 mg/L, BOD of 550-790 mg/L, TSS of 200-500 mg/L and pH varies form 6.2-6.6.	Effect of MLSS conc., Effect of Volume exchange rate, Effect of aeration time, Effect of temperature and Effect of cycles per day were studied during the work.	The removal efficiency for COD under the optimized condition was achieved round about 93%. The optimal condition of MLSS conc. at 4500 mg/L, VER at 50%, aeration time for 5 h per cycle, temperature at 30°C and 2 operation cycles per day.	Tsang et al., 2007.
Treatment of synthetic phenolic wastewater.	Two identical SBRs of working volume of 5 L were built and operated with fill, react, settle and draw periods in the ratio of 4:6:1:1 for a cycle time of 12 h. One reactor was aerated during fill and react phase while the other was aerated only in the react phase. The activated sludge seed was obtained from a domestic wastewater treatment plant and acclimatized to the base mix.	The performance of SBR was evaluated for aerated and unaerated fill phase for treating phenol containing wastewater. Effluent phenol and COD conc.	The fill mode had no significant influence on the treatment efficiencies of phenol and COD; The kinetic studies showed that increasing phenol concentration exerted an increasing inhibitory effect on the degradation rate of phenol.	Chan and Lim, 2007.

Industry/ Application	Experimental Setup/ Waste properties	Parameters observed	Result/ Conclusion/ Recommendations	Reference
Landfill leachate.	The investigations were carried out at bench scale in four SBRs operated in parallel. The reactors, with a working volume of 6 L each, and were equipped with a stirrer at regulated rotation speed (36 rpm). The leachate was supplied to the reactors by means of a peristaltic pump for 4 h of the cycle at 0.125 L/h (SBR 1), 0.2 L/h (SBR 2), 0.5 L/h (SBR 3) and 0.75 L/h (SBR 4). Experiments were carried out in four SBRs at HRT of 12, 6, 3 and 2 d.	The aim of this study was to estimate the BOD ₅ and COD removal efficiency & bio mass yield coefficient.	The conclusion of the study was: operational conditions had nearly no effect on the BOD ₅ removal efficiency, but affected the COD removal efficiency;	Kulikowska et al., 2007.
Treatment of municipal solid wastewater	The comparison of SBR with normal working procedure (Control reactor) to the SBR using Zeolite powder to increase the activity of sludge. The reactors used were of 0.3 m diameter and 0.6 m height with an effective volume of 31.1 L. The characteristics of the wastewater used in the study is- SS: 94-212 mg/L; COD: 274-421 mg/L; NH ₄ ⁺ N: 25.5-44.2 mg/L; TN: 33.5-68.7 mg/L; TP: 2.65-4.85 mg/L and pH: 6.67-7.86. The Zeolite concentration was maintained at 1000 mg/L.	The characteristics of both the SBRs in removing COD, TN, NH ₄ ⁺ N and TP; variation of DO in operating cycle; comparison of sludge was under observation during the work.	The addition of Zeolite powder could enhance the activity of the sludge and specific O ₂ utilization rate. The pollutants like COD, TN, NH ₄ ⁺ N and TP could be removed in shorter length of time. The test reactor treats 1.22 times more wastewater as compare to the control reactor.	He et al., 2007.

Industry/ Application	Experimental Setup/ Waste properties	Parameters observed	Result/ Conclusion/ Recommendations	Reference
Landfill leachate	The SBR bioreactor was of plexiglas rectangular in shape with operating volume of 50 L The SBR was operated with the cycle time of 24 h with fill phase 2 h, anoxic phase 2 h, aeration 18 h, settling 1 h, decant and idle period 1 h.	Removal of COD and BOD ₅ ; Removal of N; Change of alkalinity in the SBR system; Cyclic study; Removal effect of the full-scale SBR	The removal efficiencies of COD, BOD ₅ , TN, NH ₄ ⁺ -N were 93.76%, 98.28%, 84.74% And 9.21%, respectively.	Zhou et al., 2006.
Synthetic wastewater	Three identical SBRs were used in the study with anaerobic/aerobic sequence used in order to obtain enhanced biological phosphorus removal. The working volume of the reactor was 4 L. The operating cycle of 14 h was performed.	The aim of this study was to investigate the effect of pure cultures on the enhancement of biological phosphorus removal capability of a SBR.	Complete removal of 20 mg/L PO ₄ -P was achieved within 35 d of operation. The COD removal efficiency was 90% in all reactors.	Sarioglu, 2005.
Synthetic wastewater	Experimental setup involved in this study was consists of Four column of 127 cm height and 5 cm diameter with a working volume of 2.5 L with 20, 15, 10 and 5 min settling time respectively with 5 min for filling and 5 min for decantation and total operating cycle of 4 h. The air flow rate is maintained at 3 L/min.	Effects of settling time on aerobic granulation; effect of settling time on sludge settleability; effect of shift of settling time on aerobic granulation were observed.	The result of the study showed that the granules were successfully cultivated and become dominant only in the reactor which is operated at the smallest settling time i.e. 5 min.	Qin, 2004.

Industry/ Application	Experimental Setup/ Waste properties	Parameters observed	Result/ Conclusion/ Recommendations	Reference
Synthetic wastewater	In this comparative study a lab scale SBR operated under different conditions was consists of a fermenter with a 5 L working volume and it was microprocessor controlled for aeration, pH, agitation and DO.	The comparison of SBRs performance with three different operating schemes i.e. one with three step operation anaerobic (An)/ anoxic (Ax)/ oxic (Ox) ; four step operation (An/Ox/ Ax/Ox) and five step operation(An/Ax/Ox/Ax/Ox)	The most of the COD and ammonium were removed during the first three steps. However, Phosphate-P and nitrate-N removal efficiencies were higher in the five-step operation than with the other alternatives tested.	Kargi and Uygur, 2003.
Petroleum refineries	The experimental setup involved in this study composed of a well mixed SBR with working volume 15 L at 15°C. One third of the reactor is filled with inoculums and 3 L/h of influent flow rate is maintained. The operation cycle from fill to decant phase is of 6 h in which 4.3 h is for react phase and the rest is distributed in other phases. The experiment was repeated twice for accuracy.	The aim of the study was to treat ammoniacal nitrogen present in the waste, where phenol is present as a way to minimize ammoniacal nitrogen as well as phenol.	With this study the observation about the removal of NH_4^+ and phenol was found to be about 95% for different conc. of the above.	Silva et.al., 2002.

Industry/ Application	Experimental Setup/ Waste properties	Parameters observed	Result/ Conclusion/ Recommendations	Reference
Wastewater treatment with phenolic shock loading	This study involves the application of granulated activated carbon with SBR to treat wastewater with phenolic shock loading. Two reactors were used with the total volume of 12 L and operating volume of 10 L each. The adsorbent used was lignite based granular activated carbon with 0.75 mm diameter.	Adsorption characteristics of GAC; Step up shock loading; short term fluctuation and stepwise augmentation was studied during the work.	The results came form different experiment shows that SBR with GAC has high stability to phenol shock loading and could work as a buffer by adsorbing the high strength of influent phenol and as a supporting media for microorganisms.	Vinitnanthar at et al., 2001.
Petrochemical wastewater	The three phase experiment was used for study of different parameters in four reactors of glass cylinder with conical bottom of inside diameter 8.89 cm and capacity of 3.5 L. The working volume of SBRs is 2 L. The flow rate was 2 L/d and 400 mL/d of mixed liquor was wasted. The HRT was maintained 2 d and SRT of 10 d.	Effect of operating conditions, response to an organic shock loading and response to a phenol shock loading was observed during this work.	SBRs with shorter cycle and less amount of sludge wasted resulted in higher level of MLVSS. SBR may have high solid content while SBR reacted well for the phenolic shock loading and degraded phenol for 200 to 950 mg/L to less than 0.1 mg/L.	Hsu, 1986.

Table 3.3.2. Comparison of studies on treatment of various wastewater by sequential batch reactor.

Waste type	Reactor type	Dimension	% Conc. reduction	% COD reduction	% TKN reduction	SVI (mL/g)	HRT (d)	COD loading $\text{g/m}^3 \text{d}$	Reference
Synthetic wastewater	SBAR	I.D \times H (cm): 9 \times 90 Vol: 5.1 L	-	90.6–95.4	-	152	-	1120	Bao et al., 2009
Glucose-synthetic wastewater.	SBR	I.D. \times H (cm): 6 \times 80 Vol: 2.4 L	-	90	-	-	-	1000	Yang et al., 2008
Municipal wastewater. (BPR)	SBR	I.D. \times H (cm): 15 \times 70 Vol: 12 L	90	83.3	-	-	0.6	400	Wang et al., 2008
Resorcinol	SBR	Vol: 2 L	85.81	-	-	252.3	-	-	Sharma et al., 2010b
Palm oil refinery	SBR	Vol: 2 L	-	50	-	< 100	-	1500	Chin and Ng, 1987
Oil field produced water	MSBR	Vol: 5 L	-	90.9	-	-	20	1300	Fakhru'l-Razi et al., 2010
Piggery	SBR	Vol: 8 L	-	81	-	-	24	2028	Ng, 1987
Synthetic wastewater	SBR	I.D. \times H (cm): 10 \times 150 Vol: 8 L	-	93	92	>260	-	1760	Kim et al., 2008
Stainless steel rinse wastewater	SBR	Vol: 3 L	-	78	98	-	-	335.4	Nava et al., 2008

PAH-Polycyclic aromatic hydrocarbons; (SBR)-Sequencing batch reactor; BPR-Biological phosphorus removal; (MSBR)- Membrane-coupled sequencing batch reactor; (SBAR)- Sequencing Biological airlift reactor.

Table 3.3.3. Studies on the treatment of phenolic compounds using sequential batch reactor.

Wastewater	Reactor	Dimension	Initial Conc. (mg/L)	SRT (d)	HRT (h)	Cycle Time (h)	% Pollutant Removal	% COD Removal	Reference
2,4-di chloro phenol	SBR	Vol: 4 L; I.D.×H: 8 ×100 cm	50 - 100	-	8	-	94	95	Wang et al., 2007
Phenol	SBR	Vol: 5 L; L×W×H: 20×15×25 cm	10-100	-	-	12.	99	-	Chan and Lim, 2007
4-Nitrophenol	SBR	Vol: 5 L	320-400	16	16	8	98		Tomei et. al., 2003
Polycyclic aromatic hydrocarbons	SBR	Vol: 5 L	70	-	44-77 day	168	80		Chiavola et. al., 2010
4-Chloro phenol	SBR	Vol: 2.5 L	Phenol: 525 4-CP: 105 to 2100	-		12	Phenol-41		Monsalvo et al., 2009
Phenol and cyanides	SBR and CSTR	Vol: 5 L	Phenol: 1400 Cyanide: 100	26	30	12	93	90	Papadimitriou et al., 2009

Wastewater	Reactor	Dimension	Initial Conc. (mg/L)	SRT (d)	HRT (h)	Cycle Time (h)	% Pollutant Removal	% COD Removal	Reference
Saline	GSBR	Vol: 4 L I.D.×H: 15×40 cm	Phenol: 100-2000	-	-	17	93-99	92-99	Moussavi, 2010
Phenolic	SBR	Vol: 5 L	4NP: 40-60	16	16	8			Tomei and Annesini, 2008
Phenol and m-Cresol	SBR	Vol: 1.4 L; I.D.×H: 5×100 cm	Phenol: 200-1000	-	-	6	90-95		Farooqi et. al., 2008
Phenolic	SBR	Vol: 5 L	Phenol: 3.12	4	10	4		97	Yoong et. al., 2000
Phenolic	ASP	Vol: 11 L	Phenol: 300	-	72	-	99.3	98	Rajani et. al., 2011

GSBR: Granular SBR; ASP: Activated Sludge Process; CSTR: Continuous Stirred Tank Reactor; Vol.: Volume; I.D.×H: Internal diameter × Height; H: Height; L×W×H: Length × Width × Height

3.4 ELECTROCOAGULATION TREATMENT

Electrocoagulation (EC) is an effective alternate technique for liquid wastes trivalent cations generated by the dissolution of sacrificial anodes induce the flocculation of the dispersed pollutants contained by reduction of the zeta potential. In addition, evolution of hydrogen bubbles at the cathode results in the formation of foam. The aggregates formed can then be removed by decantation or flotation followed by settling. Efficiency of EC treatment depends on various process parameters like conductivity, pH, type of electrode used, current density (j), type of pollutant, etc. Due to this multiple ingredient, the process is complex and requires some statistically experimental design that reduces the number of experiment run with a better combination of input parameter. The application of this statistical design is to reduce the process variability and it reduces the time of trial and error experiments [Chen et al., 2012; Prasad et al., 2008; Moreno et al., 2009].

EC technique has been used for the treatment of numerous types of wastewater generated in various industries such as textile, distillery, tannery, pulp and paper, etc. It has been used for the removal of various types of pollutants such as dyes, arsenic, phenolic compounds, etc. from aqueous solutions [Jiang et al., 2002; Holt et al., 2002; Stephenson and Tennant, 2003; Mahesh et al., 2006; Aleboyeh et al., 2008; Feng et al., 2007; Thella et al., 2008; Zongoa et al., 2009; Wang et al., 2005; Can et al., 2003; Thakur et al., 2009; Khandegar and Saroha, 2013; Hariz et al., 2013; Cotillas et al., 2013]. Table 3.4.1 briefly describes utilized EC for the treatment of varieties of industrial wastewater. Ho and Chan [1986] reported electroflotation of palm oil mill effluent by lead oxide coated Ti in 0.5L reactor, 40% COD and 86% SS removal was

observed at current 0.5 A and pH 10. [Chen \[2004\]](#) reviewed the development, design and applications of electrochemical technologies in water and wastewater treatment by comparing the electro-deposition, EC, electro-flotation (EF) and electrooxidation techniques. It was considered as an established technology with possible further development in the improvement of space-time yield. EC has been in use for water production or wastewater treatment which is finding more applications using either aluminum, iron or the hybrid Al/Fe electrodes. [Feng et al. \[2007\]](#) studied treatment of tannery wastewater by EC using mild steel and aluminum electrodes. The removal rates of COD, ammonia, TOC, sulfide and colority were 68.0, 43.1, 55.1, 96.7 and 84.3%, respectively, with the initial concentrations 2413.1, 223.4, 1000.4 and 112.3 mg/L, respectively. [Aleboyeh et al. \[2008\]](#) also investigated the removal efficiency of C.I. Acid Red 14 (AR14) azo dye, from aqueous solution by an EC treatment in batch mode using iron as anode and stainless steel as cathode and reported the >91% removal efficiency at the optimized conditions.

Only few studies are available in open literature for the EC treatment of PRW which are listed in [Table 3.4.2](#). [Yavuz et al. \[2010\]](#) performed electrochemical oxidation of PRW using boron doped diamond anode (BDD), ruthenium mixed metal oxide (Ru-MMO) electrode, and electro-fenton and electrocoagulation using iron electrode. [Yan et al. \[2011\]](#) treated PRW using EC process with three dimensional multi-phase porous graphite plate electrode. Thus, previous researchers did not use the most common iron/stainless steel (SS) electrodes for the EC treatment of PRW.

Table 3.4.1. Studies on treatment of various wastewaters by electrocoagulation.

Industry/ Application	Experimental setup/ Waste properties	Optimized condition	Percentage reduction	Reference
Olive mill wastewater	<p>Reactor Material: Plexiglass Working Volume: 0.5 L</p> <p>Electrode Material: Aluminum electrode Dimension: 5 cm×6 cm×2 mm</p> <p>Waste Properties pH=4.96; COD=66.45(g/L); Conductivity=9.8 mS/cm; Polyphenol=2.4 g/L</p>	<p>$j = 75 \text{ mA/cm}^2$ pH = 4-5 $t = 30 \text{ min}$</p>	<p>COD = 76% Polyphenol = 91%</p>	<p>Adhoum and Monser, 2004</p>
Tannery liming drum wastewater	<p>Reactor Material: Plexiglass Working Volume: 0.4 L</p> <p>Electrode Material: Iron Electrode Dimension: 9.3 cm×7.5 cm×0.3 cm</p> <p>Waste Properties pH=12.3; COD=25300 (mg/L); Conductivity=37.2 mS/cm; BOD₅=10850 (mg/L), Sulphide=3000 (mg/L) Oil & Grease=185 (mg/L)</p>	<p>$j = 35 \text{ mA/cm}^2$ (COD & Sulphide) and 3.5 mA/cm^2 (Oil & Grease) pH = 3 $t = 10 \text{ min}$ Energy Consumptions: COD=5.768kWh/m³; Sulphide=0.524kWh/m³; Oil-grease=0.00015kWh/m³</p>	<p>COD = 82% Sulphide = 90% Oil & Grease = 96%</p>	<p>Sengil et al., 2009</p>
Distillery wastewater (bio-digester effluent)	<p>Reactor Material: Plexiglass Working Volume: 1.5 L</p> <p>Electrode Material: Iron Electrode Dimension: 100 cm×80 cm×2 mm</p>	<p>$j = 44.65 \text{ mA/cm}^2$ pH = 8 Electrode Gap = 2 cm $t = 120 \text{ min}$</p>	<p>COD = 50.5% Color = 95.2%</p>	<p>Kumar et al., 2009</p>

	Waste Properties pH=4.9; COD=15600(mg/L); TS=34.1 g/L; BOD ₅ =7200 (mg/L), Color= Dark Black			
Distillery wastewater	Reactor Material: Perspex Working Volume: 1.5 L Electrode Material: Stainless Steel Dimension: 10.00cm×8.00cm×0.3cm. Waste Properties pH=8.5; COD=9310(mg/L); BOD=3724(mg/L); Total solids=17(g/L); Turbidity=1400 NTU	$j = 146.75 \text{ A/m}^2$ pH = 6.75 $t = 130 \text{ min}$ $g = 1 \text{ cm}$	COD = 63.1% Color = 98.4% Electrical energy consumption = 2.76 kWh/kg	Thakur et al., 2009
Pulp and paper industry	Reactor Material: Glass Working Volume: 0.5 L Electrode Material: Aluminum. Dimension: 50mm×50mm×3 mm. Waste Properties pH=6.9–7.2; COD=620(mg/L); BOD=210(mg/L);Suspended solids=200(mg/L); Color=255(CU (Pt–Co))	$j = 15 \text{ mA/cm}^2$ pH = 7 Rotational speed = 100 rpm NaCl concentration = 1 g/L $g = 3 \text{ cm}$	Color = 94% COD = 90% BOD = 87% Electrode energy consumption = 10.1 to 12.9kWh/m ³	Sridhar et al., 2011
Synthetic hexavalent chromium	Reactor Material: Perspex Working Volume: 0.6 L Electrode Material: Aluminum Dimension: 5cm×20cm×0.5cm.	Voltage = 11 V pH = 7 $t = 18.6 \text{ min}$	Cr(VI) = 50% Electrical energy consumption = 15.46 kWh/m ³	Bhatti et al., 2011
Potato chips processing	Reactor Material: Plexiglass	$j = 200 \text{ mA/cm}^2$	COD = 65.0% Turbidity = 95%	Kobya et al., 2006

wastewater	<p>Working Volume: 250 mL</p> <p>Electrode Material: Aluminum Dimension: 45 mm×55 mm×3 mm</p> <p>Waste Properties COD, 2200–2800 mg/L; BOD, 1650–2150 mg/L; pH, 6.2–6.5; turbidity, 260–610 NTU; conductivity, 1.90–2.40 mS/cm.</p>	<p>pH = 5 $t = 30$ min</p>	Suspended Solid = 95%	
Biodiesel wastewater	<p>Reactor Material: Plexiglass Working Volume: 1 L</p> <p>Electrode Material: Aluminum (anode) and Graphite (cathode) Surface Area: 10.5×5.0 cm²</p> <p>Waste Properties pH=8.9; COD=30980 mg/L; SS, 340 mg/L; Oil & Grease=1360 mg/L; Methanol=10667 mg/L; Conductivity=350 μS/cm.</p>	<p>Voltage = 20 V pH = 6 $t = 25$ min $g = 1.5$ cm</p>	<p>COD = 55.01% Oil & Grease = 96% SS = 97.75%</p>	<p>Chavalparit and Ongwandee, 2009</p>
Synthetic dairy wastewater	<p>Reactor Material: Perspex Working Volume: 1.5 L</p> <p>Electrode Material: Iron Dimension: 9.50cm×8.50cm×0.15cm.</p> <p>Waste Properties pH=6.3–6.8; COD=3900(mg/L); Total solids=3090(mg/L); Turbidity=1744 NTU</p>	<p>270A/m^2 pH = 7 $t = 50$ min NaCl concentration = 1 g/L</p>	<p>Color = 70% Total Solid = 48.2%</p> <p>Electrical energy consumption = 2.76 kWh/kg</p>	<p>Kushwaha et al., 2010</p>
Dye-bath wastewater	<p>Reactor Material: Perspex Working Volume: 1.5 L</p> <p>Electrode</p>	<p>$j = 15.34$ mA/cm² pH = 7.2 $t = 90$ min $g = 1.5$ cm</p>	<p>COD = 91.7% Color = 99.8%</p>	<p>Mondal et al., 2012</p>

	<p>Material: Stainless Steel Dimension: 110mm×85mm×3mm.</p> <p>Waste Properties pH=6.5; COD=5660(mg/L); Color=466000 Pt-Co unit; Total solids=16.89 g/L; Conductivity=5.37 milli mho</p>		Electrical energy consumption = 7.71 kWh/kg	
Textile wastewater	<p>Reactor Material: Perspex Working Volume: 1.0 L</p> <p>Electrode Material: Aluminum and Iron Dimension: 45mm×53mm×3mm.</p> <p>Waste Properties pH=8.88; COD=2031(mg/L); Total suspended solids=102 mg/L; Conductivity=2310 mS/cm; Turbidity= NTU</p>	<p>pH for Fe electrode = 7.0 pH for Al electrode=5.0 $j=30 \text{ A/m}^2$ $t = 15 \text{ min}$ $g = 20 \text{ mm}$</p>	<p>For Fe electrode COD = 65.0% Turbidity= 83%</p> <p>For Al electrode COD = 63.0% Turbidity = 80%</p>	Bayramoglu et al., 2007
Electroplating industry effluent	<p>Reactor Material: Glass Beaker Working Volume: 200 L</p> <p>Electrode Material: Iron Dimension: 120mm×32mm×1.5mm.</p> <p>Waste Properties pH=1.65; Chromium(VI)=887.29(mg/L); Chromium(III)=1495(mg/L); Total dissolved solids=30800 mg/L; Conductivity=64.2 mS/cm</p>	<p>pH =4 $g = 0.5 \text{ cm}$ $j = 50 \text{ mA/cm}^2$</p> <p>Actual Effluent $t = 45 \text{ min}$</p> <p>Synthetic Effluent $t = 15 \text{ min}$</p>	<p>Synthetic Effluent Cr(VI) = 100 %</p> <p>Actual Effluent Cr(III) & Cr(VI) = 100 %</p>	Verma et al., 2013

j =Current density; t =Electrolysis time; g =Inter-electrode gap; COD=Chemical oxygen demand

Table 3.4.2. Studies on treatment of PRW by electrocoagulation.

Industry/ Application	Experimental Setup/ Waste properties	Optimized condition	Percentage reduction	Reference
Oil refinery wastewater	<p>Reactor Material: Perspex Reactor Dimension: 25cm×25cm×30 cm Working Volume: 3.5 L</p> <p>Electrode Material: Aluminum Dimension: 25cm×25cm×0.3cm.</p> <p>Waste Properties pH=8; COD=80-120(mg/L); BOD=40.25(mg/L); Turbidity=7.4 NTU; Phenol=13 mg/L</p>	<p>Current density =23.6mA/cm² pH = 7 Electrolysis Time = 120 min Electrode Gap=1cm</p>	<p>Phenol Concentration = 94.5%</p> <p>Electrical energy consumption = 1.8 kWh/g</p>	Abdelwahab Et al., 2009
Petroleum refinery wastewater	<p>Reactor Material: Beaker Working Volume: 0.3 L</p> <p>Electrode Material: Porous Graphite Plate Dimension: 60 mm×110 mm×2 mm</p> <p>Waste Properties pH=6.5; COD=1021mg/L; Conductivity=1423 μS/cm; Volatile Phenol=95 mg/L</p>	<p>Cell Voltage =12V pH = 6.5 Electrolysis Time = 60 min</p>	<p>COD = 92.8% Conductivity = 94.1%</p>	Yan et al., 2011
Petroleum refinery	<p>Reactor Material: Beaker</p>	<p>Current Density =21.2mA/cm²</p>	<p>Sulfide and organics expressed as COD ></p>	Hariz et al., 2013

sulfidic spent caustic waste	<p>Working Volume: 0.3 L</p> <p>Electrode Material: Iron Dimension: 100 mm×50 mm×0.5 mm</p> <p>Waste Properties Sulfide (wt%)=1-4%; COD=20-60 g/L; BOD= 5-15 g/L; TOC=6-20 g/L; Volatile Phenol=0-2 g/L</p>	pH = 9 Electrolysis Time = 30 min	80.0%	
Petroleum contaminated groundwater	<p>Reactor Material: Cylindrical Glass Cell Working Volume: 0.2 L</p> <p>Electrode Material: Aluminum; Iron; Stainless Steel Dimension: 10 cm×2 cm×0.2 cm</p> <p>Waste Properties Total petroleum hydrocarbon=64 mg/L; Sulfate =60.5 mg/L; TDS=1178 mg/L; Nitrate= 9.8 mg-N/L; Chloride=419 mg/L; Electrical conductivity=1.61 ms/cm</p>	-	Total Petroleum Hydrocarbon = 93-95 %	Moussavi et al., 2011
Petrochemical wastewater containing phenolic compounds	<p>Reactor Material: Plexi-glass Working Volume: 10 L</p> <p>Electrode Material: Aluminum Dimension: 10 cm×10 cm×0.2 cm</p> <p>Waste Properties pH=7; COD =100 mgO₂/L; Phenol=3 mg/L;</p>	Current Density = 8.59 mA/cm ² , pH = 7, NaCl concentration = 1 g/L	Phenol Compound=100% COD=75%	El-Ashtoukhy et al., 2013

	Turbidity= 8.2 NTU; Conductivity=3.5 mS/cm			
Oil wastewater from gas refinery	<p>Reactor Material: Pyrex Glass Working Volume: 0.4 L</p> <p>Electrode Material: Aluminum Dimension: 0.3 cm×3 cm×4.5 cm</p> <p>Waste Properties pH=7.6; COD=4000 mg/L; Electrical Conductivity=32 mS/cm</p>	Current density =40 mA/cm ² pH = 7 Electrolysis Time = 120 min Electrode Gap=1cm	COD=97%	Saeedil and Khalvati-Fahlyani, 2011
Petroleum Refinery Wastewater	<p>Reactor Material: Perspex Working Volume: 1.5 L</p> <p>Electrode Material: Ruthenium Mixed Metal Oxide Dimension: 4cm×3cm.</p> <p>Waste Properties pH=8.5; COD=590(mg/L); BOD=3724(mg/L); Total solids=17(g/L); Turbidity=1400 NTU; Electrical Conductivity=15.63 mS/cm Phenol=192.9 mg/L</p>	Current density =40 mA/cm ² pH = 7 Electrolysis Time = 120 min Electrode Gap=1cm	COD=97%	Yavuz et al., 2010

3.5 RESEARCH GAP

The design of any adsorption systems requires isotherm data. Most of the workers have reported equilibrium adsorption data for single component adsorption of phenolic compounds. Since, actual industrial effluents contain several phenolic compounds; therefore, equilibrium adsorption data for closely related binary and ternary compounds are also important. RHA has been shown as an effective adsorbent for the removal of metals, dyes, etc. However, a review of the literature shows that no study has been reported on individual or simultaneous adsorption of phenolic compounds onto RHA. Further studies are required on the use of RHA as an adsorbent for individual and simultaneous removal of phenol and associated compounds like catechol and resorcinol from aqueous solutions and gather experimental data on adsorption equilibrium for the binary and ternary system containing these compounds.

A review of the literature on treatment of phenolic compounds in SBR shows that most of the studies have been done on single phenolic compounds ([Table 3.3.3](#)). Disposal of sludge generated in SBR is also important; however previous investigators have scarcely dealt this aspect of wastewater treatment. Therefore, it is necessary to explore the possibility of using SBR for the treatment of wastewater containing phenolic compounds such as phenol, resorcinol and catechol. It is also necessary to characterize the sludge wasted by proximate, elemental and thermal analysis and to explore disposal of sludge along with energy recovery.

Only few studies are reported on treatment of petroleum refinery wastewater (PRW) in SBR [[Viero et al., 2008](#); [Shariati et al., 2011](#); [Kutty et al., 2011](#)]. Previous researchers did not use fill time as an operating parameter. Kinetic study and settling

studies on the treated effluent were not carried out. These studies also need to be carried out with actual PRW along with the settling characteristics of effluent after treatment.

A review of literature shows that only two studies have been reported previously for the treatment of petroleum refinery wastewater (PRW) by EC method [Yavuz et al., 2010; Yan et al., 2011]. Previous researchers did not use the most common iron/stainless steel (SS) electrodes for EC treatment of PRW. More over in these studies, the interaction of various parameters were not studied and the sludge was not characterized from disposal point of view. All these research gaps need to be filled with future studies.

The main aim and detail objectives of this present study (as given in sections 1.5) have been formulated based upon the research gaps identified in the literature (as discussed above).

ADSORPTION

4.1 GENERAL

This chapter describes the theory of adsorption, materials and methods, results and discussion for experiments carried out for individual, binary and ternary adsorption of phenol, catechol and resorcinol onto rice husk ash (RHA).

4.2 ADSORPTION THEORY

Adsorption process occurs on the surface or pores of a solid (adsorbent). Extent of adsorption is affected by the pore surface area available in the adsorbent and is a function of the concentration of adsorbate in aqueous solutions [Chiou, 2002]. Adsorption occurs if the attractive force between the solute and adsorbent is greater than the cohesive energy of the substance itself. Adsorption is typically nonlinear due to the energy heterogeneity between the available sites for adsorption.

Adsorption processes can be classified as either physical (van der Waals adsorption) or chemical (chemisorptions) depending on the type of forces between the adsorbate and the adsorbent. In physical adsorption, the individuality of the adsorbate and the adsorbent are preserved. In chemisorption, there is transfer or sharing of electron, or breakage of the adsorbate into atoms or radicals, which get attached separately to the adsorbent surface.

Structural and elemental analyses of low cost adsorbents like RHA show that they usually contain various minerals and some carbon moieties. Therefore, adsorption on low cost adsorbents is controlled by both physical and chemical forces. The main forces controlling adsorption are van der Waals forces, hydrophobicity, hydrogen bonds, polarity and steric interaction, dipole induced interaction, π - π interaction, etc. In the adsorption processes, pollutants get accumulated on adsorbent surfaces by the above mentioned interactions.

Adsorption is thought to occur in three stages, as the adsorbate concentration increases.

Stage I: First, a single layer of molecules builds up over the surface of the solid. This monolayer may be chemisorbed and is associated with a change in free energy that is a characteristic of the forces that hold it.

Stage II: As the adsorbate concentration is further increased, more layers are formed by physical adsorption; the numbers of layers which can be formed are limited by the size of the pores.

Stage III: Finally, for adsorption from the gas phase, capillary condensation may occur in which capillaries get filled with condensed adsorbate, when its partial pressure reaches a critical value relative to the size of the pore.

The amount of adsorbate adsorbed by an adsorbent from adsorbate solution is influenced by number of factors such as initial pH of solution, initial concentration of adsorbate and the adsorbent dose.

The adsorption of adsorbate from solution to adsorbent can be considered as a reversible process with equilibrium being established between the solution and the

adsorbate. Assuming a non-dissociating molecular adsorption of adsorbate molecules on adsorbent, the sorption phenomenon can be described as the diffusion controlled process.

When a solution is contacted with a solid adsorbent, molecules of adsorbate get transferred from the solution to the solid until the concentration of adsorbate in solution as well as in the solid phase are in equilibrium. At equilibrium, rate of adsorption and desorption of adsorbate become equal. The equilibrium data at a given temperature is represented by adsorption isotherm and the study of adsorption isotherm is important in a number of chemical processes ranging from the design of heterogeneous chemical reactors to purification of compounds by adsorption.

4.3 MATERIALS AND METHODS

4.3.1 Adsorbent Characterization

RHA, as obtained from a nearby paper mill (Rana paper mill, Muzaffarnagar, India) was used as such without any pretreatment except sieving to remove very fine particles. The physico-chemical characterization of RHA was performed using standard procedures. Proximate analysis was carried out using the standard procedure as given in IS code [IS 1350:1984]. Bulk density was determined by using MAC bulk density meter whereas particle size analysis was done using standard sieves. Point of zero charge (pH_{PZC}) of RHA was determined by the solid addition method [Balistrieri and Murray, 1981; Srivastava et al., 2006a].

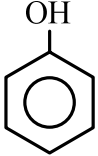
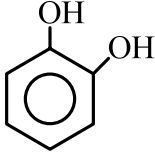
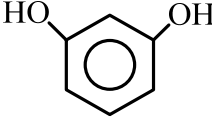
X-ray diffraction (XRD) analysis was carried out using Phillips (Holland) diffraction unit (Model PW 1140/90), with copper as the target, nickel as the filter

media, and K radiation maintained at 1.542 Å. Goniometer speed was maintained at 1°/min. Textural characteristics were determined by nitrogen adsorption at 77.15 K to determine the specific surface area and the pore diameter of RHA using an ASAP 2010 Micromeritics instrument and by Brunauer-Emmett-Teller (BET) method [Brunauer, 1938], using the software of Micromeritics. Nitrogen was used as cold bath (77.15 K). The Barrett-Joyner-Hanlenda (BJH) method [Barret et al., 1951] was used to calculate the pore size distribution. FTIR spectrometer (Thermo Nicolet, Model Magna 760) was used to determine the presence of functional groups in RHA at room temperature. Pellet (pressed-disk) technique was used for FTIR analysis. The spectral range chosen was from 4000 to 400 cm^{-1} . Carbon, hydrogen, nitrogen and sulphur (CHNS) analysis was done using Elementar Vario EL III, Elementar Analyzen systeme, GmbH, Germany.

4.3.2 Adsorbates

All chemicals used in study were of analytical reagent (AR) grades. Phenol ($\text{C}_6\text{H}_6\text{O}$) and catechol ($\text{C}_6\text{H}_6\text{O}_2$) were procured from s.d. Fine Chemicals, Mumbai, India whereas resorcinol ($\text{C}_6\text{H}_6\text{O}_2$) was procured from E. Merck, Mumbai, India. Physico-chemical and solvatochromic properties of phenol, catechol and resorcinol are given in Table 4.3.1.

Table 4.3.1. Physico-Chemical properties and solvatochromic parameter of phenol, catechol and resorcinol.

Parameter	Phenol	Catechol	Resorcinol	Reference
Chemical Structure				Buscaa et al., 2008; Suresh et al., 2012a,b
Molar mass (g/mol)	94.11	110.1	110.1	
Density (g/cm ³)	1.06	1.344	1.28	Yang et al., 2008; Kamlet et al., 1988
Solubility in water (g×100 ml ⁻¹ , 20 °C)	8.3	43	110	Huang et al., 2009
λ_{\max} (nm)	270	275	273	Yang et al., 2008; Richard et al., 2009; Mohamed et al., 2006
Dipole moment (Debye, D)	1.7	2.62	2.07	Suresh et al., 2012a,b; Kamlet et al., 1988
Melting point (°C)	43	10	110	Suresh et al., 2012a,b; Kirk and Othmer, 1981
Boiling point (°C)	182	245.5	277	
Molecular size	0.42 nm	0.55 nm × 0.55 nm	0.56 nm × 0.47 nm	Zhang et al., 2007; Huang et al., 2009
pK _a	9.95	9.25, 13	9.2, 10.9	Fiore and Zanetti, 2009; Yang et al., 2008; EHC 157, 1994

4.3.3 Batch Experimental Programme

Batch adsorption experiments were carried out to optimize the adsorption process parameters like initial pH, contact time and adsorbent dose. Experimental solutions were prepared by diluting the respective stock solution of phenol, catechol and resorcinol with double distilled water (DDW) and mixing them in the desired proportion. Each experiment was conducted in 250 mL flask containing 150 mL aqueous solution of known concentration and known mass of RHA. The flasks were kept in a constant temperature orbital shaker (CIS-24 BL, Remi Instrument, Mumbai) at 150 rpm. The samples were collected after the sorption process and analyzed for residual concentration of compounds using high performance liquid chromatography (HPLC). A symmetry column C-18 was used to separate the substrate using a mobile phase in the ratio of 6:4:0.1 of distilled water: methanol: acetic acid with a flow rate of 1 mL/min, and the injection volume was 20 μ L. The identification of each compound was based on the peak retention time of the components. Concentration of phenol, catechol and resorcinol were measured at wavelength 275, 270 and 273 nm, respectively, in HPLC. Fresh stock solution, as required, was prepared every day, and initial concentration (C_o) was ascertained before the start of each experimental run accordingly.

The equilibrium adsorption uptake ($q_{e,i}$), individual adsorption yield (Ad_i %) and total adsorption yields (Ad_{Tot} %) were calculated using the following expressions:

$$q_{e,i} = (C_{o,i} - C_{e,i})V / w, \text{ (mmol of adsorbate/g of adsorbent)} \quad (4.3.1)$$

$$Ad_i \% = 100(C_{o,i} - C_{e,i}) / C_{o,i} \quad (4.3.2)$$

$$Ad_{Tot} \% = 100 \sum (C_{o,i} - C_{e,i}) / \sum C_{o,i} \quad (4.3.3)$$

Where, C_o and C_e are initial and equilibrium adsorbate concentration (mg/L), V is the volume of the adsorbate containing solution (L) and w is the mass of the adsorbent (g).

4.3.4 Adsorption Kinetic Study

To determine the time necessary for adsorption of various adsorbate onto RHA, 150 mL of the aqueous solution containing 250 mg/L of given adsorbate (phenol, catechol and resorcinol) was taken in a series of conical flasks with 20 g/L of RHA. The flasks were kept in shaker with 150 rpm agitation speed at temperature of 30 °C. At the end of predetermined time, the flasks were taken out and the supernatant were analyzed with HPLC for adsorbate concentration. In order to investigate the kinetics of adsorption of the adsorbate on the RHA, two kinetic models namely pseudo-first-order and pseudo-second-order models were used.

Using first order kinetics, it can be shown that with no adsorbate initially present on the adsorbent, the uptake of the adsorbate by the adsorbent at any instant t is given as [Srivastava et al., 2006c]:

$$q_t = q_e [1 - \exp(-k_f t)] \quad (4.3.4)$$

Where, q_e is the amount of the adsorbate adsorbed on the adsorbent under equilibrium condition and k_f is the pseudo-first order rate constant.

The pseudo-second-order model is represented as [Blanchard et al., 1984; Ho and McKay, 1999]:

$$q_t = \frac{tk_s q_e^2}{1 + tk_s q_e} \quad (4.3.5)$$

The initial sorption rate, h (mg/g min), at $t \rightarrow 0$ is defined as:

$$h = k_s q_e^2 \quad (4.3.6)$$

4.3.5 Adsorption Isotherm Study

4.3.5.1 Single component isotherm modeling

Many theoretical and empirical models have been developed to represent the various types of adsorption isotherms. Langmuir, Freundlich, Brunauer-Emmet-Teller (BET), Redlich-Peterson (R-P), etc. are the most commonly used adsorption isotherm models for describing the dynamic equilibrium. Isotherm equations used for the study are described as follows:

4.3.5.1.1 Langmuir isotherm

This equation is based on following assumptions that:

1. Only monolayer adsorption is possible.
2. Adsorbent surface is uniform in terms of energy of adsorption.
3. Adsorbed molecules do not interact with each other.
4. Adsorbed molecules do not migrate on the adsorbent surface.

The adsorption isotherm derived by Langmuir for the adsorption of a solute from a liquid solution is given as [Langmuir, 1918]:

$$q_e = \frac{q_m K_L C_e}{1 + K_L C_e} \quad (4.3.7)$$

Where, q_e is the amount of adsorbate adsorbed per unit amount of adsorbent at equilibrium, q_m is the amount of adsorbate adsorbed per unit amount of adsorbent required for monolayer adsorption (limiting adsorbing capacity), K_L is a constant

related to enthalpy of adsorption, C_e is the concentration of adsorbate solution at equilibrium.

4.3.5.1.2 Freundlich isotherm

The heat of adsorption in many instances decreases in magnitude with an increase in extent of adsorption. This decline in heat of adsorption is logarithmic, implying that adsorption sites are distributed exponentially with respect to adsorption energy. This isotherm does not indicate an adsorption limit when coverage is sufficient to fill a monolayer. Freundlich isotherm is given as [Freundlich, 1906]:

$$q_e = K_F C_e^{1/n} \quad (4.3.8)$$

Where, K_F and n are the Freundlich constants.

Freundlich equation is most useful for dilute solutions over small concentration ranges. It is frequently applied to the adsorption of impurities from a liquid solution onto the various types of commercial adsorbents. High value of K_F and $1/n$ indicate high adsorption throughout the whole concentration range. Low value of K_F and high value of $1/n$ indicates a low adsorption throughout the whole concentration range. Low value of $1/n$ indicates high adsorption at strong adsorbate concentration.

4.3.5.1.3 Redlich-Peterson isotherm

Redlich and Peterson (R-P) [1959] model combines elements from both the Langmuir and Freundlich equation and the mechanism of adsorption is a hybrid and does not follow ideal monolayer adsorption. R-P isotherm has a linear dependence on concentration in the numerator and an exponential function in the denominator. It approaches the Freundlich model at high concentration and is in accord with the low concentration limit of the Langmuir equation. Furthermore, the R-P equation

incorporates three parameters into an empirical isotherm, and therefore, can be applied either in homogenous or heterogeneous systems due to the high versatility of the equation [Srivastava et al., 2006b]. It can be described as follows:

$$q_e = \frac{K_R C_e}{1 + a_R C_e^\beta} \quad (4.3.9)$$

Where, K_R is R–P isotherm constant (L/g), a_R is R–P isotherm constant $(L / mg)^{1/\beta}$ and β is the exponent which lies between 1 and 0.

4.3.5.2 Multi-component Isotherm Modeling

When a number of components are present in the solution, and are to be adsorbed simultaneously, the adsorbate-adsorbate and the adsorbate-adsorbent interactive effects play important roles in the overall adsorption phenomena. In general, a mixture of adsorbates can produce three possible types of behavior: synergism, antagonism and non-interaction [Ting et al., 1991; Sag et al., 1998]. For correlating the experimental adsorption data to multi-component system, single adsorbate isotherm equations have been modified to account the effects of the components on each other's adsorption. In the present study, the equilibrium adsorption data for the following multi-component systems have been studied for phenol, catechol and resorcinol adsorption onto RHA:

1. Binary systems: catechol-phenol, catechol-resorcinol and phenol-resorcinol.
2. Ternary system: phenol-catechol-resorcinol

Various multi-component isotherm equations have been developed by various researchers. Some of the multi-component isotherm model equations were tested for

their applicability to represent the experimental isotherm data. These equations are shown in Table 4.3.2.

Table 4.3.2. Multi-component isotherm models.

Multi-component isotherm models		
Non-modified Langmuir Model	$q_{e,i} = \frac{q_{m,i} K_{L,i} C_{e,i}}{1 + \sum_{j=1}^N K_{L,j} C_{e,j}}$	-
Modified Langmuir isotherm	$q_{e,i} = \frac{q_{m,i} K_{L,i} (C_{e,i} / \eta_{L,i})}{1 + \sum_{j=1}^N K_{L,j} (C_{e,j} / \eta_{L,j})}$	[Bellot and Condoret, 1993]
Extended Langmuir isotherm	$q_{e,i} = \frac{q_{\max} K_{EL,i} C_{e,i}}{1 + \sum_{j=1}^N K_{EL,j} C_{e,j}}$	[Yang, 1987]
Extended Freundlich isotherm	$q_{e,i} = \frac{K_{F,i} C_{e,i}^{(1/n_i)+x_i}}{C_{e,i}^{x_i} + y_i C_{e,i}^{z_i}}$	[Fritz and Schluender, 1974]
Sheindorf–Rebuhn–Sheintuch (SRS) Model	$q_{e,i} = K_{F,i} C_{e,i} \left(\sum_{j=1}^N a_{ij} C_{e,j} \right)^{(1/n_i)-1}$	[Sheindorf et al., 1981]
Non-modified Redlich-Peterson Model	$q_{e,i} = \frac{K_{R,i} C_{e,i}}{1 + \sum_{j=1}^N a_{R,j} C_{e,j}^{\beta,j}}$	-
Modified Redlich-Peterson Model	$q_{e,i} = \frac{K_{R,i} (C_{e,i} / \eta_{R,i})}{1 + \sum_{j=1}^N a_{R,j} (C_{e,j} / \eta_{R,j})^{\beta,j}}$	[Srivastava et al., 2006b]

Adsorption isotherm studies for single, binary and ternary systems were carried out at natural $pH_o=6.0$ and 20 g/L adsorbent dose with 150 mL of the adsorbate solutions having C_o in the range of 50-500 mg/L. After 24 h contact time, the supernatant was taken out for analysis of adsorbate concentration by HPLC. For binary and ternary systems, detection wavelength for HPLC was kept at 260 nm. Various single and multi component isotherm models have been used to correlate the experimental equilibrium data. Isotherm parameters evaluated from single component isotherm model are used for multi component modeling.

The isotherm parameters of all models were determined using MS Excel for Windows by minimizing the error function. Sum of square of errors (SSE) was employed in this study to find out the most suitable isotherm model to represent the experimental data. This error function is given as:

$$SSE = \sum_{i=1}^n (q_{e,i,exp} - q_{e,i,cal})^2 \quad (4.3.10)$$

In the above equation, the subscript 'exp' and 'calc' refer to the experimental and calculated values, respectively, and n is the number of measurements.

4.4 RESULTS AND DISCUSSION

4.4.1 Characterization of Adsorbent

The physico-chemical characteristics of RHA are presented in [Table 4.4.1](#). The average particle size of RHA was 150.5 μm whereas the bulk density and the heating value were 109.9 kg/m^3 and 9.9 MJ/kg, respectively. The BET surface area was found to be 47.2 m^2/g where as Langmuir surface area was 70.5 m^2/g . Similarly, t-plot micropore area was found to be 26.9 m^2/g and t-plot external surface area was found to be 20.2 m^2/g .

Table 4.4.1. Characterization of rich husk ash (RHA).

Parameter	Rich husk ash (RHA)
Proximate analysis	
Moisture (%)	4
Ash (%)	69.6
Volatile matter (%)	6.5
Fixed carbon (%)	19.9
Bulk density (kg/m ³)	109.9
Heating value (MJ/kg)	9.9
Average particle size (μm)	150.5
Ultimate analysis of adsorbents	
Carbon (%)	9.481
Hydrogen (%)	0.610
Nitrogen (%)	0.048
C/N ratio	196.8
Surface area of pores (m²/g)	
BET	47.2
BJH	
(a) Adsorption cumulative	20.31
(b) Desorption cumulative	15.74
BJH cumulative pore volume (cm³/g)	
Single point total	0.0332
BJH adsorption	0.1965
BJH desorption	0.0156
Average pore diameter (°A)	
BET	28.20
BJH adsorption	38.70
BJH desorption	39.73

The pore size distribution show RHA to be predominantly mesoporous in nature. BJH adsorption average pore diameter was 38.7 Å and BJH desorption average pore diameter was 39.7 Å. Total pore volume of pores was 0.033 cm³/g. BJH pore area showed that the 80% of the pore area was due to the mesopores.

4.4.2 Effect of Initial pH

The pH of the solution affects the surface charge of the adsorbents as well as the degree of ionization and speciation of different adsorbates [Elliot and Hung, 1981]. Reaction kinetics and equilibrium characteristics of the adsorbent process are pH sensitive and, therefore, any change in the system pH affects them. Adsorption of various anionic and cationic species on such adsorbents has been explained on the basis of the competitive adsorption of H⁺ and OH⁻ ions with the adsorbates.

To understand the adsorption mechanism, it is necessary to determine the point of zero charge (pH_{PZC}) of the RHA. Adsorption of cations is favored at higher pH due to the deposition of OH⁻ ions, while the adsorption of anions is favored at lower pH due to presence of H⁺ ions. The specific adsorption of cations shifts pH_{PZC} towards lower values, whereas the specific adsorption of anions shifts pH_{PZC} towards higher values. Figure 4.4.1 shows that for all the concentration of KNO₃, the zero value of the difference between initial and final pH and hence, pH_{PZC} for RHA lies at the pH_o value of 9.2.

The influence of the pH_o of the aqueous solution on the extent of adsorption of phenol, catechol and resorcinol individually onto RHA was studied at 30°C by varying pH_o in the range of 2-10. Result of experiments are shown in Figure 4.4.2. Adsorption

of compounds increase with increase in pH_o of solution upto 6. At higher pH_o (≥ 6.0), the adsorption of phenol, catechol and resorcinol is sharply decreased. The percentage adsorption were found to be 63.2%, 78.4% and 73.1%, respectively for $pH_o=6$, which is nearby its natural pH .

The uptake of phenolic compounds was low at $pH=3$, because hydrogen bonds between phenolic compounds and surface groups may block the entrance of fine pores [Terzyk, 2003]. The phenolic compounds are predominantly in the neutral molecular form. Increase in the removal efficiencies of phenol, catechol and resorcinol within pH_o 3-6 suggests the insignificant involvement of hydrogen bond between the phenolic compounds and RHA [Chen et al., 2007]. At $pH_o \leq pH_{PZC}$, the RHA surface is positively charged, and the species adsorbed at pH (6-7) are neutral molecules. In these conditions, the dispersive or van der waals interaction determine the adsorption process [Blanco-Martinez et al., 2009; Shakir et al., 2008]. The dissociation of $-OH$ groups on the phenol at high pH may inhibit the formation of hydrogen bonds between RHA and phenolic compounds, and thus reduce the adsorption as well. The increase in surface acidity of RHA at $pH_o \approx 6$ favors the dono-acceptor interaction between the electrons of the aromatic ring and the surface. This leads to an increase of the removal efficiency [Blanco-Martinez et al., 2009]. It can be seen from Figure 4.7.2 that removal efficiency of catechol and resorcinol were approximately constant at intermediate pH , which means that catechol and resorcinol exist in both neutral and anionic form in the aqueous solution. Hence, it seems judicious to assume that at this pH catechol and resorcinol are adsorbed via both electrostatic and van der waals interactions [Shakir et al., 2008]

Solubility of resorcinol is much higher than catechol. This may be the reason for lower adsorption capacity of resorcinol compared to that of catechol. In addition, the polarity of adsorbates also plays an important factor affecting adsorption of phenolic derivatives. The dipole moment of catechol (2.620 D) is much larger than that of resorcinol (2.071 D) and phenol (1.22 D), respectively [Chen, 1990]. Therefore, the interaction between the RHA and catechol is expected to be much stronger than that of resorcinol and phenol. Suresh et al. [2011d] found that the ortho-position greatly enhances the adsorption energy of compound such as catechol. Thus, cumulative effects of solubility, polarity and position of the hydroxyl group probably increased the adsorbability of catechol as compared to resorcinol and phenol onto RHA [Sun et al., 2005].

4.4.3 Effect of Adsorbent Dose (m) and Contact Time (t)

The effect of m on the adsorption of phenol, catechol and resorcinol onto RHA was studied and is shown in Figure 4.4.3. The percent removal of phenol, catechol and resorcinol increased with an increase in m from 6.67 g/L to 20 g/L. The increase in the adsorption with m can be attributed to the availability of greater surface area and more adsorption sites. The increment in percentage removal were very less for all three compounds for $m > 20$ g/L. This is due to fact that the removal efficiency depends more upon the concentration of the solution and less depends on adsorbent dose. Thus, optimized adsorbent dose for adsorption of adsorbate was taken as 20 g/L.

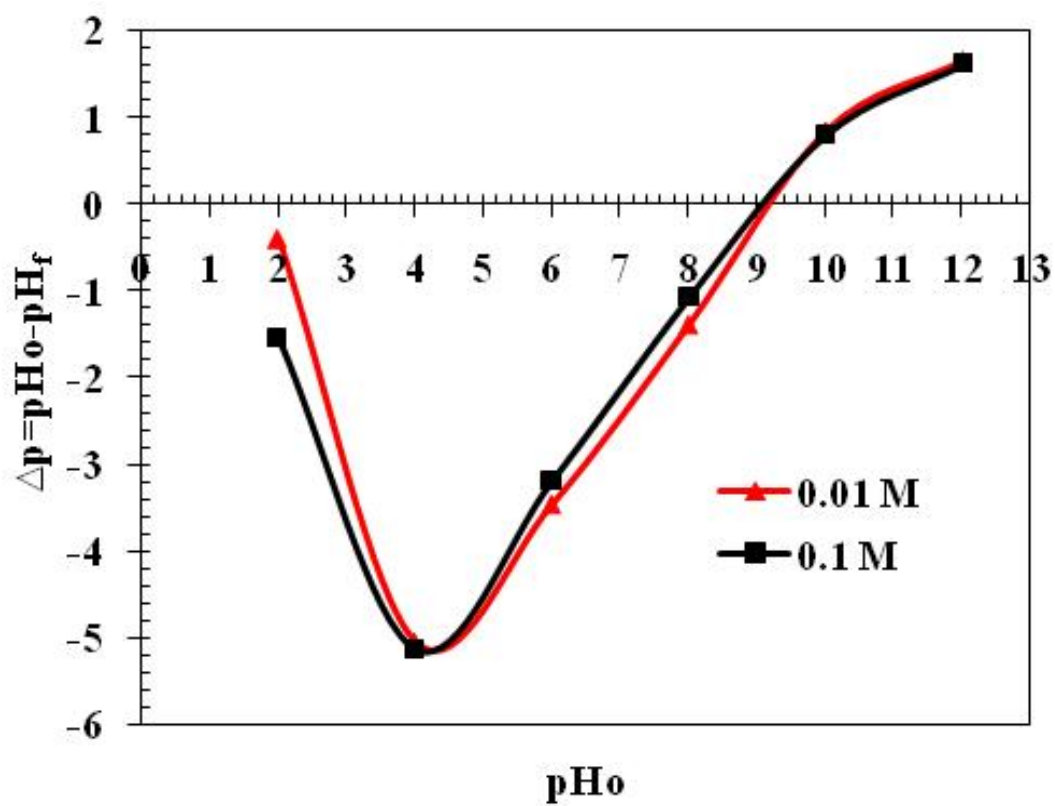


Figure 4.4.1. Point of zero charge of RHA.

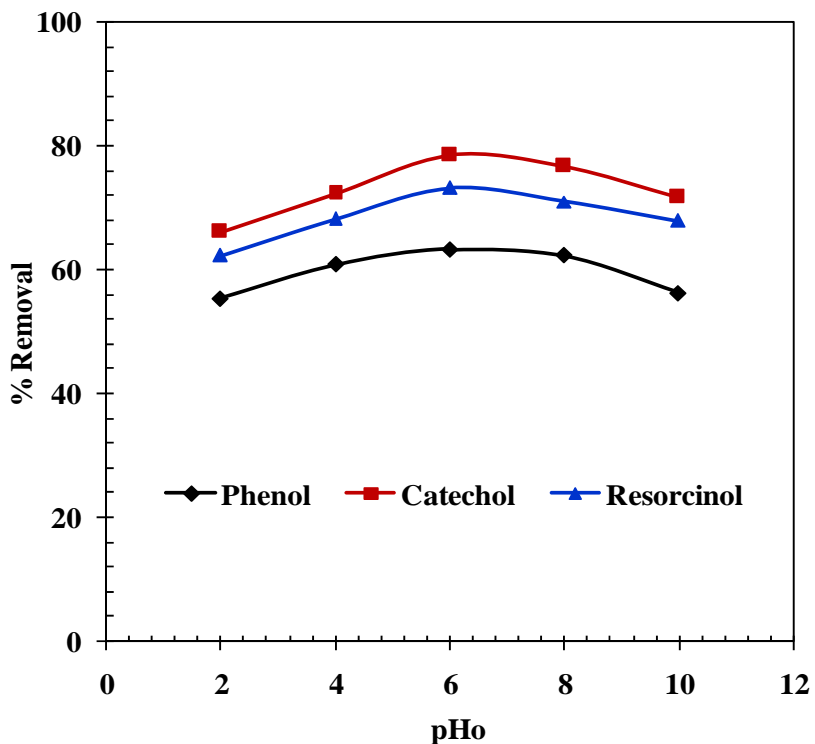


Figure 4.4.2. Effect of pH_0 on the adsorption of phenol, catechol and resorcinol by RHA, $C_0 = 250$ mg/L, $m = 20$ g/L, $t = 24$ h, $T = 30$ °C.

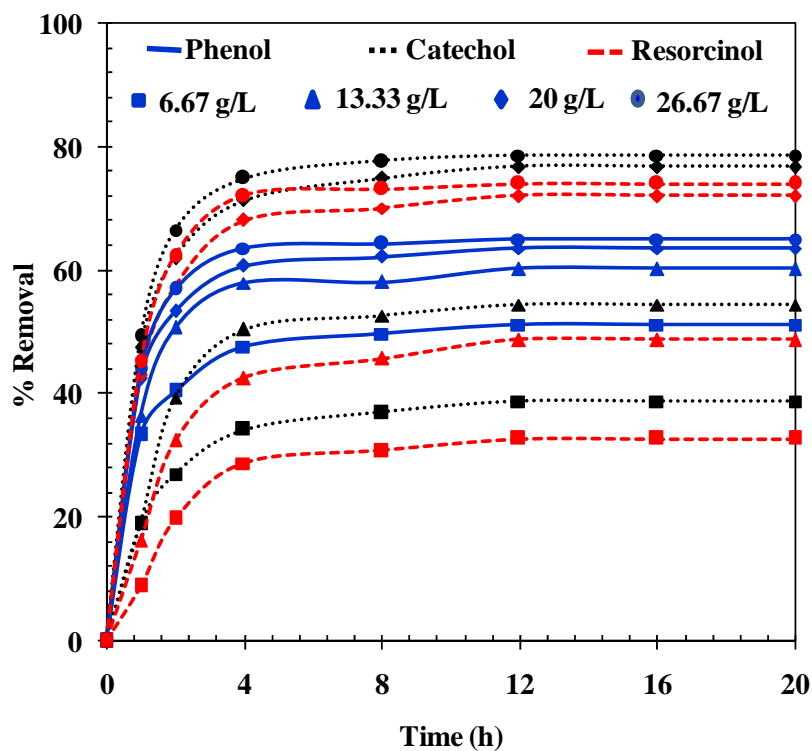


Figure 4.4.3. Effect of adsorbent dose and contact time on the adsorption of phenol, catechol and resorcinol by RHA, $C_0 = 250$ mg/L, $pH_0 = 6$, $T = 30$ °C.

The contact time between the adsorbate and the adsorbent is of significance in the wastewater treatment by adsorption. Available adsorption studies in the open literature reveal that the uptake of adsorbate species is fast at the initial stages of the contact time and, thereafter, it becomes constant. Very rapid uptake can be seen during initial hour. After 4 h, uptake of substrate becomes nearly constant. This rapid uptake of substrate indicates the efficiency of the adsorbents used for removal of phenol, catechol and resorcinol. At later stages, no significant removal was achieved due to the lesser availability of vacant surface. Contact time of 4 h was assumed to be optimum time for the adsorption of phenol, catechol and resorcinol.

4.4.4 Adsorption Kinetic Study

Two kinetic models, namely, pseudo-first-order and pseudo-second-order have been used to test their validity with the kinetic experimental adsorption data. Kinetic parameters were determined by non-linearly fitting the experimental data to the kinetic models using Marquardt's percent standard deviation (MPSD) [Marquardt, 1963], which is given as:

$$MPSD = 100 \sqrt{\frac{1}{n-p} \sum_{i=1}^n \left(\frac{q_{t,i,exp} - q_{t,i,cal}}{q_{t,i,exp}} \right)^2} \quad (4.4.1)$$

Where, $q_{t,i,exp}$ (mg/g) is the experimental value of solid phase concentration of adsorbate at time t, and $q_{t,i,cal}$ (mg/g) is the calculated value of solid phase concentration of adsorbate at time t.

The best-fit values of parameters along with the coefficient of determination (R^2) and MPSD values are given in Table 4.4.2. It was very difficult to decide the best model on the basis of R^2 value. Therefore, MPSD error function was used to find best model for experimental data. It may be seen that the adsorption kinetics can be satisfactorily and adequately represent by the pseudo second order model which has lower MPSD values as compared to the pseudo first order model. The fit of pseudo second order model is shown in Figure 4.4.4 by solid line for phenol, catechol and resorcinol removal by RHA.

Table 4.4.2. Kinetic parameter for the removal of phenol, catechol and resorcinol by RHA. $pH_0=6.0$, $C_0=250$ mg/L, $m=20$ g/L, $T=30$ °C.

Pseudo-first-order model					
	$q_{e, exp}$ (mg/g)	$q_{e, calc}$ (mg/g)	k_f (min ⁻¹)	R^2	MPSD
Phenol	7.20	6.803	0.015	0.993	15.55
Catechol	8.924	8.978	0.017	0.998	21.96
Resorcinol	8.515	8.459	0.018	0.998	7.49
Pseudo-second-order model					
	$q_{e, calc}$ (mg/g)	h (mg/g min)	k_s (g/mg min)	R^2	MPSD
Phenol	9.118	0.110	0.0013	0.998	9.51
Catechol	10.495	0.215	0.002	0.997	19.44
Resorcinol	10.689	0.174	0.0015	0.998	9.62

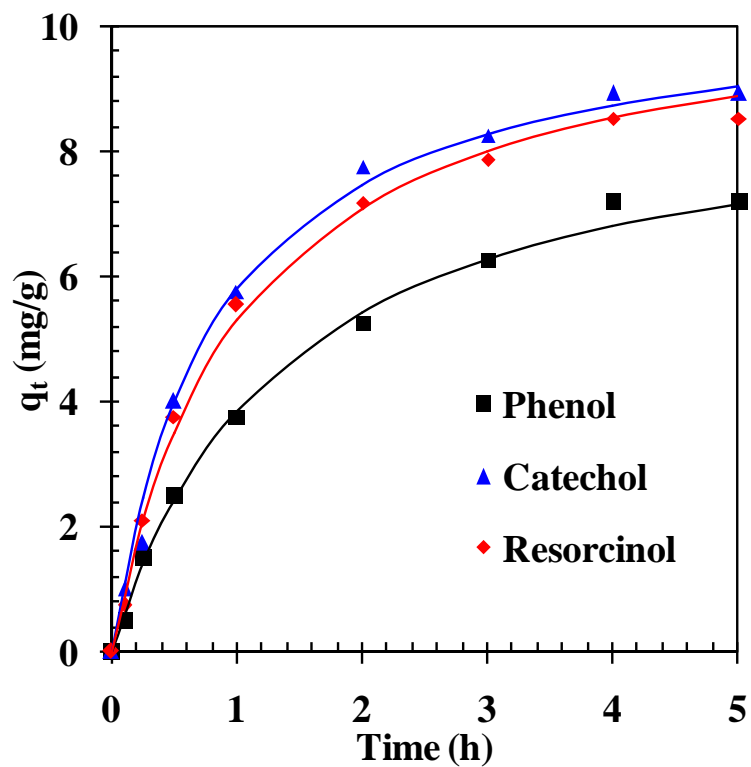


Figure 4.4.4. Pseudo-second-order kinetic plot for the removal of phenol, catechol and resorcinol by RHA, $pH_0=6.0$, $C_0=250$ mg/L, $m=20$ g/L, $T=30$ °C.

4.4.5 Adsorption Isotherm Modeling

4.4.5.1 Individual adsorption of phenol, catechol and resorcinol

The equilibrium uptakes and the adsorption yields obtained for single component phenol, catechol and resorcinol solution are shown in [Table 4.4.3](#). [Figure 4.4.5](#) illustrates that an increase in the initial concentration of phenol, catechol and resorcinol increased the equilibrium uptake. At higher concentrations, the driving force required to overcome the resistances to the mass transfer of adsorbate between the solution and the solid phases becomes greater, and thus the equilibrium uptake increases. It may also be seen in [Figure 4.4.5](#) that the adsorption capacity of RHA for catechol is greater than that of resorcinol and phenol.

The Langmuir, Freundlich and R-P isotherms are widely used for single-component adsorption data analysis. Equilibrium adsorption data for single-component aqueous solutions containing phenol, catechol and resorcinol were fitted to these three isotherm models. Results are shown in [Table 4.4.4](#) along-with R^2 and SSE values. The single-component Langmuir constant, q_m , is the monolayer saturation at equilibrium [[Langmuir, 1918](#)]. The values of q_m in [Table 4.4.3](#) indicate that the amount of catechol adsorbed per unit mass of RHA for the complete monolayer surface coverage was little higher than that of phenol and resorcinol. A large value of constant K_L , which is related to adsorbate affinity for RHA, indicates strong bonding of catechol to RHA. The value of constant $1/n$ in Freundlich isotherm [[Freundlich, 1906](#)] indicates affinity to RHA. It also indicates the heterogeneity of the adsorbent sites. RHA shows greater

heterogeneity for catechol than that for phenol and resorcinol (Table 4.4.3). The magnitude of K_F also showed the higher uptake of catechol than that of resorcinol and phenol by RHA. For favorable adsorption, value of R-P constant (β) normally lies between 0 and 1.

It may be seen in Table 4.4.4 that the SSE values are lower and R^2 values are higher for R-P or Freundlich isotherm fitting than that for Langmuir indicating better representation of isotherm data by R-P or Freundlich isotherms. However, the difference in SSE or R^2 values for any of the isotherms is marginal and isotherm can be represented by any of the R-P, Freundlich or Langmuir isotherms. Allen et al. [2004] mentioned that Freundlich and Langmuir equation show good fit for moderate concentration range data with two constants, however, wide concentration range cannot be fitted with two constants. R-P equation contains three parameters and represents wide range of concentration data.

The FTIR spectra analysis of blank RHA and individually loaded phenol, catechol and resorcinol onto RHA have been studied in the range of 400-4000 cm^{-1} wave numbers (Figure 4.4.6) to understand the change of function group after loading of phenol, catechol and resorcinol onto RHA. FTIR shows a broad peak in the region 3320-3600 cm^{-1} in blank RHA. This band for the hydroxyl group is due to -OH deformation vibrations and -OH stretching frequencies which suggested the presence of alcoholic or phenolic components [Zhou et al., 2007]. It may be seen that the adsorbate loaded RHA has much sharper peak as compared to blank-RHA which has broader

peak. The peaks at 2815 cm^{-1} in blank RHA may be due to the $-\text{CH}$ stretching of phenolic rings or due to the symmetric CH_3 stretch of the methoxyl group. These peaks get shifted to higher wave numbers 2830 , 2834 and 2854 cm^{-1} in phenol, resorcinol and catechol loaded RHA, respectively. Blank RHA show peaks at 1355 and 1593 cm^{-1} . These peaks may be due to OH deformation and stretching of $\text{C}=\text{C}$ aromatic rings [Zhou et al., 2007; Terzyk, 2001]. The band at 1355 cm^{-1} could also be due to both OH in-plane bending and CH bending [Sharma et al., 2004]. The strong band observed around 1091 cm^{-1} may be assigned to $\text{C}-\text{O}$ stretching in aryl ethers. In adsorbate loaded-RHA spectra, not only the intensity of these band increases but also shift in peaks is observed indicating utilization of these groups for adsorption purpose [Vasudevan and Stone, 1996]. Substitution of functional groups on benzene ring provides different inductive and resonance effects [Star et al., 2003]. π -donating strength of the host aromatic ring is known to be enhanced by the substitution of hydroxyl group which is an electron-donating functional group. This increases the adsorption affinity of the phenolic compounds to RHA [Lin and Xing, 2008]. FTIR analysis shows that the interaction between RHA and adsorbates (phenol, catechol and resorcinol) happens with the help of $-\text{OH}$ groups. Since π - π dispersive interactions become stronger with an increase in the number of hydroxyl groups [Suresh et al., 2011b]. Therefore, the adsorption of phenol is less than the catechol and resorcinol onto RHA.

Table 4.4.3. Individual adsorption equilibrium uptakes and yields of phenol, catechol and resorcinol adsorption at different initial concentrations onto rice husk ash.

C_o	C_e	q_e	Ad%
(mmol/L)	(mmol/L)	(mmol/g)	-
Phenol			
0.266	0.212	0.003	20.250
2.597	1.421	0.059	45.294
5.173	3.254	0.096	37.112
7.830	5.300	0.127	32.316
10.480	6.774	0.185	35.361
13.510	9.083	0.221	32.773
Catechol			
0.229	0.162	0.003	29.434
0.865	0.368	0.025	57.450
2.141	0.906	0.062	57.677
6.747	3.767	0.149	44.167
8.952	4.757	0.210	46.860
13.525	7.430	0.305	45.068
Resorcinol			
0.239	0.169	0.004	29.454
0.465	0.238	0.011	48.718
1.164	0.519	0.032	55.448
2.553	1.270	0.064	50.262
5.225	2.960	0.113	43.346
6.687	4.093	0.130	38.795
8.958	5.092	0.193	43.156
13.510	7.947	0.278	41.176

Table 4.4.4. Isotherm parameter fitted on isotherm model for the removal of phenol, catechol and resorcinol by rice husk ash.

Adsorbate	Henry	R^2	SSE
Phenol	$q_{e,P} = 0.026C_{e,P}$	0.977	0.0010
Catechol	$q_{e,P} = 0.042C_{e,P}$	0.990	0.0009
Resorcinol	$q_{e,P} = 0.036C_{e,P}$	0.987	0.0010
Adsorbate	Langmuir	R^2	SSE
Phenol	$q_{e,P} = \frac{0.85 \times 0.038C_{e,P}}{1 + 0.038C_{e,P}}$	0.980	0.0006
Catechol	$q_{e,C} = \frac{2.22 \times 0.0212C_{e,C}}{1 + 0.0212C_{e,C}}$	0.990	0.0007
Resorcinol	$q_{e,R} = \frac{0.81 \times 0.056C_{e,R}}{1 + 0.056C_{e,R}}$	0.972	0.0008
Adsorbate	Freundlich	R^2	SSE
Phenol	$q_{e,P} = 0.036C_{e,P}^{0.819}$	0.983	0.0005
Catechol	$q_{e,C} = 0.052C_{e,C}^{0.88}$	0.991	0.0006
Resorcinol	$q_{e,R} = 0.046C_{e,R}^{0.841}$	0.975	0.0007
Adsorbate	Redlich-Peterson	R^2	SSE
Phenol	$q_{e,P} = \frac{1.08C_{e,P}}{1 + 28.72C_{e,P}^{0.186}}$	0.983	0.0005
Catechol	$q_{e,C} = \frac{3.32C_{e,C}}{1 + 63.34C_{e,C}^{0.121}}$	0.991	0.0006
Resorcinol	$q_{e,R} = \frac{2.87C_{e,R}}{1 + 61.86C_{e,R}^{0.161}}$	0.975	0.0007

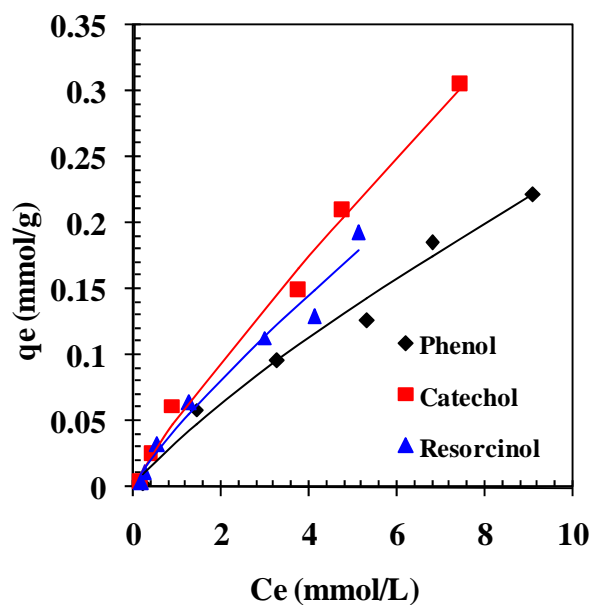


Figure 4.4.5. Equilibrium adsorption isotherms for the individual adsorption of phenol, catechol and resorcinol onto rice husk ash. Experimental data represented by points and R-P isotherm fitting represented by lines.

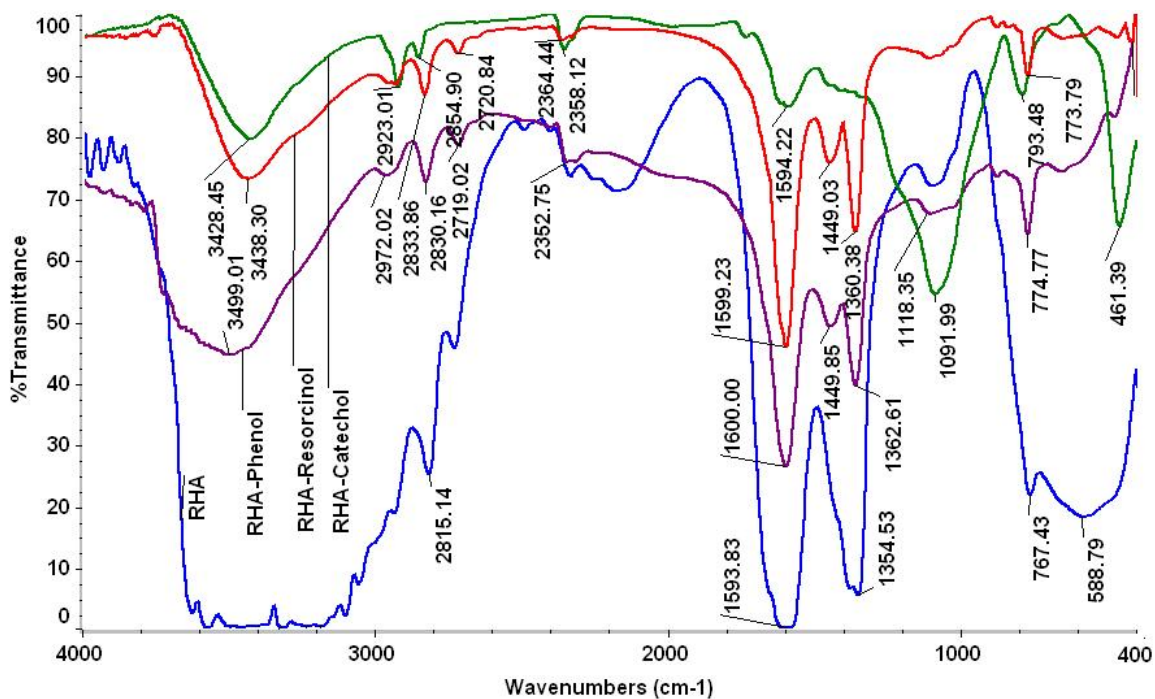


Figure 4.4.6. FTIR analysis of raw RHA, phenol, catechol and resorcinol loaded RHA.

4.4.5.2 Binary adsorption of catechol-phenol, catechol-resorcinol and phenol-resorcinol

Binary adsorption isotherm data for phenol-catechol, catechol-resorcinol and phenol-resorcinol systems onto RHA were collected by taking four solutions of each adsorbate having different initial concentrations of the adsorbate. Thus, a total of 16 experiments were performed for catechol-phenol, catechol-resorcinol and phenol-resorcinol systems. These initial concentrations along with equilibrium adsorption values for phenol-catechol, catechol-resorcinol and phenol-resorcinol systems are summarized in [Tables 4.4.5, 4.4.6 and 4.4.7](#), respectively.

The binary adsorption data of phenol-catechol, catechol-resorcinol and phenol-resorcinol onto RHA have been fitted to various multi-component isotherm models, viz., non-modified, modified and extended Langmuir models; extended Freundlich and SRS models; non-modified and modified R-P models. The parametric values of all the multicomponent adsorption models and the SSE value between the experimental and calculated q_e values for the entire data set of phenol-catechol, catechol-resorcinol and phenol-resorcinol are also given in [Tables 4.4.8, 4.4.9 and 4.4.10](#), respectively. The comparisons of the experimental and calculated q_e values of phenol-catechol, catechol-resorcinol and phenol-resorcinol in mixtures are also presented by the parity plots in [Figure 4.4.7, 4.4.8 and 4.4.9](#), respectively.

It may be seen that the equilibrium uptake of phenol decreases with an increase in resorcinol concentration and vice versa. For instance, at 5.17 ± 0.01 mmol/L initial phenol concentration, in the absence of resorcinol and in the presence of 0.853 mmol/L resorcinol concentration, adsorbed phenol quantities at equilibrium are found to be

0.096 and 0.066 mmol/g, respectively. Similarly at 5.2 ± 0.1 mmol/L initial resorcinol concentration, in the absence of phenol and in the presence of 0.89 mmol/L phenol concentration, adsorbed resorcinol quantities at equilibrium are found to be 0.113 and 0.107 mmol/g, (Table 4.4.3 and Table 4.4.7) respectively. Thus, the combined effect of phenol and resorcinol on the total sorption is antagonistic. Similarly, the combined effect of catechol-phenol and catechol-resorcinol on the total sorption is antagonistic in nature (Table 4.4.3, Table 4.4.5 and Table 4.4.6).

The binary adsorption data of catechol-phenol, catechol-resorcinol and phenol-catechol aqueous solution onto RHA have been fitted to various multi-component isotherm models using SSE error function. The multi-component non-modified R-P model (equations 4.4.2, 4.4.3 and 4.4.4) showed poor fit to catechol-phenol (CP system), catechol-resorcinol (CR system) and phenol-catechol (PC system) experimental data.

$$\text{CP: } q_{e,C} = \frac{3.321C_{e,C}}{1 + (63.336C_{e,C}^{0.121} + 28.722C_{e,P}^{0.186})}; q_{e,P} = \frac{1.080C_{e,P}}{1 + (63.336C_{e,C}^{0.121} + 28.722C_{e,P}^{0.186})} \quad \text{SSE}=0.0682 \quad (4.4.2)$$

$$\text{CR: } q_{e,C} = \frac{3.321C_{e,C}}{1 + (63.34C_{e,C}^{0.121} + 61.86C_{e,R}^{0.161})}; q_{e,R} = \frac{2.87C_{e,R}}{1 + (63.34C_{e,C}^{0.121} + 61.86C_{e,R}^{0.161})} \quad \text{SSE}=0.048 \quad (4.4.3)$$

$$\text{PC: } q_{e,P} = \frac{1080C_{e,P}}{1 + (28.72C_{e,P}^{0.186} + 61.86C_{e,R}^{0.161})}; q_{e,R} = \frac{2.87C_{e,R}}{1 + (28.72C_{e,P}^{0.186} + 61.86C_{e,R}^{0.161})} \quad \text{SSE}=0.024 \quad (4.4.4)$$

To improve the accuracy of non-modified R-P model, an interaction term, $\eta_{RP,i}$, was incorporated in the competitive non-modified R-P model to formulate the modified

competitive R-P model. The value of $\eta_{RP,i}$ depends upon the characteristic of each adsorbate and also on the concentration of the other adsorbate. All the modified R-P coefficients ($\eta_{RP,i}$) estimated were found to be slightly less than 1.0 indicating that the use of $\eta_{RP,i}$ increased the fitting in modified R-P model (equations 4.4.5, 4.4.6 and 4.4.7).

$$\text{CP: } q_{e,C} = \frac{3.321(C_{e,C}/0.67)}{1+(63.336(C_{e,C}/0.67)^{0.121}+28.722(C_{e,P}/0.163)^{0.186})}; q_{e,P} = \frac{1.08(C_{e,P}/0.163)}{1+(63.336(C_{e,C}/0.675)^{0.121}+28.722(C_{e,P}/0.163)^{0.186})} \quad \text{SSE}=0.0040 \quad (4.4.5)$$

$$\text{CR: } q_{e,C} = \frac{3.321(C_{e,C}/0.49)}{1+(63.34(C_{e,C}/0.49)^{0.121}+61.86(C_{e,R}/0.323)^{0.161})}; q_{e,R} = \frac{2.871(C_{e,R}/0.323)}{1+(63.34(C_{e,C}/0.49)^{0.121}+61.86(C_{e,R}/0.323)^{0.161})} \quad \text{SSE}=0.0051 \quad (4.4.6)$$

$$\text{PR: } q_{e,P} = \frac{1.08(C_{e,P}/0.393)}{1+(28.72(C_{e,P}/0.393)^{0.186}+61.86(C_{e,R}/0.767)^{0.161})}; q_{e,R} = \frac{2.871(C_{e,R}/0.767)}{1+(28.72(C_{e,P}/0.393)^{0.186}+61.86(C_{e,R}/0.767)^{0.161})} \quad \text{SSE}=0.0103 \quad (4.4.7)$$

The multi-component non-modified Langmuir model shown by following set of equations showed a poor fit to the experimental data (SSE=0.011):

$$\text{CP: } q_{e,C} = \frac{2.22 \times 0.021 C_{e,C}}{1+(0.04 C_{e,P} + 0.021 C_{e,C})}; q_{e,P} = \frac{0.85 \times 0.04 C_{e,P}}{1+(0.04 C_{e,P} + 0.021 C_{e,C})} \quad \text{SSE}=0.0251 \quad (4.4.8)$$

$$\text{CR: } q_{e,C} = \frac{2.22 \times 0.021 C_{e,C}}{1+(0.056 C_{e,R} + 0.021 C_{e,C})}; q_{e,R} = \frac{0.81 \times 0.056 C_{e,R}}{1+(0.021 C_{e,C} + 0.056 C_{e,R})} \quad \text{SSE}=0.0135 \quad (4.4.9)$$

$$\text{PR: } q_{e,P} = \frac{0.85 \times 0.04 C_{e,C}}{1+(0.056 C_{e,R} + 0.04 C_{e,P})}; q_{e,R} = \frac{0.81 \times 0.056 C_{e,R}}{1+(0.04 C_{e,P} + 0.056 C_{e,R})} \quad \text{SSE}=0.011 \quad (4.4.10)$$

As discussed earlier, Langmuir isotherm does not well represents the single component adsorption behavior. Therefore, non-modified Langmuir model is also not

able to represent the multi-component adsorption behavior. For that reason, modified isotherms related to the individual isotherm parameters and the correction factors are used.

To improve the accuracy of non-modified Langmuir model, [Bellot and Condoret \[1993\]](#) incorporated an interaction term, $\eta_{L,i}$, in the competitive non-modified Langmuir model to formulate the modified competitive Langmuir model. The value of $\eta_{L,i}$ depends upon the characteristic of each adsorbate and also on the concentration of other adsorbates. Interaction terms for Langmuir model ($\eta_{L,i}$) in the modified Langmuir model (equations 4.4.11, 4.4.12 and 4.4.13) significantly improved the fit of the non-modified Langmuir model (equations 4.4.8, 4.4.9 and 4.4.10) as shown by decrease in SSE values:

$$CP: q_{e,C} = \frac{2.23 \times 0.021 (C_{e,C}/0.87)}{1 + (0.021 (C_{e,C}/0.87) + 0.04 (C_{e,P}/0.51))}; q_{e,P} = \frac{0.85 \times 0.04 (C_{e,P}/0.51)}{1 + (0.021 (C_{e,C}/0.87) + 0.04 (C_{e,P}/0.51))} \quad SSE=0.0047 \quad (4.4.11)$$

$$CR: q_{e,C} = \frac{2.23 \times 0.021 (C_{e,C}/0.861)}{1 + (0.021 (C_{e,C}/0.861) + 0.056 (C_{e,R}/0.64))}; q_{e,R} = \frac{0.81 \times 0.056 (C_{e,R}/0.64)}{1 + (0.056 (C_{e,R}/0.64) + 0.021 (C_{e,C}/0.861))} \quad SSE=0.0044 \quad (4.4.12)$$

$$PR: q_{e,P} = \frac{0.85 \times 0.04 (C_{e,P}/1.11)}{1 + (0.04 (C_{e,P}/1.11) + 0.056 (C_{e,R}/1.08))}; q_{e,R} = \frac{0.81 \times 0.056 (C_{e,R}/0.64)}{1 + (0.056 (C_{e,R}/1.08) + 0.04 (C_{e,P}/1.11))} \quad SSE=0.0105 \quad (4.4.13)$$

[Yang \[1987\]](#) gave an extended Langmuir isotherm model for multi-component systems assuming that the surface sites are uniform, and that all the adsorbate molecules in the solution compete for the same surface sites. The use of the extended

Langmuir model on binary system of catechol-phenol, catechol-resorcinol and phenol-resorcinol (equations 4.4.14, 4.4.15 and 4.4.16) improved the fit of the binary adsorption data over non-modified and modified competitive Langmuir models:

$$CP: q_{e,C} = \frac{2.96 \times 0.017 C_{e,C}}{1 + (0.017 C_{e,C} + 0.02 C_{e,P})}; q_{e,P} = \frac{2.96 \times 0.02 C_{e,P}}{1 + (0.017 C_{e,C} + 0.02 C_{e,P})} \quad SSE=0.0041 \quad (4.4.14)$$

$$CR: q_{e,C} = \frac{0.51 \times 0.137 C_{e,C}}{1 + (0.137 C_{e,C} + 0.167 C_{e,R})}; q_{e,R} = \frac{0.51 \times 0.167 C_{e,R}}{1 + (0.137 C_{e,C} + 0.167 C_{e,R})} \quad SSE=0.0039 \quad (4.4.15)$$

$$PR: q_{e,P} = \frac{0.161 \times 0.542 C_{e,C}}{1 + (0.542 C_{e,P} + 0.711 C_{e,R})}; q_{e,R} = \frac{0.161 \times 0.711 C_{e,R}}{1 + (0.542 C_{e,P} + 0.711 C_{e,R})} \quad SSE=0.0055 \quad (4.4.16)$$

Constant K_i (Table 4.4.8, 4.4.9 and 4.4.10) in the extended Langmuir model reflects the affinity between RHA and the adsorbates in the binary system. The value of K_i for catechol-phenol was found to be 0.017 and 0.020 L/mmol; for catechol-resorcinol was found to be 0.137 and 0.167 L/mmol; and for phenol-resorcinol was found to be 0.542 and 0.712 L/mmol; respectively. The overall total adsorbate uptakes (q_{\max}) for catechol-phenol, catechol-resorcinol and phenol-resorcinol by RHA were found to be 2.96, 0.51 and 0.16 mmol/g, respectively, which is much lower than the sum of the maximum total capacities of catechol-phenol (2.22+0.85=3.07 mmol/g), catechol-resorcinol (2.22+0.81=3.03 mmol/g) and phenol-resorcinol (0.85+0.81=1.66 mmol/g) resulting from the single component adsorption. Thus, it seems that phenol and resorcinol compete more as compared to catechol and resorcinol and catechol and phenol for same adsorption sites present on RHA. For this reason, mono-component Langmuir model is not able to represent the single component adsorption data as competitive adsorption behavior.

Sheindorf-Rebhum-Sheintuch (SRS) model is applicable to those systems where adsorption energies of sites are exponentially distributed, and that each component individually obeys the single-component Freundlich isotherm. The isotherm coefficients, except for the adsorption competition coefficient (a_{ij}), are known from the single component isotherm fitting data [Sheindorf et al., 1981]. The adsorption competition coefficient (a_{ij}) describes the inhibition to the adsorption of component i by component j . The values of a_{ij} for the multicomponent SRS model were evaluated by minimizing the SSE. For systems which are represented by the SRS model, product of the competition coefficients a_{ij} and a_{ji} is close to unity [Srivastava et al., 2008a,b]. The binary adsorption of catechol-phenol, catechol-resorcinol and phenol-resorcinol onto RHA can be represented by following form of SRS equations:

$$\text{CP: } q_{e,C} = 0.052C_{e,C} \left(0.001C_{e,P} + C_{e,C} \right)^{(0.88-1)} ; q_{e,P} = 0.036C_{e,P} \left(C_{e,P} + 0.001C_{e,C} \right)^{(0.82-1)} \quad \text{SSE}=0.0205 \quad (4.4.16)$$

$$\text{CR: } q_{e,C} = 0.052C_{e,C} \left(C_{e,C} + 0.001C_{e,R} \right)^{(0.88-1)} ; q_{e,R} = 0.046C_{e,R} \left(0.001C_{e,C} + C_{e,R} \right)^{(0.841-1)} \quad \text{SSE}=0.010 \quad (4.4.17)$$

$$\text{PR: } q_{e,P} = 0.036C_{e,P} \left(C_{e,P} + 2.1101C_{e,R} \right)^{(0.823-1)} ; q_{e,R} = 0.046C_{e,R} \left(2.5043C_{e,P} + C_{e,R} \right)^{(0.841-1)} \quad \text{SSE}=0.010 \quad (4.4.18)$$

A higher value of a_{PR} suggests that the adsorption of phenol onto RHA was more significantly affected by the presence of resorcinol and catechol. Thus, the SRS model was not able to satisfactorily represent the binary sorption data.

Fritz and Schlunder [1974] gave an extended Freundlich isotherm for binary mixtures of phenolic substitutes on activated carbon. Extended Freundlich isotherm

gives better fit for systems with significant non-ideal effects and heterogeneous surfaces [McKay and Al-Duri, 1991]. Since RHA surface is heterogeneous in nature and Freundlich model represented the mono-component isotherm data, therefore, extended Freundlich model also gave satisfactory fit to the binary experimental equilibrium data. The adsorption of catechol-phenol, catechol-resorcinol and phenol-resorcinol sorption onto RHA from binary mixture can be represented by following forms of extended Freundlich model equations:

$$\text{CP: } q_{e,C} = \frac{0.052C_{e,C}^{0.89}}{C_{e,C}^{0.01} + 14.985C_{e,P}^{465.22}}; q_{e,P} = \frac{0.036C_{e,P}^{0.82}}{C_{e,P}^{0.001} + 1.55C_{e,C}^{1.55}} \quad \text{SSE}=0.0797 \quad (4.4.19)$$

$$\text{CR: } q_{e,C} = \frac{0.0517C_{e,C}^{10.671}}{C_{e,C}^{9.791} + 0.001C_{e,R}^{0.2040}}; q_{e,R} = \frac{0.0457C_{e,R}^{77.474}}{C_{e,R}^{76.634} + 11.669C_{e,C}^{205.117}} \quad \text{SSE}=0.034 \quad (4.4.20)$$

$$\text{PR: } q_{e,P} = \frac{0.0361C_{e,P}^{0.8236}}{C_{e,P}^{-0.0001} + 1.064 \times 10^{-5} C_{e,R}^{0.918}}; q_{e,R} = \frac{0.0457C_{e,R}^{0.841}}{C_{e,R}^{-0.0019} + 9.903 \times 10^{-7} C_{e,P}^{10.096}} \quad \text{SSE}=0.0079 \quad (4.4.21)$$

The comparisons of the experimental and calculated q_e values of catechol-phenol, catechol-resorcinol and phenol-resorcinol in mixtures are also presented by the parity plots in Figures 4.4.4, 4.4.5 and 4.4.6, respectively. To determine the best fit model for both binary adsorption system, SSE values of different isotherm models were compared. Extended Langmuir model (SSE=0.0041, SSE=0.0039 and SSE=0.0055) showed best-fits for the experimental binary adsorption data for all the systems. It seems that components of both binary adsorbates compete for the same adsorption sites on RHA. Thus, extended Langmuir model which assumes overlapping of sites for different adsorbates better represents the isotherm data.

Table 4.4.5. Comparison of individual and total adsorption equilibrium uptakes and yields found at different catechol (C) concentrations in the absence and presence of increasing concentrations of phenol (P) onto RHA.

$C_{o,C}$	$C_{o,P}$	$C_{e,C}$	$C_{e,P}$	$q_{e,C}$	$q_{e,P}$	$Ad_C\%$	$Ad_P\%$	$Ad_{Tot}\%$
(mmol/l)	(mmol/l)	(mmol/l)	(mmol/l)	(mmol/g)	(mmol/g)	-	-	-
0.496	0.459	0.140	0.179	0.018	0.014	71.810	60.940	66.590
0.552	1.019	0.157	0.495	0.020	0.026	71.640	51.410	58.520
0.454	2.511	0.119	1.171	0.017	0.067	73.800	53.340	56.470
0.508	5.470	0.143	2.318	0.018	0.158	71.750	57.620	58.820
0.916	0.586	0.359	0.229	0.028	0.018	60.840	60.920	60.870
0.860	1.042	0.286	0.525	0.029	0.026	66.770	49.590	57.360
0.908	2.589	0.327	1.333	0.029	0.063	64.040	48.530	52.560
0.871	4.949	0.286	2.505	0.029	0.122	67.150	49.390	52.040
2.237	0.572	1.082	0.200	0.058	0.019	51.620	64.990	54.340
2.082	1.021	0.935	0.470	0.057	0.028	55.090	53.970	54.720
2.061	2.490	0.984	1.322	0.054	0.058	52.250	46.900	49.320
2.191	5.232	1.055	2.385	0.057	0.142	51.830	54.420	53.650
3.919	0.555	2.145	0.243	0.089	0.016	45.270	56.130	46.610
4.257	1.082	2.260	0.682	0.100	0.020	46.910	37.000	44.900
4.563	2.822	2.286	1.476	0.114	0.067	49.900	47.700	49.060
4.171	5.067	2.208	2.362	0.098	0.135	47.060	53.380	50.530

Table 4.4.6. Comparison of individual and total adsorption equilibrium uptakes and yields found at different catechol (C) concentrations in the absence and presence of increasing concentrations of resorcinol (R) onto RHA.

$C_{o,C}$	$C_{o,R}$	$C_{e,C}$	$C_{e,R}$	$q_{e,C}$	$q_{e,R}$	Ad_C %	Ad_R %	Ad_{Tot} %
(mmol/l)	(mmol/l)	(mmol/l)	(mmol/l)	(mmol/g)	(mmol/g)	-	-	-
0.511	0.470	0.147	0.120	0.018	0.018	71.280	74.500	72.820
0.486	0.963	0.126	0.438	0.018	0.026	74.000	54.500	61.040
0.537	2.244	0.154	0.892	0.019	0.068	71.430	60.240	62.400
0.506	4.505	0.144	2.250	0.018	0.113	71.560	50.060	52.230
0.896	0.482	0.273	0.179	0.031	0.015	69.580	62.760	67.190
0.962	0.922	0.342	0.419	0.031	0.025	64.410	54.570	59.590
0.917	2.253	0.309	0.909	0.030	0.067	66.280	59.650	61.570
0.921	4.477	0.363	2.069	0.028	0.120	60.570	53.790	54.950
2.275	0.476	1.119	0.166	0.058	0.015	50.810	65.090	53.280
2.228	0.927	0.939	0.438	0.064	0.024	57.870	52.710	56.350
2.259	2.336	0.943	0.883	0.066	0.073	58.260	62.180	60.260
2.272	4.462	0.981	1.948	0.065	0.126	56.820	56.350	56.510
4.473	0.408	2.410	0.122	0.103	0.014	46.120	70.040	48.120
4.501	0.892	2.341	0.390	0.108	0.025	47.980	56.270	49.350
4.508	2.331	2.175	0.906	0.117	0.071	51.750	61.130	54.950
4.481	4.479	2.519	2.190	0.098	0.114	43.780	51.100	47.440

Table 4.4.7. Comparison of individual and total adsorption equilibrium uptakes and yields found at different resorcinol (R) concentrations in the absence and presence of increasing concentrations of Phenol (P) onto RHA.

$C_{o,R}$	$C_{o,P}$	$C_{e,R}$	$C_{e,P}$	$q_{e,R}$	$q_{e,P}$	Ad_R %	Ad_P %	Ad_{Tot} %
(mmol/l)	(mmol/l)	(mmol/l)	(mmol/l)	(mmol/g)	(mmol/g)	-	-	-
0.862	0.582	0.472	0.472	0.020	0.005	45.3	18.9	34.6
1.250	0.911	0.664	0.361	0.029	0.027	46.9	60.3	52.5
2.654	0.865	1.215	0.365	0.072	0.025	54.2	57.8	55.1
5.151	0.891	3.013	0.576	0.107	0.016	41.5	35.3	40.6
0.778	1.007	0.459	0.529	0.016	0.024	41.0	47.5	44.7
1.473	1.436	0.658	0.612	0.041	0.041	55.3	57.4	56.4
3.106	1.570	1.604	0.876	0.075	0.035	48.4	44.2	47.0
5.155	1.537	3.059	0.842	0.105	0.035	40.7	45.2	41.7
0.436	2.548	0.055	0.956	0.019	0.080	87.5	62.5	66.1
0.838	2.605	0.228	1.292	0.030	0.066	72.8	50.4	55.8
1.966	2.436	0.849	1.372	0.056	0.053	56.8	43.7	49.5
4.004	2.580	2.356	1.503	0.082	0.054	41.2	41.7	41.4
0.420	4.883	0.127	3.331	0.015	0.078	69.7	31.8	34.8
0.853	5.180	0.423	3.857	0.021	0.066	50.4	25.6	29.1
2.173	5.303	1.269	3.589	0.045	0.086	41.6	32.3	35.0
4.213	5.305	2.990	3.836	0.061	0.073	29.0	27.7	28.3

Table 4.4.8. Multi-component isotherm parameter values for the simultaneous removal of phenol and catechol by RHA.

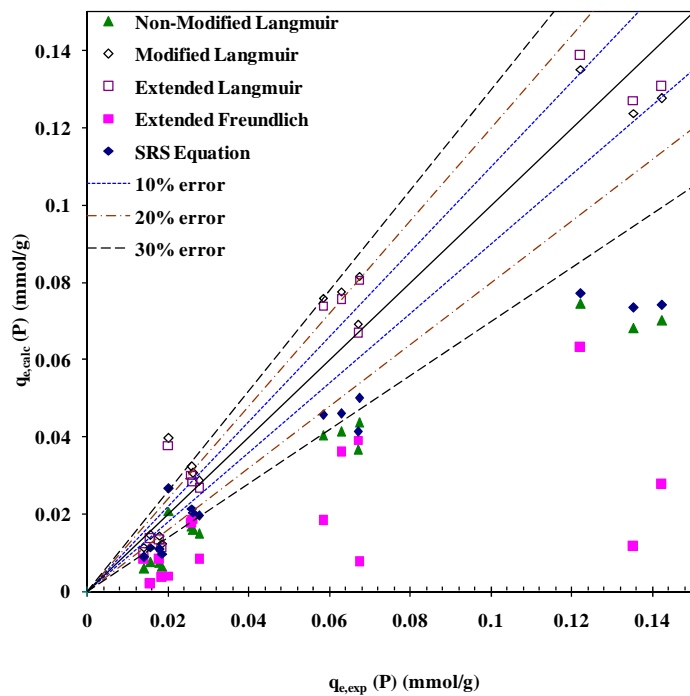
Multicomponent isotherm models	Parameter	Phenol	Catechol
Non-modified Langmuir model	R^2	0.94	0.98
	SSE	0.0251	
Non-modified R-P model	R^2	0.94	0.97
	SSE	0.0683	
Modified Langmuir model	$\eta_{L,i}$	0.507	0.870
	R^2	0.93	0.97
	SSE	0.0047	
Extended Langmuir model	K_i	0.020	0.017
	q_{\max}	2.961	
	R^2	0.94	0.98
	SSE	0.0041	
Modified R-P model	$\eta_{RP,i}$	0.163	0.675
	R^2	0.94	0.97
	SSE	0.0040	
Extended Freundlich model	x_i	0.001	0.010
	y_i	1.549	14.985
	z_i	1.549	465.225
	R^2	0.50	0.21
	SSE	0.0797	
SRS model	a_{ij}	1	0.001
	a_{ij}	0.001	1
	R^2	0.93	0.98
	SSE	0.0206	

Table 4.4.9. Multi-component isotherm parameter values for the simultaneous removal of catechol and resorcinol by RHA.

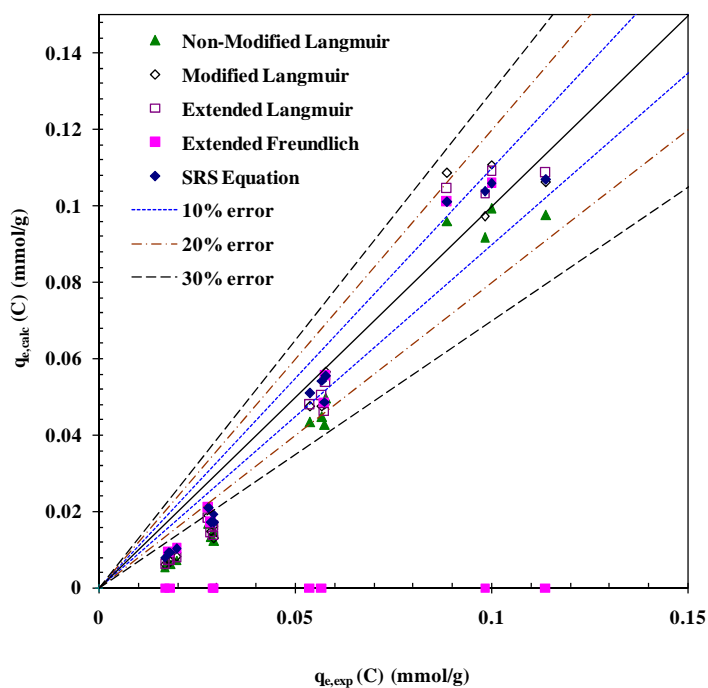
Multicomponent isotherm models	Parameter	Catechol	Resorcinol
Non-modified Langmuir model	R^2	0.95	0.95
	SSE	0.0135	
Non-modified R-P model	R^2	0.94	0.94
	SSE	0.048	
Modified Langmuir model	$\eta_{L,i}$	0.681	0.640
	R^2	0.95	0.96
	SSE	0.0044	
Extended Langmuir model	K_i	0.137	0.167
	q_{\max}	0.507	
	R^2	0.95	0.94
	SSE	0.0039	
Modified R-P model	$\eta_{RP,i}$	0.492	0.323
	R^2	0.94	0.94
	SSE	0.0051	
Extended Freundlich model	x_i	9.790	76.633
	y_i	0.001	11.669
	z_i	0.204	205.117
	R^2	0.95	0.53
	SSE	0.0340	
SRS model	a_{ij}	1	0.001
	a_{ij}	0.001	1
	R^2	0.96	0.96
	SSE	0.0100	

Table 4.4.10. Multi-component isotherm parameter values for the simultaneous removal of phenol and resorcinol by RHA.

Multicomponent isotherm models	Parameter	Phenol	Resorcinol
Non-modified Langmuir model	R^2	0.63	0.85
	SSE	0.011	
Non-modified R-P model	R^2	0.64	0.84
	SSE	0.024	
Modified Langmuir model	$\eta_{L,i}$	1.110	1.077
	R^2	0.62	0.85
	SSE	0.0105	
Extended Langmuir model	K_i	0.542	0.712
	q_{\max}	0.161	
	R^2	0.71	0.88
	SSE	0.0055	
Modified R-P model	$\eta_{RP,i}$	0.393	0.767
	R^2	0.64	0.84
	SSE	0.0103	
Extended Freundlich model	x_i	0.0001	0.0001
	y_i	1.0635E-05	9.9034E-07
	z_i	9.918	10.096
	R^2	0.64	0.92
	SSE	0.0079	
SRS model	a_{ij}	1	2.1101
	a_{ij}	2.5043	1
	R^2	0.64	0.86
	SSE	0.010	

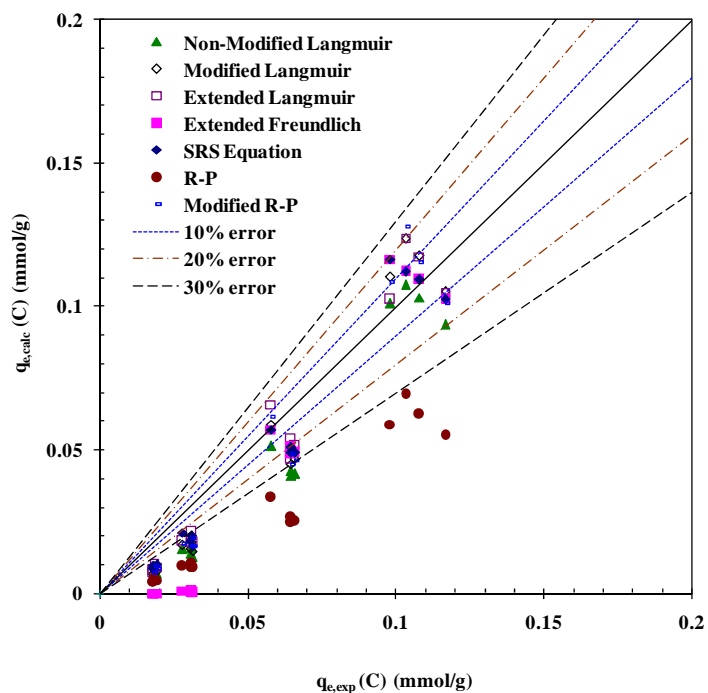


(a) Phenol

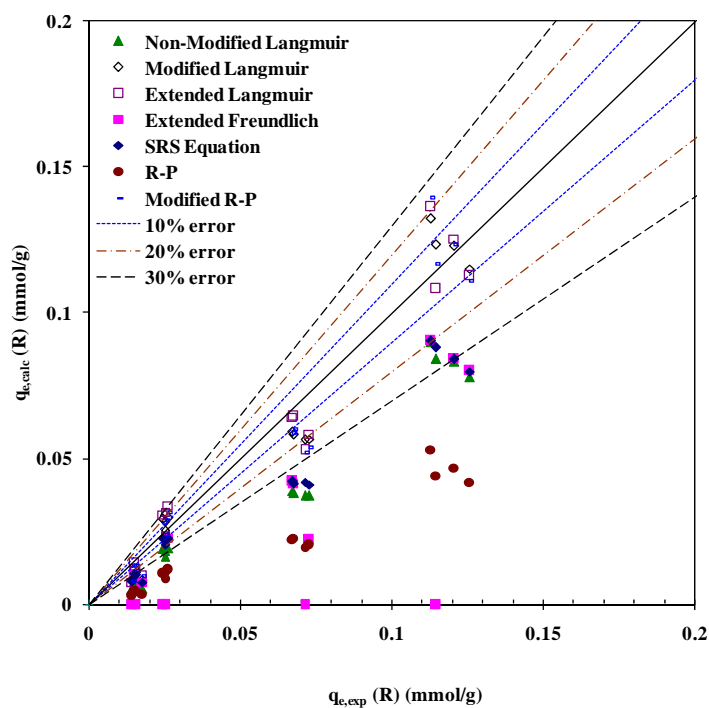


(b) Catechol

Figure 4.4.7. Comparison of the experimental and calculated q_e values for phenol and catechol adsorption from a binary mixture of phenol and catechol.

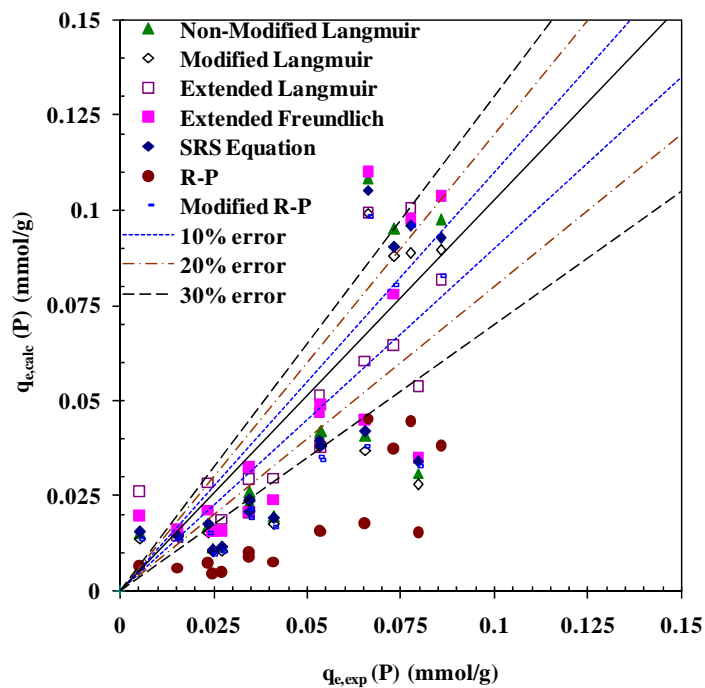


(a) Catechol

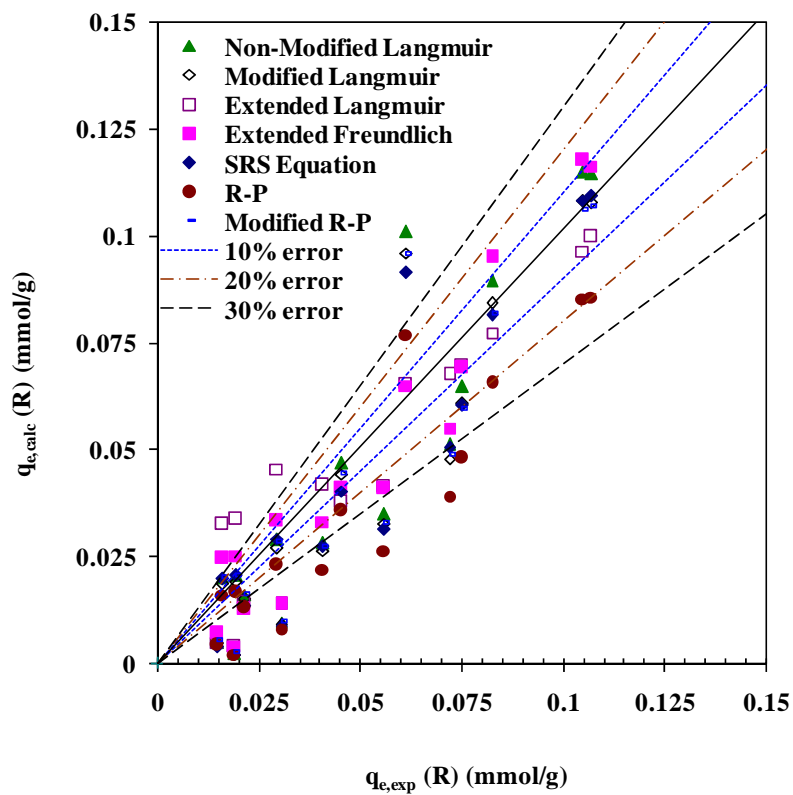


(b) Resorcinol

Figure 4.4.8. Comparison of the experimental and calculated q_e values for catechol and resorcinol adsorption from a binary mixture of catechol and resorcinol.

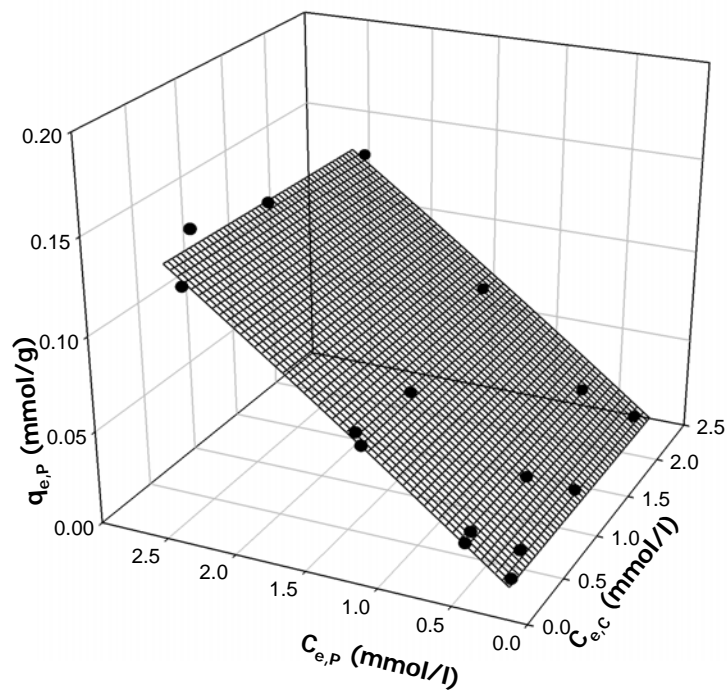


(a) Phenol

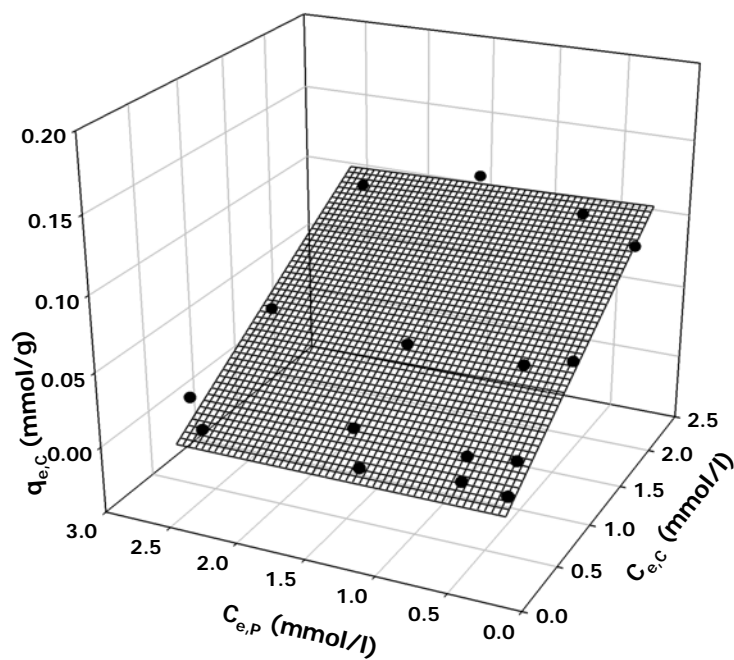


(b) Resorcinol

Figure 4.4.9. Comparison of the experimental and calculated q_e values for phenol and resorcinol adsorption from a binary mixture of phenol and resorcinol.

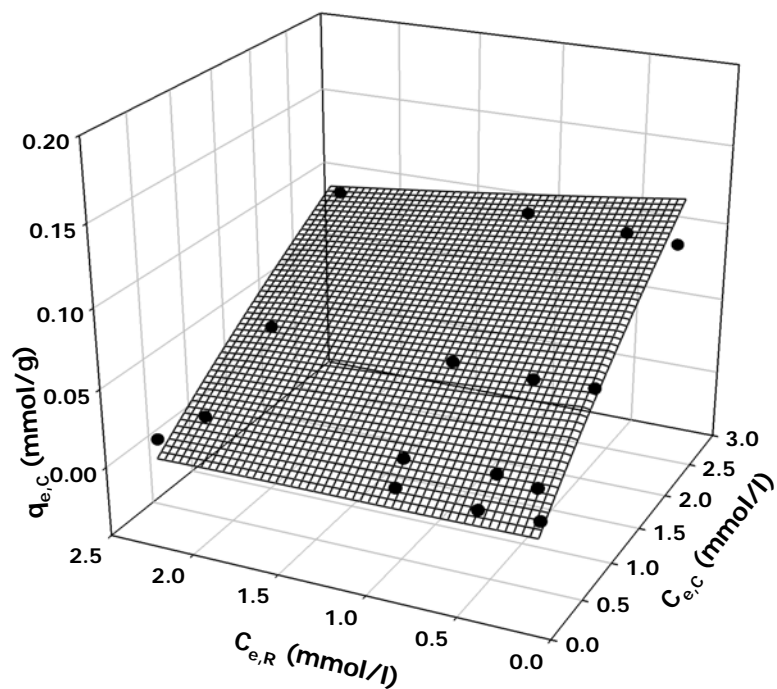


(a) Phenol

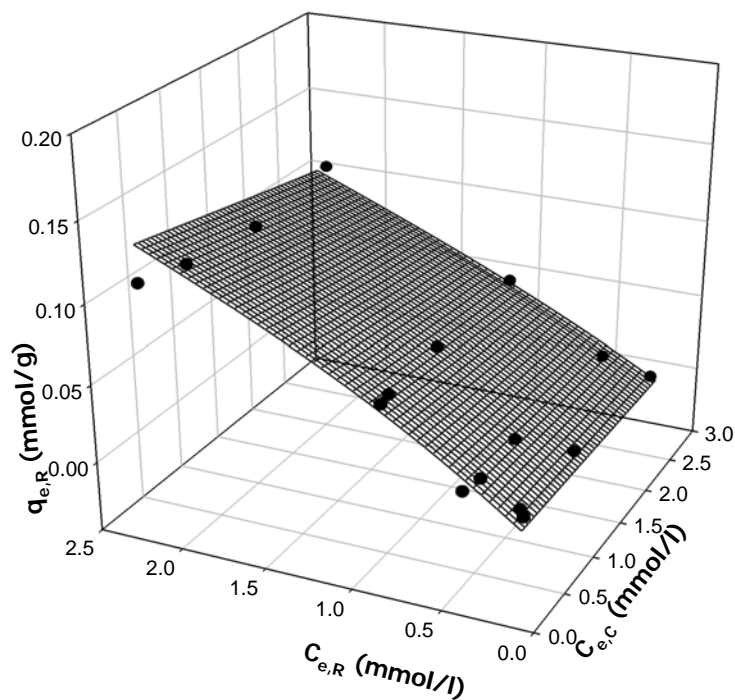


(b) Catechol

Figure 4.4.10. Binary adsorption isotherms of simultaneous phenol and catechol adsorption onto RHA. The surfaces are predicted by the extended Langmuir model and the symbols are experimental data. (a) Phenol uptake and (b) Catechol uptake.

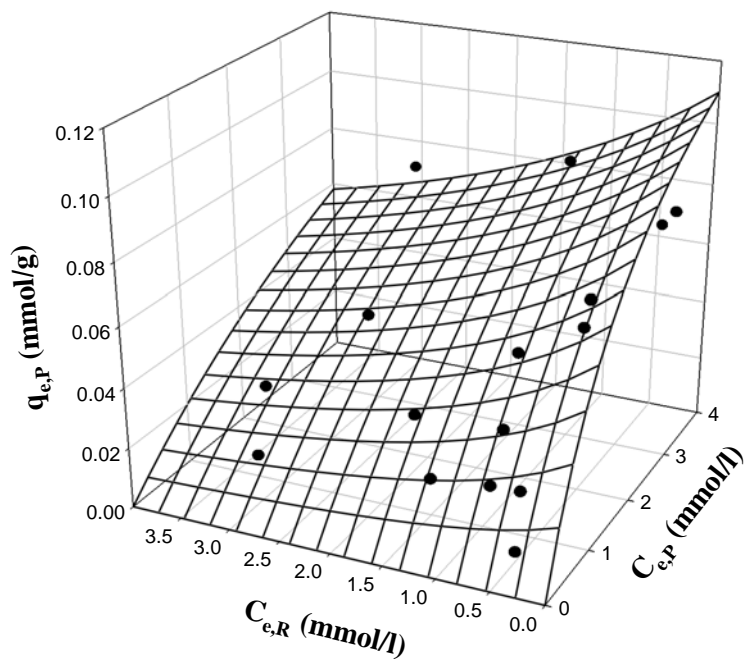


(a) Catechol

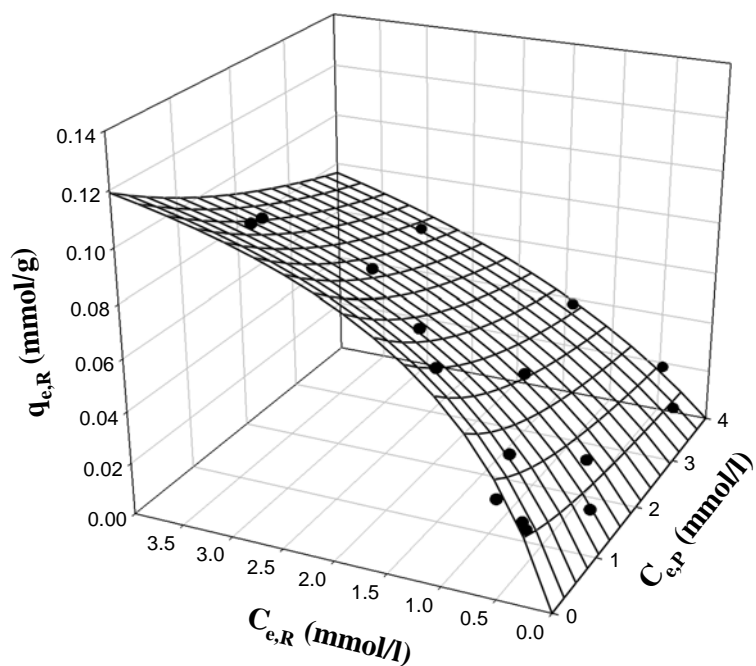


(b) Resorcinol

Figure 4.4.11. Binary adsorption isotherms of simultaneous catechol and resorcinol adsorption onto RHA. The surfaces are predicted by the extended Langmuir model and the symbols are experimental data. (a) Catechol uptake and (b) Resorcinol uptake.



(a) Phenol



(b) Resorcinol

Figure 4.4.12. Binary adsorption isotherms of simultaneous phenol-resorcinol adsorption onto RHA. The surfaces are predicted by the extended Langmuir model and the symbols are experimental data. (a) Phenol uptake and (b) Resorcinol uptake

4.4.5.3 Ternary adsorption of phenol, catechol and resorcinol

Equilibrium isotherms data for ternary adsorption of phenol, catechol and resorcinol onto RHA are given in Table 4.4.11. The ternary adsorption isotherm data was analyzed by using non-modified Langmuir, modified Langmuir, extended-Langmuir, SRS, non-modified and modified R-P models. The parametric and SSE values of all the multi-component adsorption models for the adsorption of phenol, catechol and resorcinol by RHA from ternary systems of phenol-catechol-resorcinol are given in Table 4.4.12.

The multi-component non-modified Langmuir model showed a poor fit to the experimental data with SSE values of 0.2356 for phenol-catechol-resorcinol systems. The values of the modified Langmuir coefficient ($\eta_{L,i}$) deviate from one for both the systems indicating that non-modified multi-component Langmuir model related to the individual isotherm parameters could not be used to predict the ternary system adsorption. However, the use of the interaction term, $\eta_{L,i}$, improved the fit of the modified-Langmuir model as shown by lower of SSE values (0.1063) of modified-Langmuir model in comparison to non-modified Langmuir model.

$$\begin{aligned}
 q_{e,P} &= \frac{0.85 \times 0.04 (C_{e,P} / 2.31)}{1 + (0.04 (C_{e,P} / 2.31) + 0.021 (C_{e,C} / 0.38) + 0.056 (C_{e,R} / 0.11))} \\
 q_{e,C} &= \frac{2.22 \times 0.21 (C_{e,C} / 0.38)}{1 + (0.04 (C_{e,P} / 2.31) + 0.021 (C_{e,C} / 0.38) + 0.056 (C_{e,R} / 0.11))} \\
 q_{e,R} &= \frac{0.81 \times 0.056 (C_{e,R} / 0.38)}{1 + (0.04 (C_{e,P} / 2.31) + 0.021 (C_{e,C} / 0.38) + 0.056 (C_{e,R} / 0.11))}
 \end{aligned}
 \quad \text{SSE}=0.1063 \quad (4.4.22)$$

The multi-component extended-Langmuir model has been found to adequately describe the adsorption equilibria of the ternary system of Cr(VI), Cu(II) and Cd(II) for a biosorbent *R. arrhizus* [Sag et al., 2002]. This model also showed good fitting of the data for

present binary adsorption systems also. For ternary system the overall total adsorbate uptakes (q_{max}) for phenol-catechol-resorcinol system is 0.2735 mmol/g. These values are considerably lower than the sum of the maximum total capacities of phenol, catechol and resorcinol resulting from the single component adsorption systems. For that reason, the adsorption sites of adsorbates in ternary systems of phenol-catechol-resorcinol is highly overlapping. The information obtained from the maximum capacities seems to violate the basic assumptions of the Langmuir model [Sag et al., 2003]. The equations as suggested by extended Langmuir model are:

$$q_{e,P} = \frac{0.27 \times 0.18 C_{e,P}}{1 + (0.18 C_{e,P} + 1.74 C_{e,C} + 3.93 C_{e,R})}; \quad q_{e,C} = \frac{0.27 \times 1.74 C_{e,C}}{1 + (0.18 C_{e,P} + 1.74 C_{e,C} + 3.93 C_{e,R})}; \quad (4.4.23)$$

$$q_{e,R} = \frac{0.27 \times 3.93 C_{e,R}}{1 + (0.18 C_{e,P} + 1.74 C_{e,C} + 3.93 C_{e,R})} \quad SSE=0.0798$$

Non-modified Redlich-Peterson (R-P) model gave high SSE values (0.2054), however, modified R-P model improved the fit considerably. The fits of the following modified R-P model (SSE=0.1031 for phenol-catechol-resorcinol) are comparably better than the single component based modified Langmuir models:

$$q_{e,P} = \frac{1.08(C_{e,P}/0.53)}{1 + (28.722(C_{e,P}/0.533)^{0.186} + 63.34(C_{e,C}/0.16)^{0.121} + 61.86(C_{e,R}/0.32)^{0.161})}$$

$$q_{e,C} = \frac{3.32(C_{e,C}/0.163)}{1 + (28.722(C_{e,P}/0.533)^{0.186} + 63.34(C_{e,C}/0.16)^{0.121} + 61.86(C_{e,R}/0.32)^{0.161})} \quad SSE=0.1031 \quad (4.4.24)$$

$$q_{e,R} = \frac{2.87(C_{e,R}/0.163)}{1 + (28.722(C_{e,P}/0.533)^{0.186} + 63.34(C_{e,C}/0.16)^{0.121} + 61.86(C_{e,R}/0.32)^{0.161})}$$

The multi-component SRS model applies to those systems where each component individually obeys the single-component Freundlich isotherm. The isotherm coefficients can be determined from the mono-component isotherm except for the adsorption

competition coefficients, a_{ij} , which have to be determined experimentally. The competition coefficients, a_{ij} , describe the inhibition to the adsorption of component i by component j . The three components were individually found to obey the single-component Freundlich model. The main assumptions incorporated in the derivation are that for each component in a multi-component adsorption, adsorption energies of sites are exponentially distributed. A comparison of the competition coefficients in the adsorption isotherm equation for phenol-catechol-resorcinol shows that the uptake of the phenol was strongly affected by the presence of catechol or resorcinol ($a_{12}=1827.8$ and $a_{13}=24.77$ values are very high), while the inhibition exerted in the reverse situation is not that strong ($a_{21}=0.077$ or $a_{31}=0.031$ are not that high). Also, resorcinol adsorption onto RHA was more affected by catechol ($a_{32}=0.528$) as compared to that of catechol by resorcinol ($a_{23}=0.0174$). SRS model for the ternary adsorption of phenol-catechol-resorcinol can be represented by the following sets of equations:

$$\begin{aligned}
 q_{e,P} &= 0.036C_{e,P} \left(C_{e,P} + 1827.83C_{e,C} + 24.75C_{e,R} \right)^{(0.82-1)} \\
 q_{e,C} &= 0.052C_{e,C} \left(0.077C_{e,P} + C_{e,C} + 0.017C_{e,R} \right)^{(0.88-1)} \quad \text{SSE}=0.1670 \quad (4.4.25) \\
 q_{e,R} &= 0.046C_{e,R} \left(0.031C_{e,P} + 0.528C_{e,C} + C_{e,R} \right)^{(0.841-1)}
 \end{aligned}$$

Overall, extended Langmuir model best represented the ternary equilibrium data of phenol, catechol and resorcinol adsorption onto RHA. For plotting 3-D adsorption isotherm surfaces for ternary systems, the residual concentration of one of the adsorbate has been taken as a parameter in these plots. A 3-D diagram is plotted on the basis of the randomly generated data, and the experimental data are fitted to a smooth surface according to the appropriate input equation. The multi-component extended Langmuir model can be used to

simulate the equilibrium sorption behavior of the ternary system through 3-D plots.

The adsorption isotherm surfaces for phenol-catechol-resorcinol system, as shown in Figures 4.4.13 and 4.4.14, respectively, were created by using the multi-component extended Langmuir model and smoothed and fitted to the experimental adsorption data. When both catechol and phenol were present in the solution together and the effect of resorcinol was ignored, reduction of the phenol uptake was observed with increasing catechol concentrations (Figure 4.4.13a). The uptake of catechol, however, decreased marginally with increasing equilibrium phenol concentrations (Figure 4.4.13b). Thus inhibition effect of catechol was more pronounced than phenol. Figure 4.4.14 shows the plots of unadsorbed catechol and resorcinol concentrations in solution at equilibrium against the catechol, resorcinol and total (catechol+resorcinol) uptakes by RHA. The initial concentration of phenol was taken as a parameter. It is found that the catechol or resorcinol uptake by RHA was strongly affected by the presence of resorcinol or catechol. The deviations of the predicted data from the experimental data for resorcinol were much more pronounced in the 3-D adsorption isotherm plots (Figure 4.4.13b). Since the expected increase in the inhibitory effects caused by the presence of the other substrate at increasing concentrations was not observed, the predicted equilibrium uptake for resorcinol was higher than the experimental value.

Table 4.4.11. Comparison of individual and total adsorption equilibrium uptakes and yields found at different Resorcinol concentrations in the absence and presence of increasing concentrations of Phenol ions onto rice husk ash.

$C_{o,P}$	$C_{o,C}$	$C_{o,R}$	$C_{e,P}$	$C_{e,C}$	$C_{e,R}$	$q_{e,P}$	$q_{e,C}$	$q_{e,R}$	$Ad_P\%$	$Ad_C\%$	$Ad_R\%$	$Ad_{Tot}\%$
(mmol/L)			(mmol/L)			(mmol/g)			-	-	-	-
0.525	3.631	1.759	0.440	1.378	0.067	0.004	0.113	0.085	16.190	62.059	96.197	68.144
0.525	0.848	0.413	0.388	0.048	0.178	0.007	0.040	0.012	26.117	94.342	57.040	65.663
0.556	0.910	4.046	0.505	0.177	2.221	0.003	0.037	0.091	9.205	80.589	45.109	47.344
0.579	2.055	3.397	0.335	0.330	1.052	0.012	0.086	0.117	42.066	83.927	69.044	71.525
0.585	4.104	0.614	0.426	0.914	0.062	0.008	0.160	0.028	27.212	77.717	89.851	73.551
0.593	2.288	1.205	0.208	0.168	0.058	0.019	0.106	0.057	64.924	92.669	95.155	89.375
0.607	2.130	1.963	0.245	0.560	0.058	0.018	0.079	0.095	59.662	73.699	97.037	81.635
0.609	4.230	1.259	0.355	1.153	0.060	0.013	0.154	0.060	41.709	72.743	95.231	74.289
0.635	3.663	3.488	0.522	1.468	1.081	0.006	0.110	0.120	17.702	59.925	69.017	60.557
0.637	2.361	1.308	0.169	0.428	0.078	0.023	0.097	0.062	73.527	81.894	94.030	84.341
0.945	0.955	1.354	0.507	0.324	0.331	0.022	0.032	0.051	46.367	66.102	75.543	64.301
0.967	0.756	0.399	0.249	0.023	0.039	0.036	0.037	0.018	74.292	96.953	90.351	85.382
0.968	3.799	0.414	0.602	1.045	0.105	0.018	0.138	0.016	37.784	72.495	74.763	66.191
1.008	0.634	2.316	0.860	0.396	1.288	0.007	0.012	0.051	14.753	37.456	44.361	35.712
1.026	2.101	3.820	0.979	0.601	2.104	0.002	0.075	0.086	4.587	71.394	44.903	46.960
1.035	3.892	3.688	0.839	1.548	1.859	0.010	0.117	0.092	18.989	60.219	49.602	50.720
1.069	4.183	2.043	0.952	1.780	0.993	0.006	0.120	0.053	10.931	57.445	51.413	48.941
1.074	0.872	4.073	0.736	0.022	2.178	0.017	0.043	0.095	31.483	97.471	46.514	51.216

1.077	0.865	2.015	0.598	0.085	0.686	0.024	0.039	0.067	44.464	90.155	65.977	65.406
1.081	0.874	0.821	0.319	0.061	0.253	0.038	0.041	0.028	70.456	93.020	69.234	77.200
1.085	2.229	2.088	0.880	0.544	0.946	0.010	0.084	0.057	18.897	75.590	54.687	56.127
2.398	0.429	3.689	1.973	0.091	2.318	0.021	0.017	0.069	17.706	78.779	37.153	32.736
2.526	0.447	0.807	1.726	0.066	0.115	0.040	0.019	0.035	31.689	85.242	85.753	49.558
2.558	0.456	0.437	1.490	0.065	0.059	0.053	0.020	0.019	41.749	85.699	86.465	53.220
2.677	2.191	0.887	2.084	0.278	0.387	0.030	0.096	0.025	22.151	87.314	56.405	52.240
2.686	0.912	2.090	2.453	0.190	0.859	0.012	0.036	0.062	8.673	79.177	58.933	38.448
2.691	0.482	2.135	1.797	0.066	0.746	0.045	0.021	0.070	33.223	86.401	65.082	50.870
2.790	4.475	0.903	2.484	1.509	0.349	0.015	0.148	0.028	10.964	66.275	61.328	46.834
2.808	0.955	0.893	2.059	0.130	0.179	0.037	0.041	0.036	26.668	86.406	79.956	49.143
4.879	0.447	3.858	3.970	0.082	2.398	0.045	0.018	0.073	18.622	81.590	37.839	29.761
5.008	0.464	0.815	3.415	0.071	0.162	0.080	0.020	0.033	31.811	84.767	80.167	41.989
5.073	2.148	0.834	4.186	0.267	0.215	0.044	0.094	0.031	17.493	87.581	74.270	42.060
5.113	0.456	0.429	3.261	0.063	0.091	0.093	0.020	0.017	36.226	86.273	78.912	43.080
5.122	0.458	2.077	4.066	0.085	0.954	0.053	0.019	0.056	20.622	81.570	54.090	33.347
5.249	0.894	2.144	4.700	0.203	0.949	0.027	0.035	0.060	10.452	77.234	55.731	29.370
5.291	4.405	0.867	4.177	1.146	0.298	0.056	0.163	0.029	21.062	73.977	65.702	46.793
5.367	2.277	2.174	4.898	0.451	0.747	0.024	0.091	0.071	8.744	80.191	65.667	37.918
5.428	1.079	4.565	4.741	0.189	2.423	0.034	0.045	0.107	12.661	82.506	46.930	33.599
5.616	1.007	0.995	4.444	0.145	0.191	0.059	0.043	0.040	20.873	85.592	80.804	37.259

Table 4.4.12. Multi-component isotherm parameter values for the simultaneous removal of phenol and catechol by rice husk ash.

	Non-modified Langmuir Model			Non-modified R-P Model
SSE	0.2356			0.2854
	Modified Langmuir Model		Extended Langmuir Model	
Adsorbate	$\eta_{L,i}$		K_i	q_{\max}
Phenol	2.3101		0.1862	0.2735
Catechol	0.3825		1.7382	
Resorcinol	0.7441		3.9361	
SSE	0.1063		0.0798	
	SRS Model			Modified R-P Model
Adsorbate	a_{ij}	a_{ij}	a_{ij}	$\eta_{RP,i}$
Phenol	1	1827.8	24.77	0.5289
Catechol	0.077	1	0.0174	0.1601
Resorcinol	0.031	0.528	1	0.3242
SSE	0.1670			0.1031

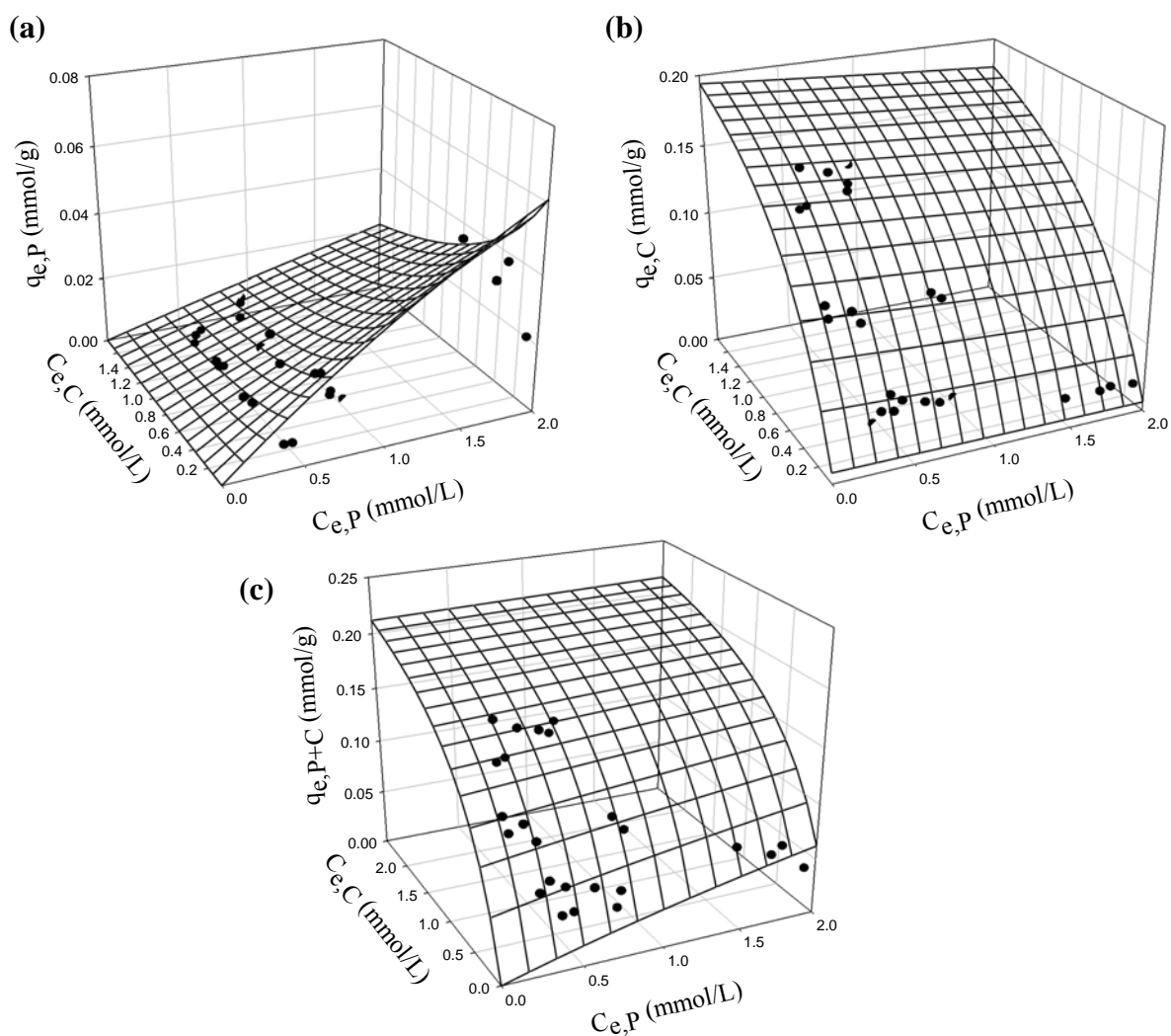


Figure 4.4.13. Three-dimensional adsorption isotherm surfaces created by using a multicomponent extended Langmuir model for the phenol + catechol + resorcinol systems with $C_{e,R}$ as a parameter. (a) The effect of catechol concentration on the equilibrium uptake of phenol; (b) the effect of phenol concentration on the equilibrium uptake of catechol; (c) the effect of phenol and catechol concentration on the equilibrium total uptake of phenol + catechol by RHA.

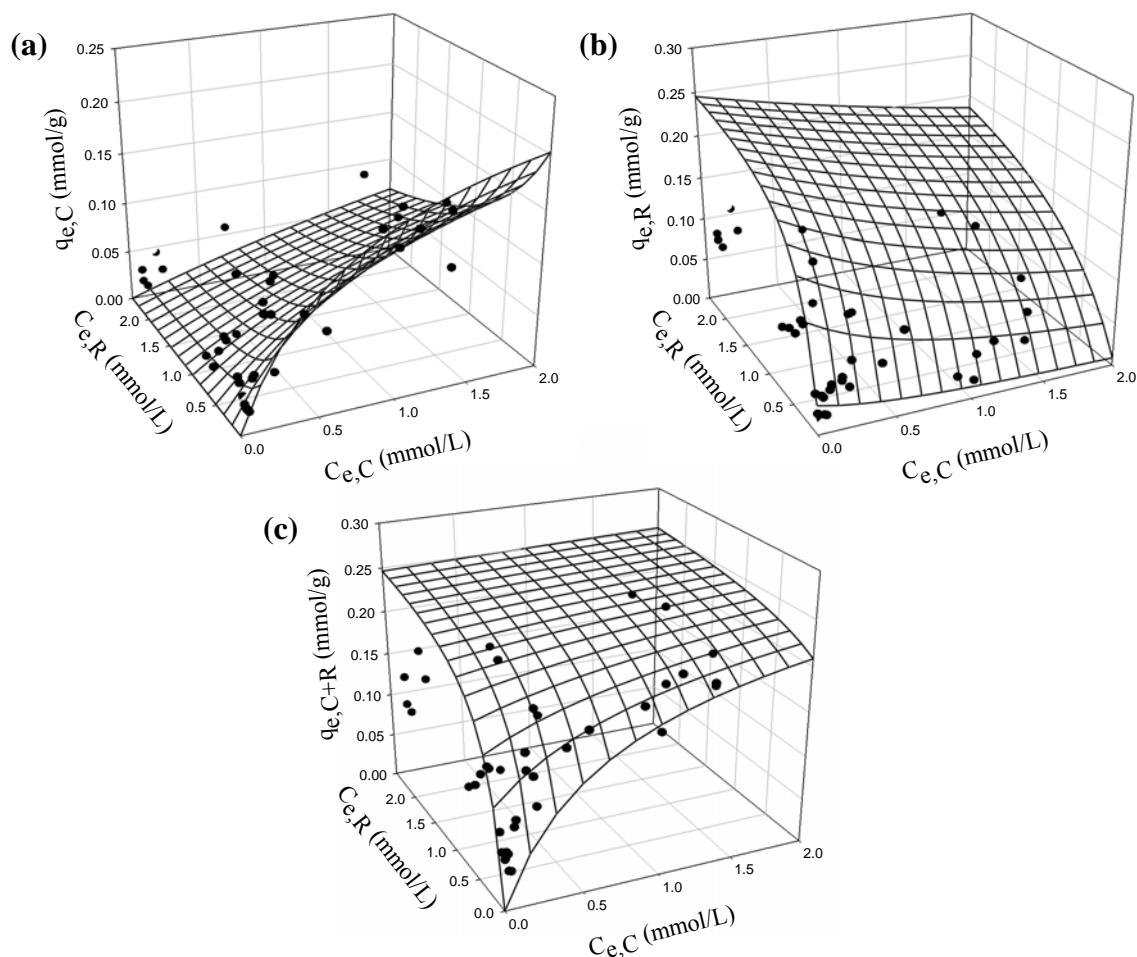


Figure 4.4.14. Three-dimensional adsorption isotherm surfaces created by using a multicomponent extended Langmuir model for the phenol + catechol + resorcinol systems with $C_{e,P}$ as a parameter. (a) The effect of resorcinol concentration on the equilibrium uptake of catechol; (b) the effect of catechol concentration on the equilibrium uptake of resorcinol; (c) the effect of catechol and resorcinol concentration on the equilibrium total uptake of catechol + resorcinol by RHA.

SEQUENTIAL BATCH REACTOR

5.1 GENERAL

This chapter deals with the biological treatment of synthetic wastewater containing phenolic compounds (phenol, catechol and resorcinol) and actual petroleum refinery wastewater (PRW) using sequential batch reactor (SBR). Process parameters like hydraulic retention time (HRT) and fill time of wastewater were varied to maximize the treatment efficiencies.

5.2 SEQUENTIAL BATCH REACTOR

SBR process is a sequential operation of activated sludge process (ASP) in which all major steps: fill, react, settle and decant phase occur in the same tank in sequence. Compared to conventional ASP, SBR eliminates the need of primary and secondary clarifiers, and return sludge storage tank. It can be applied to treat wastewaters having high concentration of chemical oxygen demand (COD), biological oxygen demand (BOD), phenolic compounds and other hazardous pollutants [Silva et al., 2002; Barrios-Martinez et al., 2006]. According to a 1999 U.S. EPA report, SBR is no more than an activated-sludge plant that operates in time rather than space.

SBR has been shown to be a cost effective treatment of hazardous organic pollutants found in industrial wastewater. In addition, SBR has several advantages over

conventional continuous flow systems like ASP [[Wastewater technology fact sheet, USEPA, 1999](#); [Arora et al., 1985](#)].

- Equalization, primary clarification (in most cases), biological treatment, and secondary clarification can be achieved in a single reactor vessel.
- Operation flexibility and control.
- Potential capital cost savings by eliminating clarifiers and other equipments.
- The possibility of using only the partial capacity of the plant during low wastewater generation.

5.2.1 Operation of Sequential Batch Reactor

SBRs are variable-volume, non-steady-state, suspended-growth biological wastewater treatment reactors. The treatment process is characterized by a repeated treatment cycle consisting of a series of sequential process phases: fill, react, settle, decant and idle. These steps can be altered for different operational applications. The importance of the interactions between these considerations vary depending on fill strategy and cycle time control strategy. Operating strategy must be capable of accurately adjusting the intercycle phase times to prevent loss of biological treatment or volumetric capacity [[Irvine et al., 1989](#)]. [Figure 5.2.1](#) shows cycle of SBR.

All the SBR systems have five steps in common, which are carried out in sequence as follows:

Fill: Wastewater flows into the reactor and get mixed with the biomass already present in the reactor. Mixing and aeration can be varied to create the following three different conditions:

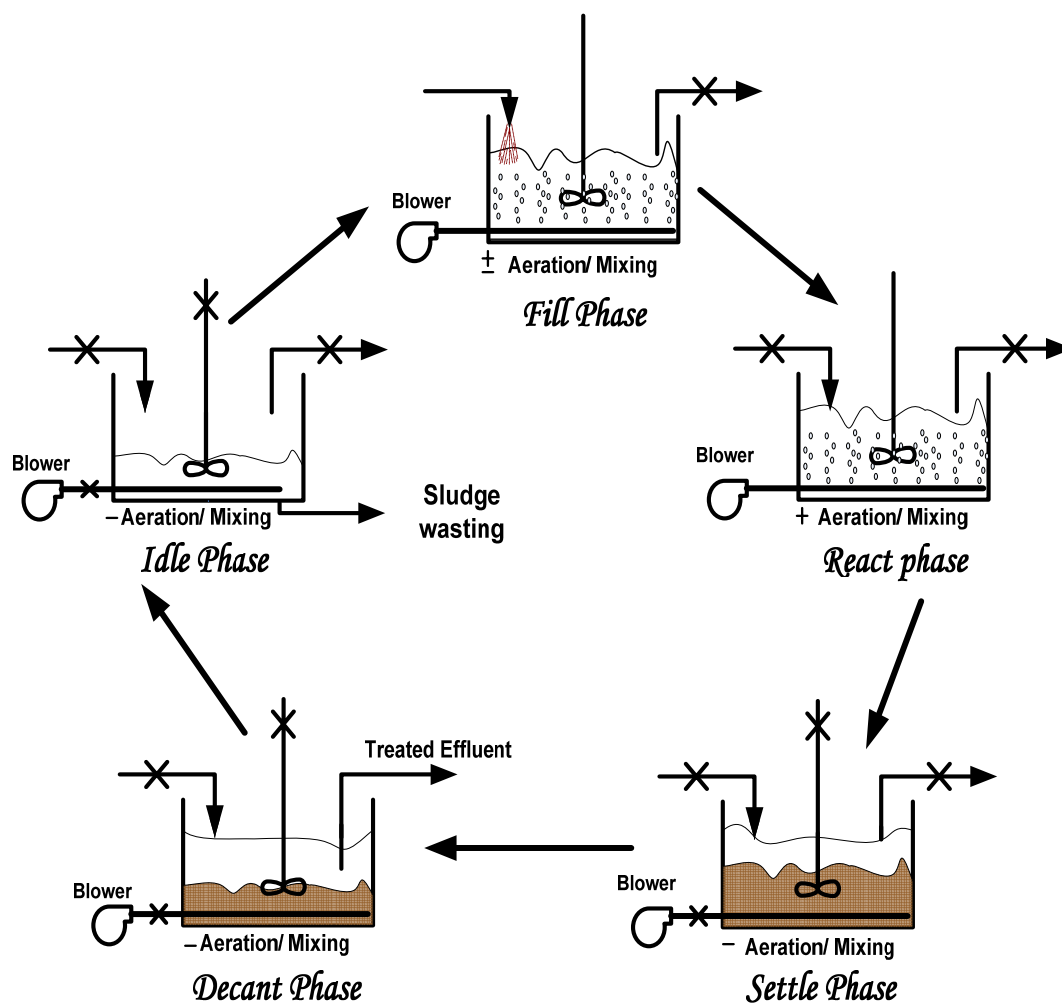


Figure 5.2.1. Sequencing batch reactor (SBR) operation principle.

- **Static Fill:** Under static-fill condition, influent wastewater enters into the reactor with no mixing and/or aeration.
- **Mixed Fill:** Under the condition of mixed-fill, influent is mixed with biomass present in the reactor but aeration remains off. As there is no aeration, an anoxic condition appears.
- **Aerated Fill:** In condition of aerated-fill, both the aeration and the stirrer are switched on. Aerobic and anoxic environment are created inside the reactor by keeping on/off oxygen supply to the reactor. Aerated fill can reduce the aeration time required in the react step.

React: Depending on the conditions applied: anaerobic, anoxic or aerobic reactions, substrate present in the wastewater are consumed by the biomass. This phase allows for further reduction or "polishing" of wastewater parameters. Most of the carbonaceous BOD removal occurs in the react phase.

Settle: After sufficient time of reaction aeration and mixing, the activated sludge tends to settle as a flocculent mass, forming a distinctive interface with the clear supernatant. This phase is a critical part of the cycle, because if the solids do not settle rapidly, some sludge can be drawn off during the subsequent decant phase and thereby degrade effluent quality.

Decant: Clear supernatant (treated wastewater) is removed from the reactor. Floating decanters maintain the inlet orifice slightly below the water surface to minimize the removal of solids in the effluent. Floating decanters offer operator flexibility to vary fill and draw volumes.

Idle: This is the time between cycles and is useful when there is more than one reactor. It is used to adjust the cycle time of influent flow rate and the operating strategy between SBR reactors. Sludge wasting is also performed during this phase.

5.2.2 Operating Parameters in SBR Process

The treatment efficiency of SBR depends on the operating parameters such as phase duration, HRT and organic loading, sludge retention time (SRT), temperature, pH, mixed liquor suspended solids (MLSS), mixed liquor volatile suspended solids (MLVSS), dissolved oxygen (DO) concentration and the strength of wastewater.

Cycle time: A cycle in SBR comprises of fill, react, settle, decant and idle phase. The total cycle time (t_C) is the sum of all these phases.

$$t_C = t_F + t_R + t_S + t_D + t_I \quad (5.2.1)$$

Where, t_F is the fill time (h), t_R is the react time (h), t_S is the settle time (h), t_D is the decant time (h) and t_I is the idle time (h).

Volume exchange ratio and hydraulic retention time (HRT): Due to filling and decanting phase during a cycle, SBR operate with varying volume. Volume exchange ratio (VER) for a cycle is defined as V_F/V_T . Where, V_F is the filled volume of wastewater and decanted effluent for a cycle, and V_T is the total working volume of the reactor.

HRT for the continuous system is defined as:

$$\text{HRT} = \frac{V_T}{Q} \quad (5.2.2)$$

Where, Q is the daily wastewater flow rate. For SBR systems:

$$Q = V_F \times N_C \quad (5.2.3)$$

Where, N_C is the number of cycles per day and defined as:

$$N_C = \frac{24}{t_C} \quad (5.2.4)$$

Therefore, HRT for the SBR systems may be given as:

$$\text{HRT} = \frac{t_C}{V_F / V_T} \times \frac{1}{24} \quad (5.2.5)$$

Solid retention time (SRT): In biological systems of wastewater treatment, waste or surplus sludge is directly withdrawn from the reactor to control the sludge age (SRT).

SRT determines the time (d) for which the biomass is retained in the reactor.

$$\text{SRT} = \frac{V_T \times X \times t_C}{V_W \times X_W \times 24} \quad (5.2.6)$$

Where, X is the MLSS in the reactor with full filled (mg/L), X_W is the MLSS in waste stream (mg/L) and V_W is the waste sludge volume (L).

5.3 MATERIALS AND METHODS

5.3.1 Experimental Setup

The reactor was prepared from plexi glass, with the dimension of 7.37 cm × 40.64 cm (radius × height) and having 5 L working volume. Aquarium sintered sand diffusers were placed at the bottom centre of the reactor which maintained the desired DO level in the reactor. Agitation at constant 100 rpm was done for proper distribution of air and nutrient in the reactor. Experiment setup was assembled with online DO and pH measuring instruments. Wastewater was fed from top and was withdrawn from the

side of the reactor. DO concentration inside the reactor was maintained between 2-5 mg/L during the experiments by controlling the flow of air through air rotameter. pH probe was dipped in the reactor for continuous monitoring of change in pH during the reaction time. Addition of feed and the wasting of sludge were done with peristaltic pumps. MLSS concentration was controlled between 1200 to 2600 mg/L and 2500 to 3500 mg/L with a sludge age of approximately 20 and 30 days for synthetic phenolic wastewater and PRW, respectively. Excess sludge, which grew during the aeration stage, was drawn out at the end of every operating cycle, in order to maintain proper MLSS concentration. The reactors were operated in an isothermal chamber with controlled temperature at $30\pm 1^{\circ}\text{C}$. [Figure 5.3.1](#) and [Figure 5.3.2](#) show schematic diagrams and actual photographs of experiment setup, respectively.

5.3.2 Experimental Procedure

Reactor was operated on a fill-and-draw basis at instantaneous fill mode. Total operating volume of wastewater and activated sludge in the reactor was kept at 5 L. For synthetic wastewater containing phenol, catechol and resorcinol, the total cycle time was 12 h which consisted of 10 h react phase, 1 h settling phase, 0.5 h decant phase and 0.5 h idle phase. For PRW, the total cycle time was of 8 h out of which 6 h was react time, 1 h was settling time, 1 h was decanting and idle time. HRT and fill time of PRW were varied in the range 0.56-3.33 d and 0.5-2.0 h, respectively.

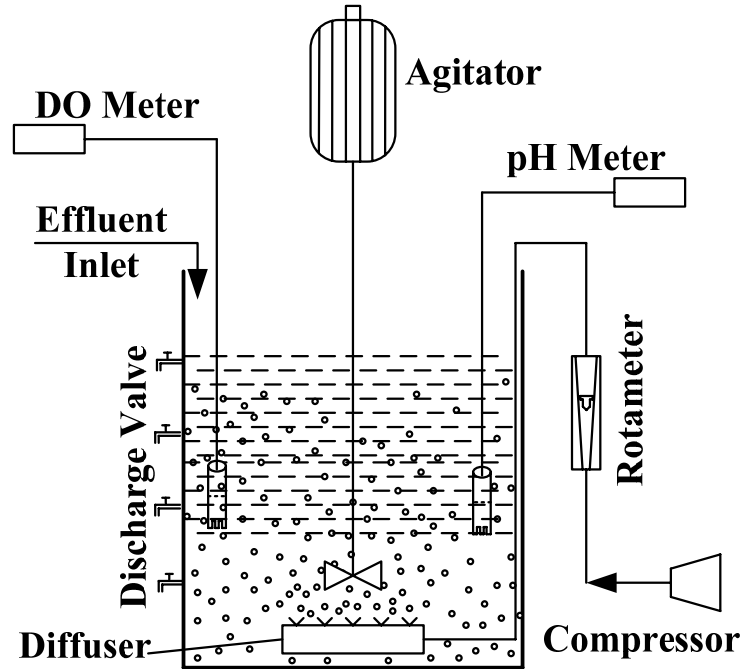


Figure 5.3.1. Schematic diagram of experiment setup.



Figure 5.3.2. Actual photograph of experiment setup. (1) Reactor, (2) Agitator, (3) Peristaltic Pump, (4) Rotameter, (5) pH/DO meter, (6) Discharge collection beaker, (7) Compressor

The media was aerated and agitated (100 rpm) vigorously during the oxic (aerobic) operation. Agitation provided optimal mixing and improved the overall organic matter consumption rates [Samantha et al., 2005].

Samples were withdrawn from the reactor time to time and at the end of the react phase for analysis. Samples were filtered with filter paper (Whatman filter paper no. 42 of pore size ca. 2.5 μm) and then examined for concentration. At the end of react phase, the biomass was settled for 1 h and the amount of the treated wastewater was removed. Settled organisms were used for the next treatment operation. Sludge wasting was done from the reactor daily before settling to adjust the sludge age. Optimization of fill time led to decrement in react time which decreased the total cycle time.

5.3.3 Analytical Measurements

The synthetic substrate was prepared fresh daily with distilled water. The sample was taken initially and after the completion of 12 h cycle. The samples were filtered and analyzed for the phenol, catechol and resorcinol concentration. The concentration of phenol, catechol and resorcinol in the aqueous solution were determined at 260 nm wavelength using high performance liquid chromatograph (HPLC) supplied by Waters (India) Pvt. Ltd., Bangalore. A mixture of 40% methanol, 1% acetic acid and rest millipore water obtained from Milli-Q purification system was used as a solvent in a symmetry C₁₈ column having size: 4.6 mm x 150 mm. Flow rate of solvent in the column was 0.5 mL/min.

Actual PRW was kept in cold condition and was analyzed before and after of each experimental run. COD, MLSS and MLVSS were also determined in accordance to standard methods and IS code [APHA, 1995; IS 355-1984]. For estimation of COD,

samples were digested for 2 h at 150°C in digestion unit (DRB 200, HACH, USA). After digestion, sample was cooled and tested in double beam UV visible spectrophotometer (HACH, DR 5000, USA), for the measurement of COD. TOC estimation was done using TOC-VCPH, SHIMADZU, ASI-V instrument.

The proximate analysis of the wasted AS was done as per Indian Standards [IS-1350]. The heating value of the sludge was estimated by using a standard adiabatic bomb calorimeter equipped with a digital firing unit (Toshniwal, Bombay).

To study the distribution of the elements in AS before and after the treatment of refinery wastewater energy dispersive X-ray (EDX) QUANTA, Model 200 FEG, USA spectra of the dried AS were taken.

Thermal analysis of raw and used AS was carried out using a thermal analysis (TA) instrument (Perkin- Elmer Pyris Diamond). Thermogravimetric analysis (TGA), differential thermogravimetric (DTG) and the derivative thermal (DTA) analyses were carried out from data and plots obtained from the instrument. TA instrument operated with the following specifications: weight of the sample, 10-15 mg (max. 100 mg); temperature range, ambient to 1000 °C. The thermo-analytical curves of the solid samples were obtained from this instrument under air atmospheres with a flow rate of 0.2 L/min.

FTIR spectra analysis was performed in the wavelength range of 400-4000 cm^{-1} at room temperature. Samples were mixed with potassium bromide (KBr) and pellet was formed which was further used in the FTIR spectrometer for analysis (Thermo Nicolet, Model Magna 760).

Some of the instruments used for analysis of various parameter is given in [Table 5.3.1](#)

Table 5.3.1. Analytical techniques/instruments/equipment used in the determination of various parameters.

Parameter	Analytical Technique/Method	Make/method
pH	Digital pH meter.	NIG 333, Toshniwal, New Delhi.
BOD	27 °C, 3 days incubation.	BOD-Oxidirect, Aqualitic, Germany
COD	UV visible spectrophotometer	HACH, DR 5000, USA
Settleability & Filterability	Column and Beuchner Funnel.	Gravity settling and filtration.
Morphology	Scanning electron microscope.	LEO 435 VP, England.
EDAX	Energy Dispersive X-ray spectrometer (FE-SEM).	QUANTA 200 FEG.
Heating value	Bomb calorimeter, IS 1350, Part II.	Toshniwal, Bombay.
Oxidation characteristics	TG/DTG/DTA analyzer.	Perkin Elmer Pyris Diamond.

5.4 TREATMENT OF SYNTHETIC WASTEWATER CONTAINING PHENOLIC COMPOUNDS (PHENOL, CATECHOL AND RESORCINOL) [Thakur et al., 2013a]

5.4.1 Characteristic of Wastewater and Acclimatization of Sludge

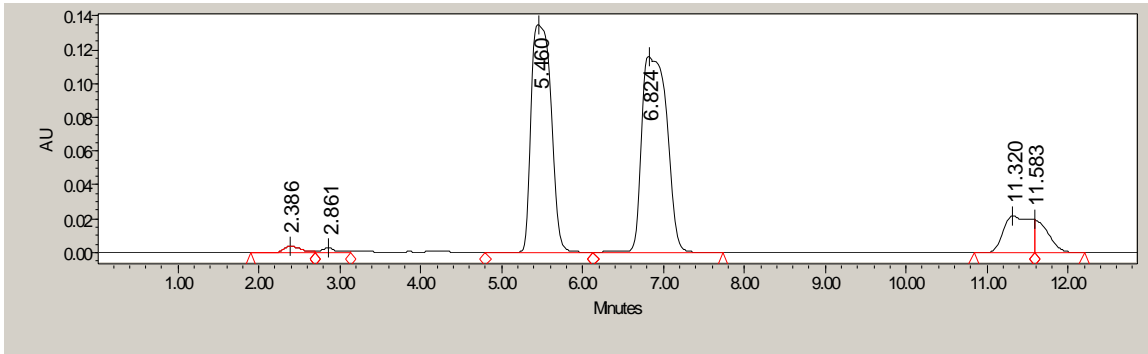
Analytical (AR) grade phenol (C_6H_6O) and catechol ($C_6H_6O_2$) were procured from s.d. Fine Chemicals, Mumbai, India whereas resorcinol ($C_6H_6O_2$) was procured from E. Merck, Mumbai, India. The synthetic wastewater, used in the present study, was made by dissolving following compounds (concentration in mg/L) in distilled water: phenol (200), catechol (200), resorcinol (200). Synthetic wastewater, thus prepared had initial COD of 700 ± 20 mg/L. [Figure 5.4.1](#) show the HPLC reading of phenol, catechol and resorcinol peaks.

Activated sludge was collected from sewage treatment plant located in Rishikesh, Uttaranchal, India. The sludge was first screened for the removal of coarse and bigger particles and then it was aerated for 1-2 d [Sharma et al., 2010b; Thakur et al., 2013a,f]. It was transferred into the reactor and aerated again for 3-5 d for acclimatization of the sludge with the wastewater. During the acclimatization period, nutrients like glucose (150 mg/L), $\text{Na}_2\text{HPO}_4 \cdot 12\text{H}_2\text{O}$ (100 mg/L) and NH_4Cl (150 mg/L) were added with wastewater for the growth of microbe. As the microbes adapted to the wastewater, addition of nutrient was stopped.

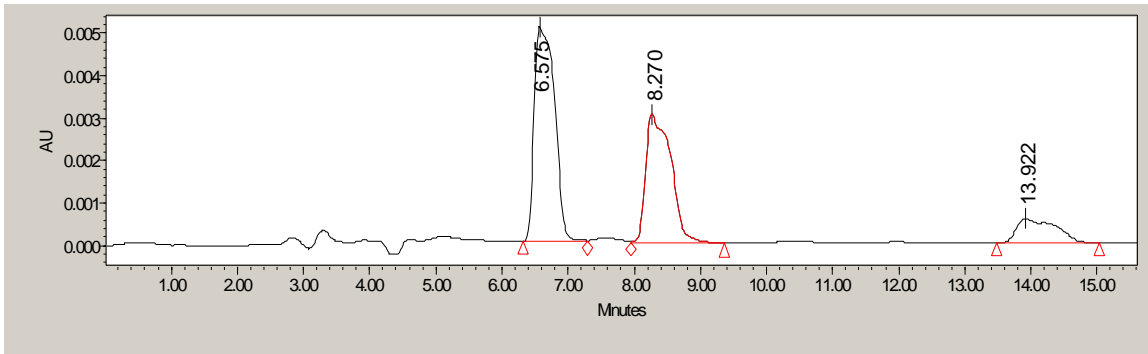
5.4.2 Effect of HRT

The HRT represents the average period of time wastewater remained in the system. The effect of HRT on the biodegradation of phenol, resorcinol and catechol was studied with HRTs of 0.625, 0.714, 0.833, 1, 1.25, 1.667, and 2.5 d at instantaneous fill condition. The COD and phenol, resorcinol and catechol removal efficiencies during the treatment in the SBR with varying HRT are shown in Figure 5.4.2. Variation in biomass concentration with HRT is shown in Figure 5.4.3.

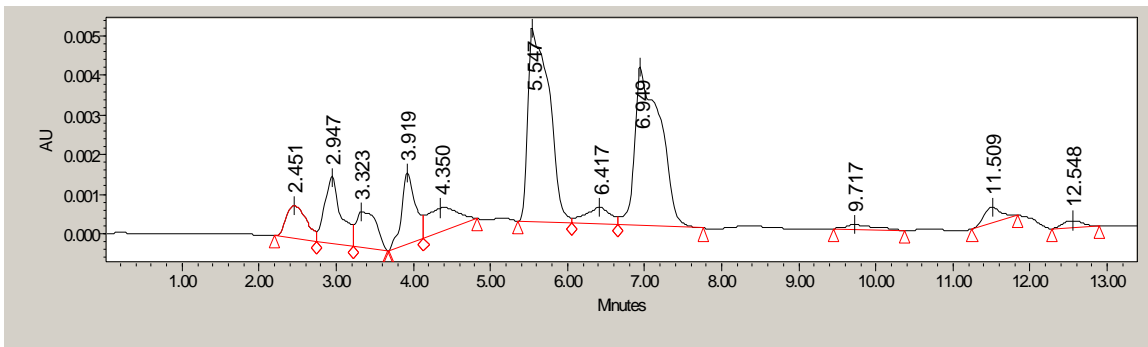
Results obtained from the experiment shows that an increase in HRT from 0.625 d to 1.25 d increases the COD and phenol, resorcinol and catechol removal efficiencies. This may be due to the fact that higher HRT gives longer contact time between biomass in the reactor and the wastewater, and thus better degradation rates. It may be seen in Figure 5.4.3 that the MLSS and MLVSS concentration is highest at HRT=1.25 d. Thus, higher growth rate of microorganisms during 0.625-1.25 d increases the removal efficiencies.



(a)



(b)



(c)

Figure 5.4.1. Peaks corresponding to phenol, catechol and resorcinol present in wastewater before and after treatment in SBR. (a) before treatment, (b) after treatment, 1.25 d HRT and instantaneous fill, (c) after treatment, 1.25 d HRT and 1.5 h fill time.

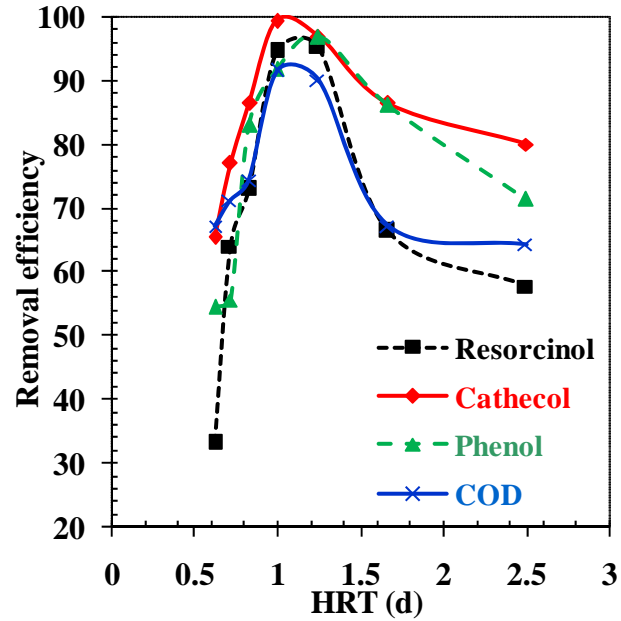


Figure 5.4.2. Effect of hydraulic retention time (HRT) on the removal of resorcinol, catechol, phenol and COD at SRT=20 d, instantaneous filling.

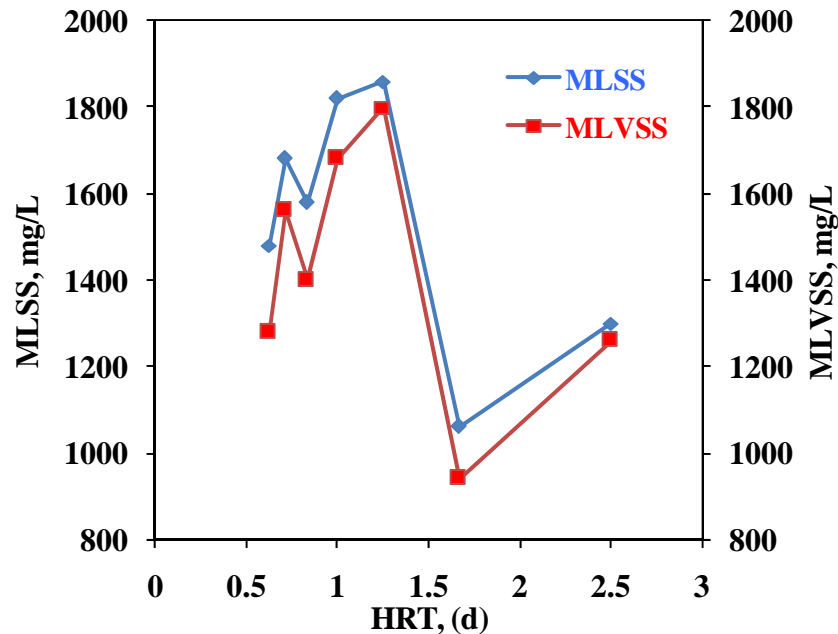


Figure 5.4.3. Effect of hydraulic retention time (HRT) on the final MLSS and MLVSS concentration at SRT=20 d, instantaneous filling.

Further increase in HRT from 1.25 d to 2.5 d decreases COD and phenol, resorcinol and catechol removal efficiencies (Figure 5.4.2). It may also be seen in Figure 5.4.3 that the MLSS and MLVSS concentration decrease with an increase in HRT from 1.25 to 2.5 d. The decrease in the COD, phenol, resorcinol and catechol removal efficiencies at very high HRT, thus, may be due to lower growth rate of microorganisms and accumulation of older cells.

5.4.3 Effect of Fill Time

In this part of the study, HRT was kept constant at 1.25 d whereas fill time was varied in the range of 0.5 - 2 h. The removal efficiencies with varying fill time are shown in Figure 5.4.4. Variation of biomass concentration with the fill time is depicted in Figure 5.4.5. Results showed that an increase in fill time from 0.5 h to 1.5 h increase the MLSS concentration from 1900 to 2100 mg/L. However, further increase in fill time to 2 h decreased the MLSS concentration to 1780 mg/L. Thus results obtained from the experiment show that an increase in fill time from 1.5 - 2 h decrease the removal efficiency of substrates (Figure 5.4.4). This may be due to the fact that lower fill time gives short contact time between biomass in the reactor and the waste water, and thus reduced degradation rates.

5.4.4 Characterization of Sludge

To maintain appropriate level of MLSS concentration within the reactor, some amount of sludge is wasted after every cycle which prevents the problem of sludge bulking and excessive growth of filamentous bacteria and maintains the efficiency of SBR. The amount of sludge wasted depends on HRT and SRT.

Sludge obtained at the bottom of settling tank or that obtained at the top of the filter media can further be utilized as a fuel. Physico-chemical and thermal characteristics of the dried AS were determined to come across its proper disposal option. The sludge wasted during the idle phase of the cycle was collected, filtered, dried in desiccators, and stored in glass containers.

Proximate analysis of wasted sludge was done as per Indian Standards. Moisture content, volatile matter, ash and fixed carbon of sludge were found to be 4.1%, 40.3%, 13.7% and 41.9%, respectively. [Figure 5.4.6](#) displays the EDX spectra as well the relative percentage of elements present in the raw and used AS obtained after treatment of wastewater. Raw and used AS was found to contain 35.95% and 37.54% oxygen; 44.77% and 50.19% carbon, respectively. The increase in carbon content (5.42%) was due to the presence of organics which were removed from the wastewater during the treatment process. The increased peak intensity for carbon in the AS was also due to the growth of biomass in the SBR. Relative percentage of magnesium, aluminum, phosphorus and calcium decreased in the treated AS as compared to that in raw AS due to the utilization of these elements as nutrients for the growth of microorganism.

Thermal stability of AS is directly dependent on the decomposition temperature of its various organics. AS contains high amount of carbon and oxygen. At high temperature, the organics present in AS decompose, producing CO (200-600°C), CO₂ (450-1000°C) [[Puri and Walker, 1966](#)], water vapor and free hydrogen (500-1000°C). The thermo-gravimetric analysis curves (TGA, DTA and DTG) of raw AS under oxidizing atmosphere are shown in [Figure 5.4.7a](#).

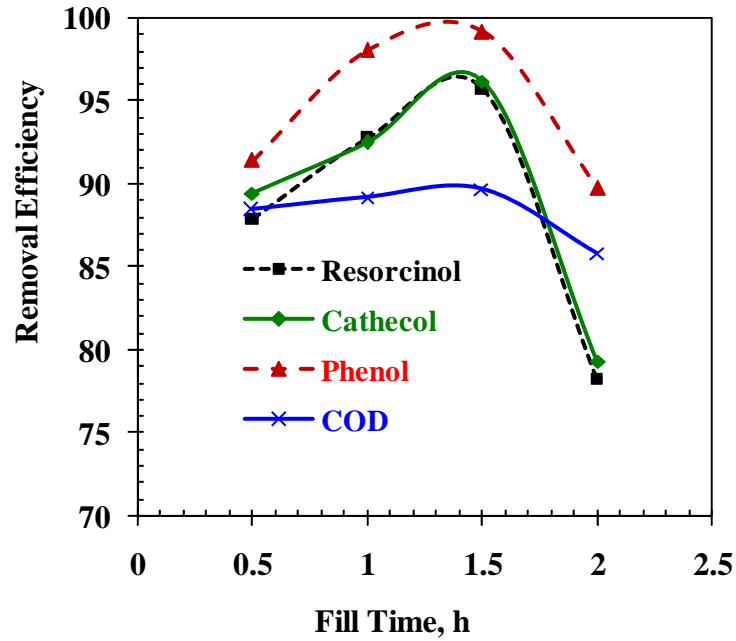


Figure 5.4.4. Effect of fill time on the on the removal of resorcinol, catechol, phenol and COD at SRT=20 d and HRT=1.25 d.

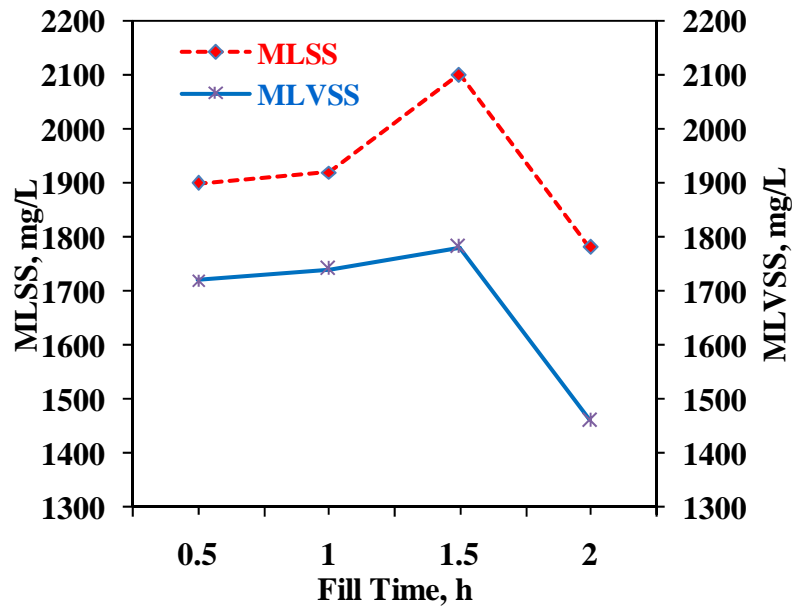
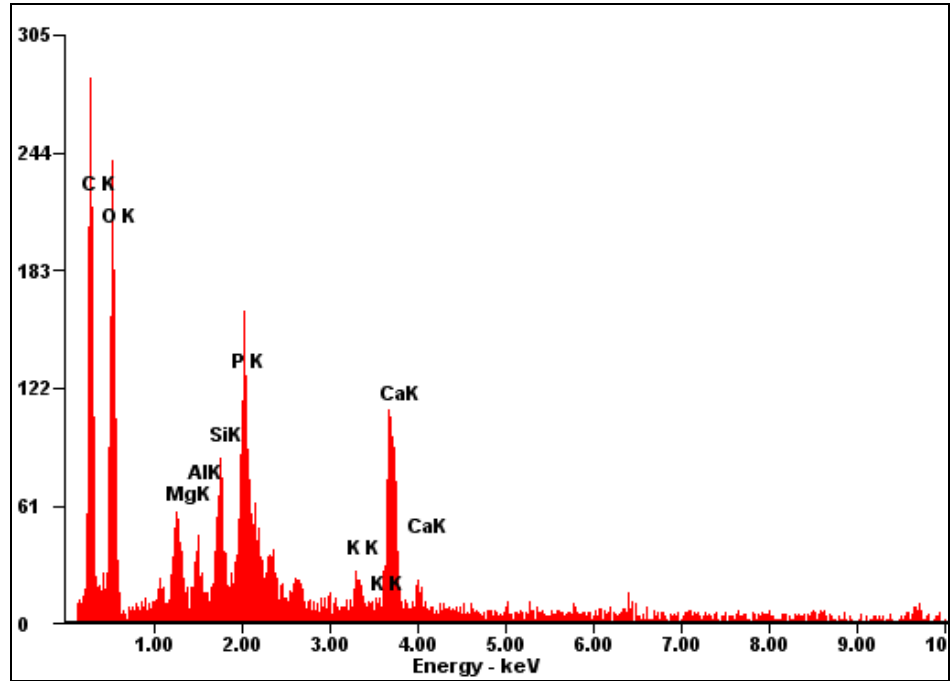


Figure 5.4.5. Effect of fill time on the final MLSS and MLVSS concentration at SRT=20 d and HRT=1.25 d.

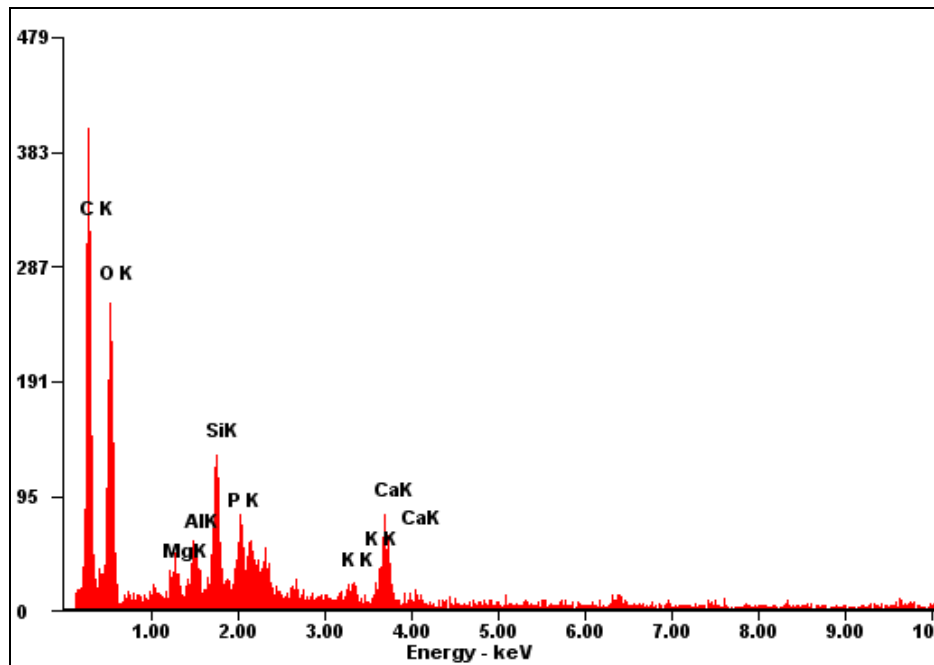
Three different zones can be envisaged: from room temperature to 200°C, from 200 to 550/600°C, and from 550/600 to 1000°C.

Main weight loss was recorded in the second zone, while first and third zone correspond to comparatively small weight losses. For raw AS, first zone corresponds to removal of moisture and light volatiles upto 200°C with a total loss of about 12%. This initial zone is followed by active oxidation zone from 200 to 550°C with total degradation of 58.4%. Subsequently, the sample weight decreased very slowly with total degradation of 5.3% in the third zone upto 1000°C. The residue left at 1000°C is ash and is about 24.3% of the original sample weight. Thermal degradation characteristics of treated AS shows (Figure 5.4.7b) removal of moisture and light volatiles of about 13% up to temperature of 200°C followed by an active oxidation zone between 200 and 600°C. Total degradation during this zone is about 65.3%. Beyond 600°C, the sample weight almost remained constant with total degradation of 1.8% upto 1000°C. Raw and treated AS do not show any endothermic transition between room temperature and 300°C, indicating the lack of any phase change during the heating process [Ng et al., 2002]. The strong exothermic peak centered on 530°C for raw AS and 580°C for treated AS is due to the oxidative degradation of the sample.

The heating value of the sludge was found to be 12.03 MJ/kg. This sludge can be utilized for making blended fuel briquettes with other organic fuels, which can be further used as a fuel in furnaces. The bottom ash obtained after its combustion can be blended with the cementitious mixture. This mixture can be used in construction purposes, thus, recovering energy from the sludge.

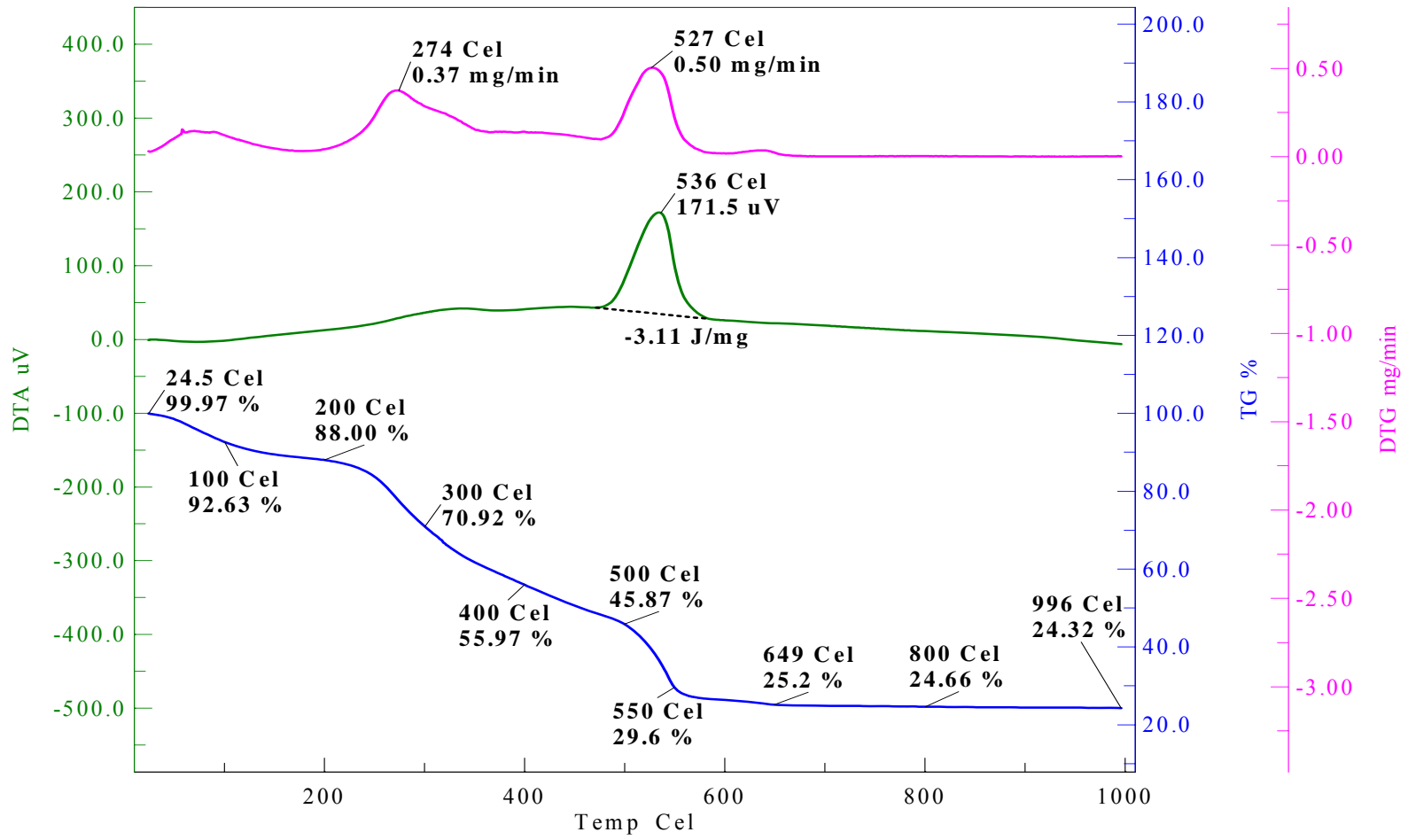


Before treatment

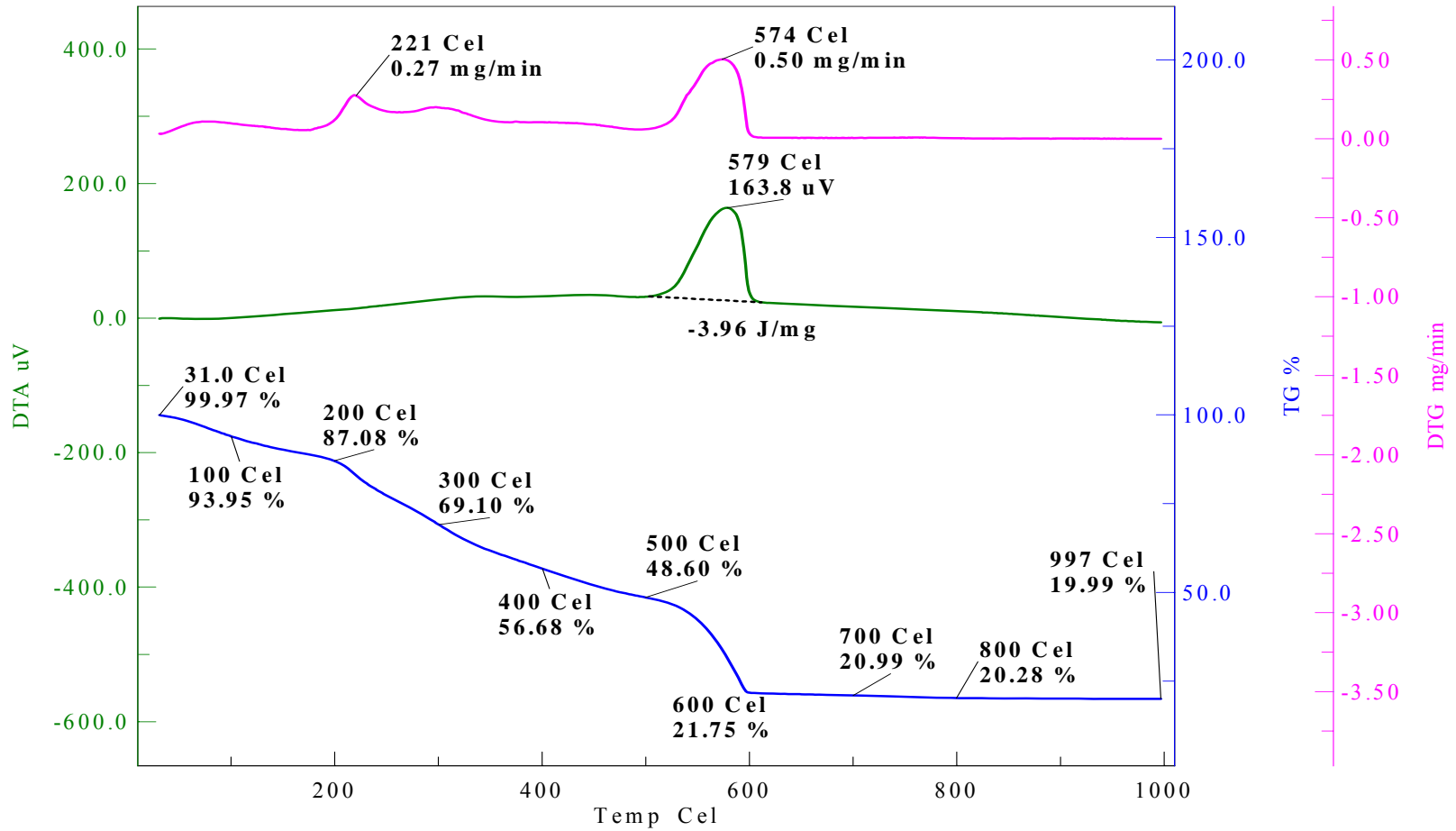


After treatment

Figure 5.4.6. EDX of activated sludge before and after treatment.



(a)



(b)

Figure 5.4.7. DTA-DTA-TG plot of activated sludge in various conditions in air atmosphere (a) before and (b) after growth.

5.5 TREATMENT OF ACTUAL PETROLEUM REFINERY (PRW) WASTEWATER

5.5.1 Characteristics of Wastewater and Acclimatization of Sludge

Activated sludge was collected from a sewage treatment plant located in Haridwar, Uttarakhand, India. Coarse and bigger particles were removed from the sludge and fed into the reactor. The reactor was initially filled with 4 L of activated sludge and 1 L of PRW along with nutrients such as NH_4Cl , $\text{Na}_2\text{HPO}_4 \cdot 12\text{H}_2\text{O}$, $\text{CaCl}_2 \cdot \text{H}_2\text{O}$, Na_2CO_3 , glucose and micronutrients such as NaCl , KCl , $\text{MgSO}_4 \cdot 7\text{H}_2\text{O}$, NaHCO_3 . Sludge acclimatization was performed for 30 d [Thakur et al., 2013e]. As the activated sludge adapted to reactor condition, volume of effluent was increased and nutrient amount was decreased as shown in Table 5.5.1. The total volume of activated sludge and PRW was maintained at 5 L throughout the experiment. DO inside the reactor was always maintained above 2 mg/L during the acclimatization, and experimental runs.

Table 5.5.1. Details of acclimatization procedure for SBR.

Time (d)	Volume of PRW (L)	Nutrient concentration (mg/L)					No. of cycles of 12 h each
		NH_4Cl	$\text{Na}_2\text{HPO}_4 \cdot 12\text{H}_2\text{O}$	$\text{CaCl}_2 \cdot \text{H}_2\text{O}$	Na_2CO_3	Glucose	
0-4	1	150	150	50	150	300	8
4-10	1	100	100	30	100	150	12
10-13	1.5	100	100	30	100	150	6
13-17	1.5	50	50	20	50	50	8
17-21	2	50	50	20	50	50	8
21-26	2	0	0	0	0	0	10
26-30	2.5	0	0	0	0	0	8

Actual PRW was collected from common wastewater treatment plant of local petroleum refinery of India. The sample was collected after the skimming of oil and emulsion removal. Main characteristics of the PRW are shown in [Table 5.5.2](#).

Table 5.5.2. Characterization of PRW before and after treatment by SBR.

Parameter (mg/L) except pH and Conductivity	Before Treatment	After Treatment
pH	8±0.5	7±0.5
Chemical Oxygen Demand (COD)	350±25	100±25
Total Organic Carbon (TOC)	70±10	17±5
Total Carbon (TC)	140±20	20±5
Phenol	10	0.1
Hardness (as CaCO₃)	180	
Total Dissolved Solid	900	400
Conductivity (µs/cm)	1317	
Chloride	261.062	60.613
Fluoride	2.933	0.797
Bromide	1.192	0.124
Sulfate	118.963	0.017
Nitrate	3.761	0.967

5.5.2 Effect of HRT on COD and TOC Removal

HRT, which is defined as the time the wastewater takes to pass through the system, for SBRs was calculated using the formula [\[Thakur et al., 2013a\]](#):

$$\text{HRT} = \frac{V_T}{V_F} \frac{1}{N_c} = \frac{V_T}{V_F} \frac{T_c}{24} \quad (5.5.1)$$

Where, V_F is the fill volume (L) and V_T is the total working volume of 5 L which is the sum of V_F and sludge volume (V_S). N_c is number of cycles per day and T_c

is the total cycle time of 10 h. Different V_F (0.5, 1, 1.5, 2, 2.5 and 3) were used to vary the HRT during instantaneous fill conditions. Effect of HRT on biodegradation of PRW was analyzed in the form of COD and TOC removal. [Figure 5.5.1a](#) and [Figure 5.5.1\(b\)](#) illustrate the change in COD and TOC removal efficiencies with change in HRT, respectively. Percentage COD and TOC removal increased with an increase in HRT from 0.56 ($V_F=3$ L) to 0.83 d ($V_F=2$ L) indicating higher biological conversion in the reactor. Maximum COD and TOC removal efficiencies of $\approx 77\pm 2\%$ and $80\pm 3\%$ were observed at 0.83 d HRT. These efficiencies were maintained for HRT of 1.11 d ($V_F=1.5$ L) also. Further increase in HRT led to decrease in COD and TOC removal efficiencies. [Neczaj et al. \[2008\]](#) and [Kushwaha et al. \[2013\]](#) have reported similar trend for the treatment of landfill leachate and dairy wastewaters. Details of experiment run for effect of HRT is given in [Table 5.5.3](#).

[Figure 5.5.2a](#) shows change in pH values during SBR operation at different HRT. It may be seen that pH decreased initially and attained a minimum value and then increased up to a maximum and became nearly constant. The initial decrease in pH is due to degradation of organic matter into acids and release of hydrogen ions. Increase in the hydrogen ion concentration leads to nitrification process in the reactor until a minimum value of pH is attained.

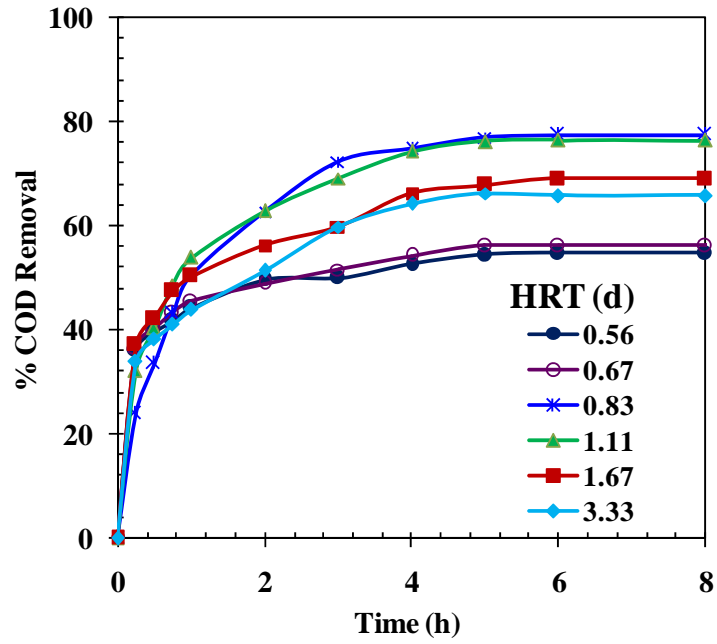
Nitrogen removal takes place via nitrification and denitrification, which, causes decrease and increase in pH, respectively. During nitrification, alkalinity is used up which is supplied from PRW itself. Therefore, during nitrification process, pH gets reduced up to pH 4 with time ([Figure 5.5.2a](#)) [[Kushwaha et al., 2013](#)]. At this pH (~ 4), all the alkalinity present in PWR gets consumed [[Peavy, 1985](#)], and therefore, the nitrification process stops. This minimum value in the pH profile is called ammonia valley and corresponds to the end of nitrification. At the same time when ammonia valley is attained, DO level is low and nearly anoxic condition is attained. After the ammonia valley, the pH increases from pH ~ 4 to ~ 7 due to the stripping of CO_2 , which is produced by oxidation of carbonaceous material, and ongoing denitrification. Thereafter, pH becomes nearly constant showing complete denitrification and end of CO_2 evolution [[Kushwaha et al., 2013](#)]. [Figure 5.5.2a](#) shows that at higher HRT, pH of the solution decreased rapidly then it increased slowly.

Table 5.5.3. Effect of HRT with instantaneous fill on COD and TOC removal efficiency.

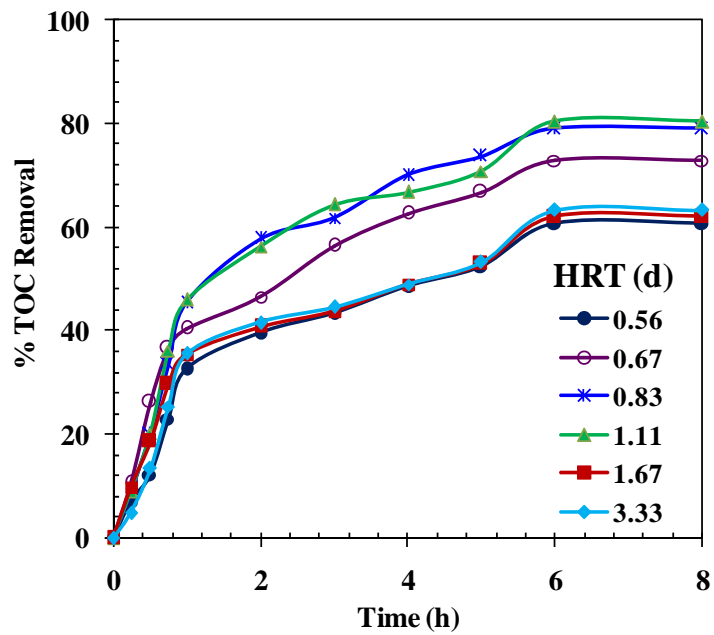
RUN	V_F	V_{SI}	VER (V_F/V_T)	HRT (d)	COD _{eff} (mg/L)	% COD removal	TOC _{eff} (mg/L)	% TOC removal	MLSS (mg/L)	SVI (mL/g)
1	0.5	4.5	0.1	3.33	86	65.74	20.46	63.25	2192	182.5
2	1	4	0.2	1.67	78	68.92	21.12	62.07	2153	162.6
3	1.5	3.5	0.3	1.11	84	76.34	16.08	80.40	2664	168.9
4	2	3	0.4	0.83	94	77.29	19.58	79.03	2896	172.7
5	2.5	2.5	0.5	0.67	144	56.10	19.92	72.88	2340	183.8
6	3	2	0.6	0.56	126	54.68	21.7	60.72	2410	186.7

A review of the literature shows that oxygen deficiency leads to growth of filamentous micro-organisms [Gaval and Pernell, 2003]. Filamentous growth induced by a low DO level requires increasing the DO concentration in the bulk fluid. High amount of DO above 5 mg/L may also lead to shearing of biomass and cause bulkier sludge. Excess growth of filamentous bacteria may lead poor sludge settleability and effluent with high turbidity [Wilean and Balmer, 1999]. The ultimate consequence of filamentous growth is the failure of the aerobic sludge SBR [Liu and Liu, 2006]. Figure 5.5.2b shows the change in DO level during SBR operation. Decrease in DO level indicates that organic matters present in the wastewater are being degraded by aerobic microbes present in the reactor. DO level in the present study was maintained above 2-5 mg/L to avoid excess filament growth and bulking of sludge.

Change in MLSS concentration was also studied with respect to change in HRT. Results are shown in Figure 5.5.3.

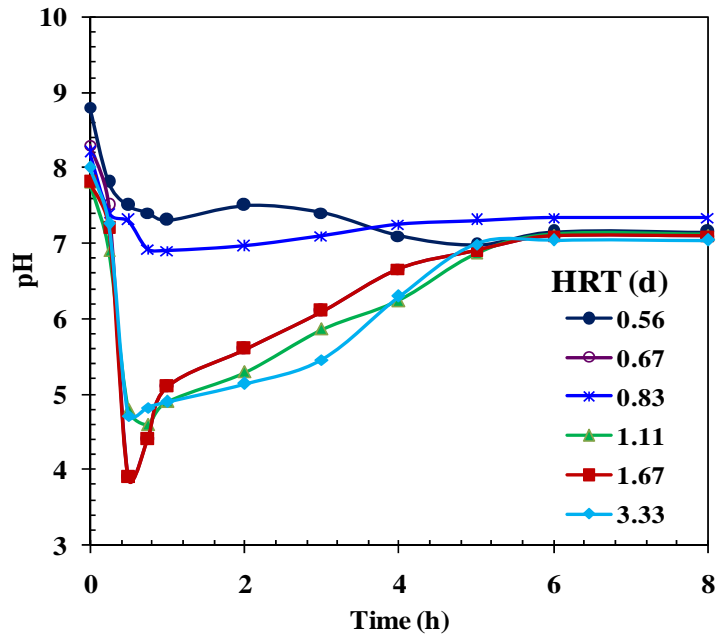


(a)

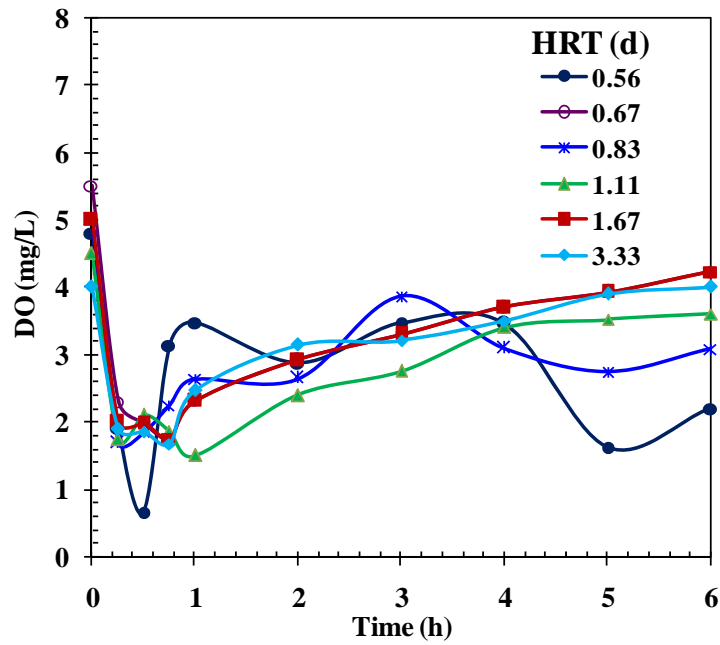


(b)

Figure 5.5.1. Effect of HRT on (a) COD removal, and (b) TOC removal.



(a)



(b)

Figure 5.5.2. Effect of HRT on (a) pH, and (b) dissolved oxygen.

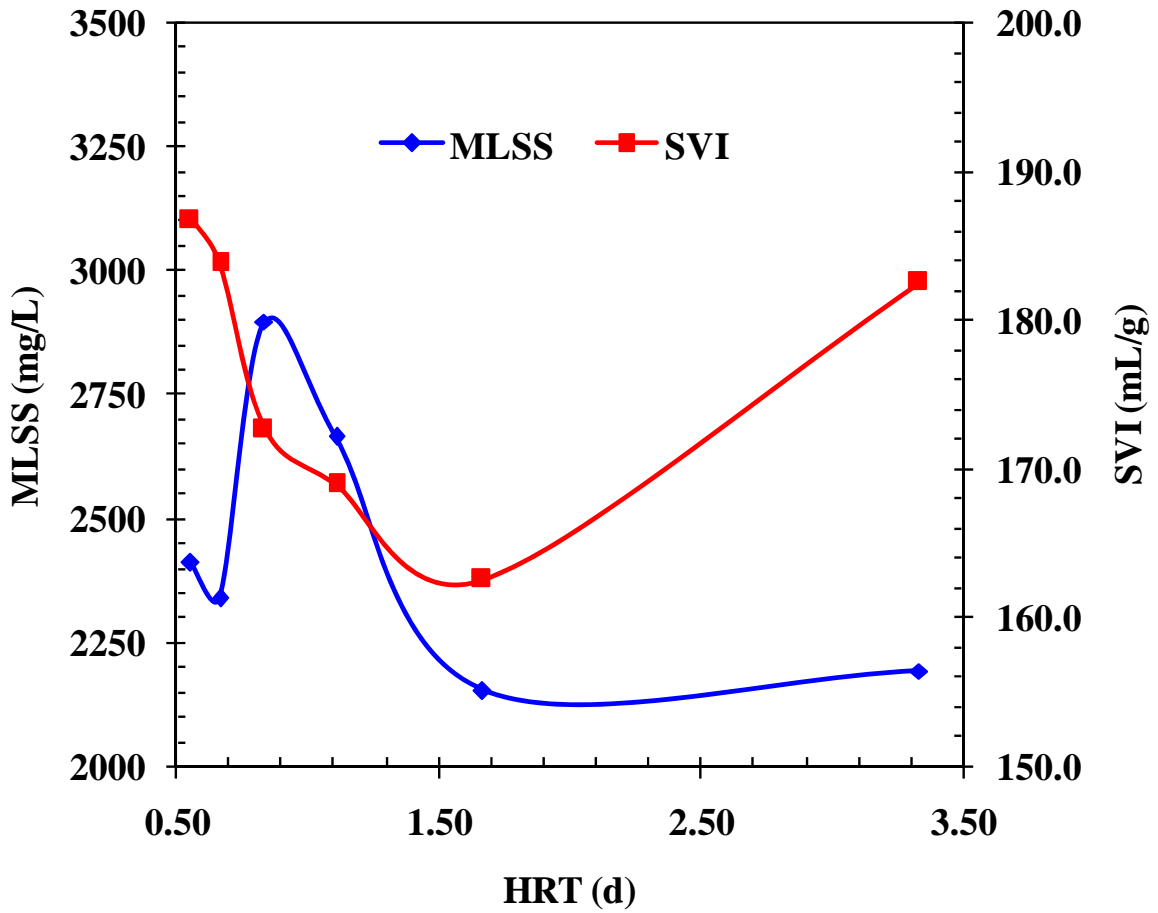


Figure 5.5.3. Effect of HRT on MLSS and SVI.

SVI is commonly used as an indicator of sludge settleability as well as filamentous growth in activated sludge processes. It may be seen that the value of SVI in the slurry decreased initially with an increase in HRT and then increased at higher HRT values. Higher growth rate of microorganism was observed when HRT was increased from 0.56 to 0.83 d. COD and TOC removal efficiencies decreased as the HRT increased beyond 1.11 d. This may be due to lower growth rate of microorganism and accumulation of older cells. HRT of 0.83 d (with fraction of SBR being filled in each cycle being 0.4) was selected as optimum HRT for further optimization of fill time.

5.5.3 Effect of Fill Time on COD and TOC Removal

In this study, fill time (t_F) of the SBR was varied in the range of 0.5-2 h. During filling process, aeration and agitation were also done, so that the degradation of organic compounds present in PRW also occurred during the fill phase itself. [Figure 5.5.4a](#) and [Figure 5.5.4b](#) show the effect of fill time in percentage removal of COD and TOC respectively.

At the end of fill period for $t_F=0.5, 1.0$ and 2.0 h, COD removal efficiency were found to be 58, 65.7 and 74.1%, respectively; and TOC removal efficiency were found to be 28.5, 51.1 and 59.3%, respectively. It may be noted that during instantaneous filling with $HRT_{opt}=0.83$ d (given in previous section), COD removal efficiencies of 33.57%, 50.48% and 62.56% and TOC removal efficiencies of 20.1%, 45.4% and 57.7% were observed with the corresponding react time of 0.5 h, 1.0 h and 2.0 h, respectively. Therefore, it can be concluded that fill time increases the removal rate and hence, reduces the react time. Overall, maximum COD and TOC removal of 79.7% and 83.3% were

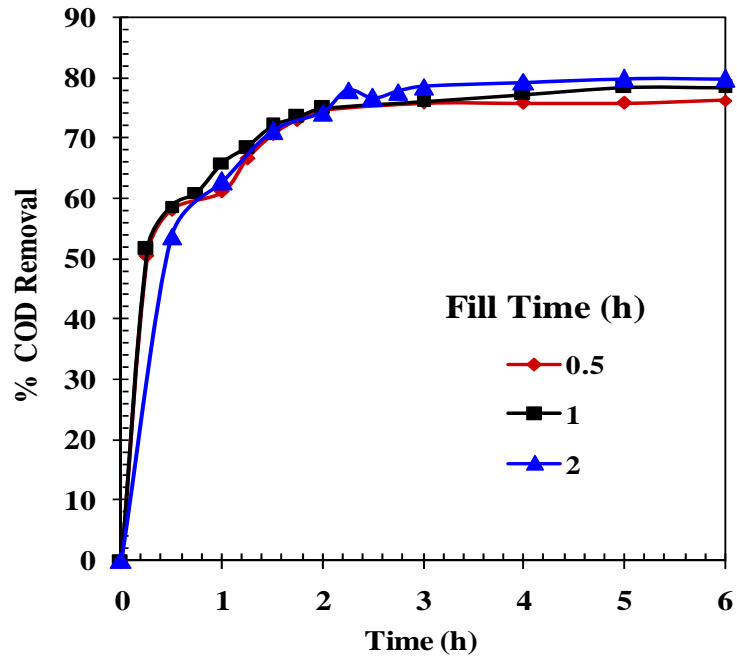
observed at 2 h fill time. At the end of further react time for 2 h, COD and TOC removal efficiency of 79.7% and 83.5%, respectively, were found. Figure 5.5.5a shows that the pH decreases during treatment at various fill times as was observed during treatment in instantaneous mode. Figure 5.5.5b gives details of DO profile in the reactor during this optimization of fill time. DO variation was found to be highest for $t_F=0.5$ h and least for $t_F=2$ h. Least variation in DO during experimental run with $t_F=2$ h may be due to slow filling and continuous treatment of PRW.

It may be seen in Figure 5.5.6 that an increase in fill time increased the MLSS concentration which in turn increased the SVI value. Higher value of SVI for the experimental run with $t_F=2$ h is due to the presence of optimum amount of DO during this run. Table 5.5.4 give the details of COD and TOC removal which varying fill time.

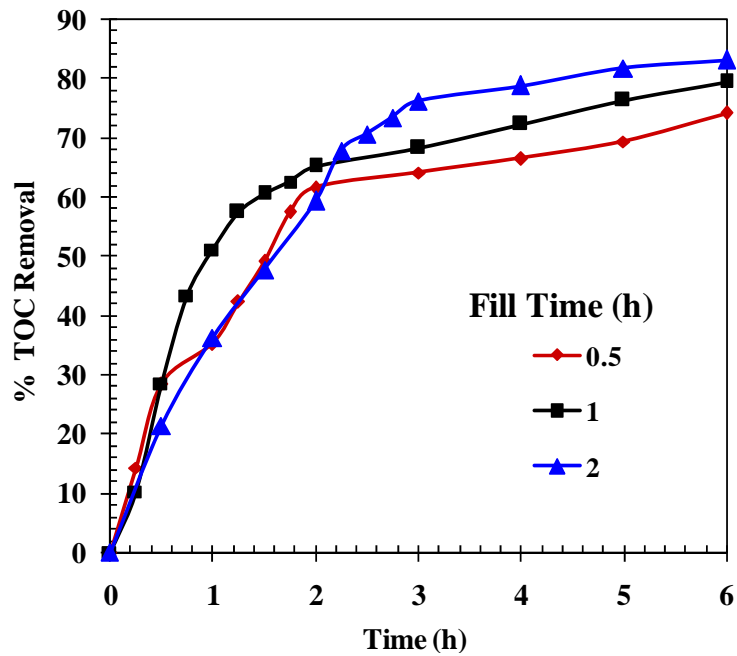
Table 5.5.4. Variation in fill time with HRT 0.83 d on COD and TOC removal efficiency.

Run	t_F	COD _{eff} (mg/L)	% COD removal	TOC _{eff} (mg/L)	% TOC removal	MLSS (mg/L)	SVI (mL/g)
1	0.5 h	88	76.15	19.47	76.83	2606	145.82
2	1.0 h	75	78.57	14.90	80.40	2795	161.00
3	2.0 h	75	79.73	13.84	83.53	2880	173.61

Overall, based on observations in Figure 5.5.1 and Figure 5.5.4, it is recommended to treat PRW in SBR having fill phase of 2 h and react phase of 2 h with fraction of SBR being filled in each cycle being 0.4.

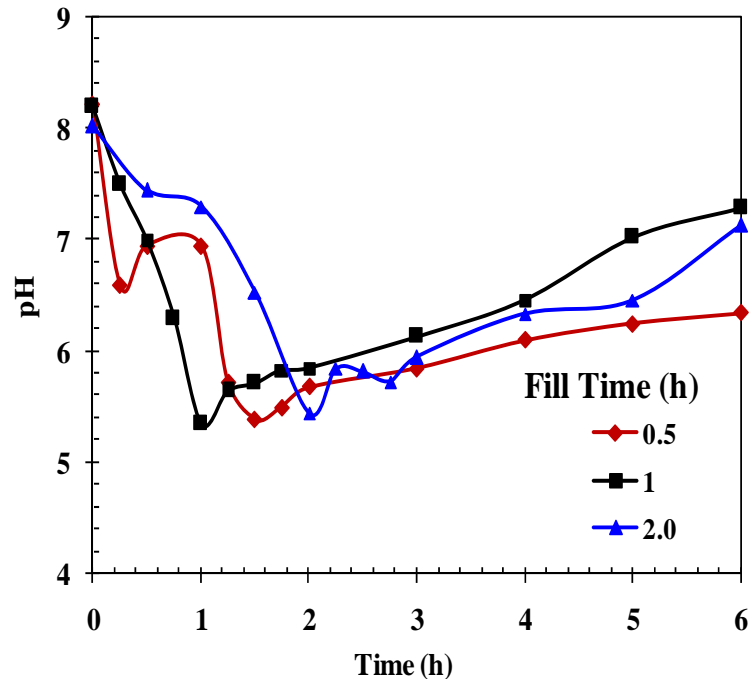


(a)

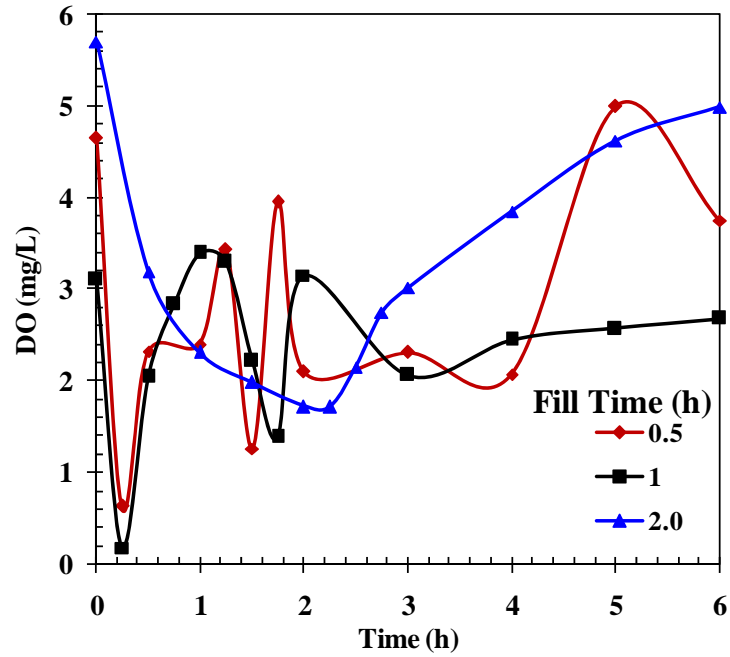


(b)

Figure 5.5.4. Effect of fill time on (a) COD removal, and (b) TOC removal.



(a)



(b)

Figure 5.5.5. Effect of fill time on (a) pH, and (b) dissolved oxygen.

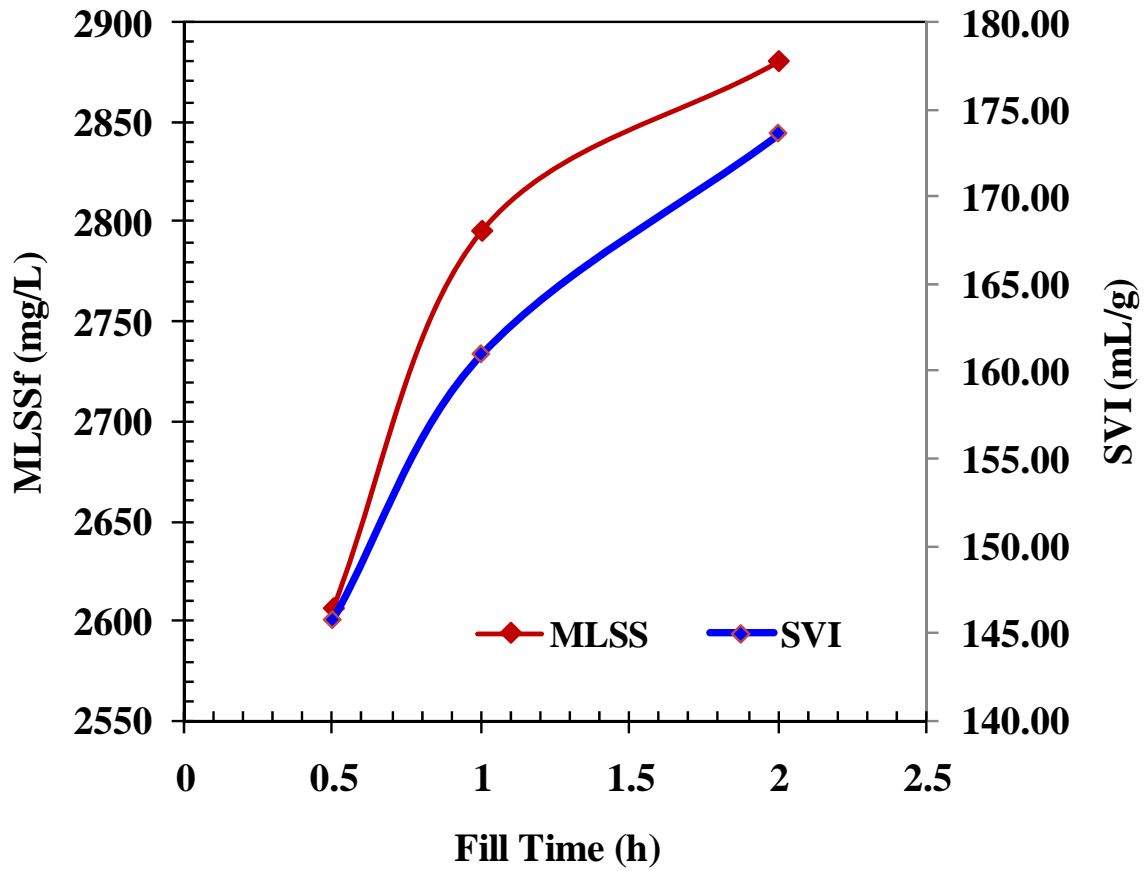


Figure 5.5.6. Effect of fill time on MLSS and SVI.

5.5.4 Determination of Kinetic Parameters

During biological treatment of PRW, micro-organisms consume the organics present in PRW and new biological cells or biomass is produced. Therefore, to understand the performance of the process kinetic study, determination of the values of kinetic parameters is necessary.

Kinetic study was performed for treatment of PRW in terms of COD removal under instantaneous filling of PRW to SBR and with varying HRT (in the range of 0.56-3.33 h). In the log growth phase and endogenous phase, variation of biomass concentration can be represented by following rate equation [Peavy et al., 2009]:

$$\frac{dX}{dt} = \mu X - k_d X \quad (5.5.2)$$

Where, μ is the specific growth rate constant (h^{-1}), X is the biomass concentration (MLSS) (mg/L) and k_d is the endogenous coefficient (h^{-1}). In the endogenous phase, increase in biomass is very slow. Therefore, endogenous coefficient (k_d) may be neglected and the above equation reduces to following log growth phase rate equation:

$$\frac{dX}{dt} = \mu X \quad (5.5.3)$$

In the exponential phase, the specific growth rate (μ) is obtained from the end of exponential growth phase and is calculated by [Marrot et al., 2006]:

$$\mu = \frac{\ln(X_2 / X_1)}{t_2 - t_1} \quad (5.5.4)$$

Yield coefficient (Y) can be calculated using the following equation:

$$Y = \frac{dX}{dS} = \frac{X_2 - X_1}{S_2 - S_1} \quad (5.5.5)$$

The specific rate of substrate utilization (q) can be calculated using the following relationship between q , μ and Y [Monod, 1949; Okpokwasili and Nweke, 2005]:

$$q = \frac{1}{X} \frac{dS}{dt} = \frac{1}{X} \frac{dX}{dt} \frac{dS}{dX} = \frac{\mu}{Y} \quad (5.5.6)$$

Calculated values of μ , Y and q at various HRTs are shown in Table 5.5.5. It may be seen that the values of μ , Y and q increase with an increase in HRT till HRT value of 1.11 d. Further increase in HRT decrease the value of μ , Y and q . Since the values of μ , Y and q are not much different for HRT values at 0.83 d and 1.11 d and the amount of PRW treated with HRT=0.83 ($V_F=2$ L) is much higher than that for HRT=1.11 d ($V_F=1.5$ L), therefore, HRT of 0.83 d was considered as optimum.

Table 5.5.5. Kinetic constant for COD degradation of PRW in SBR at various HRT.

HRT (d)	COD _f (mg/L)	MLSS _i (mg/L)	MLSS _f (mg/L)	μ	Y	q
0.56	144	3230	3380	0.0076	0.7281	0.0104
0.67	126	3020	3230	0.0112	0.9375	0.0120
0.83	94	2750	3020	0.0156	1.0547	0.0148
1.11	84	2430	2750	0.0206	1.2030	0.0171
1.67	86	2240	2430	0.0135	0.7197	0.0188
3.33	78	2059	2240	0.0140	0.6654	0.0211

5.5.5 Characterization of Wastewater and Activated Sludge

Figure 5.5.7 shows the FTIR analysis of untreated PRW and the treated effluent at optimized condition. The broad peak at ≈ 3455 cm^{-1} for untreated and treated PRW originate from stretching of hydrogen bonds in hydroxyl groups. This band may also be attributed to the presence of N-H vibrations. A series of peaks from 2873-2969 cm^{-1} are due to aliphatic CH_2 and/or carbon-hydrogen stretching in methyl and methylene groups

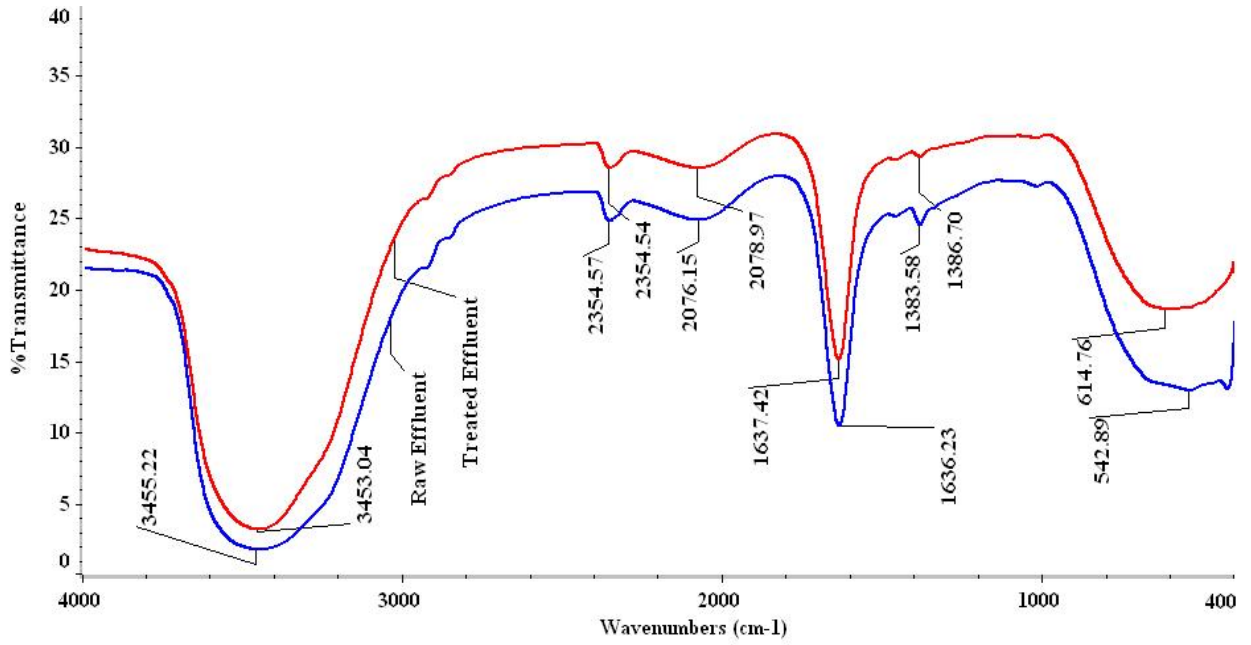


Figure 5.5.7. FTIR of treated and raw refinery wastewater by SBR.

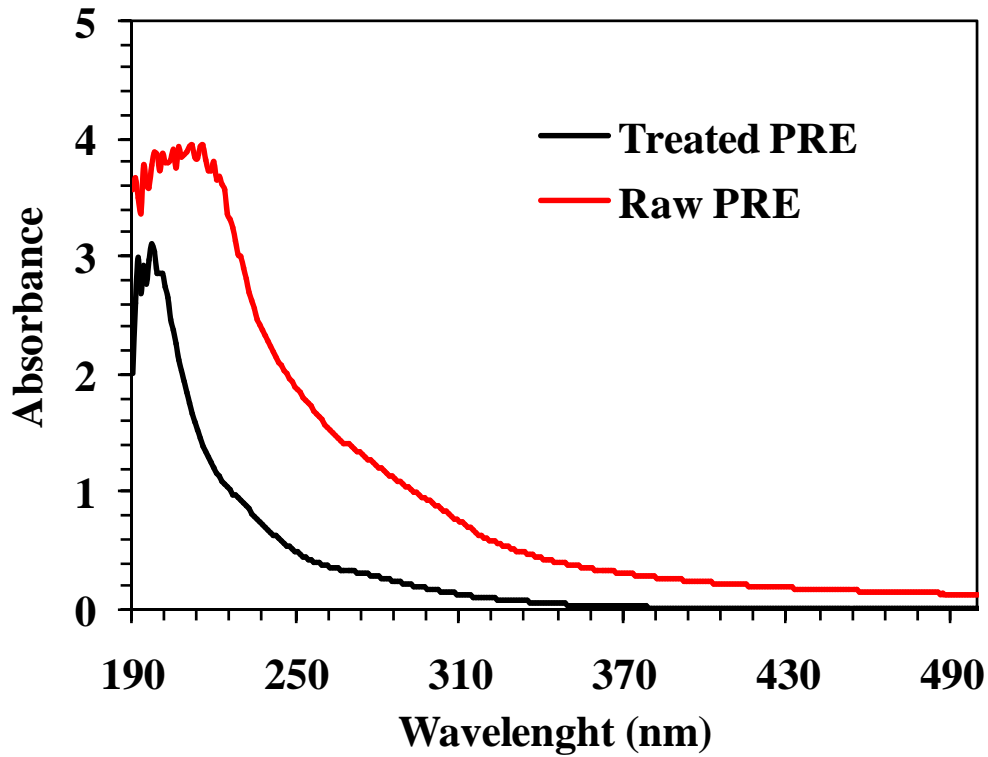


Figure 5.5.8. UV spectrum analysis of treated and raw refinery wastewater by SBR.

[Barber et al., 2001]. The band in the region $2000\text{--}2400\text{ cm}^{-1}$ is associated with OH, CH and C=O stretching vibrations. The peak observed at $\approx 1635\text{ cm}^{-1}$ corresponds to presence of amides [Leenheer et al., 2001]. Several small peaks ranging from 1380 cm^{-1} to 1456 cm^{-1} are due to carbon–hydrogen bending vibrations of methyl and methylene groups [Bright et al., 2010]. Peaks near 614 cm^{-1} and 542 cm^{-1} are associated with silicate minerals [Lingbo et al., 2005]. At lower frequencies, the vibrations are dominated by O-H band. It may be seen that transmittance of all the peaks and bands increased in treated PRW as compared to the untreated PRW indicating degradation of various compounds (containing these functional groups) during SBR operation.

Degradation of PRW before and after treatment was also studied using UV–visible analysis in the range of $190\text{--}490\text{ nm}$ (Figure 5.5.8). Presence of aromatic rings in PRW is indicated by peaks at $\approx 200\text{ nm}$. Untreated PRW shows peaks in range of $200\text{--}230\text{ nm}$ (representing mono-aromatic rings) which get faded in treated PRW. This study shows that different bonds were broken and aromatic rings were mineralized during SBR treatment.

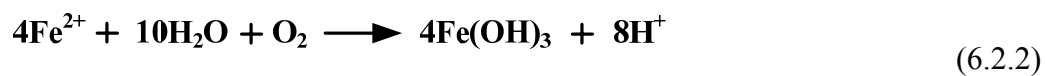
ELECTROCOAGULATION

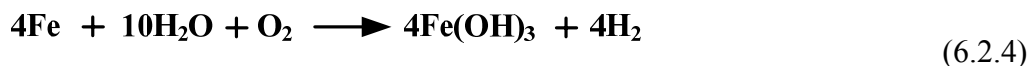
6.1 GENERAL

This chapter describes the theory, materials and methods, results and discussion regarding treatment of petroleum refinery wastewater (PRW) using electrocoagulation method.

6.2 ELECTROCOAGULATION THEORY

Electrocoagulation (EC) treatment method works on the principle of increase in ionic concentration which reduces the zeta potential and neutralizes colloidal particle charge by well known mechanism of sweep flocculation [Duan et al., 2003]. EC treatment occurs sequentially as electrolytic reactions take place on the surface of electrodes. Metal ions generation take place at anode and hydrogen gas generation take place at cathode according to equation 6.2.1 and 6.2.3, respectively. Generated metal ions react with the colloids present in wastewater and subsequent precipitation of metal hydroxide take place in aqueous phase (as given in equation 6.2.2). Overall reaction taking place in the reactor can be represented by equation 6.2.4 [Keshmirizadeh et al., 2011].





Treatment steps involved in EC process are: electrolytic reactions at electrode surfaces; formation of coagulants in the aqueous phase; and adsorption of soluble or colloidal pollutants on coagulants and removal by sedimentation or flotation [Can et al., 2003]. EC method can be used in batch and continuous mode depending on the amount of wastewater to be treated. In batch system, certain amount of wastewater is fed into the reactor and after an appropriate time wastewater is taken out for further analysis. In continuous system, a feed pump is provided which continuously feeds the wastewater and treated effluent is taken out continuously.

EC is highly versatile and works on principle of generation of metal hydroxides and dispersed gas bubbles during electrolysis. Characteristics of wastewater and selection of process parameters play a vital role in removal efficiency of EC process. Efficiency of EC treatment depends on various process parameters like conductivity, pH, type of electrode used, current density (j), type of pollutant, etc. Thus, EC process is complex and are controlled by multiple parameters and requires some statistical experimental design that may reduce the number of experimental runs with a better combination of input parameters. The application of this statistical design is to reduce the process variability which in turn reduces the time of trial and error experiments [Chen et al., 2012; Prasad et al., 2008; Moreno et al., 2009].

EC technique has been used for the treatment of numerous types of wastewater generated in various industries such as textile, distillery, tannery, pulp and paper, etc. It has been used for the removal of various types of pollutants such as dyes, arsenic, phenolic compounds, etc. from aqueous solutions [Jiang et al., 2002; Mahesh et al.,

2006; Feng et al., 2007; Thella et al., 2008; Zongoa et al., 2009; Wang et al., 2005; Can et al., 2003; Thakur et al., 2009].

6.3 MATERIALS AND METHODS

6.3.1. Wastewater

Characterization of wastewater used in this study has been described in section 5.5.1 of Chapter V.

6.3.2. Experimental Setup

A laboratory scale rectangular reactor of perspex glass, prepared with a working volume of 1.5 L, was used for the batch EC experiments. Schematic diagram and actual photograph of EC experimental setup is shown in [Figure 6.3.1](#) and [Figure 6.3.2](#), respectively. Stainless steel (SS) sheet was procured from local supplier and was cut into required shape. Four SS plate electrodes were used in the present study. For the cleaning of iron electrodes, they were first degreased and then treated with 15% HCl, followed by washing with distilled water and oven drying prior to their use in the ECT experiments. Dimensional characteristics of the reactor and SS electrode are shown in [Table 6.3.1](#).

Inter-electrode gap was varied in the range of 0.5-2.5 cm. A digital direct current power supply (0–20 V, 0–5 A) was used to maintain constant current in the range of 1-5 A during the run. Solution was agitated with magnetic stirrer during the experimental run so as to achieve proper mixing. Electrode inside the reactor was placed 1 cm above the bottom of reactor to achieve proper agitation.

Zeta potential was measured using Malverian Instruments, Zetasizer Nano Series, UK.

Table 6.3.1. Dimensional characteristics of EC-cell.

Reactor Characteristics	
Material	Plexiglass
Reactor type	Batch
Dimensions (mm)	110 × 110 × 125 (length × width × height)
Working volume (L)	1.5
Stirring mechanism	Magnetic bar
Electrode Characteristics	
Material (Anode and Cathode)	Stainless steel
Shape	Rectangular plate
Size of each plate (mm)	80×80
Thickness (mm)	3
Plate arrangement	Parallel
Submergence	Full

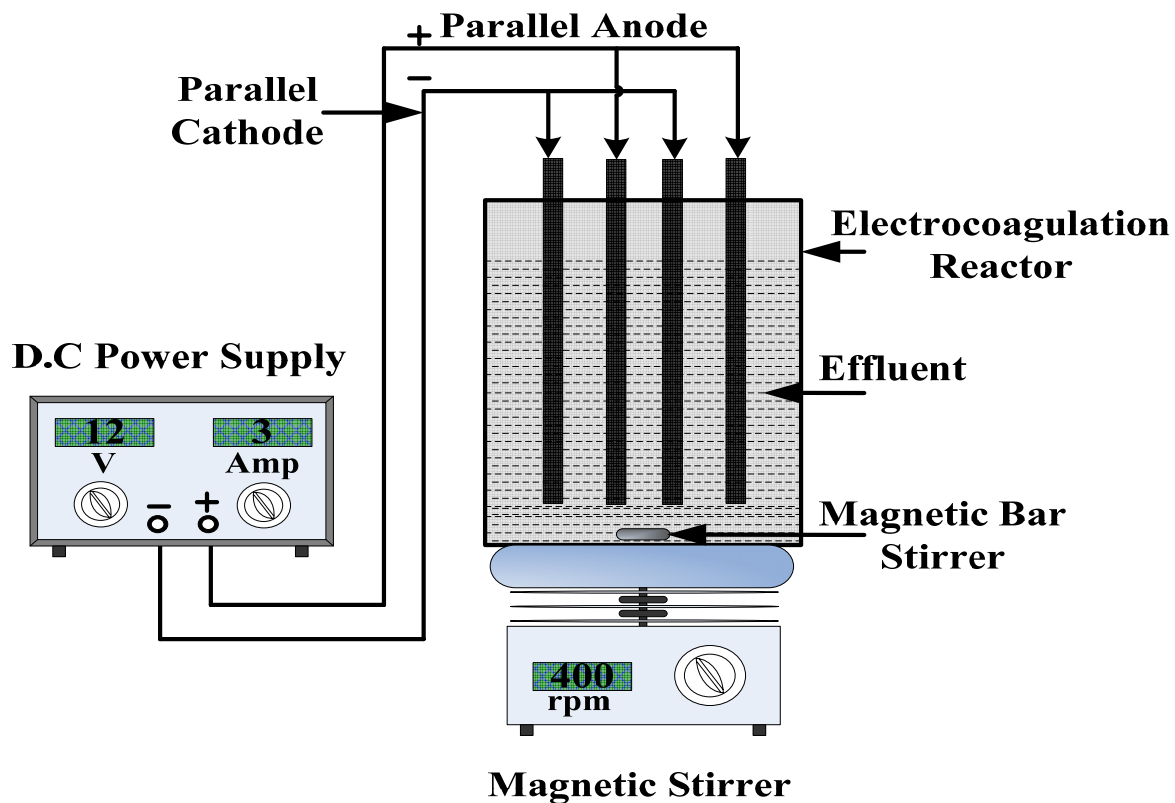


Figure 6.3.1. Schematic diagram of experimental setup.

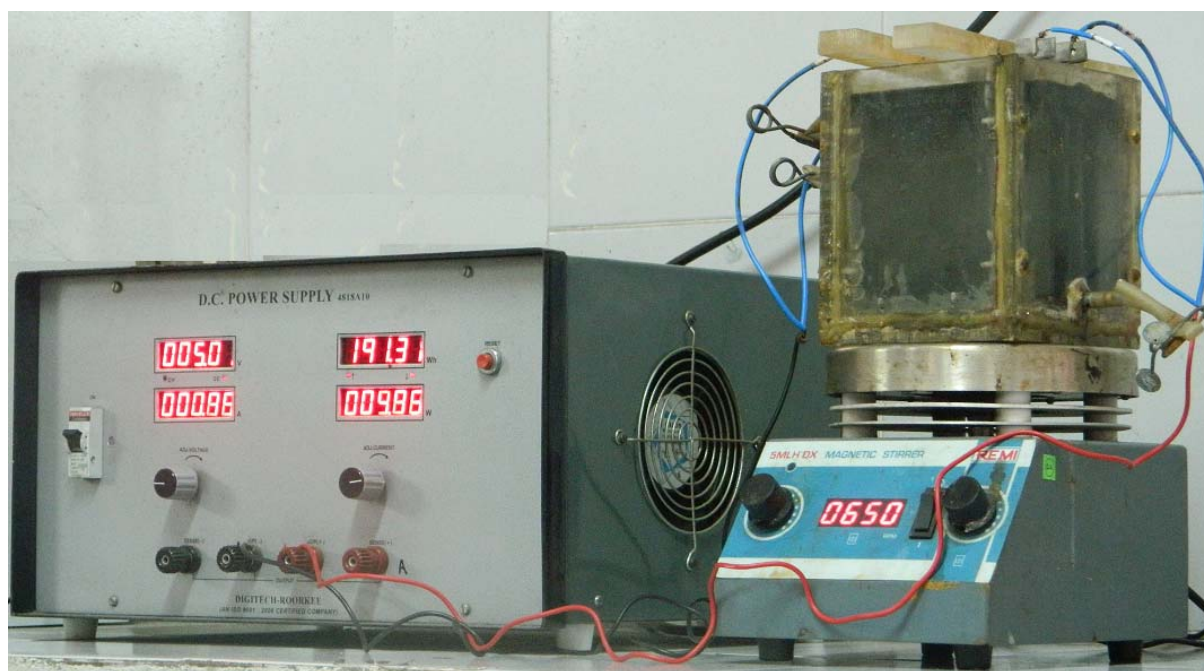


Figure 6.3.2. Actual photograph of experimental setup.

6.3.3. Experimental Design and Procedure

In the present study, experiments for EC treatment of PRW were designed using response surface methodology (RSM). RSM is an effective statistical tool for collection of mathematical and statistical information useful for developing, improving and optimizing processes and can be used to evaluate the relative significance of several affecting parameters even in the presence of complex interactions. The main advantage of RSM is the reduced number of experiments needed to provide sufficient information to optimise the process. Four factor five level central composite (CC) design has been used in the present study. Data obtained were analyzed by Design expert software version 6.0.8 (STAT-EASE Inc., Minneapolis, USA).

Five-level four factors (namely pH_o : 2–10; j : 39.06–195.31 A/m²; g : 0.5–2.5 cm and t : 30–150 min) have been taken as input parameters and percentage COD removal (Y_1) and TOC removal (Y_2) have been taken as responses of the system. For statistical calculations, levels for the four parameters X_i (X_1 (J), X_2 (m), X_3 (t), X_4 (pH_o)) were coded as x_i according to the following relationship [Thakur et al., 2009]:

$$x_i = \frac{(X_i - X_o)}{\delta X} \quad (6.3.1)$$

Where, x_i is coded (dimensionless) value of parameter X_i , X_o is value of the parameter X_i , at the centre point, and δX represents the step change. Based on this, the levels were designated as -2, -1, 0, +1, and +2. Values of various parameters at various coded points are given in Table 6.3.2 and the CC design matrix is given in Table 6.3.3.

Initial pH of PRW was adjusted using 0.1 N NaOH and 0.1 N HCl with j kept constant throughout each experimental run. After the completion of the run, residual

COD and TOC were estimated. Percentage removal was calculated using the following relationship:

$$\text{Percent COD removal (Y)} = \frac{(C_0 - C_f)100}{C_0} \quad (6.3.2)$$

Where, C_f is the final COD concentration (mg/L) after t (min).

Desirability function approach was used to simultaneously optimize two responses of the present study [Derringer and Suich, 1980].

Table 6.3.2. Parameters and their level used to design the experiment runs.

Variable, Unit	Factors	Level				
		-2	-1	0	1	2
Initial pH, pH ₀	X ₁	2	4	6	8	10
Current density, j (A/m ²)	X ₂	39.06	78.12	117.19	156.25	195.31
Inter-electrode distance, g (cm)	X ₃	0.5	1	1.5	2	2.5
Time of electrolysis, t (min)	X ₄	30	60	90	120	150

Simultaneous optimization combines all the different responses into one composite requirement. One-sided desirability d_i of any one response is given by:

$$d_i = \begin{cases} 0 & \text{if } Y_i \leq Y_{i-\min} \\ \left[\frac{Y_i - Y_{i-\min}}{Y_{i-\max} - Y_{i-\min}} \right]^r & \text{If } Y_{i-\min} < Y_i < Y_{i-\max} \\ 1 & \text{if } Y_i \geq Y_{i-\max} \end{cases} \quad (6.3.3)$$

Where, Y_i is response value, $Y_{i-\min}$ and $Y_{i-\max}$ are the minimum and maximum acceptable values of response i , and r is a positive constant that is used to determine scale of desirability [Kushwaha et al., 2010].

Table 6.3.3. Full factorial design with actual and predicted values of percentage COD and TOC removal.

Std. order	pH ₀ (X ₁)	j (X ₂)	g (X ₃)	t (X ₄)	Y ₁ (COD removal)		Y ₂ (TOC removal)	
					Y _{1exp} (%)	Y _{1pre} (%)	Y _{2exp} (%)	Y _{2pre} (%)
1	4	78.12	1	60	27.72	23.36	23.48	25.29
2	8	78.12	1	60	26.64	28.73	17.77	16.00
3	4	156.25	1	60	44.00	42.46	19.65	19.78
4	8	156.25	1	60	33.94	30.43	17.91	16.71
5	4	78.12	2	60	19.10	21.79	15.06	14.05
6	8	78.12	2	60	20.19	18.86	16.95	16.45
7	4	156.25	2	60	52.51	48.82	15.81	18.75
8	8	156.25	2	60	26.47	28.49	25.26	27.36
9	4	78.12	1	120	32.41	28.96	38.42	34.54
10	8	78.12	1	120	41.52	44.89	28.06	26.12
11	4	156.25	1	120	51.27	52.28	37.85	39.36
12	8	156.25	1	120	54.95	50.82	37.93	37.16
13	4	78.12	2	120	21.01	24.20	16.50	18.71
14	8	78.12	2	120	31.73	31.84	23.88	21.96
15	4	156.25	2	120	58.98	55.46	33.75	33.73
16	8	156.25	2	120	41.67	45.70	44.01	43.21
17	2	117.19	1.5	90	32.78	36.74	34.01	31.78
18	10	117.19	1.5	90	34.56	32.35	28.96	31.97
19	6	39.06	1.5	90	18.63	16.57	15.53	18.66
20	6	195.31	1.5	90	45.75	49.46	36.90	34.61
21	6	117.19	0.5	90	35.00	39.38	21.08	23.74
22	6	117.19	2.5	90	35.32	32.69	20.46	18.57
23	6	117.19	1.5	30	26.31	29.24	11.84	10.19
24	6	117.19	1.5	150	53.21	52.04	32.87	35.29
25	6	117.19	1.5	90	43.12	43.71	20.41	22.02
26	6	117.19	1.5	90	45.46	43.71	24.25	22.02
27	6	117.19	1.5	90	40.43	43.71	18.78	22.02
28	6	117.19	1.5	90	46.47	43.71	25.55	22.02
29	6	117.19	1.5	90	39.70	43.71	19.50	22.02
30	6	117.19	1.5	90	46.96	43.71	23.70	22.02

One-sided desirability d_i transforms each response into a value between 0 and 1. All the desirabilities are combined to form overall desirability (D) which is given by following function:

$$D = (d_1 \times d_2 \times d_3 \dots)^{1/k} \quad (6.3.4)$$

Where, $0 \leq D \leq 1$ and k is the number of responses.

6.4 RESULTS AND DISCUSSION

6.4.1. Statistical Analysis and Fitting of Second-Order Polynomial Equation

The responses, Y_1 and Y_2 , measured according to the conditions of various operational parameters are shown in [Table 6.3.3](#). Various types of models such as linear, interactive, quadratic and cubic models were fitted to the experimental data. The model adequacies were checked by sequential model sum of squares test and model summary statistics test which required calculation of coefficient of determination (R^2), adjusted- R^2 and statistical significance check by F-test. Results of the adequacies test are given in [Table 6.4.1](#), which suggest that the quadratic model is significant. Both tests suggested second order polynomial to be used for further data analysis. Experimental data were, therefore, fitted to quadratic second-order polynomial model as given below:

$$Y = b_o + \sum_{i=1}^4 b_i X_i + \sum_{i=1}^4 b_{ii} X_i^2 + \sum_{i=j}^3 \sum_{i=j+1}^4 b_{ij} X_{ij} \quad (6.4.1)$$

Where, Y is the predicted response b_o , b_i , b_{ii} , b_{ij} are the model coefficients and X_i is the uncoded independent variable. Fitting quality of polynomial models was checked

by analysis of variance (ANOVA) for each response. ANOVA results are shown in [Table 6.4.2](#) and [Table 6.4.3](#) for Y_1 and Y_2 , respectively.

ANOVA showed that j and t are highly significant terms, whereas, j^2 and $pH_o \times j$ are significant terms for response Y_1 . For response Y_2 , j and t are highly significant terms, and pH_o^2 , $pH_o \times g$, $j \times g$ and $j \times t$ are significant terms.

The final quadratic equations in terms of coded factors for Y_1 and Y_2 are given below:

$$Y_1 = +43.77 - 2.26X_1 + 16.47X_2 - 3.31X_3 + 11.42X_4 - 9.16X_1^2 - 10.76X_2^2 - 7.67X_3^2 - 3.07X_4^2 - 17.48X_1X_2 - 8.30X_1X_3 + 10.57X_1X_4 + 7.97X_2X_3 + 4.25X_2X_4 - 3.19X_3X_4 \quad (6.4.2)$$

$$Y_2 = +22.05 + 0.12X_1 + 7.94X_2 - 2.55X_3 + 12.59X_4 + 9.85X_1^2 + 4.55X_2^2 - 0.87X_3^2 + 0.72X_4^2 + 6.25X_1X_2 + 11.68X_1X_3 + 0.87X_1X_4 + 10.26X_2X_3 + 10.38X_2X_4 - 4.60X_3X_4 \quad (6.4.3)$$

Values in front of various terms in the coded model indicate the intensity and the algebraic sign (+/-) indicates the direction of the influence of the process variables on the response [[Cruz-Gonzalez et al., 2010](#)]. Quadratic polynomial model gives R^2 value of 0.9273 and 0.9333 for Y_1 and Y_2 , respectively.

Corresponding values of adjusted R^2 are 0.8595 and 0.8705, respectively. [Joglekar and May \[1987\]](#) suggested that R^2 should be at least 0.80 for a good fit while in the present study R^2 value of COD and TOC were 0.93 which indicates that only 7% of total variation could not be explained by the empirical quadratic model [[Olmez et al., 2009](#)].

Table 6.4.1. Adequacy of the models tested for Y_1 and Y_2 .

Source	Sequential model sum of squares						Model summary statistics					
	Sum of Squares	DF	Mean Square	F Value	Prob> F	Remark	Std. Dev.	R ²	Adjusted R ²	Predicted R ²	PRESS	Remarks
COD removal (Y_1)												
Mean	42399.53	1	42399.53									
Linear	2500.65	4	625.16	13.14	<0.0001		6.90	0.6777	0.6261	0.5325	1724.98	
2FI	574.15	6	95.69	2.96	0.0328		5.69	0.8333	0.7455	0.6021	1468.41	
Quadratic	347.10	4	86.78	4.85	0.0103	Suggested	4.23	0.9273	0.8595	0.6376	1337.44	Suggested
Cubic	218.50	9	24.28	2.93	0.1017	Aliased	2.88	0.9865	0.9349		+	Aliased
Residual	49.57	6	8.28									
Total	46089.59	30	1536.32									
TOC removal (Y_2)												
Mean	18556.65	1	18556.65									
Linear	1360.21	4	340.05	11.39	<0.0001		5.46	0.6458	0.5891	0.4671	1122.38	
2FI	407.84	6	67.97	3.82	0.0115		4.22	0.8394	0.7549	0.6457	746.20	
Quadratic	197.19	4	49.30	5.24	0.0076	Suggested	3.07	0.93330	0.8705	0.6956	641.07	Suggested
Cubic	93.65	9	10.41	1.32	0.3807	Aliased	2.81	0.9775	0.8913		+	Aliased
Residual	47.38	6	7.90									
Total	20662	30	688.79									

DF: degree of freedom, PRESS: Predicted residual sum of square, 2FI: two factor interaction.

Table 6.4.2. ANOVA for response surface quadratic model for Y_1 .

Source	Coefficient estimate	Sum of Squares	DF	Mean Square	F Value	Prob>F	
Model		3421.89	14	238.6906	13.67	<0.0001	Highly Significant
Intercept	43.77						
X_1	-2.26	30.74	1	30.74	1.72	0.2095	
X_2	16.47	1618.87	1	1618.87	90.55	<0.0001	Highly Significant
X_3	-3.31	65.87	1	65.87	3.68	0.0741	
X_4	11.42	781.93	1	781.93	43.74	<0.0001	Highly Significant
X_1^2	-9.16	143.69	1	143.69	8.04	0.0125	
X_2^2	-10.76	198.84	1	198.84	11.12	0.0045	Significant
X_3^2	-7.67	100.70	1	100.70	5.63	0.0314	
X_4^2	-3.07	16.11	1	16.11	0.90	0.3575	
X_1X_2	-17.48	302.61	1	302.61	16.93	0.0009	
X_1X_3	-8.30	68.85	1	68.85	3.85	0.0685	
X_1X_4	10.57	111.70	1	111.70	6.25	0.0245	
X_2X_3	7.97	62.92	1	62.92	3.52	0.0802	
X_2X_4	4.25	17.90	1	17.90	1.00	0.3328	
X_3X_4	-3.19	10.15	1	10.15	0.57	0.4628	
Residual		268.16	15	17.88			
Lack of Fit		219.74	10	21.97	2.27	0.1894	Not Significant
Pure Error		48.43	5	9.69			
Cor Total		3690.06	29				

Table 6.4.3. ANOVA for response surface quadratic model for Y_2 .

Source	Coefficient estimate	Sum of Squares	DF	Mean Square	F Value	Prob>F	
Model		1965.24	14	140.37	14.93	<0.0001	Highly Significant
Intercept	22.05						
X_1	0.12	0.087	1	0.087	0.00928	0.9245	
X_2	7.94	376.42	1	367.42	40.03	<0.0001	Highly Significant
X_3	-2.55	38.96	1	38.96	4.14	0.0598	
X_4	12.59	950.93	1	950.93	101.14	<0.0001	Highly Significant
X_1^2	9.85	166.24	1	166.24	17.68	0.0008	Significant
X_2^2	4.55	35.52	1	35.52	3.78	0.0710	
X_3^2	-0.87	1.29	1	1.29	0.14	0.7165	
X_4^2	0.72	0.89	1	0.89	0.094	0.7628	
X_1X_2	6.25	38.66	1	38.66	4.11	0.0607	
X_1X_3	11.68	136.37	1	136.37	14.50	0.0017	Significant
X_1X_4	0.87	0.75	1	0.75	0.080	0.7814	
X_2X_3	10.26	104.23	1	104.23	11.08	0.0046	Significant
X_2X_4	10.38	106.71	1	106.71	11.35	0.0042	Significant
X_3X_4	-4.60	21.12	1	21.12	2.25	0.1547	
Residual		141.04	15	9.40			
Lack of Fit		101.41	10	10.14	1.28	0.4147	Not Significant
Pure Error		39.63	5	7.93			
Cor Total		2106.28	29				

6.4.2. Effects of Parameters

Three-dimensional response surface graphs for responses Y_1 , Y_2 and desirability with respect to various operational parameters namely pH_o , j , g and t are shown in [Figure 6.4.1](#) and [Figure 6.4.2](#). The operating parameters, pH and j influence the coagulant generation rate that affect the removal of pollutants from wastewater. [Figure 6.4.1](#) shows that as the pH of the solution changes from acidic medium to basic medium, COD and TOC removal efficiencies of the EC increase. This is due to formation of polymeric species, amorphous hydroxide precipitates and other iron complexes in the pH range of 4-7. As the pH increases beyond 9, less formation of these reactive flocs decreases the removal efficiencies [[Chavalparit and Ongwande, 2009](#); [Gurses et al., 2002](#); [Tir and Moulai-Mostefa, 2008](#)]. Current density (j) plays an important role in increasing the quantity of flocs. As the j increases, higher formation of flocs takes place which causes higher removal of COD and TOC as seen from [Figure 6.4.1](#). It may also be seen that the overall desirability, given by equation 6.3.3 and 6.3.4 (detailed calculation procedure for overall desirability is given in later sections) increases with an increase in j and pH. As the j and time of electrolysis increase towards higher range, desirability also increases to its maximum value of 1. [Figure 6.4.2](#) shows the effect of t and g on COD and TOC removal efficiencies. When the value of t increases, an increment occurs in the concentration of ions and their hydroxide flocs by Faraday's law. This increases the COD and TOC removal efficiencies. It may be seen in figures that g has very marginal affect on COD and TOC removal efficiencies and that the maximum COD and TOC removal efficiencies occur at $g=1.5$ cm.

6.4.3. Optimization Analysis

The experimental design results were optimized using the approximating functions of percentage COD and TOC removal efficiencies as given in equations 6.4.2 and 6.4.3, respectively. Optimization of design parameters namely j , pH, t and g was done with an aim to simultaneously maximize COD (Y_1) and TOC (Y_2) removal efficiencies. This optimization of parameters was done by maximizing the desirability function.

For calculating individual desirability, minimum acceptable values of responses (Y_{i-min}) that have been considered are those which do not depend on any factors and interaction of factors. Maximum values of responses (Y_{i-max}) are those to which the responses are likely to reach. For Y_1 and Y_2 , minimum values are 43.77% and 22.05%, respectively. Maximum values for both the responses were taken as 100%. Thus, one-sided desirability of Y_1 (d_1) is achieved as follow:

$$d_1 = \begin{cases} 0 & \text{if } Y_1 \leq 43.77 \\ \left[\frac{Y_1 - 43.77}{100 - 43.77} \right] & \text{If } 43.77 < Y_1 < 100 \\ 1 & \text{if } Y_1 \geq 100 \end{cases} \quad (6.4.4)$$

In a same way, one-sided desirability of Y_2 (d_2) is given as:

$$d_2 = \begin{cases} 0 & \text{if } Y_2 \leq 22.05 \\ \left[\frac{Y_2 - 22.05}{100 - 22.05} \right] & \text{If } 22.05 < Y_2 < 100 \\ 1 & \text{if } Y_2 \geq 100 \end{cases} \quad (6.4.5)$$

In the above both equations $r=1$. The overall desirability D is calculated by the following equation:

$$D = \sqrt{d_1 d_2} \quad (6.4.6)$$

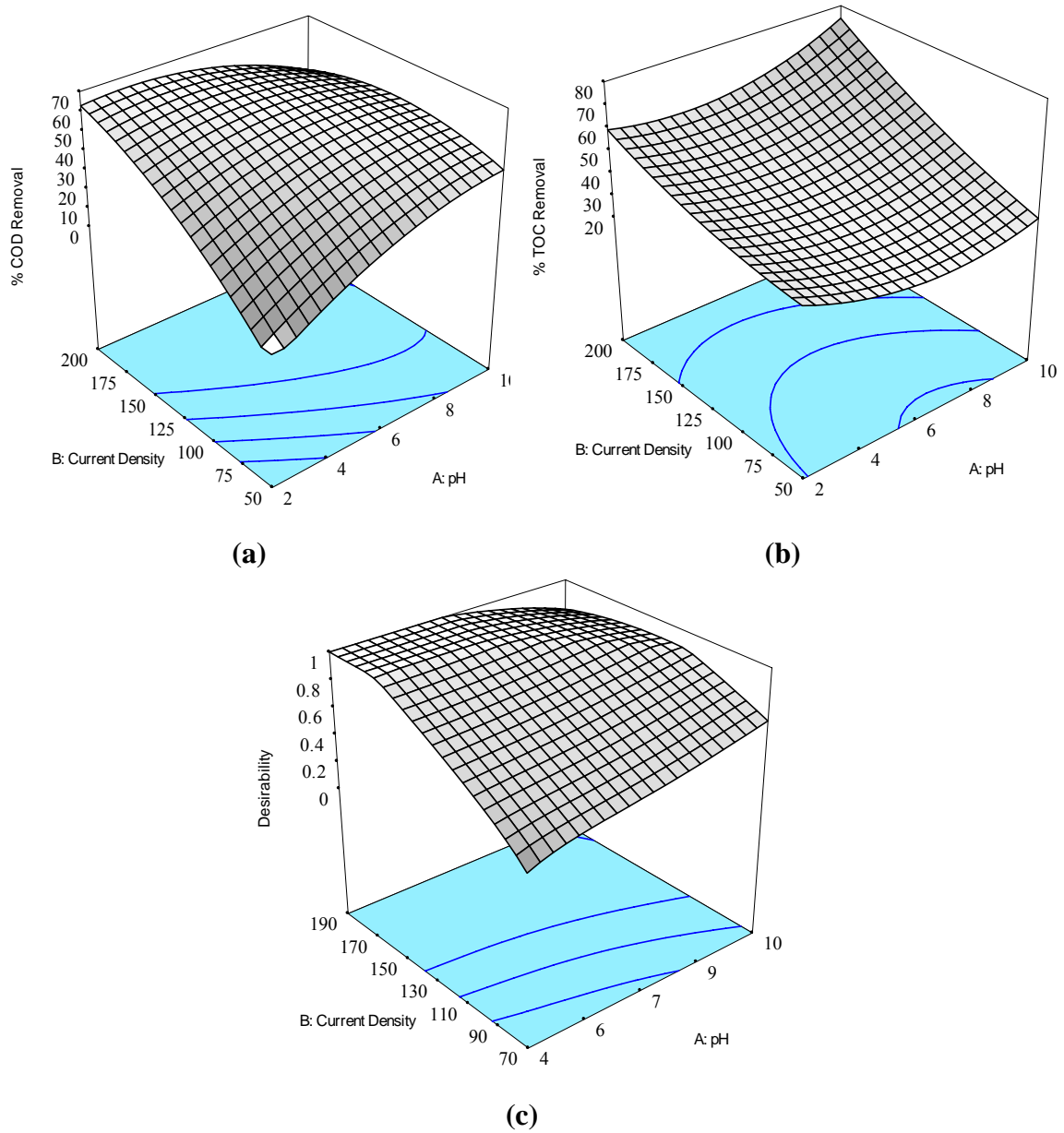


Figure 6.4.1. Effect of current density (A/m²) and pH on (a) COD removal, (b) TOC removal, and (c) desirability factor.

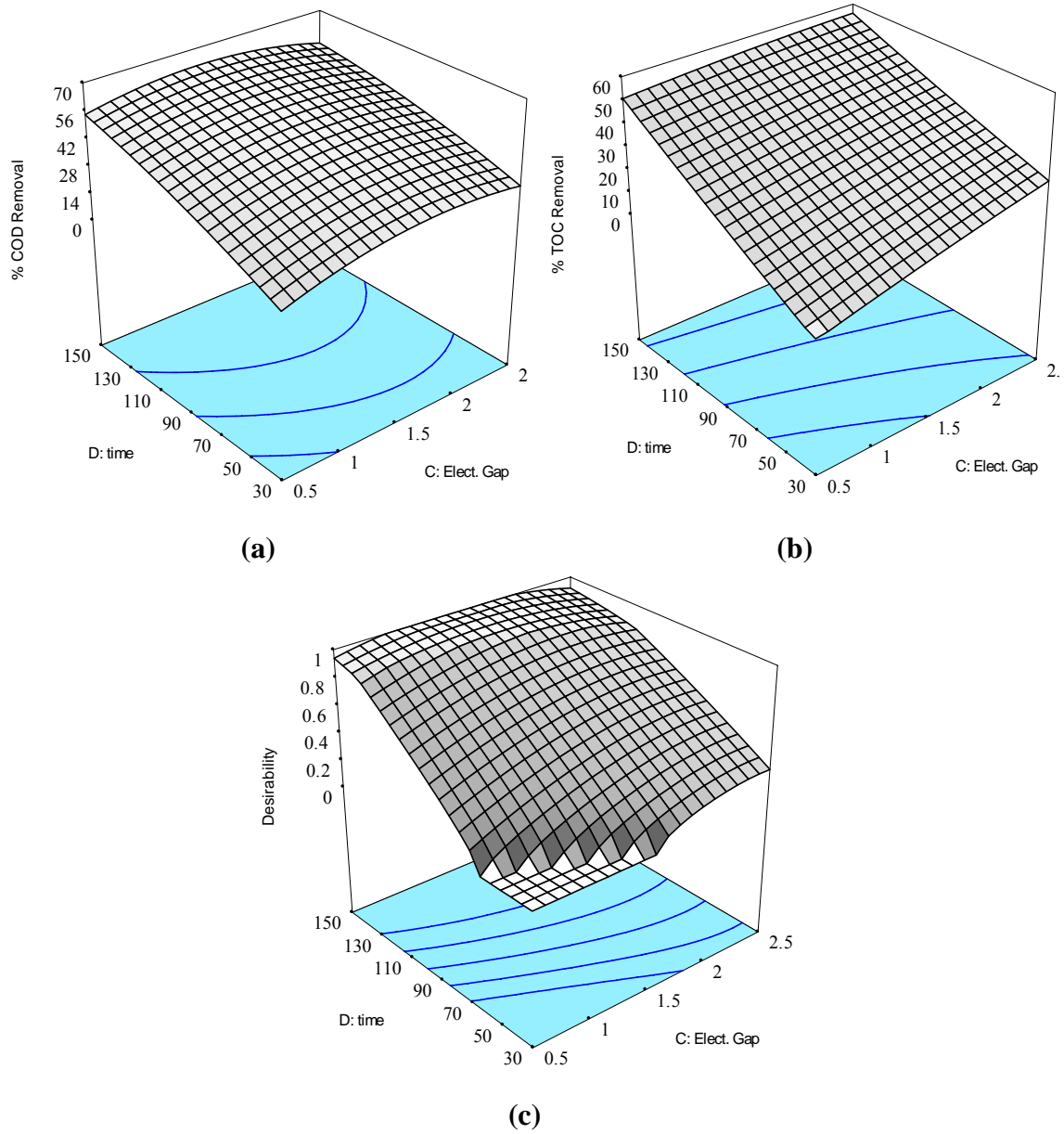


Figure 6.4.2. Effect of time (min) and electrode gap (cm) on (a) COD removal, (b) TOC removal, and (c) desirability factor.

The optimum values of operational parameters were found to be: pH=6, $j=182$ A/m², $g=1.5$ cm and $t=145$ min which gave an overall $D=0.515$. Under these optimized conditions, 62% COD removal and 52% TOC removal were predicted. In order to validate the optimization, three runs at these optimum conditions were conducted which gave an average of 60.8% COD and 51.1% TOC removal efficiencies.

Government of India has prescribed maximum COD and Fe values of 250 mg/L and 3 mg/L, respectively, for discharge of treated effluents into inland surface water bodies [CPCB, 2012]. Treated PRW was found to contain maximum 1 mg/L of Fe. Thus, the treated PRW meets the effluent discharge limit set by Government of India.

6.4.4. Mechanism Study

EC degradation before and during treatment (at various treatment time) was studied using UV–visible analysis (190–490 nm) (Figure 6.4.3). A peak was observed at 220 nm, which may be assigned to the aromatic rings of organics present in wastewater. The peak which appeared in the range of 200-230 nm in the untreated wastewater, faded after the treatment. This study shows that different bonds were broken and most of the aromatic rings were mineralized during EC treatment with SS electrode.

Zeta potential of EC solution was measured with time during treatment at optimum conditions so as to understand electrostatic interaction between various iron species generated and the colloidal particles present in PRW. The variation of zeta potential of EC solution is given in Figure 6.4.4. It may be seen that zeta potential value initially decreased (in terms of absolute value) and moved towards neutral side. This decrease is because of charge neutralization of the colloids present in PRW which

causes zeta potential to decrease. However, beyond 20 min of treatment, zeta potential becomes more negative with time. This is because of the fact that majority of colloidal pollutant particles initially present in PRW get removed in first 20 min of treatment and settle to the bottom. Remaining colloids present in the solution have high stability, and thus, don't get removed. These highly stable colloids only get removed by adsorption onto iron hydroxide precipitates which are heavier particles and settle easily. Removal of these highly stable colloids again decreases the zeta potential [Singh et al., 2013a,b].

To understand the treatment mechanism of EC process, FTIR analysis of untreated and treated PRW at optimized condition and the sludge generated was done. FTIR spectra is shown in Figure 6.4.5 and the major peaks are identified in Table 6.4.5. FTIR spectra of untreated and treated PRW shows a broad band between 3000 and 3700 cm^{-1} with peak at $\approx 3450 \text{ cm}^{-1}$. This band is due the presence of OH groups of phenolic compounds present in PRW. This may also be due to the presence of the tertiary amine group and N-H bending in the PRW. Zhou et al. [2007] suggested that the presence of alcoholic compounds or hydroxyl group show OH deformation vibrations and -OH stretching frequencies. The band in the region 2400-2000 cm^{-1} is due to OH, CH and C=O stretching vibrations. The peak observed in range 1625-1645 cm^{-1} corresponds to amide in-plane bending and also due to C=C stretching [Terzyk, 2001; Leenheer et al., 2001]. Conversion of the tertiary amine group to secondary and primary amines is shown by emergence of a peak at $\approx 1384 \text{ cm}^{-1}$ [Mollah et al., 2010]. It is seen in Figure 6.4.5 that the transmittance of various peaks increases after treatment of PRW suggesting that the quantities of various functional groups initially present in PRW decrease after EC treatment.

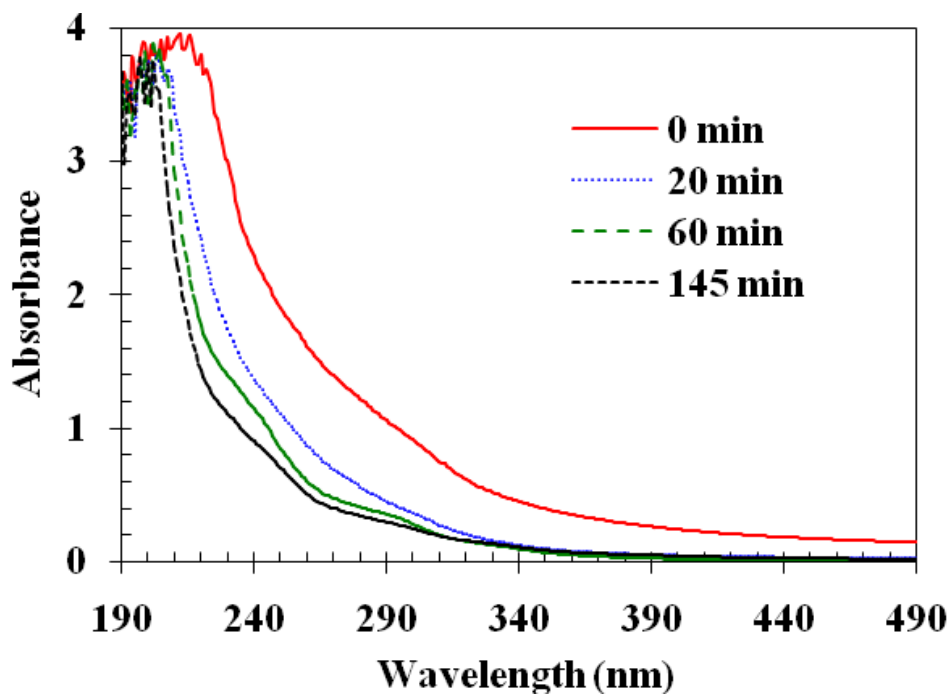


Figure 6.4.3. UV-visible spectra of PRW at different time intervals during the EC treatment at $\text{pH}_0=6.0$, $j=182 \text{ A/m}^2$, $g=1.5 \text{ cm}$.

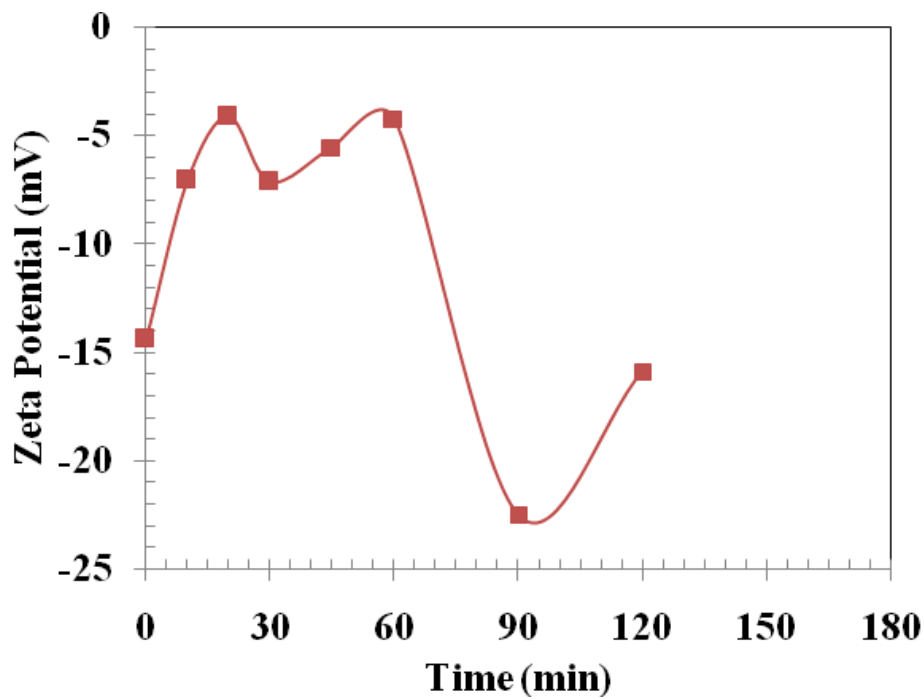


Figure 6.4.4. Variation of zeta potential with time in the EC reactor at optimum condition of treatment, $\text{pH}_0=6.0$, $j=182 \text{ A/m}^2$, $g=1.5 \text{ cm}$.

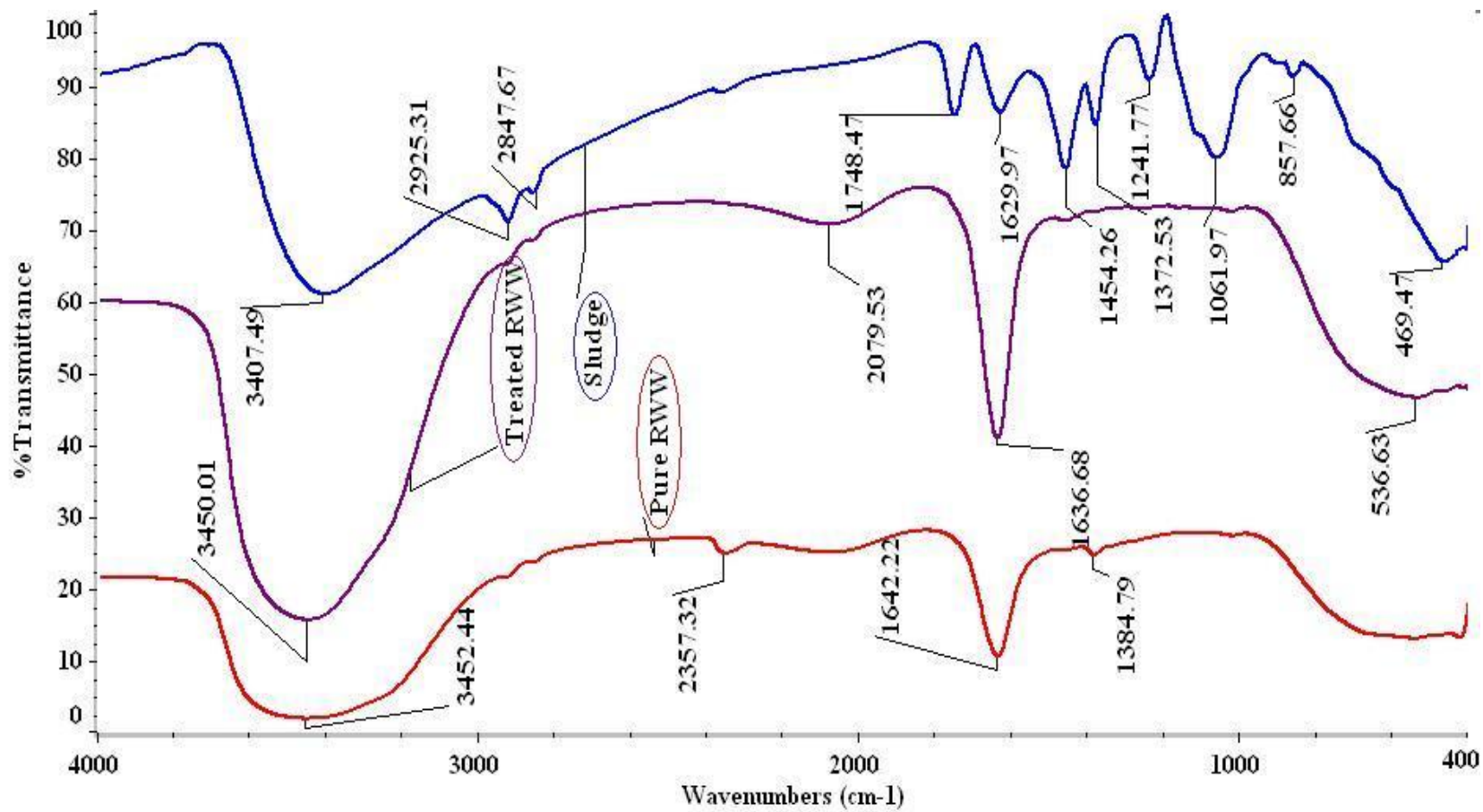


Figure 6.4.5. FTIR of sludge generated, treated and raw refinery wastewater by EC.

Table 6.4.4. FTIR band assignment for untreated and treated PRW and sludge generated during EC experiment.

Band Assignments	Untreated PRW	Treated PRW	Sludge
Primary amine ($-\text{NH}_2$)	3452.44 (br)	3450.01 (br)	3407.49 (br)
Phenyl ring C–H and CLC stretching			2925.31 (sh), 2847.67(w)
O-H bending	1642.22 (s)	1636.68(s)	1629.97 (s)
Aromatic ring stretching	1384.79 (w)		
O-H/C-H deformation			1454.26 (sh)
CH_3 deformation, O-H deformation			1241.77 (sh), 1372.53 (sh)
Aromatic ring stretching, C-O stretching, Out of plane O-H vibration of carbonyl group			1061.97(br), 857.66 (w)
CO_2 deformation		536.63 (w)	469.47 (w)

(s)-strong; (br)-broad; (sh)-shoulder; (w)-weak

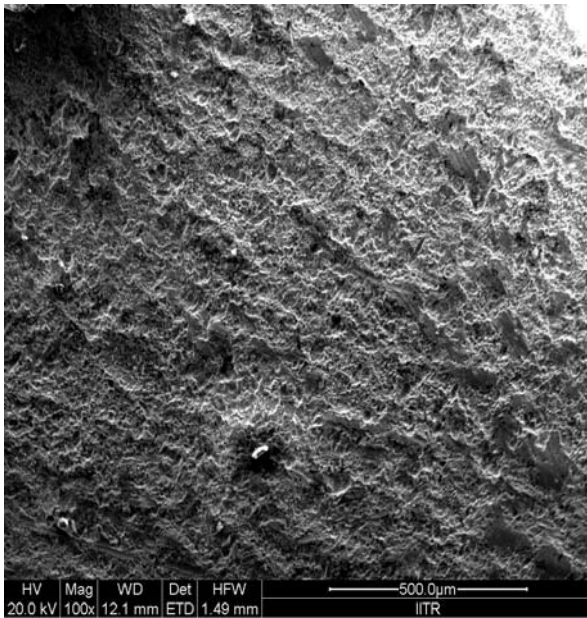
The spectra of sludge shows a broad peak at 3407.49 cm^{-1} which shows the presence of both free and hydrogen bonded $-\text{OH}$ groups. Peaks from 2925 cm^{-1} to 2847 cm^{-1} are due to carbon-hydrogen stretching in methyl and methylene groups [Barber et al., 2001]. A peak of carbonyl group is observed at 1748 cm^{-1} . The strong band observed around 1061 cm^{-1} for sludge may be assigned to C–O stretching in aryl ethers. Some characteristic peaks of sludge in the finger print region (1500 to 500 cm^{-1}) show presence of mono and para-benzene substituted derivatives. Overall, sludge is found to contain a number of functional groups initially present in PRW. During EC treatment, compounds initially present in PRW, get degraded by various oxidizing agents formed in-situ. Also, these pollutants and various intermediates formed during degradation get entrapped by iron hydroxide precipitates and settle to the bottom of EC reactor and form the sludge. Therefore, FTIR analysis of sludge shows similar peaks as found in untreated PRW.

6.4.5. Physico-Chemical Analysis of Electrodes and Residues

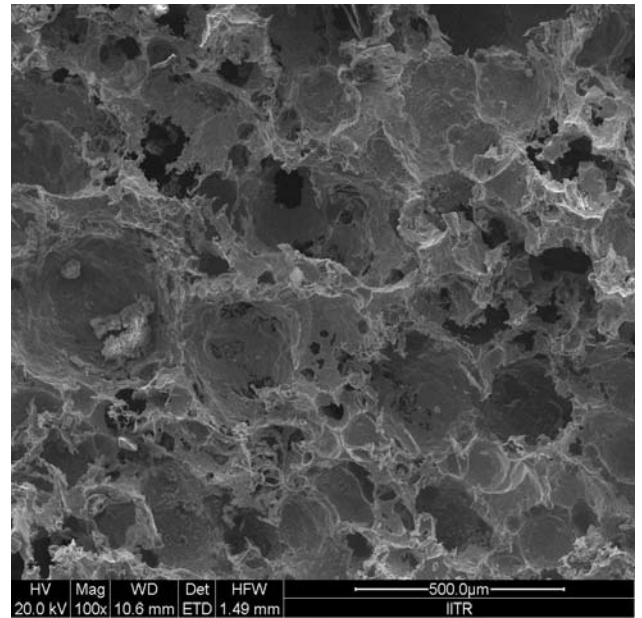
To investigate the changes that occur in the anode during the EC of PRW, and to understand the amount of iron going into the sludge various physico-chemical analysis were performed. Scanning electron micrographs (SEM) (Figure 6.4.6) were used to detect the changes on the surface of electrode [Kushwaha et al., 2010]. SEM image of fresh SS electrode (Figure 6.4.6a) shows rough surface whereas the SEM of the same electrode after several cycles of EC experiments (Figure 6.4.6b) shows a number of dents in the size range of 50–500 μm [Thakur et al., 2009]. These dents are formed around the nucleus of the active sites where the electrode dissolution took place producing ionic iron species and hydroxide. SEM images of dried sludge (Figure 6.4.6c) obtained during the EC process shows crystalline nature [Thakur et al., 2009]. Distribution of elements present in sludge generated by EC of PRW was checked by energy dispersive X-ray (EDX) analysis. Sludge was found to contain O (27.32%), Fe (49.55%), Cr (11.01%), C (5.66%), Ni (4.64%), Ca (0.87%), Al (0.50%) and Si (0.45%). Thus, sludge was found to contain high amount of iron, oxygen and carbon.

Figure 6.4.7 shows the thermogravimetric analysis of sludge under air atmosphere. TGA analysis was performed to understand the degradation kinetics of sludge in the presence of air at the heating rate of 10 $^{\circ}\text{C}/\text{min}$. TGA of sludge shows $\approx 7.38\%$ loss in weight when the temperature of furnace was increased from 25 to 100 $^{\circ}\text{C}$. This loss was due to the presence of moisture and bound water in the samples. In this temperature range, maximum rate of degradation was found to be 120 $\mu\text{g}/\text{min}$ as shown in differential thermal gravimetric (DTG) plot.

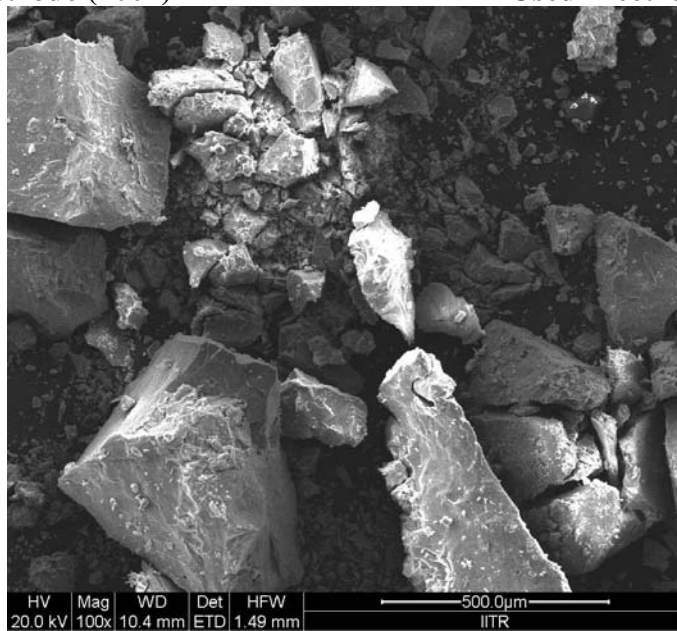
In the temperatures range of 100-400 $^{\circ}\text{C}$, weight loss was found to be $\approx 16.7\%$. This weight loss is generally associated with the evolution of CO_2 and CO [Thakur et al., 2009]. In the last temperature range between 400 and 1000 $^{\circ}\text{C}$, very marginal weight loss of $\approx 3.1\%$ was observed due to oxidation of sludge. A weak exothermic peak was observed between 200-240 $^{\circ}\text{C}$ due to oxidative degradation of the samples. In this region, the change of phase takes place due to which 95 $\mu\text{g}/\text{min}$ of mass was consumed as seen from DTG plot [Thakur et al., 2009].



Fresh Electrode (100x)



Used Electrode (100x)



Sludge (100x)

Figure 6.4.6. SEM images of fresh and used stainless steel electrode and sludge generated during experiment.

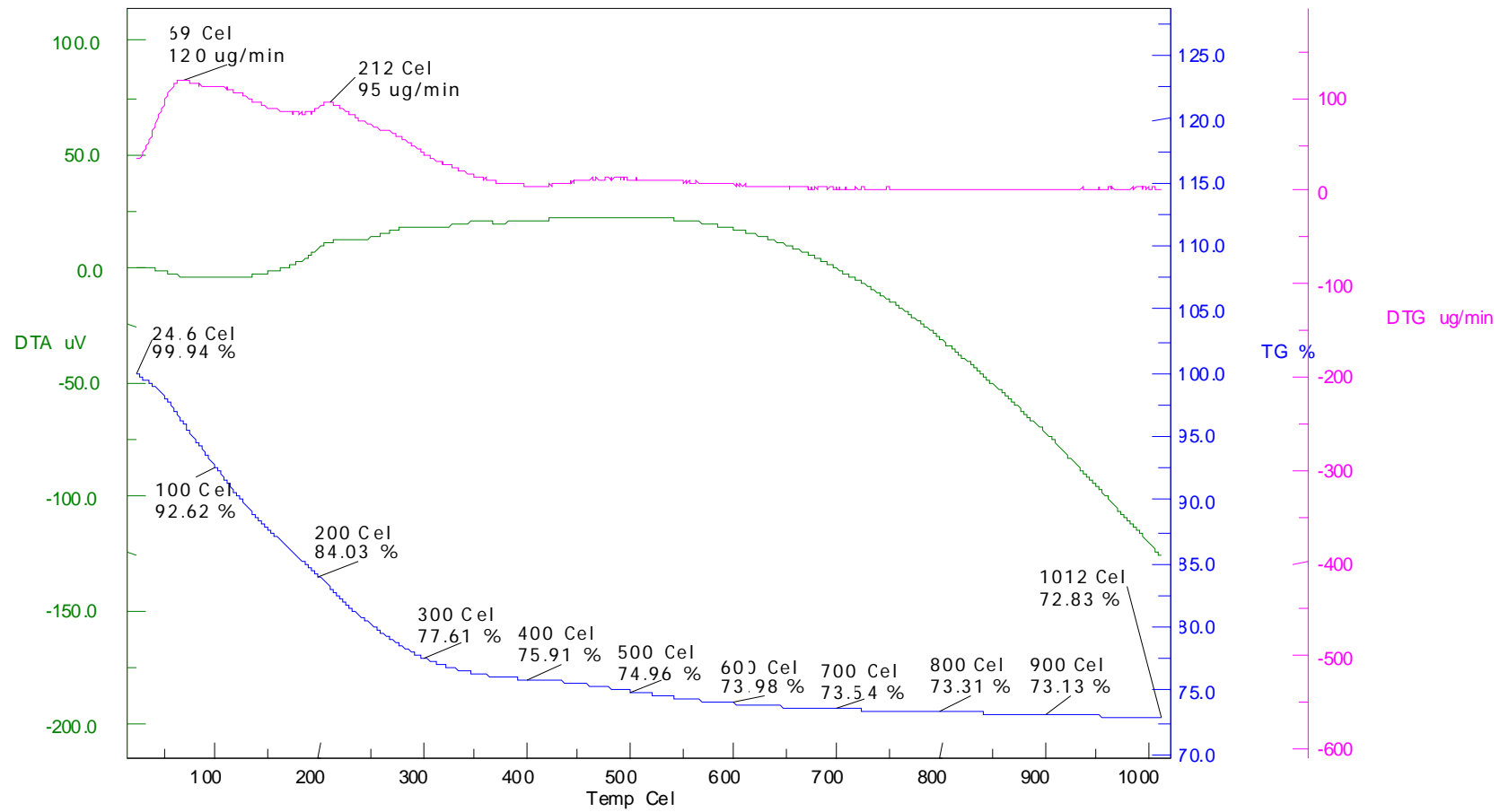


Figure 6.4.7. Thermogravimetric analysis of sludge under air atmosphere.

CONCLUSIONS AND RECOMMENDATIONS

7.1 CONCLUSIONS

In the present study, work was carried out as per the aims and objectives given in section 1.5 which themselves were decided on the basis of the literature survey presented in Chapter 3 and the research gaps identified in section 3.5. First, treatment of synthetic wastewater containing phenol, catechol and resorcinol was studied using adsorption onto rice husk ash (RHA) and sequential batch reactor (SBR). Thereafter, treatment of actual petroleum refinery wastewater (PRW) was studied using SBR and electrocoagulation (EC) with stainless steel (SS) electrode.

7.1.1 Treatment of Synthetic Wastewater Containing Phenol, Catechol and Resorcinol

On the basis of the results and discussion presented heretofore for the treatment of synthetic wastewater containing phenol, catechol and resorcinol using adsorption (Chapter IV) and sequential batch reactor (SBR) (Chapter V, section 5.3), following major conclusions can be drawn:

Adsorption

- Optimum conditions for individual adsorptive removal of phenol, catechol and resorcinol by RHA were found to be: natural pH, adsorbent dose of 20 g/L and contact time ≈ 16 h.
- The adsorption kinetics was found to be well-represented by the pseudo-second-order kinetic model and the adsorption processes could be well described by a two-stage diffusion model.
- For the individual adsorption, Redlich-Peterson isotherm well-represented the equilibrium adsorption of phenol, catechol and resorcinol.
- The adsorption of phenol, catechol and resorcinol from the binary and ternary solutions onto RHA was found to be antagonistic in nature.

- The competitive extended-Freundlich model best-fitted the equilibrium binary and ternary adsorption data of phenol, catechol and resorcinol onto RHA.
- For a mixture containing phenol, catechol and resorcinol (each 250 mg/L), phenol, catechol and resorcinol removal efficiencies were found to be 42.32%, 76.89% and 59.94%, respectively.

SBR

- For treatment of synthetic wastewater simultaneously containing phenol, catechol and resorcinol in SBR, optimum HRT was found to be 1.25 d with volume exchange ratio of 0.4.
- Phenol, catechol, resorcinol and COD removal efficiencies increased during filling of wastewater in the reactor as the filling time was increased from 0.5 to 2.0 h.
- For a mixture containing phenol, catechol and resorcinol (each 200 mg/L), phenol, catechol, resorcinol and COD removal efficiencies were found to be 99%, 96%, 95% and 89%, respectively, at optimum condition of HRT=1.25 d and fill time=1.5 h.

7.1.2 Treatment of Actual PRW

Similarly, on the basis of the results and discussion presented heretofore for the treatment of actual PRW using SBR (Chapter V, section 5.4) and EC method with SS electrode (Chapter VI), following major conclusions can be drawn:

SBR

- Optimum HRT for treatment of actual PRW was found to be 0.83 d with volume exchange ratio of 0.4.
- COD and TOC removal efficiencies increased during filling of PRW in the reactor as filling time was increased from 0.5 to 2.0 h.
- At optimum condition (HRT=0.83 d and fill time=2 h), COD and TOC removal efficiencies were found to be 79% and 83%, respectively.

EC method

- Full factorial central composite (CCD) design was used to study the effect of four key process parameters on the reduction of COD and total organic carbon

TOC from PRW. The parameters used in this study were initial pH (pH_0): 2–10; current density (j): 39.06–195.31 A/m²; inter-electrode distance (g): 1–2.5 cm and electrolysis time (t): 30–150 min.

- Optimized operating condition of $\text{pH}_0=6.0$, $j=182$ A/m², $g=1.5$ cm and $t=145$ min gave COD and TOC removal efficiencies of 62% and 52%, respectively.
- UV-visible study showed that different bonds were broken and most of the aromatic rings were mineralized during EC treatment with SS electrode.
- FTIR study showed that transmittance of various peaks increased after treatment of PRW suggesting that the quantity of various functional groups initially present in PRW decreased after EC treatment.
- TGA study showed that the residues generated during EC of PRW can be used as a fuel in boilers/incinerators, or can be used for the production of fuel-briquettes.

Finally, optimum conditions and performance of various methods for the treatment of synthetic wastewater containing phenolic compounds and actual PRW studied are as follows:

Water	Treatment Method	Initial Concentration (mg/l)	Optimum Conditions	Final Concentration (mg/l)
Synthetic wastewater containing phenol, catechol and resorcinol	Adsorption by RHA	$C_0=250$ each	$m=20$ g/L, $t=8$ h, $\text{pH}_0=6$	Phenol=144.2; Catechol=57.8; Resorcinol=100.2
	SBR	$C_0=200$ each; COD=700±25	HRT=1.25 d, VER=0.4, $t_f=1.5$ h, $t_R=8$ h, $\text{pH}_0=6$	Phenol=2; Catechol=8; Resorcinol=10; COD=77
Actual PRW	SBR	pH=8±0.5; COD=350±25; TOC=70±10; TC=140±20; Phenol=10; TDS=900	pH=8±0.5, HRT=0.83 d, VER=0.4, $t_f=2$ h, $t_R=6$ h,	pH=7±0.5; COD=100±25; TOC=17±5; TC=20±5; Phenol=0.1; TDS=400
	EC		$\text{pH}_0=6.0$, $j=182$ A/m ² , $g=1.5$ cm and $t=145$	pH=10; COD=130±25; TOC=33±5; TC=53±5; Phenol=1; TDS=621.62

Major conclusions drawn from the comparative analysis are:

- For synthetic wastewater simultaneously containing phenol, catechol and resorcinol, comparison of treatment efficiencies shows that the SBR treatment worked better than adsorption by RHA.
- For treatment of actual PRW also, SBR was found to give higher treatment efficiency than EC method, however, it requires higher treatment time as compared to EC treatment.

7.2 RECOMMENDATIONS

Based on the experiences gained during the present work, the following recommendations are being made for future research:

- Column and scale-up studies should be conducted to evaluate the suitability of RHA as adsorbent for the removal of phenol and its derivatives from wastewater.
- Anoxic phase should be study for better efficiency of SBR and membrane technology can be used as post-treatment option for reducing suspended solids.
- Non-toxic electrodes in combinations (anode and cathode) in series and bipolar arrangement and in both batch and continuous electrochemical reactors need to be study and compared for their adoption in EC treatment.
- Since the EC treatment is not able to remove the COD and TOC completely, it may further be treated by other methods like SBR, adsorption to meet the stipulated regulatory discharge standards of the effluents.
- Studies may be carried out for reutilizing and reusing the SBR and EC generated sludge for wastewater treatment either as an adsorbent or by making nano-particles through thermal route.

REFERENCES

1. Abdelwahab, O.; Amin, N.K.; El-Ashtoukhy, E.S.Z. Electrochemical removal of phenol from oil refinery wastewater. *Journal of Hazardous Material*, *163*, 711–716, (2009).
2. Abdelwahab, O.; Nemr, A.E.; Sikaily, A.E.; Khaled, A. Use of rice husk for adsorption of direct dyes from aqueous solution: a case study of direct F. Scarlet. *Egyptian Journal of Aquatic Research*, *31*, 1110-0354, (2005).
3. Adhoum, N.; Monser, L. Decolourization and removal of phenolic compounds from olive mill wastewater by electrocoagulation. *Chemical Engineering and Processing*, *43*, 1281–1287, (2004).
4. Aghav, R.M.; Kumar, S.; Mukherjee, S.N. Artificial neural network modeling in competitive adsorption of phenol and resorcinol from water environment using some carbonaceous adsorbents. *Journal of Hazardous Material*, *188*, 67-77, (2011).
5. Ahmaruzzaman, M. Adsorption of phenolic compounds on low-cost adsorbents: a review. *Advances in Colloid and Interface Science*, *143*, 48–67, (2008).
6. Aksu, Z.; Yener, J. A comparative adsorption/boisorption study of monochlorinated phenols onto various sorbent. *Waste Management*, *21*, 695-702, (2001).
7. Al Zarooni, M.; Elshorbagy, W. Characterization and assessment of Al Ruwais refinery wastewater. *Journal of Hazardous Material*, *136*, 398–405, (2006).
8. Alam, M.Z.; Muyibi, S.A.; Toramae, J. Statistical optimization of adsorption processes for removal of 2, 4-dichlorophenol by activated carbon derived from oil palm empty fruit bunches. *Journal of Environmental Science*, *19*, 674–677, (2007).
9. Aleboyeh, A.; Daneshvar, N.; Kasiri, M.B. Optimization of C.I. Acid Red 14 azo dye removal by electrocoagulation batch process with response surface methodology. *Chemical Engineering and Processing*, *47*, 827–832, (2008).

10. Allen, S.J.; McKay, G.; Porter, J.F. Adsorption isotherm models for basic dye adsorption by peat in single and binary component systems. *Journal of Colloid and Interface Science*, 280, 322–333, (2004).
11. APHA, Standard Methods for the Examination of Water and Wastewater. *American Public Health Association*, (19th ed.), Washington, DC (1995).
12. Arana, J.; Melian, E.P.; Lopez, V.M.R.; Alonso, A.P.; Rodriguez, J.M.D.; Diaz, O.G.; Pena, J.P. Photocatalytic degradation of phenol and phenolic compounds Part I. Adsorption and FTIR study. *Journal of Hazardous Material*, 146, 520–528 (2007).
13. Armagan, B.; Ozdemir, O.; Turan, M.; Celik, M.S. The removal of reactive azo dyes by natural and modified zeolites. *Journal of Chemical Technology and Biotechnology*, 78(7), 725–732, (2003).
14. Arora, M.L.; Barth, E.F.; Umphres, M.B. Technology evaluation of sequencing batch reactors. *Journal of the Water Pollution Control Federation*, 57, 867–875, (1985).
15. Assessment of atmospheric emissions from petroleum refining. *Radian Corp.*, (1980).
16. Bagajewicz, M. A review of recent design procedures for water networks in refineries and process plants. *Computer and Chemical Engineering*, 24, 2093–2113, (2000).
17. Balistrieri, L.S.; Murray, J.W. The surface chemistry of goethite (α -FeOOH) in major ion seawater. *Journal of American Society*, 281(6), 788–806, (1981).
18. Bansal, M.; Garg, U.; Singh, D.; Garg V.K. Removal of Cr (VI) from aqueous solutions using pre-consumer processing agricultural waste: A case study of rice husk. *Journal of Hazardous Material*, 162, 312–320, (2009).
19. Bao, R.; Yu, S.; Shi, W.; Zhang, X.; Wang, Y. Aerobic granules formation and nutrients removal characteristics in sequencing batch airlift reactor (SBAR) at low temperature. *Journal of Hazardous Material*, 168, 1334–1340, (2009).
20. Barber, L.B.; Leenheer, J.A.; Noyes, T.I.; Stiles, E.A. Nature and transformation of dissolved organic matter in treatment wetlands. *Environment Science and Technology*, 35, 4805–4816, (2001).

21. Barrett, E.P.; Joyner, L.G.; Halenda, P.P. The Determination of pore volume and area distributions in porous substances. I. computations from nitrogen isotherms. *Journal of American Chemical Society*, *73*, 373-380, (1951).
22. Barrios-Martinez, A.; Barbot, E.; Marrot, B.; Moulin, P.; Roche, N. Degradation of synthetic phenol-containing wastewaters by MBR. *Journal of Membrane Science*, *281*, 288-296, (2006).
23. Bay, S.M.; Zeng, E.Y.; Lorenson, T.D.; Tran, K.D.; Alexander, C. Temporal and spatial distributions of contaminants in sediments of Santa Monica Bay. California, *Marine Environmental Research*, *56*, 255 – 276, (2003).
24. Bayram, E.; Hoda, N.; Ayranci, E. Adsorption/electrosorption of catechol and resorcinol onto high area activated carbon cloth. *Journal of Hazardous Material*, *168*, 1459–1466, (2009).
25. Bayramoglu, M.; Eyvaz, M.; Kobya, M. Treatment of the textile wastewater by electrocoagulation Economical evaluation. *Chemical Engineering Journal*, *128*, 155–161, (2007).
26. Beg, M.U.; Saeed, T.; Al-Muzaini, S.; Beg, K.R.; Al-Bahloul, M. Distribution of petroleum hydrocarbon in sediment from coastal area receiving industrial effluents in kuwait. *Ecotoxicology and Environmental Safety*, *54*, 47-54, (2003).
27. Bellot, J.C.; Condoret, J.S. Modelling of liquid chromatography equilibrium. *Process Biochemistry*, *28*, 365-376 (1993).
28. Benyahia, F; Abdulkarim, M; Embaby, A; Rao, M. The 7th Annual U.A.E. *University Research Conference*, Al Ain, UAE, (2006).
29. Bertin, L.; Di Gioia, D.; Barberio, C.; Salvadori, L.; Marchetti, L.; Fava, F. Biodegradation of polyethoxylated nonylphenols in packed-bed biofilm reactors. *Industrial and Engineering Chemistry Research*, *46*, 6681–6687, (2007).
30. Beszedits, S.; Silbert, M.D. Treatment of phenolic wastewaters, B & L information services. *Toronto*, (1990).
31. Bhatnagar, R.; Mall, I.D.; Joshi, H.; Srivastava, V.C. Electrochemical treatment of acrylic dye bearing textile wastewater: optimization of operating parameters. *Desalination Water Treatment*, 1-12, (2013), DOI: 10.1080/19443994.2013.786653.

32. Bhattacharya, P.K.; Jayan, R.; Bhattacharjee, C. A combined biological and membrane-based treatment of prehydrolysis liquor from pulp mill. *Separation Purification and Technology*, 45, 119–130, (2005).
33. Bhatti, M.S.; Reddy, A.S.; Kalia, R.K.; Thukral, A.K. Modeling and optimization of voltage and treatment time for electrocoagulation removal of hexavalent chromium. *Desalination*, 269, 157–162, (2011).
34. Blanchard, G.; Maunaye, M.; Martin, G. Removal of heavy metals from water by means of natural zeolites. *Water Research*, 18, 1501-1507, (1984).
35. Blanco-Martinez, D.A.; Giraldo, L.; Moreno-Pirajan, J.C. Effect of the pH in the adsorption and in the immersion enthalpy of monohydroxylated phenols from aqueous solutions on activated carbons. *Journal of Hazardous Material*, 169, 291-296, (2009).
36. BP Statistical Review of world Energy of World Energy, June, (2013).
37. Bright, A.; Renuga, D.T.S.; Gunasekaran, S. Spectroscopical vibrational band assignment and qualitative analysis of biomedical compounds with cardiovascular activity. *International Journal of ChemTech Research*, 2, 379-388, (2010).
38. Brunauer S.; Emmett, P.H.; Teller, E. Adsorption of gases in multimolecular layers.
39. Buscaa, G.; Berardinelli, S.; Resini, C.; Arrighi, L. Technologies for the removal of phenol from fluid streams: A short review of recent developments. *Journal of Hazardous Material*, 160, 265–288, (2008).
40. Cam, L.M.; Hung, T.V.; Thu, N.T.; Khu, L.V.; Phu, N.H. Activated carbon (AC) containing transition metal oxides (MeOx) in phenol adsorption and catalytic oxidation of adsorbed phenol by hydrogen peroxide. *International Conference on Biology, Environment and Chemistry*, Singapore, (2011).
41. Can, O.T.; Bayramoglu, M.; Kobya, M. Decolorization of reactive dye solutions by electrocoagulation using aluminum electrodes. *Industrial and Engineering Chemistry Research*, 42, 3391-3396, (2003).
42. Care Rating, Indian Crude oil Industry, February, (2013). <http://www.careratings.com/Portals/0/ResearchReports/BrochureIndianCrudeOilIndustry.pdf>

43. Carucci, A.; Majone, M.; Ramadori, R.; Rossetti, S. Biological phosphorus removal with different organic substrates in an anaerobic/aerobic sequencing batch reactor. *Water Science and Technology*, 35, 161–168, (1997).
44. Chan, C-H.; Lim, P-E. Evaluation of sequencing batch reactor performance with aerated and unaerated FILL periods in treating phenol-containing wastewater. *Bioresource Technology*, 98, 1333–1338, (2007).
45. Chavalparit, O.; Ongwandee, M. Optimizing electrocoagulation process for the treatment of biodiesel wastewater using response surface methodology. *Journal of Environment and Science*, 21, 1491–1496, (2009).
46. Chen, G. Electrochemical technologies in wastewater treatment. *Separation and Purification Technology*, 38, 11 – 41, (2004).
47. Chen, G.R. Chemical Industry Encyclopedia. *Chemical Industry Press, Beijing, China*, 1, 352, (1990).
48. Chen, W.; Duan, L.; Zhu, D.Q. Adsorption of polar and nonpolar organic chemicals to carbon nanotubes. *Environment Science and Technology*, 41, 8295-8300, (2007).
49. Chen, W-J.; Su, W-T.; Hsu, H-Y. Continuous flow electrocoagulation for MSG wastewater treatment using polymer coagulants via mixture-process design and response-surface methods. *Journal of the Taiwan Institute of Chemical Engineering*, 43, 246–255 (2012).
50. Chen, Z.; Huang, G.H.; Li J.B. A GIS-based modeling system for petroleum waste management. *Water Science and Technology*, 47, 309–317, (2003).
51. Chiavola, A.; Baciocchi, R.; Gavasci, R. Biological treatment of PAH-contaminated sediments in a Sequencing Batch Reactor. *Journal of Hazardous Material*, 184, 97-104, (2010).
52. Chin, K.K.; Ng, W.J. Palm oil refinery effluent treatment by sequencing batch reactors. *Biological Wastes*, 20, 101-109, (1987).
53. Chiou, C.T. Partition and adsorption of organic contaminants in environmental systems. *John Wiley and Sons, Inc.*, (2002).

54. Coelho, A.; Castro, A.V.; Dezotti, M.; Sant Anna, Jr.G.L. Treatment of petroleum refinery sour water by advanced oxidation processes. *Journal of Hazardous Material*, 137, 178–184, (2006).
55. Colmenarejo, M.F.; Bustos, A.; Garcia, M.G.; Borja, R.; Banks, C.J. An analysis of the factors that influence biological phosphorus removal (BPR) in a sequencing batch anaerobic/aerobic reactor. *Bioprocess Engineering*, 19, 171-4, (1998).
56. Colunga, A.M.; Martinez, S.G. Effects of population displacements on biological phosphorus removal in a biofilm SBR. *Water Science and Technology*, 34, 303–313, (1996).
57. Cordero, T.; Mirasol, J.R.; Bedia, J.; Gomis, S.; Yustos, P.; Garcia-Ochoa, F.; Santos, A. Activated carbon as catalyst in wet oxidation of phenol: Effect of the oxidation reaction on the catalyst properties and stability. *Applied Catalysis B: Environ.*, 81, 122-131, (2008).
58. Cotillas, S.; Llanos, J.; Canizares, P.; Mateo, S.; Rodrigo, M.A. Optimization of an integrated electro-disinfection/ electrocoagulation process with Al bipolar electrodes for urban wastewater reclamation. *Water Research*, 47, 1741-1750, (2013)
59. CPCB, Pollution Control Acts, Rules and Notifications Issued There Under. *Central Pollution Control Board*, Ministry of Environment and Forests, Delhi, India (2006).
60. Cruz-Gonzalez, K.; Tores-Lopez, O.; Garcia-Leon, A.; Guzman-Mar, J.L.; Reyes, L.H.; Hernandez-Ramirez, A.; Peralta-Herandez, J.M. Determination of optimum parameter for Acid Yellow 36 decolorization by electron-fenton process using BDD cathode. *Chemical Engineering Journal*, 160, 199-206, (2010).
61. Dague, R.R.; Habben, C.E.; Pidaparti, S.R. Initial studies on the anaerobic sequencing batch reactor. *Water Science and Technology*, 26, 2429-2532, (1992).
62. Damaris, N.M.; Paul, M.S.; Rachel, M.N.; Geoffrey, N.K. Adsorption and detection of some phenolic compounds by rice husk ash of Kenyan origin. *Journal of Environmental Monitoring*, 4, 978–984, (2002).

63. Danesh, S.; Oleszkiewicz, J.A. Use of a new anaerobic-aerobic sequencing batch reactor system to enhance biological phosphorus removal. *Water Science and Technology*, 35, 137-44, (1997).
64. Demirci S., Erdogan B., Ozcimder R. Wastewater treatment at the petroleum refinery Kirikkale Turkey using some coagulant and Turkishh clays as coagulant aids. *Water Research*, 32, 3495–3499, (1997).
65. Derringer, G.; Suich, R. Simultaneous optimization of several response variables. *Journal of Quality Technology*, 12, 214-219, (1980).
66. Diyaudeen, B.H.; Daud, W.M.A.W.; Aziz, A.R.A. Treatment technologies for petroleum refinery effluents: A review. *Process Safety and Environmental Protection*, 89, 95–105, (2011).
67. Doggett, T.; Rascoe, A. Global energy demand seen up 44 percent by 2030. <http://www.reuters.com/articles/GCAGreenBusiness/idUSN2719528620090527> [accessed 17.09.2009].
68. Dold, P.L. Current practice for treatment of petroleum refinery wastewater and toxics removal. *Water Quality Research Journal of Canada*, 24(3), 363– 390, (1989).
69. Dorn, P.B. Case histories the petroleum industry. In: Ford, D.L. (Ed.), Toxicity Reduction: Evaluation and Control. *Water Quality Management Library, Technomic Publishing Company, Lancaster, PA*, 3, 183-223, (1998).
70. Duan, J.; Gregory, J. Coagulation by hrdolysing metal salts. *Advanced Journal of Colloid and Interface Science*, 100–102, 475-502, (2003).
71. EHC 157, International programme on chemical safety (IPCS), *Environmental Health Criteria 157*, Hydroquinone, (1994).
72. El-Ashtouky, E-S.Z.; El-Taweel, Y.A.; Abdelwahab, O.; Nassef, E.M. Treatment of petrochemical wastewater containing phenolic compounds by electrocoagulation using a fixed bed electrochemical reactor. *International Journal of Electrochemical Science*, 8, 1534-1550, (2013).
73. Elliott, H.A.; Huang, C.P. Adsorption characteristics of some Cu(II) complexes on alumina silicates. *Water Research*, 15, 849-854, (1981).

74. El-Naas, M.H.; Al-Zuhair, S.; Al-Lobaney, A.; Makhlof, S. Assessment of electrocoagulation for the treatment of petroleum refinery wastewater. *Journal of Environmental Management*, *91*, 180-185, (2009b).
75. El-Naas, M.H.; Al-Zuhair, S.; Alhajja, M.A. Reduction of COD in refinery wastewater through adsorption on Date-Pit activated carbon. *Journal of Hazardous Material*, *173*, 750-757, (2009a).
76. El-Naas, M.H.; Al-Zuhair, S.; Alhajja, M.A. Removal of phenol from petroleum refinery wastewater through adsorption on date-pit activated carbon. *Chemical Engineering Journal*, *162*, 997-1005, (2010).
77. El-Said, A.G.; Badawy, N.A.; Garamon, S.E. Adsorption of cadmium (II) and mercury (II) onto natural adsorbent rice husk ash (RHA) from aqueous solutions: study in single and binary system. *Journal of American Society*, *6*, 400-409, (2010).
78. Fakhru'l-Razi, A.; Pendashteh, A.; Abidin, Z.Z.; Abdullah, L.C.; Biak, D.R.A.; Madaeni, S.S. Application of membrane-coupled sequencing batch reactor for oil field produced water recycle and beneficial re-use. *Bioresource Technology*, *101*, 6942-6949, (2010).
79. Fang, H.H.P.; Liang, D.W.; Zhang, T.; Liu, Y. Anaerobic treatment of phenol in wastewater under thermophilic condition. *Water Research*, *40*, 427-434, (2006).
80. Farooqi, I.H.; Basheer, F.; Ahmad, T. Studies on biodegradation of phenols and m-cresols by upflow anaerobic sludge blanket and aerobic sequential batch reactor. *Global Nest Journal*, *10*, 39-46, (2008).
81. Feng, J.W.; Sun, Y.B.; Zheng, Z.; Zhang, J.B.; Li, S.; Tian, Y.C. Treatment of tannery wastewater by electrocoagulation. *Journal of Environmental Science*, *19*, 1409-1415, (2007).
82. Fiore, S.; Zanetti, M.C. Sorption of phenols: Influence of groundwater pH and of soil organic carbon content. *American Journal of Environmental Science*, *5(4)*, 546-554, (2009).
83. Freundlich, H.M.F. Over the adsorption in solution. *Journal of Physical Chemistry*, *57*, 385-471, (1906).

84. Fritz, W.; Schluender, E.U. Simultaneous adsorption equilibria of organic solutes in dilute aqueous solutions on activated carbon. *Chemical Engineering Science*, 29, 1279-1282, (1974).
85. Gasim, H. A.; Kutty, S. R. M.; Isa, M. H. Biodegradability of petroleum refinery wastewater in batch reactor. *Proceeding of ICSBI-10, Kuala Lumpur Malaysia*, (2010).
86. Gaval, G.; Pernell, J.J. Impact of the repetition of oxygen deficiencies on the filamentous bacteria proliferation in activated sludge. *Water Research*, 37, 1991–2000, (2003).
87. Gomkale, A.V.; Kumar, Y.; Jain, S.K. Environmental Issues of Indian Petroleum Refining Industry. *Chemical Engineering World*, 9, 95-98, (1996).
88. Gupta, V.K.; Sharma, S.; Yadav, I.S.; Mohan, D. Utilization of bagasse fly ash generated in sugar industry for the removal and recovery of phenol and p-nitrophenol from wastewater. *Journal of Chemical Technology and Biotechnology*, 71, 180–186, (1998).
89. Gurses, A.; Yalcin, M.; Dogar, C. Electrocoagulation of some reactive dyes: A statistical investigation of some electrochemical variables. *Waste Management*, 22, 491–499, (2002).
90. Hariz, I.B.; Halleb, A.; Adhoum, N.; Monser, L. Treatment of petroleum refinery sulfidic spent caustic wastes by electrocoagulation. *Separation and Purification Technology*, 107, 150–157, (2013).
91. Hasan, D.B.; Aziz, A.R.A.; Daud W.M.A.W. Oxidative mineralisation of petroleum refinery effluent using Fenton-like process. *Chemical Engineering and Research Design*, 90, 298–307, (2012).
92. Hasan, D.B.; Daud W.M.A.W.; Aziz, A.R.A. Treatment technologies for petroleum refinery effluents: A review. *Process Safety and Environmental Protection*, 89, 95–105, (2011).
93. He, S.B.; Xue, G.; Kong, H.; Li, X. Improving the performance of sequencing batch reactor (SBR) by the addition of zeolite powder. *Journal of Hazardous Material*, 142, 493–499, (2007).

94. Ho, C.C.; Chan, C.Y. The application of lead dioxide-coated Titanium anode in the Electroflotation of Palm oil mill effluent. *Water Research*, 20(12), 1523-1527, (1986).
95. Ho, Y.S.; McKay, G. Pseudo-second order model for sorption processes. *Process Biochemistry*, 34, 451-465, (1999).
96. Holt, P.K.; Barton, G.W.; Wark, M.; Mitchell, C.A. A quantitative comparison between chemical dosing and electrocoagulation. *Colloids and Surfaces A: Physicochemical and Engineering Aspects*, 211, 233-248, (2002).
97. Hsu, E.H. Treatment of a petrochemical wastewater in sequencing batch reactors. *Environmental Progress and Sustainable Energy*, 5, 71-81, (1986).
98. Huang, J. Treatment of phenol and p-cresol in aqueous solution by adsorption using a carbonylated hypercrosslinked polymeric adsorbent. *Journal of Hazardous Material*, 168, 1028-1034, (2009).
99. Huang, J.; Huang, K.; Yan, C. Application of an easily water-compatible hypercrosslinked polymeric adsorbent for efficient removal of catechol and resorcinol in aqueous solution. *Journal of Hazardous Material*, 167, 69-74, (2009).
100. Imagawa, A.; Seto, R.; Nagaosa, Y. Adsorption of chlorinated hydrocarbons from air and aqueous solutions by carbonized rice husk. *Carbon*, 38, 623, (2000).
101. Industries Effluent Standard. *CPCB, New Delhi*, (2012).
102. IPIECA, International Petroleum Industry Environmental Conservation Association. Petroleum refining water/wastewater use and management: IPIECA Operations Best Practice Series. *London, UK*, (2010).
103. Irvine, R.L.; Ketchum, L.H. Sequencing batch reactors for biological wastewater treatment. *Critical Reviews In Environmental Control*, 18, 255-294, (1989).
104. IS 1350 (part I), Methods of Test for Coal and Coke, Proximate Analysis, Bureau of Indian Standards, Manak Bhawan, New Delhi, India (1984)
105. IS 355:1984, Methods of Determination of Chemical Composition of Ash of Coal and Coke, Proximate Analysis, Bureau of Indian Standards, Manak Bhawan, New Delhi, India (1984)

106. Jiang, J.Q.; Graham, N.; Andre, C.; Geoff, H.K.; Brandon, N. Laboratory study of electro-coagulation-floatation for water treatment. *Water Research*, 36, 4064-4078, (2002).
107. Joglekar, A.M.; May, A.T. Product excellence through design of experiments. *Cereal Foods World*, 32, 857-868, (1987).
108. Jou, C.G.; Huang, G. A pilot study for oil refinery wastewater treatment using a fixed film Bioreactor. *Advance Environmental Research*, 7, 463-469, (2003).
109. Kaleta, J. Removal of phenol from aqueous solution by adsorption. *Canadian Journal of Civil Engineering*, 33, 546-551, (2006).
110. Kamble, S.P.; Mangrulkar, P.A.; Bansiwala, A.K.; Rayalu, S.S. Adsorption of phenol and o-chlorophenol on surface altered fly ash based molecular sieves. *Chemical Engineering Journal*, 138, 73-83, (2008).
111. Kamlet, M.J.; Doherty, R.M.; Abraham, M.H.; Marcus, Y.; Taft, R.W. Linear solvation energy relationships an improved equation for correlation and prediction of octanol-water partition coefficients of organic nonelectrolytes (including strong hydrogen bond donor solutes). *Journal of Physical Chemistry*, 92, 5244-5255 (1988)
112. Kargi, F.; Uygur, A. Nutrient removal performance of a five-step sequencing batch reactor as a function of wastewater composition. *Process Biochemistry*, 38, 1039-1045, (2003).
113. Katzer, J.; Ramage, M.; Sapre, A. Petroleum Refining: Poised for Profound Changes. *Chemical Engineering Process*, 41-51, (2000).
114. Keshmirizadeh, E.; Yousefi, S.; Rofouei, M.K. An investigation on the new operational parameter effective in Cr(VI) removal efficiency: A study on electrocoagulation by alternating pulse current. *Journal of Hazardous Materials*, 190, 119-124, (2011).
115. Khaing, T-H.; Li, J.; Li, Y.; Wai, N.; Wong, F. Feasibility study on petrochemical wastewater treatment and reuse using a novel submerged membrane distillation bioreactor. *Separation and Purification Technology*, 74, 138-143, (2010).

116. Khandegar, V.; Saroha, A.K. Electrocoagulation for the treatment of textile industry effluent A review. *Journal of Environmental Management*, 128, 949-963, (2013)
117. Khanna, S.K.; Malhotra, P. Kinetics and mechanism of phenol adsorption on fly ash. *Indian Journal of Environmental Health*, 19, 224-37 (1977).
118. Khieu, D.Q.; Quang, D.T.; Lam, T.D.; Phu, N.H.; Lee, J.H.; Kim, J.S. Fe-MCM-41 with highly ordered mesoporous structure and high Fe content: Synthesis and application in heterogeneous catalytic wet oxidation of phenol. *Journal of Inclusion Phenomena and Macrocyclic Chemistry*, 65, 73-81, (2009).
119. Kim, C.Y.; Choi, H.M.; Cho, H.T. Effect of deacetylation on sorption of dyes and chromium on chitin. *Journal of Applied Polymer Science*, 63(6), 725-736, (1997).
120. Kim, I.S.; Kim, S.M.; Jang A. Characterization of aerobic granules by microbial density at different COD loading rates. *Bioresource Technology*, 99, 18-25, (2008).
121. Kirk, R.E.; Othmer, D.F. *Encyclopedia of Chemical Technology*. 2nd edn, 462-492, Wiley, New York, (1966).
122. Knop, A.; Pilato, L.A. Phenolic Resins - Chemistry, Applications and Performance, *Springer-Verlag*, (1985).
123. Kobya, M.; Hiz, H.; Senturk, E.; Aydiner, C.; Demirbas, E. Treatment of potato chips manufacturing wastewater by electrocoagulation. *Desalination*, 190, 201-211, (2006).
124. Kulikowska, D.; Klimiuk, E.; Drzewicki, A. BOD₅ and COD removal and sludge production in SBR working with or without anoxic phase. *Bioresource Technology*, 98, 1426-1432, (2007).
125. Kumar, A.; Kumar, S.; Kumar, S. Adsorption of resorcinol and catechol on granular activated carbon: Equilibrium and kinetics. *Carbon*, 41, 3015-3025, (2003).
126. Kumar, M.; Ponselvan, F.I.A.; Malviya, J.R.; Srivastava, V.C.; Mall, I.D. Treatment of bio digester effluent by electrocoagulation using iron electrodes. *Journal of Hazardous Material*, 165, 345-352, (2009).

127. Kumar, S.; Upadhyay, S.N.; Upadhya, Y.D. Removal of phenols by adsorption on fly ash. *Journal of Chemical Technology and Biotechnology*, 37, 281-290, (1987)
128. Kumar, S.; Zafar, M.; Prajapati, J.K.; Kumar, S.; Kannepalli, S. Modeling studies on simultaneous adsorption of phenol and resorcinol onto granular activated carbon from simulated aqueous solution. *Journal of Hazardous Material*, 185, 287–294, (2011).
129. Kushwaha, J.P.; Srivastava, V.C.; Mall, I.D. Organics removal from dairy wastewater by electrochemical treatment and residue disposal. *Separation and Purification Technology*, 76,198–205 (2010).
130. Kushwaha, J.P.; Srivastava, V.C.; Mall, I.D. Studies on electrochemical treatment of dairy wastewater using aluminum electrode. *AIChE Journal*, 57, 2589-2598, (2011).
131. Kushwaha, J.P.; Srivastava, V.C.; Mall, I.D. Sequential batch reactor for dairy wastewater treatment: Parametric optimization, kinetics and waste sludge disposal. *Journal of Environmental Chemical Engineering*, (2013), DOI: 10.1016/j.jece.2013.08.018.
132. Kutty, S.R.M.; Gasim, H.A.; Khamaruddin, P.F.; Malakahmad, A. Biological treatability study for refinery wastewater using bench scale sequencing batch reactor systems. *WIT Transactions on Ecology and the Environment*, 145, ISSN 1743-3541 (2011) doi:10.2495/WRM110621
133. Lakshmi, U.R.; Mall, I.D.; Srivastava, V.C.; Latye, D.H. Rice husk ash as an effective adsorbent: Evaluation of adsorptive characteristics for Indigo Carmine dye. *Journal of Environmental Management*, 90, 710-720, (2009).
134. Langmuir, I. The adsorption of gases on plane surfaces of glass, mica and platinum. *Journal of American Chemical Society*, 40, 1361-1403, (1918).
135. Lataye, D.H.; Mishra, I.M.; Mall, I.D. Pyridine sorption from aqueous solution by rice husk ash (RHA) and granular activated carbon (GAC): Parametric, kinetic, equilibrium and thermodynamic aspects. *Journal of Hazardous Material*, 154, 858–870, (2008).

136. Lee, L.Y.; Hu, J.Y.; Ong, S.L.; Ng, W.J.; Ren, J.H.; Wong, S.H. Two-stage SBR for treatment of oil refinery wastewater. *Water Science and Technology*, *50*, 243–249, (2004).
137. Leenheer, J.A.; Rostad, C.E.; Barber, L.B. Nature and chlorine reactivity of organic constituents from reclaimed water in groundwater, Los Angeles County, California. *Environmental Science and Technology*, *35*, 3869–3876, (2001).
138. Li, Y.; Yan, L.; Xiang, C.; Hong, L.J. Treatment of oily wastewater by organic inorganic composite tubular ultrafiltration (UF) membranes. *Desalination*, *196*, 76–83, (2006).
139. Lin, D.; Xing, B. Adsorption of phenolic compounds by carbon nanotubes: role of aromaticity and substitution of hydroxyl groups. *Environmental Science and Technology*, *42*, 7254-7259, (2008).
140. Lingbo, L.; Song, Y.; Congbi, H.; Guangbo, S. Comprehensive characterization of oil refinery effluent-derived humic substances using various spectroscopic approaches. *Chemosphere*, *60*, 467–476, (2005).
141. Liu, Y.; Liu Qi. Causes and control of filamentous growth in aerobic granular sludge sequencing batch reactors. *Biotechnology Advances*, *24*, 115–127, (2006).
142. Lorenz, K. Secondary treatment of power-plant phenol waste with fly ash and cinders. *Gesubdb Lng*, *75*, 189, (1954).
143. Ma, F.; Guo, J.B.; Zhao, L.J.; Chang, C.C.; Cui, D. Application of bioaugmentation to improve the activated sludge system into the contact oxidation system treating petrochemical wastewater. *Bioresource Technology*, *100*, 597–602, (2009).
144. Mahesh, S.; Prasad, B.; Mall, I.D.; Mishra, I.M. Electrochemical degradation of pulp and paper mill wastewater part I. COD and color removal. *Industrial and Engineering Chemistry Research*, *45*, 2830–2839, (2006).
145. Malik, P.K. Use of activated carbons prepared from sawdust and rice-husk for adsorption of acid dyes: a case study of acid yellow 36. *Dyes and Pigments*, *56*, 239-249, (2003).
146. Mall, I.D. Petrochemical Process Technology, *Macmillan India Limited*, 1st Edition (2006).

147. Mall, I.D.; Upadhyay, S.N.; Sharma, Y.C. A review on economical treatment of wastewaters and effluents by adsorption. *International Journal of Environmental Studies*, 51, 77-124, (1996).
148. Mall, I.D.; Srivastava, V.C.; Agarwal, N.K. Removal of Orange-G and Methyl Violet dyes by adsorption onto bagasse fly ash—kinetic study and equilibrium isotherm analyses. *Dyes and Pigments*, 69, 210–223, (2006).
149. Mane, V.; Mall, I.D.; Srivastava, V.C. Kinetic and equilibrium isotherm studies for the adsorptive removal of brilliant green dye from aqueous solution by rice husk ash. *Journal of Environmental Management*, 84, 390-400, (2007).
150. Marquardt, D.W. An algorithm for least-squares estimation of nonlinear parameters, *Journal of the Society for Industrial and Applied Mathematics*, 11, 431-441, (1963).
151. Marrot, B.; Barrios-Martinez, A.; Moulin, P.; Roche, N. Biodegradation of high phenol concentration by activated sludge in an immersed membrane bioreactor. *Biochemical Engineering Journal*, 30, 174–183, (2006).
152. McKay, G.; Al-Duri, B. Extended empirical Freundlich isotherm for binary systems: a modified procedure to obtain the correlative constants. *Chemical Engineering Process*, 29, 133-138, (1991).
153. Mizzouri, N.; Shaaban, M. Performance study of SBR system for petroleum wastewater treatment. Proceedings of the International Conference on the Environment and Natural Resources (ICENR). *The Changing Environment: Challenges for Society*, University Salaya, Thailand, (2010).
154. Mizzouri, N.S.; Shaabana, M.G. Individual and combined effects of organic, toxic, and hydraulic shocks on sequencing batch reactor in treating petroleum refinery wastewater. *Journal of Hazardous Materials*, 250–251, 333– 344, (2013).
155. Mohamed, F.S.; Khater, W.A.; Mostafa, M.R. Characterization and phenols sorptive properties of carbons activated by sulphuric acid. *Chemical Engineering Journal*, 116, 47-52, (2006).
156. Mollah, M.Y.A.; Gomes, J.A.G.; Das, K.K.; Cocke, D.L. Electrochemical Treatment of Orange II Dye Solution-Use of Aluminum Sacrificial Electrodes

- and Flocculation Characterization. *Journal of Hazardous Material*, 174, 851–858, (2010).
157. Mondal, B.; Srivastava, V.C.; Mall, I.D. Electrochemical treatment of textile printing wastewater by stainless steel electrodes: multiple response optimization and residue analysis. *Journal of Environmental Science and Health, Part A*, 47, 2040–2051, (2012).
158. Mondal, B.; Srivastava, V.C.; Kushwaha, J.P.; Bhatnagar, R.; Singh, S.; Mall, I.D. Parametric and multiple response optimization for the electrochemical treatment of textile printing dye-bath effluent. *Separation Purification Technology*, 109, 135–143, (2013).
159. Mondal, P.; Balomajumder, C. Treatment of resorcinol and phenol bearing wastewater by simultaneous adsorption biodegradation (SAB): optimization of process parameters. *International Journal of Chemical Reactor Engineering*, 5, S1 (2007).
160. Monod, J. The growth of bacterial cultures. *Annual Review of Microbiology*, 3, 371-394, (1949).
161. Monsalvo, V.M.; Mohedano, A.F.; Casas, J.A.; Rodriguez, J.J. Cometary biodegradation of 4-chlorophenol by sequencing batch reactors at different temperatures. *Bioresource Technology*, 100, 4572–4578, (2009).
162. MoPNG, Basic Statistics on Indian Petroleum & Natural Gas, Ministry of Petroleum & Natural Gas (MoPNG), *Government of India, New Delhi, Economic Division*, (2012).
163. Moreno, C.H.A.; Cocke, D.L.; Gomes, J.A.G.; Morkovsky, P.; Parga, J.R.; Peterson, E.; Garcia, C. Electrochemical reactions for electrocoagulation using iron electrodes. *Industrial and Engineering Chemistry Research*, 48, 2275–2282, (2009).
164. Moussavi, G.; Barikbin, B.; Mahmoudi, M. The removal of high concentrations of phenol from saline wastewater using aerobic granular SBR. *Chemical Engineering Journal*, 158, 498–504, (2010).

165. Moussavi, G.; Khosravi, R.; Farzadkia, M. Removal of petroleum hydrocarbons from contaminated groundwater using an electrocoagulation process: Batch and continuous experiments. *Desalination*, 278, 288–294, (2011).
166. Mukherjee, S.; Kumar, S.; Misra, A.K.; Fan, M. Removal of phenols from water environment by activated carbon, bagasse ash and wood charcoal. *Chemical Engineering Journal*, 129, 133–142, (2007).
167. Nava, Y.F.; Maranon, E.; Soons, J.; Castrillon, L. Denitrification of wastewater containing high nitrate and calcium concentrations. *Bioresource Technology*, 99, 7976–7981, (2008).
168. Neczaj, E.; Kacprzak, M.; Kamizela, T.; Lach, J.; Okoniewska, E. Sequencing batch reactor system for the co-treatment of landfill leachate and dairy wastewater. *Desalination*, 222, 404-409, (2008).
169. Ng, J.C.Y.; Cheung, W.H.; McKay, G. Equilibrium studies of the sorption of Cu(II) ions chitosan. *Journal of Colloid and Interface Science*, 255, 64-74, (2002).
170. Ng, W.J. Aerobic Treatment of Piggery Wastewater with the Sequencing Batch Reactor. *Biolog. Wast.*, 22, 285-294, (1987).
171. Nigarn, P.; Banat, L.M.; Singh, D.; Marchant, R. Microbial process for decolourisation of textile effluents containing azo, diazo and reactive dyes, *Process Biochemistry*, 31, 435, (1996).
172. Okpokwasili, G.C.; Nweke, C.O. Microbial growth and substrate utilization kinetics. *African Journal of Biotechnology*, 5, 305-317, (2005).
173. Olmez, T. The optimization of Cr(VI) reduction and removal by electrocoagulation using response surface methodology. *Journal of Hazardous Material*, 162, 1371–1378, (2009).
174. Pachouri, A. Optimization and performance evaluation of sequential batch reactor for the treatment of petroleum refinery wastewater. *Master of Technology Dissertation Report*, Department of Chemical Engineering, Indian Institute of Technology Roorkee, (2008).

175. Panizza, M.; Bocca, C.; Cerisola, G. Electrochemical treatment of wastewater containing polyaromatic organic pollutants. *Water Research*, 34, 2601±2605, (2000)
176. Papadimitriou, C.A.; Samaras, P.; Sakellariopoulos, G.P. Comparative study of phenol and cyanide containing wastewater in CSTR and SBR activated sludge reactors. *Bioresource Technology*, 100, 31–37, (2009).
177. Peavy, H.S.; Rowe, D.R.; Tchobanoglous, G. Environmental Engineering. *MCGRAW-HILL Higher Education*, (2009).
178. Petroleum Refining Hazardous Waste Generation , *U.S. EPA, Office of Solid Waste*, (1994).
179. Prasad, R.K.; Kumar, R.R.; Srivastava, S.N. Design of optimum response surface experiment for electrocoagulation of distillery spent wash. *Water Air Soil Pollution*, 191, 5-13, (2008).
180. Prasad, R. Petroleum Refining Technology, *Khanna Publishers, 1st edition*, (2000).
181. Puri, B.R.; Walker, P.L. Chemistry and Physics of Carbon. *New York: Marcel Dekker*, (1966).
182. Purkait, M.K.; DasGupta, S.; De, S. Micellar enhanced ultrafiltration of phenolic derivatives from their mixtures. *Journal of Colloid and Interface Science*, 285, 395–402, (2005).
183. Puyol, D.; Mohedano, A.F.; Sanz, J.L.; Rodriguez, J.J., 2009. Comparison of UASB and EGSB performance on the anaerobic biodegradation of 2,4-dichlorophenol. *Chemosphere*, 76, 1192–1198, (2009).
184. Qadeer, R. A study of the adsorption of phenol by activated carbon from aqueous solutions. *Turkish Journal of Chemistry*, 26, 357-361, (2002).
185. Qin, L.; Liu, Y. Effect of settling time on aerobic granulation in sequencing batch reactor. *Biochemical Engineering Journal*, 21, 47–52, (2004).
186. Rahman, M.M.; Al-Malack, M.H. Performance of a cross-flow membrane bio-reactor (CF-MBR) when treating refinery wastewater. *Desalination*, 191, 16-26, (2006).

187. Rajani, R.M.; Sreekanth, D.; Himabindu, V. Degradation of mixture of phenolic compounds by activated sludge processes using mixed consortia. *International Journal of Energy and Environment*, 2, 151-160, (2011).
188. Rameshraj, D.; Srivastava, V.C.; Kushwaha, J.P.; Mall, I.D. Quinoline adsorption onto granular activated carbon and bagasse fly ash. *Chemical Engineering Journal*, 181–182, 343–351, (2012).
189. Rastegara, S.O.; Mousavia, S.M.; Shojaosadatia, S.A.; Sheibanib, S. Optimization of petroleum refinery effluent treatment in a UASB reactor using response surface methodology. *Journal of Hazardous Material*, 197, 26-32, (2011).
190. Redlich, O.; Peterson, D.L. A useful adsorption isotherm, *Journal of Physical Chemistry*, 63, 1024, (1959).
191. Rengaraj, S.; Moon, S.H.; Sivabalan, R.; Arabindoo, B.; Murugesan, V. Agricultural solid waste for the removal of organics: adsorption of phenol from water and wastewater by palm seed coat activated carbon, *Waste Management*, 22, 543-548, (2002).
192. Richard, D.; Nunez, M.D.L.D.; Schweich, D. Adsorption of complex phenolic compounds on active charcoal: Adsorption capacity and isotherms. *Chemical Engineering Journal*, 148, 1–7, (2009).
193. Saeedil, M.; Khalvati-Fahlyani, A. Treatment of oily wastewater of a gas refinery by electrocoagulation using aluminum electrodes. *Water Environment Research*, 83, 256-264, (2011).
194. Sag, Y.; Akcael, B.; Kutsal, T. Application of multicomponent adsorption models to the biosorption of Cr(VI), Cu(II), and Cd(II) ions on *Rhizopus arrhizus* from ternary metal mixtures. *Chemical Engineering Communications*, 190, 797-812, (2003).
195. Sag, Y.; Akcael, B.; Kutsal, T. Ternary biosorption equilibria of chromium(VI), copper(II), and cadmium(II) on *Rhizopus arrhizus*, *Separation Science and Technology*, 37, 279-308, (2002).
196. Sag, Y.; Kaya, A.; Kutsal, T. The simultaneous biosorption of Cu (II) and Zn on *Rhizopus arrhizus*: Application of the adsorption models. *Hydrometallurgy*, 50 (3), 297–314, (1998).

197. Sahinkaya, E.; Dilek, F.B. Effect of feeding time on the performance of a sequencing batch reactor treating a mixture of 4-CP and 2,4-DCP. *Journal of Environmental Management*, 83, 427–436, (2007).
198. Samantha, C.; Suzana, M.; Jose, A.; Rodrigues, D.; Eugenio, F.; Marcelo, Z. Feasibility of treating partially soluble wastewater in anaerobic sequencing batch biofilm reactor (ASBBR) with mechanical stirring. *Bioresource Technology*, 96, 517–519, (2005).
199. Santos, F.V.; Azevedo, E.B.; Sant’Anna Jr., G.L.; Dezotti, M. Photocatalysis as a tertiary treatment for petroleum refinery wastewaters. *Brazil Journal of Chemical Engineering*, 23, 450–460, (2006).
200. Sarfaraz, S.; Thomas, S.; Tewari, U.K.; Iyengar, L. Anoxic treatment of phenolic wastewater in sequencing batch reactor. *Water Research*, 38, 965–971, (2004).
201. Sarioglu, M. Biological phosphorus removal in a sequencing batch reactor by using pure cultures. *Process Biochemistry*, 40, 1599–1603, (2005).
202. Sengil, I.A.; Kulac, S.; Ozacarc, M. Treatment of tannery liming drum wastewater by electrocoagulation. *Journal of Hazardous Material*, 167, 940-946, (2009).
203. Serafim, A.J. Solid Retention Time on Carbon Adsorption of Organics in Secondary Effluents from Treatment of Petroleum Refinery Waste. PhD Thesis, Texas A&M University, (1979).
204. Shakir, K.; Ghoneimy, H.F.; Elkafrawy, A.F.; Beheir, S.G.; Refaat, M. Removal of catechol from aqueous solutions by adsorption onto organophilic-bentonite. *Journal of Hazardous Material*, 150, 765-773, (2008).
205. Shariati, S.R.P.; Bonakdarpour, B.; Zare, N.; Ashtiani, F.Z. The effect of hydraulic retention time on the performance and fouling characteristics of membrane sequencing batch reactors used for the treatment of synthetic petroleum refinery wastewater. *Bioresource Technology*, 102, 7692–7699, (2011).
206. Sharma, R.K.; Wooten, J.B.; Baliga, V.L.; Lin, X.; Chan, W.G.; Hajaligol, M.R. Characterisation of chars from pyrolysis of lignin. *Fuel*, 83, 1469–1482, (2004).

207. Sharma, S.; Mukhopadhyay, M.; Murthy, Z.V.P. Treatment of chlorophenols from wastewaters by advanced oxidation processes. *Separation and Purification Reviews*, *42*, 263-295, (2013)
208. Sharma, Y.C.; Uma; Sinha, A.S.K.; Upadhyay, S.N. Characterization and adsorption studies of *Cocos nucifera L.* activated carbon for the removal of methylene blue from aqueous solutions. *Journal of Chemical Engineering Data*, *55*, 2662–2667, (2010a).
209. Sharma, V.; Srivastava, V.C.; Kushwaha, J.P.; Mall I.D. Studies on biodegradation of resorcinol in sequential batch reactor. *International Biodeterioration and Biodegradation*, *64*, 764-768, (2010b).
210. Sharma, S.; Mukhopadhyay, M.; Murthy, Z.V.P. Degradation of 4-chlorophenol in wastewater by organic oxidants. *Industrial and Engineering Chemistry Research*, *49*, 3094-3098, (2010c)
211. Sheindorf, C.; Rebhum, M.; Sheintuch, M. A Freundlich-type multicomponent isotherm. *Journal of Colloid and Interface Science*, *79*, 136-142, (1981).
212. Silva, M.R.; Coelho, M.A.Z; Araujo O.Q.F. Minimization of phenol and ammonical nitrogen in refinery wastewater employing biological treatment. *Engenharia Termica, Edicao Especial*, 33-37, (2002).
213. Singh, S.; Srivastava, V.C.; Mall, I.D. Mechanism of dye degradation during electrochemical treatment mechanism of dye degradation during electrochemical treatment. *Journal of Physical Chemistry C*, *117*(29), 15229–15240, (2013a).
214. Singh, S.; Srivastava, V.C.; Mall, I.D. Mechanistic study of electrochemical treatment of basic green 4 dye with aluminium electrodes through zeta potential, TOC, COD and color measurement, and characterization of residues. *RSC Advances*, (2013b), DOI: 10.1039/C3RA41605D.
215. Smith, B.; Koonce, T.; Hudson, S. Decolorizing dye wastewater using chitosan. *American Dyestuff Reporter*, *82*(10), 18-36, (1993).
216. Soto, M.L.; Moure, A.; Dominguez, H.; Parajo, J.C. Recovery, concentration and purification of phenolic compounds by adsorption: A review. *Journal of Food Engineering*, *105*, 1–27, (2011).

217. Sridhar, R.; Sivakumar, V.; Prince Immanuel, V.; Prakash Maran, J. Treatment of pulp and paper industry bleaching effluent by electrocoagulant process. *Journal of Hazardous Material*, 186, 1495–1502, (2011).
218. Srivastava, V.C.; Mall, I.D.; and Mishra, I.M. Equilibrium modelling of ternary adsorption of metal ions onto rice husk ash. *Journal of Chemical Engineering Data*, 54, 705-711, (2009).
219. Srivastava, V.C.; Mall, I.D.; Mishra, I.M. Characterization of mesoporous rice husk ash (RHA) and adsorption kinetics of metal ions from aqueous solution onto RHA. *Journal of Environmental Management*, 134, 257–267, (2006a).
220. Srivastava, V.C.; Mall, I.D.; Mishra, I.M. Equilibrium modelling of single and binary adsorption of cadmium and nickel onto bagasse fly ash. *Chemical Engineering Journal*, 117, 79-91, (2006b).
221. Srivastava, V.C.; Swamy, M.M.; Mall, I.D.; Prasad, B.; Mishra, I.M. Adsorptive removal of phenol by bagasse fly ash and activated carbon: Equilibrium, kinetics and thermodynamics. *Colloids and Surfaces A: Physicochemical and Engineering Aspects*, 272, 89–104, (2006c).
222. Srivastava, V.C.; Mall, I.D.; Mishra, I.M. Antagonistic competitive equilibrium modeling for the adsorption of ternary metal ions mixtures onto bagasse fly ash. *Industrial and Engineering Chemistry Research*, 47, 3129-3137, (2008a).
223. Srivastava, V.C.; Mall, I.D.; Mishra, I.M. Removal of cadmium(II) and zinc(II) metal ions from binary aqueous solution by rice husk ash. *Colloids and Surfaces A: Physicochemical and Engineering Aspects*, 312, 172–184, (2008b).
224. Srivastava, V.C.; Mall, I.D.; Mishra, I.M. Treatment of pulp and paper mill wastewaters with poly aluminium chloride and bagasse fly ash. *Colloids and Surfaces A: Physicochemical and Engineering Aspects*, 260, 17–28, (2005).
225. Star, A.; Han, T.R.; Gabriel, J.C.P.; Bradley, K.; Gruner, G. Interaction of aromatic compounds with carbon nanotubes: correlation to the hammett parameter of the substituent and measured carbon nanotube FET response. *Nano Letters*, 3, 1421-1423, (2003).

-
226. Stephenson, R.; Tennant, B. New electrocoagulation process treats emulsified oily wastewater at Vancouver Shipyards. *Environmental Science & Engineering*, (2003).
227. Stepnowski, P.; Siedlecka, E.M.; Behrend, P.; Jastorff, B. Enhanced photodegradation of contaminants in petroleum refinery wastewater. *Water Research*, *36*, 2167–2172, (2002).
228. Stringfellow, W.T.; Alvarez-Cohen, L. Evaluating the relationship between the sorption of PAHs to bacterial biomass and biodegradation. *Water Research*, *33*, 2535–2544, (1999).
229. Sun, Y.; Chen, J.; Li, A.; Liu, F.; Zhang, Q. Adsorption of resorcinol and catechol from aqueous aqueous solution by aminated hypercrosslinked polymers. *Reactive and Functional Polymers*, *64*, 63–73, (2005).
230. Sun, Y.; Zhang, Y.; Quan, X. Treatment of petroleum refinery wastewater by microwave-assisted catalytic wet air oxidation under low temperature and low pressure. *Separation and Purification Technology*, *62*, 565–570, (2008).
231. Suresh, S.; Srivastava, V.C.; Mishra, I.M. Adsorption of catechol, resorcinol, hydroquinone, and their derivatives: a review. *International Journal of Energy and Environmental Engineering*, (2012a).
232. Suresh, S.; Srivastava, V.C.; Mishra, I.M. Adsorptive removal of aniline by granular activated carbon from aqueous solutions with catechol and resorcinol. *Environmental Technology*, *33*, 773-81, (2012b).
233. Suresh, S.; Srivastava, V.C.; Mishra, I.M. Adsorption of hydroquinone in aqueous solution by granular activated carbon. *Journal of Environmental Engineering*, *137*, 1145-1157, (2011a).
234. Suresh, S.; Srivastava, V.C.; Mishra, I.M. Adsorptive removal of phenol from binary aqueous solution with aniline and 4-nitrophenol by granular activated carbon, *Chemical Engineering Journal*, *171*, 997, (2011b).
235. Suresh, S.; Srivastava, V.C.; Mishra, I.M. Isotherm, Thermodynamics, Desorption, and Disposal Study for the Adsorption of Catechol and Resorcinol onto Granular Activated Carbon. *Journal of Chemical Engineering Data*, *56*, 811–818, (2011c).

236. Suresh, S.; Srivastava, V.C.; Mishra, I.M. Study of catechol and resorcinol adsorption mechanism through granular activated carbon characterization, pH and Kinetic Study. *Separation Science and Technology*, *46*, 1750–1766, (2011d).
237. Tancredi, N.; Medero, N.; Moller, F.; Piriz, J.; Plada, C.; Cordero, T. Phenol adsorption onto powdered and granular activated carbon, prepared from Eucalyptus wood. *Journal of Colloid and Interface Science*, *279*, 357–363, (2004).
238. Tansel, B.; Regula, J.; Shalewitz, R. Evaluation of ultrafiltration process performance for treatment of petroleum contaminated waters. *Water, Air, and Soil Pollution*, *126*, 291-305, (2001).
239. Terzyk, A.P. Further insights into the role of carbon surface functionalities in the mechanism of phenol adsorption. *Journal of Colloid and Interface Science*, *268*, 301 (2003).
240. Terzyk, A.P. The influence of activated carbon surface chemical composition on the adsorption of acetaminophen (paracetamol) in vitro. Part II. TG, FTIR, and XPS analysis of carbons and the temperature dependence of adsorption kinetics at the neutral pH. *Colloids and Surfaces A: Physicochemical and Engineering Aspects*, *177*, 23-45, (2001).
241. Thakur, C.; Srivastava, V.C.; Mall, I.D. Electrochemical treatment of a distillery wastewater: Parametric and residue disposal study. *Chemical Engineering Journal*, *148*, 496-505, (2009).
242. Thakur, C.; Srivastava, V.C.; Mall, I.D. Effect of hydraulic retention time and filling time on simultaneous biodegradation of phenol, catechol, and resorcinol in a sequencing batch reactor. *Archives of Environmental Protection*, *39*, 1-9, (2013a).
243. Thakur, C.; Srivastava, V.C.; Mall, I.D. Equilibrium modeling of binary adsorption of phenol and resorcinol onto rice husk ash. *Theoretical Foundation of Chemical Engineering* (2013b). (Manuscript Accepted)
244. Thakur, C.; Srivastava, V.C.; Mall, I.D. Modelling of binary isotherm behaviour for the adsorption of catechol with phenol and resorcinol onto rice husk ash. *Environmental Engineering and Management Journal*, (2013c). (Communicated)

-
245. Thakur, C.; Srivastava, V.C.; Mall, I.D. Electrocoagulation treatment of actual petroleum refinery wastewater using stainless steel electrode. *Separation and Purification Technology*, (2013d). (Communicated)
246. Thakur, C.; Srivastava, V.C.; Mall, I.D. Aerobic degradation of actual petroleum refinery wastewater in sequential batch reactor. (2013e). (Communicated)
247. Thakur, C.; Dembla, A.; Srivastava, V.C.; Mall, I.D. Removal of 4-chlorophenol in sequencing batch reactor with and without granular-activated carbon. *Desalination and Water Treatment*, Doi: 10.1080/19443994.2013.803684, 1-9, (2013f).
248. Thella, K.; Verma, B.; Srivastava, V.C.; Srivastava, K.K. Electrocoagulation study for the removal of arsenic and chromium from aqueous solution. *Journal of Environmental Science and Health, Part A*, 43, 554–562, (2008).
249. Ting, Y.P.; Lavson, F.; Prince, I.G.; Uptake of cadmium and zinc by the alage *C.vulgaris*: Part II: Multi-ion species. *Biotechnology Bioengineering*, 37, 445-52, (1991).
250. Tir, M.; Moulai-Mostefa, N. Optimization of oil removal from oily wastewater by electrocoagulation using response surface method. *Journal of Hazardous Material*, 158, 107–115, (2008).
251. Tiwari, D.P.; Singh, D.K.; Saksena, D.N. Hg(II) adsorption from aqueous solutions using rice-husk ash. *Journal of Environmental Engineering*, 121, 479-481, (1995).
252. Tomei M.C.; Annesini, M.C.; Luberti, R.; Cento, G.; Senia, A. Kinetics of 4 nitrophenol biodegradation in a sequencing batch reactor. *Water Research*, 37, 3803–3814, (2003).
253. Tomei, M.C.; Annesini, M.C. Biodegradation of phenolic mixtures in a sequencing batch reactor a kinetic study. *Environmental Science and Pollution Research*, 15, 188–195, (2008).
254. Toth, J. *Adsorption: Theory, Modeling, and Analysis*. Surfactant Science Series. Marcel Dekker, New York, 107, (2002).

255. Tsang, Y.F.; Hua, F.L.; Chua, H.; Sin, S.N.; Wang, Y.J. Optimization of biological treatment of paper mill effluent in a sequencing batch reactor. *Biochemical Engineering Journal*, 34, 193–199, (2007).
256. Tyagi, R.D.; Tran, F.T.; Chowdhury, A.K.M.M. Biodegradation of petroleum refinery wastewater in a modified rotating biological contactor with polyurethane foam attached to the disks. *Water Research*, 27, 91-99, (1993).
257. USEPA, Wastewater technology fact sheet, Sequencing Batch Reactors. *U.S. Environmental Protection Agency*, 832-F-99-073, (1999).
258. Vasudevan, D.; Stone, A.T. Adsorption of catechols, 2-aminophenols, and 1,2-phenylenediamines at the metal hydroxide/water interface: Effect of ring substituents on the adsorption onto TiO₂. *Environmental Science & Technology*, 30, 1604-1613, (1996).
259. Verma, S.K.; Khandegar, V.; Saroha, A.K. Removal of chromium from electroplating industry effluent using electrocoagulation. *Journal of Hazardous, Toxic, and Radioactive Waste*, 17, 146-152, (2013).
260. Viero, A.F.; De Melo, T.M.; Torres, A.P.R.; Ferreira, N.R.; Sant'Anna Jr.G.L.; Borges, C.P.; Santiago, V.M.J. The effects of long-term feeding of high organic loading in a submerged membrane bioreactor treating oil refinery wastewater. *Journal of Membrane Science*, 319, 223–230, (2008).
261. Vinitnantharat, S.; Cha, W.S.; Lshibashi, Y.; Ha, S.R. Stability of biological activated Carbon-Sequencing batch reactor (BAC-SBR) to phenol shock loading. *Thammasat International Journal of Science and Technology*, 6, 27-32, (2001).
262. Wagner, K.; Schulz, S. Adsorption of Phenol, Chlorophenols, and Dihydroxybenzenes onto Unfunctionalized Polymeric Resins at Temperatures from 294.15 K to 318.15 K. *Journal of Chemical Engineering Data*, 46, 322-330, (2001).
263. Wang, D.; Li, X.; Yang, Q.; Zeng, G.; Liao, D.; Zhang, J. Biological phosphorus removal in sequencing batch reactor with single-stage oxic process. *Bioresource Technology*, 99, 5466–5473, (2008).

-
264. Wang, J.W.; Bejan, D.; Bunce, N.J. Electrochemical method for remediation of arsenic-contaminated nickel electro-refining baths. *Industrial and Engineering Chemistry Research*, *44*, 3384-3388, (2005).
265. Wang, S.G.; Liu, X.W.; Zhang, H.Y.; Gong, W.X.; Sun, X.F.; Gao, B.Y. Aerobic granulation for 2,4-dichlorophenol biodegradation in a sequencing batch reactor. *Chemosphere*, *69*, 769-775 (2007).
266. Wei, L.; Guo, S.; Yan, G.; Chen, C.; Jiang, X. Electrochemical pretreatment of heavy oil refinery wastewater using a three-dimensional electrode reactor, *Electrochimica Acta*, *55*, 8615-8620, (2010).
267. Wilean, B.M.; Balmer, P. The effect of dissolved oxygen concentration on the structure, size and size distribution of activated sludge flocs. *Water Research*, *33*, 391-400, (1999).
268. Wongjunda, J.; Saueprasearsit, P. Biosorption of Chromium (VI) Using Rice Husk Ash and Modified Rice Husk Ash. *Environmental Research Journal*, *4*, 244-250, (2010).
269. World Petroleum Scenario. *Petro Zine*, BP, (2011).
http://www.bharatpetroleum.co.in/YourCorner/petrozine/quart2_2011/index.html
270. Yan, L.; Ma, H.; Wang, B.; Wang, Y.; Chen, Y. Electrochemical treatment of petroleum refinery wastewater with three-dimensional multi-phase electrode. *Desalination*, *276*, 397-402, (2011).
271. Yang, R.T. Gas Separation by Adsorption Processes, *Boston, MA: Butterworths*, (1987).
272. Yang, S.F.; Li, X.Y.; Yu, H.Q. Formation and characterisation of fungal and bacterial granules under different feeding alkalinity and pH conditions. *Process Biochemistry*, *43*, 8-14, (2008).
273. Yavuz, Y.; Koparal, A.S.; Ogutveren, U.B. Treatment of petroleum refinery wastewater by electrochemical methods. *Desalination*, *258*, 201-205, (2010).
274. Yoong, E.T.; Lant, P.A.; Greenfield, P.F. In situ respirometry in an SBR treating wastewater with high phenol concentrations. *Water Resource*, *34*, 239-245, (2000).

275. Yu, H.Q.; Gu, G.W. Treatment of phenolic wastewater by sequencing batch reactors with aerated and unaerated fills. *Waste Management*, *16*, 561-566, (1996).
276. Zarooni, M.A.; Elshorbagy, W. Characterization and assessment of Al Ruwais refinery wastewater. *Journal of Hazardous Material*, *136*, 398-405, (2006).
277. Zhang, W.M.; Xu, Z.W.; Pan, B.C.; Zhang, Q.J.; Du, W.; Zhang, Q.R.; Zheng, K.; Zhang, Q.X.; Chen, J.L. Adsorption enhancement of laterally interacting phenol/aniline mixture onto nonpolar adsorbent. *Chemosphere*, *66*, 2044-2049, (2007).
278. Zhao, X.; Wang, Y.; Ye, Z.; Borthwick, A.G.L.; Ni, J. Oil field wastewater treatment in biological aerated filter by immobilized microorganisms. *Process Biochemistry*, *41*, 1475-1483, (2006).
279. Zhou, Q.; Frost, R.L.; He, H.; Xi, Y.; Liu, H. Adsorbed para-nitrophenol on HDTMAB organoclay-A TEM and infrared spectroscopic study. *Journal of Colloid and Interface Science*, *307*, (2007).
280. Zhou, S.; Zhang, H.; Yong, S. Combined treatment of landfill leachate with fecal supernatant in SBR. *Journal of Zhejiang University SCIENCE B*, *7*, 397-403, (2006).
281. Zongoa, I.; Maiga, A.H.; Wethe, J.; Valentina, G.; Leclerca, J.; Paternottea, G.; Lapiquea, F. Electrocoagulation for the treatment of textile wastewaters with Al or Fe electrodes: Compared variations of COD levels, turbidity and absorbance. *Journal of Hazardous Material*, *169*, 70-76, (2009).

BIO-DATA

Name : Chandrakant Thakur
Father Name : Shri. Mohan Singh Thakur
Date of Birth : 27th November, 1984
Permanent Address : St: No.-35, Qr/No.-3/A,
Nandini Mines, Distt: Durg
Chhattisgarh-490036 (India)
Email : chandrakant.thakur@gmail.com
Marital Status : Single

Educational Qualification:

1. S.S.C.: Gandhi Memorial Higher Secondary School, Nandini Mines in 2000.
2. H.S.C.: Gandhi Memorial Higher Secondary School, Nandini Mines in 2002.
3. B.E. (Chemical): National Institute of Technology, Raipur in 2006.
4. M.Tech (Chemical): Indian Institute of Technology Roorkee, Roorkee in 2008.

Professional Experience:

Process Engineer (4th Aug'08 to 27th Nov'09)
Pyramid Consulting and Engineering Pvt. Ltd

Publications:

International Journal - 5
Conferences - 4

PUBLICATION FROM THESIS

Research Publication in Journals

1. Thakur, C., Srivastava, V.C., Mall, I.D. "Effect of hydraulic retention time and filling time on simultaneous biodegradation of phenol, catechol, and resorcinol in a sequencing batch reactor", Archives of Environmental Protection, 39, 69-80, (2013). **(Published)**
2. Thakur, C., Srivastava, V.C., Mall, I.D. "Equilibrium modeling of binary adsorption of phenol and resorcinol onto rice husk ash", Theoretical Foundation of Chemical Engineering. (2013) **(Accepted)**
3. Thakur, C., Srivastava, V.C., Mall, I.D. "Modelling of binary isotherm behaviour for the adsorption of catechol with phenol and resorcinol onto rice husk ash", Environmental Engineering and Management Journal. **(Communicated)**
4. Thakur, C., Srivastava, V.C., Mall, I.D. "Electrochemical treatment of actual petroleum refinery wastewater using stainless steel electrode", Separation and Purification Technology. **(Communicated)**
5. Thakur, C., Srivastava, V.C., Mall, I.D. "Aerobic degradation of actual petroleum refinery wastewater in sequential batch reactor". International Biodeterioration and Biodegradation. **(Communicated)**

Research Publication in Conference Proceeding

1. Thakur, C., Srivastava, V.C., Mall, I.D. "Adsorption Study on removal of phenolic compounds by rice husk ash", RACEE-2012_Abstract_79, NIT Rourkela, (2012), 127.
2. Thakur, C., Srivastava, V.C., Mall, I.D. "Adsorption Study on removal of phenolic compounds by baggase fly ash", 7th Uttarakhand State Science & Technology Congress, 5, (2012), 160.
3. Thakur, C., Prateek, Srivastava, V.C., Mall, I.D. "Adsorption of Ternary Mixture of Phenol, Catechol and Resorcinol from aqueous solution by Rice Husk Ash", ICACE 2013, NIT Raipur.